

**INVESTIGATION INTO THE POTENTIAL OF
METHYLENE BLUE AND ITS DERIVATIVES TO BE
USED IN THE PHOTODYNAMIC THERAPY OF
NON-PIGMENTED AND PIGMENTED CELLS**

By

LESLEY RICE, BSc. (Hons), MSc.

**A thesis submitted in partial fulfilment of the requirements for the degree of
Doctor of Philosophy**

UNIVERSITY OF CENTRAL LANCASHIRE

MARCH 2001

ABSTRACT

Photodynamic therapy (PDT) is a novel treatment for malignant disease. The first step is intravenous injection of a light-absorbing, cytotoxic drug (the photosensitizer) that is then allowed time to accumulate in malignant tissue. The second step involves local activation of the photosensitizer with long (red) wavelength light, delivered usually from a laser. Subsequent to irradiation, highly reactive singlet molecular oxygen (Type II mechanism) is likely to be the most damaging cytotoxic species *in vivo*. The porphyrin molecule, Photofrin®, is the only photosensitizer currently registered for clinical use but is associated with several problems. Most disappointing is the fact that Photofrin® accumulates not only in malignant tissue but also in other organs, such as the liver, kidney and spleen. Its long persistence in the skin commonly causes severe photosensitization reactions in patients for up to three months post-treatment. Photofrin® also has poor light absorption properties within the therapeutic window (600 to 800 nm) for PDT. Furthermore, PDT with Photofrin® has proved of no use in the treatment of malignant melanoma due, possibly, to competition between the photosensitizer and melanin for light absorption.

Second-generation photosensitizers have tended to be porphyrin-based molecules, many of which have reached various stages of clinical trial. Of non porphyrin-based compounds, the cationic dye, methylene blue (MB), used traditionally as a nuclear stain in histology, has proved also to be an efficient photosensitizer, with maximum light absorption properties within the therapeutic window for PDT. Its use as a selective stain for tumour tissue in the bladder led first to its investigation in humans for the PDT of bladder cancer and inoperable tumours of the oesophagus. Radiolabelled MB has also recently been used as a tracer for metastatic melanoma in humans. The disadvantages of MB are an inherent (dark) toxicity and its rapid reduction *in vivo* to the inactive form, leuco-methylene blue (LMB).

This study found the cytotoxicity of MB to be enhanced by illumination and that successive methylation of the molecule corresponds to both increased light and dark toxicities in the EMT-6 (murine mammary), the SK-23 (murine melanoma) and SK-MEL-28 (human melanoma) cell lines. The increased toxicities may be due to increased resistance to reduction (MB<NMB<MMB<DMMB), improved singlet

oxygen quantum yield (MB<MMB<DMMB<NMB), increased hydrophobicity (MB<MMB<DMMB<NMB), improved cellular uptake (MB<MMB<DMMB \approx NMB) and/or changes in intracellular targeting and localisation. MB is known to target the nucleus but it was proposed that the increased hydrophobicities could lead to the mitochondrial targeting of the derivatives. The intracellular localisation of the photosensitizers following incubation was studied using both fluorescence and confocal microscopy. Here, confocal microscopy showed that none of the four photosensitizers, including MB itself, target the nucleus prior to illumination. DMMB and NMB in particular appear to be confined to small subcellular bodies within the cytoplasm. However, the precise locations of the photosensitizers, prior to illumination, were not established during the course of this study. Nevertheless, confocal microscopy showed that, upon illumination, all four photosensitizers rapidly relocalise within the nucleus.

Since photosensitizers that localise in mitochondria are found to be more efficient inducers of apoptosis than photosensitizers that target other subcellular sites, the ability of the photosensitizers, MB, MMB, DMMB and NMB, to induce apoptosis in EMT-6, SK-23 and SK-MEL-28 cells in culture was investigated in this study. The methods used were visual examination of cell morphology, by use of the cyanine dye, JC-1, and the use of the FluorAce® Apopain Assay Kit from Biorad, in cells that had been exposed to the photosensitizers. From these, it was concluded that an apoptotic cell killing mechanism might play an important role in the photocytotoxicity of the photosensitizers, moreso for DMMB and NMB.

The overall purpose of this project was to assess the potential of the derivatives of MB to be used in the PDT of cancer, with a special emphasis on malignant melanoma, since this is a field of cancer treatment where PDT has had no success. Although methyl substitution of MB did not abolish the inherent toxicity of the molecule, it is possible to assess the potential usefulness of the photosensitizers by examination of the light: dark differential. In fact, the light:dark differential was improved for all the derivatives of MB in all three cell lines. Nevertheless, NMB consistently performed the best, achieving maximum photocytotoxicity at concentrations that caused very little toxicity in the dark. The presence of melanin made no difference to the photosensitizing capabilities of the photosensitizers in melanoma cells.

In terms of a clinical application of the current work, PDT employing phenothiazinium photosensitizers is not suggested procedurally for the removal of primary melanoma, since this is routinely performed by excision. However, due to the demonstrated efficacy of MB in tracing microsattellites and its use in sentinel lymph node tracing, it may be of use in the photodynamic treatment of local metastatic lymph infiltration immediately post-surgery, as an alternative to lymphadenectomy. At present, MB is used routinely in various tracing or demarcation procedures, either visible or scintillographic, without reported toxicity. The derivatives used in the present *in vitro* study were all more effective in terms of the photodynamic effect and it is thus possible that future clinical developments in this direction may be feasible.

ACKNOWLEDGEMENTS

I would like to thank the many, many people who have assisted and supported me during the course of my PhD research. I am particularly grateful to my supervisors, Professor David Phoenix, Dr. Mark Wainwright and Dr. Jack Waring, for their faith in me and for guiding me through what has been a thoroughly enjoyable learning experience. For practical help, I wish particularly to thank Dr. Mark Tobin at the Daresbury Laboratories in Cheshire, who provided expert tuition in the field of confocal microscopy. I thank the technicians, academic staff and fellow researchers at the University of Central Lancashire and the Lancashire Centre for Medical Studies for their friendship, interest, advice and support. A big thank-you goes to George Georgiou for his patience and perseverance in developing all my microscopic images. I acknowledge funding from the University Bursary Scheme, the Chorley and District Hospitals Fund and the BBSRC. Finally, a very special thank-you goes to my husband, Peter, and children, Josephine, Lydia and Ashley, and to my Mum for their constant love and encouragement, and who serve to remind me that there is more to life than writing up my PhD thesis!

CONTENTS

	PAGE
<u>ABSTRACT</u>	i
<u>ACKNOWLEDGEMENTS</u>	iv
<u>CONTENTS</u>	v
<u>FIGURES & TABLES</u>	xi
<u>ABBREVIATIONS</u>	xv
CHAPTER ONE: GENERAL INTRODUCTION	1
1.1 Cancer	2
1.1.1 Cancer Aetiology and Epidemiology	2
1.1.2 Conventional Cancer Therapy	3
1.2 Photodynamic Therapy	4
1.2.1 Clinical Practice	4
1.2.2 Advantages of Photodynamic Therapy	6
1.2.3 Light Dosimetry	7
1.2.4 Light Sources in Photodynamic Therapy	8
<i>Non-Laser Systems</i>	8
<i>Laser Systems</i>	8
1.3 The Photochemical Reaction	10
1.3.1 Photosensitization	10
1.3.2 Light Absorption	12
1.3.3 Cellular Effects	13
1.3.4 Vascular Effects	15
1.3.5 Immunologic Effects	16
1.4 Development of Photodynamic Therapy	17
1.4.1 Early History	17
1.4.2 First-generation Photosensitizers: the Porphyrins	19
1.4.3 Modern History	20
1.4.4 Photofrin®	22
1.4.5 Current Status of Photodynamic Therapy	24
1.4.6 Disadvantages of Photofrin®	25
1.5 Future Directions	26
1.5.1 Second-generation Photosensitizers: Porphyrin-based Compounds	26
<i>Phthalocyanines and Naphthalocyanines</i>	27
<i>5-Aminolaevulinic Acid/Protoporphyrin IX</i>	28
<i>meta-Tetrahydroxyphenyl Chlorin (m-THPC, Temoporfin, Foscan®)</i>	31
<i>Benzoporphyrin Derivative-Monoacid Ring A (BPD-MA, Verteporfin)</i>	33
<i>Mono-L-aspartylchlorin e₆ (MACE)</i>	35

<i>Tin Ethyl Etiopurpurin (SnET2, Purlytin®)</i>	36
<i>Lutetium Texaphyrin (PCI-0123, Lu-Tex)</i>	37
1.5.2 Second-generation photosensitizers: Cationic Dyes	38
1.6 Aim of Project	41
CHAPTER TWO: CYTOTOXICITY OF METHYLENE BLUE AND ITS DERIVATIVES AGAINST THE EMT-6 CELL LINE	42
2.1 <u>ABSTRACT</u>	43
2.2 <u>INTRODUCTION</u>	44
2.3 <u>MATERIALS AND METHODS</u>	51
2.3.1 General Reagents	51
2.3.2 Photosensitizers	51
2.3.2.1 Preparation	51
2.3.2.2 Singlet Oxygen Measurements	51
2.3.2.3 Hydrophobicity Values (Log <i>P</i>)	52
2.3.2.4 Reduction Rates	52
2.3.3 Cell Culture	53
2.3.3.1 Maintenance of the EMT-6 Cell Line	53
2.3.3.2 Growth Kinetics of the EMT-6 Cell Line	54
2.3.3.3 Cytotoxicity of the Photosensitizers against the EMT-6 Cell Line	54
2.3.3.4 Light Dose Study	55
2.3.3.5 Uptake of the Photosensitizers in EMT-6 Cells	55
2.4 <u>RESULTS</u>	57
2.4.1 Photosensitizers	57
2.4.1.1 Absorption Spectra	57
2.4.1.2 Singlet Oxygen	57
2.4.1.3 Hydrophobicity Values (Log <i>P</i>)	59
2.4.1.4 Reduction Rates	59
2.4.2 Cell Culture Experiments	60
2.4.2.1 Growth Kinetics of the EMT-6 Cell Line	60
2.4.2.2 Cytotoxicity of the Photosensitizers in EMT-6 Cells	60
2.4.2.3 Light Dose Study	63
2.4.2.4 Uptake of the Photosensitizers in EMT-6 Cells	64
2.5 <u>DISCUSSION</u>	66

CHAPTER THREE: CYTOTOXICITY OF METHYLENE BLUE AND ITS DERIVATIVES AGAINST THE SK-23 AND SK-MEL-28 MELANOMA CELL LINES	70
3.1 <u>ABSTRACT</u>	71
3.2 <u>INTRODUCTION</u>	72
3.3 <u>MATERIALS & METHODS</u>	77
3.3.1 Reagents and Photosensitizers	77
3.3.1.1 Preparation	77
3.3.2 Cell culture	77
3.3.2.1 Maintenance of the SK-23 and SK-MEL-28 Cell Lines	77
3.3.2.2 Growth kinetics of the SK-23 and SK-MEL-28 Cell Lines	77
3.3.2.3 Cytotoxicity of the Photosensitizers against SK-23 and SK-MEL-28 Cells	78
3.3.2.4 Light Dose Study	78
3.3.2.5 Uptake of the Photosensitizers in SK-23 and SK-MEL-28 Cells	78
3.3.3 Melanin Binding Studies	78
3.3.3.1 Absorption Spectrophotometry	78
3.3.3.2 Absorption Spectra	79
3.4 <u>RESULTS</u>	80
3.4.1 Cell Culture Experiments	80
3.4.1.1 Growth Kinetics of the SK-23 and SK-MEL-28 Cell Lines	80
3.4.1.2 Cytotoxicity of the Photosensitizers in SK-23 and SK-MEL-28 Cells	81
3.4.1.3 Light Dose Study	86
3.4.1.4 Uptake of the Photosensitizers in SK-23 and SK-MEL-28 Cells	86
3.4.2 Melanin Binding Experiments	88
3.4.2.1 Absorption Spectrophotometry	88
3.4.2.2 Absorption Spectra	88
3.5 <u>DISCUSSION</u>	90

CHAPTER FOUR: SUBCELLULAR LOCALISATION OF METHYLENE BLUE AND ITS DERIVATIVES IN PIGMENTED AND NON-PIGMENTED CELLS IN CULTURE	92
4.1 <u>ABSTRACT</u>	93
4.2 <u>INTRODUCTION</u>	94
4.3 <u>MATERIALS AND METHODS</u>	101
4.3.1 Localisation Studies	101
4.3.1.1 Fluorescence Microscopy	101
4.3.1.2 Scanning Laser Confocal Microscopy	101
4.3.1.3 Image Processing	102
4.3.2 Effect of Photosensitizers on Mitochondrial Respiration	102
4.3.2.1 Preparation of Liver Homogenates	102
4.3.2.2 Protein Estimation	102
4.3.2.3 Mitochondrial Respiration	102
4.3.2.4 Calculation of Data	103
4.4 <u>RESULTS</u>	104
4.4.1 Localisation Studies	104
4.4.1.1 Fluorescence Microscopy	104
4.4.1.2 Confocal Microscopy	104
4.4.2 Effect of Photosensitizers on Mitochondrial Respiration	114
4.4.2.1 Protein Estimation	114
4.4.2.2 Mitochondrial Respiration	114
4.5 <u>DISCUSSION</u>	116

CHAPTER 5: EVIDENCE FOR INDUCTION OF APOPTOSIS BY METHYLENE BLUE AND ITS DERIVATIVES IN EMT-6, SK-23 AND SK-MEL-28 CELLS IN CULTURE	120
5.1 <u>ABSTRACT</u>	121
5.2 <u>INTRODUCTION</u>	122
5.3 <u>METHODS & MATERIALS</u>	130
5.3.1 Cell Morphology	130
5.3.2 Detection of Apoptosis using JC-1	130
5.3.2.1 JC-1	130
5.3.2.2 Effect of Concentration on the Fluorescence Spectrum of JC-1	131
5.3.2.3 Effect of Ionic Strength on the Fluorescence Spectrum of JC-1	131
5.3.2.4 Effect of pH on the Fluorescence Spectrum of JC-1	132
5.3.2.5 Fluorescence Microscopy with JC-1 to detect Apoptosis in Cell Cultures	132
5.3.2.6 Fluorometric Determination of Apoptosis in Cell Cultures using JC-1	132
5.3.3 The FluorAce® Apopain Assay	133
5.3.3.1 Apopain/Caspase 3	133
5.3.3.2 The FluorAce® Apopain Assay Kit	134
5.3.3.3 Cell Cultures	134
5.3.3.4 Preparation of Cell Extracts	134
5.3.3.5 Apopain Assay	134
5.3.3.6 Inhibition of Apopain Activity (Negative Control)	135
5.4 <u>RESULTS</u>	136
5.4.1 Cell Morphology	136
5.4.2 Detection of Apoptosis using JC-1	136
5.4.2.1 JC-1	136
5.4.2.2 Effect of Concentration on the Fluorescence Spectrum of JC-1	136
5.4.2.3 Effect of Ionic Strength on the Fluorescence Spectrum of JC-1	136
5.4.2.4 Effect of pH on the Fluorescence Spectrum of JC-1	139
5.4.2.5 Fluorescence Microscopy with JC-1 to detect Apoptosis in Cell Cultures	139
5.4.2.6 Fluorometric Determination of Apoptosis in Cell Cultures using JC-1	139

5.4.3	Detection of Apoptosis using the FluorAce® Apopain Assay Kit	145
5.4.3.1	Apopain Assay	145
5.4.3.2	Inhibition of Apopain Activity (Negative Control)	145
5.5	<u>DISCUSSION</u>	147
CHAPTER SIX: CLOSING DISCUSSION		151
CHAPTER SEVEN: REFERENCES		159
CHAPTER EIGHT: APPENDIX		187
PRESENTATIONS & PUBLICATIONS		191

FIGURES & TABLES

		PAGE
Figure 1.	Jablonski diagram showing possible transitions of aromatic molecules following light excitation.	12
Figure 2.	Chemical mechanisms of photosensitization.	13
Figure 3.	Chemical structure of haematoporphyrin derivative.	19
Table 1.	Significant historical events leading to the development of PDT.	21
Figure 4.	Chemical structures of phthalocyanine and naphthalocyanine molecules.	27
Figure 5.	Chemical structures of 5-aminolaevulinic acid/protoporphyrin IX.	28
Figure 6.	The haem biosynthetic pathway.	29
Figure 7.	Chemical structure of <i>meso</i> -tetra(<i>m</i> -hydroxyphenyl)chlorin.	31
Figure 8.	Chemical structure of benzoporphyrin derivative-monoacid ring A.	33
Figure 9.	Chemical structure of mono-L-aspartylchlorin e_6 .	35
Figure 10.	Chemical structure of tin ethyl etiopurpurin.	36
Figure 11.	Chemical structure of a texaphyrin molecule.	37
Figure 12.	Chemical structure of 5-ethylamino-9-[α]thiazinium chloride.	41
Figure 13.	Schematic representation of the photosensitizers.	50
Table 2.	Physicochemical data for the photosensitizers.	57
Figure 14.	Absorption spectra of the photosensitizers.	58
Figure 15.	Rates of reduction for the photosensitizers.	59
Figure 16.	Growth kinetics of the murine, mammary tumour cell line, EMT-6.	60
Figure 17.	Effect of light on the EMT-6 cell line.	61
Figure 18.	Photocytotoxicity and dark toxicity of the photosensitizers against the EMT-6 cell line.	62
Table 3.	Toxicity data and light:dark ratios for the photosensitizers against the EMT-6 cell line.	63

Figure 19.	Photocytotoxicity of the photosensitizers against the EMT-6 cell line as a function of light dose.	64
Figure 20.	Uptake of the photosensitizers into EMT-6 cells over a range of concentrations.	65
Figure 21.	Uptake of the photosensitizers, MB, MMB, DMMB and NMB at 5 μ M concentrations into EMT-6 cells over three hours.	65
Figure 22.	Growth kinetics of the murine [SK-23] and human [SK-MEL-28] cell lines.	80
Figure 23.	Photocytotoxicity and dark toxicity of the photosensitizers in the SK-23 cell line.	82
Figure 24.	Photocytotoxicity and dark toxicity of the photosensitizer in the SK-MEL-28 cell line.	83
Table 4.	Toxicity data and light:dark ratios for the photosensitizers in the SK-23 cell line.	84
Table 5.	Toxicity data and light:dark ratios for the photosensitizers in the SK-MEL-28 cell line.	84
Figure 25.	Photocytotoxicity of the photosensitizers in the SK-23 and SK-MEL-28 cell lines as a function of light dose.	85
Figure 26.	Uptake of the photosensitizers, into SK-23 cells and SK-MEL-28 cells over a range of concentrations.	87
Figure 27.	Uptake of the photosensitizers into SK-23 cells and SK-MEL-28 cells over a period of three hours.	87
Figure 28.	Percentage binding of the photosensitizers to melanin.	88
Figure 29.	Absorption spectra for the photosensitizers and their compositions with synthetic melanin.	89
Figure 30.	Intracellular targets for hydrophilic and hydrophobic Photosensitizers.	99
Figure 31.	Subcellular localisation of the photosensitizers, pre-incubated for three hours with typical EMT-6 cells, as shown by fluorescence microscopy.	106
Figure 32.	Subcellular localisation of the photosensitizers, pre-incubated for three hours with typical SK-MEL-28 cells, as shown by confocal microscopy.	107

Figure 33.	Subcellular localisation of MMB in a typical SK-MEL-28 cell, using a flow-through method, as shown by confocal microscopy.	108
Figure 34.	Subcellular localisation of MB, pre-incubated for three hours with SK-MEL-28 cells, as shown by confocal microscopy.	109
Figure 35.	Subcellular localisation of the photosensitizers, pre-incubated for three hours with SK-23 cells, as shown by confocal microscopy.	110
Figure 36.	Subcellular localisation of MB in a typical SK-23 cell, using a flow-through method, as shown by confocal microscopy.	111
Figure 37.	Subcellular localisation of MMB in a typical SK-23 cells, using a flow-through method, as shown by confocal microscopy.	111
Figure 38.	Subcellular localisation of DMMB in typical SK-23 cells, using a flow-through method, as shown by confocal microscopy.	112
Figure 39.	Subcellular localisation of NMB in typical SK-23 cells, using a flow-through method, as shown by confocal microscopy.	113
Figure 40.	Effect of photosensitizers on oxygen utilisation in isolated rat mitochondria.	115
Figure 41.	Apoptosis induction <i>via</i> caspase activation for mitochondria-specific and plasma membrane bound photosensitizers.	125
Figure 42.	Light microscope images of SK-23 cells incubated with DMMB.	137
Figure 43.	Effect of concentration, ionic strength and pH on the fluorescence spectrum of JC-1.	138
Figure 44.	Fluorescent microscopy with JC-1 to detect apoptosis in cell cultures.	140
Figure 45.	J-aggregate formation in EMT-6 cells following various exposures to phenothiazinium photosensitizers.	141
Figure 46.	J-aggregate formation in SK-23 cells following various exposures to phenothiazinium photosensitizers.	142

Figure 47.	J-aggregate formation in SK-MEL-28 cells following various exposures to phenothiazinium photosensitizers.	143
Figure 48.	J-aggregate formation in EMT-6, SK-23 and SK-MEL-28 cells following one-hour incubation with phenothiazinium photosensitizers.	144
Figure 49.	Detection of apoptosis in cultures of EMT-6, SK-23 and SK-MEL-28 cells exposed to phenothiazinium photosensitizers using the FluorAce® Apopain Assay Kit.	146

ABBREVIATIONS

Ac-DEVD-CMK	chloromethyl ketone
ACR	acceptor control ratio
AIDS	acquired immune deficiency syndrome
5-ALA	5-aminolaevulinic acid
AlPc	aluminium phthalocyanine
AlPcS2	disulfonated aluminium phthalocyanine
ANT	adenine nucleotide translocase
ARMD	age-related macular degeneration
ATP	adenosine triphosphate
BAEE	1 μ molN-(α)-benzoyl-L-arginine ethyl ester
BCC	basal cell carcinoma
BPD-MA	benzoporphyrin derivative-monoacid ring A (Verteporfin®)
BSA	bovine serum albumin
CaCl₂	calcium chloride
cAMP	cyclic adenosine monophosphate
<i>C. elegans</i>	<i>Caenorhabditis elegans</i>
CHAPS	3-[(3-cholamidopropyl)dimethylammonio]-1-propane-sulfonate
CW	continuous wave
DHE	dihaematoporphyrin ether
DHFR	dihydrofolate reductase
DMMB	dimethyl methylene blue
DMSO	dimethyl sulfoxide
DNA	deoxyribonucleic acid
DPIBF	1,3-diphenylisobenzofuran
DTIC	decabazine
DTT	DL-dithiothreitol
EDTA	ethylenediaminetetraacetic acid
EtNBS	ethylamino-9-diethylaminobenzo[<i>a</i>]thiazinium chloride
FADH₂	reduced flavin nicotinamide dinucleotide

FDA	Food and Drug Administration (U.S.)
HBSS	Hanks' balanced salt solution
HEPES	N-[2-hydroxyethyl]piperazine-N'-[2-ethanesulfonic acid]
Hp	haematoporphyrin
HpD	haematoporphyrin derivative
IC₅₀	inhibitory concentration for a 50 % effect
IC₉₀	inhibitory concentration for a 90 % effect
ICE	interleukin-1-converting enzyme
IL-2	interleukin-2
IL-1β	interleukin-1 β
IPA	International Photodynamic Association
JC-1	5,5',6,6'-tetrachloro-1,1',3,3'- tetraethylbenzimidazolylcarbocyanine iodide
KCl	potassium chloride
K₂HPO₄	potassium phosphate
LDL	low density lipoprotein
LMB	leuco-methylene blue
LMM	lentigo malignant melanoma
MACE	mono-L-aspartylchlorin <i>e</i> ₆ (Npe ₆)
MB	methylene blue
MgCl₂	magnesium chloride
MMB	methyl methylene blue
8-MOP	8-methoxypsoralen (methoxsalen)
MPTP	mitochondrial permeability transition pore
m-THPC	<i>meta</i> -tetrahydroxyphenyl chlorin (Temoporfin, Foscan®)
MTT	3-[4,5-dimethylthiazol-2-yl]-2,5-diphenyl-2 <i>H</i> -tetrazolium bromide
NaCl	sodium chloride
NAD⁺	nicotinamide adenine dinucleotide
NADH	reduced nicotinamide adenine dinucleotide
NADPH	reduced nicotinamide adenine dinucleotide phosphate
Nc	naphthalocyanine
Nd:YAG	QS neodymium:yttrium-aluminium-garnet laser
NMB	new methylene blue <i>N</i>

$^1\text{O}_2$	singlet oxygen
PBGD	porphobilinogen deaminase
PBS	phosphate buffered saline
Pc	phthalocyanine
PCI-0123	lutetium texaphyrin (Lu-Tex)
PDT	photodynamic therapy
PGE₂	prostaglandin E ₂
PgP	p-glycoprotein
PKC	protein kinase C
PMSF	phenylmethylsulfonyl fluoride
PpIX	protoporphyrin IX
QS	Q-switched
SCC	squamous cell carcinoma
Smase	sphingomyelinase
SnET2	tin ethyl etiopurpurin, Purlytin®
SSM	superficial spreading melanoma
T₁	triplet lifetime
TNFα	tumour necrosis factor- α
TPPS4	tetraphenylporphine sulfonate
Z-DEVD-AFC	carbonyloxy-Asp-Glu-Val-Asp-7-amino-4-trifluoromethyl coumarin

CHAPTER ONE.
GENERAL INTRODUCTION.

1.1 Cancer

1.1.1 Cancer Aetiology and Epidemiology

Cancer is not a single disease, but is a generic term for over a hundred different types of tumour that have become invasive or malignant. In the developed world, most people will be touched by cancer at some point during their lifetime, as approximately one person in three develops the disease, and the disease will end the life of approximately one person in five [Rennie & Rusting, 1996].

Cancers are classified according to the tissue and cell types from which they derive and include carcinomas (from epithelial cells), melanomas (of the skin), sarcomas (from connective tissue or muscle cells), leukaemias and lymphomas (from haemopoietic and immune systems), gliomas (of the central nervous system) and retinoblastomas (of the eye). Almost any tissue can develop malignancies, indeed a single tissue may yield several types, each distinguishable by its own unique features [Ritchie, 1970]. In the west, the incidence of most cancers has risen in step with advances in industry and technology and is linked with overexposure to carcinogens such as tobacco smoke, high fat diets, ultraviolet light and toxic chemicals in the environment. It is also established that many different types of cancer, accounting for as many as fifteen per cent of the world's cancer deaths, are viral, bacterial or parasitic in origin [Trichopoulos *et al.*, 1996]. Worldwide there are more serious epidemiological problems than cancer, but the disease is of interest in a broader scientific context since it arises from disturbances in the fundamental life processes of the multicellular organism [Weinberg, 1996]. It is now known that virtually all cancers are derived from a single mutation in the DNA of a single cell. Indeed, cancers generally develop as a result of the progressive mutation by different carcinogens of three main sets of cellular genes [Soloman *et al.*, 1991]. These are the growth-promoting proto-oncogenes, the growth-inhibitory tumour-suppressor genes and a group of genes active in DNA repair, which together control the growth and differentiation of normal cells [Soloman *et al.*, 1991]. Once the ancestral cell (and its descendents) has accumulated a series of such mutations, it is able to escape all controlling signals and becomes capable of uncontrolled division and metastasis (migration to and colonization at distant sites of the body) [Ruoslahti, 1994].

1.1.2 Conventional Cancer Therapy

There are several families of chemotherapeutic drugs that induce cell death by disruption of various biochemical processes, including dysregulation of the cell cycle [Hellman & Vokes, 1996]. A typical target is topoisomerase II, the enzyme responsible for separating the DNA double helix into two strands in preparation for replication. Topoisomerase II temporarily cleaves one strand of DNA, passes the other strand through the break, before reattaching the two cut ends together. Topoisomerase inhibitors include CPT-11 and the single, most widely used, conventional chemotherapeutic agent, adriamycin, also known as doxorubicin [Hellman & Vokes, 1996]. Adriamycin is an anthracycline antibiotic that acts primarily on the plasma membrane of cells leading to disruption of signal transduction systems with, most notably, increased activation of protein kinase C (PKC) [Murphree *et al.*, 1981]. PKC causes malfunction of topoisomerase II, preventing the reattachment of the DNA strand breaks in dividing cells, thus causing these cells to die [Liu, 1989].

Other chemotherapeutic drugs include antimetabolic agents, alkylating agents and the plant alkaloids [Hellman & Vokes, 1996]. Antimetabolites are usually analogues of molecules involved in various biochemical pathways in the living cell. Methotrexate is a prime example of such a drug and is a chemical analogue of folic acid. It functions, in part, by binding to the enzyme dihydrofolate reductase (DHFR) which normally converts folic acid into adenine and guanine. This drug thus prevents cell division by incapacitating the cell's ability to synthesise new DNA. Other examples of chemotherapeutic agents that behave in this way are fluorouracil and gemcitabine [Hellman & Vokes, 1996]. Alkylating agents (cyclophosphamide and chlorambucil are examples) form chemical bonds with particular DNA nucleotides, causing defects in the normal double helical DNA molecule. The damage may involve breaks or inappropriate links between or within strands of DNA that will trigger cellular suicide if not corrected by DNA repair mechanisms. Finally, plant alkaloids (such as vinblastine, vinorelbine, paclitaxel and docetaxel) prevent cell division by binding to the protein, tubulin [Hellman & Vokes, 1996]. Tubulin is a component of microtubules, the network of fibres responsible for chromosomal separation during cell division. Drugs that interfere with the assembly or disassembly of these tubulin fibres also prevent successful cell division.

Despite the multitude of advances made in the field of modern medicine, the identification of a single, proven treatment regime for cancer continues to prove elusive. Since carcinomas arise from within the host's own cell population [Section 1.1.1], normal and malignant cells have few differences that can be targeted by selective, pharmacological, anticancer regimes. Consequently, the conventional treatments for cancer (surgery, radiotherapy and chemotherapy) often prove to be more disabling than the disease itself. Conventional chemotherapeutic drugs are widely used but, unfortunately, have only a limited degree of selectivity for neoplastic cells and are disadvantaged by their toxicity towards normal tissues. The side effects encountered as a result of this acutely increase patient morbidity. In addition, and without doubt the major obstacle to effective cancer treatment, is the resistance of tumour cells to a whole range of structurally unrelated compounds. This phenomenon of broad resistance is termed pleiotropism or multidrug resistance (MDR) [Kartner & Ling, 1989; Moscow & Cowan, 1988]. One of the major areas in cancer research is, therefore, the development of tumour-specific drugs. Advances in gene therapy and immunotherapy offer hope for the future but are still largely experimental and used only as adjuncts to conventional cancer treatments.

1.2 Photodynamic Therapy

1.2.1 Clinical Practice

Photodynamic therapy (PDT) is a largely experimental approach to the treatment of localised malignant and pre-malignant lesions [Gomer, 1989]. It has three major requirements: a photosensitizing drug (a dye), long (red) wavelength light and molecular oxygen. To date, the majority of clinical PDT has been carried out using only porphyrin-based compounds, commonly the sole registered PDT drug, Photofrin®. PDT induces cell death by the porphyrin-sensitized photo-oxidation of biological matter, which may be achieved either by endogenous or exogenous means [Henderson & Dougherty, 1992]. In either case, administration of treatment is a bimodal process. Endogenous photosensitization requires the topical application of an inactive prodrug and will be discussed later [Section 1.5.1]. Exogenous photosensitization is the more common method and usually involves first the intravenous injection of a light-absorbing, cytotoxic drug (the photosensitizer) that is, ideally, inert until illuminated.

This is then allowed time to accumulate in malignant tissue and it is important to delay the illumination step until a time when the ratio of drug level between malignant and adjacent normal tissues is at a maximum. The second step involves local activation of the photosensitizer with light of a high fluence and of an appropriate wavelength delivered usually from a laser [Section 1.2.4]. All photosensitizers exhibit a characteristic absorption spectrum and, generally speaking, each can be activated at wavelengths that fall within this particular range. However, because of its absorption by haemoglobin and other pigments such as melanin, there is only minimal penetration of short-wave visible light into blood-containing tissue, and deep penetration of light into tissue is a necessity for the treatment of larger and deeply lying (millimetre range) tumours. Haemoglobin has significant absorptions near 425, 544 and 577 nm, making it necessary to have illumination wavelengths > 600 nm. At wavelengths > 1200 nm, light absorption by water molecules becomes substantial. At wavelengths between 850 and 900 nm, the photons may not have sufficient energy to participate in a photochemical reaction [Section 1.3]. For these reasons, the light delivery range in the red and near infrared regions of the visible spectrum (600 to 800 nm) has been determined as the 'therapeutic window' for clinical treatment. Moreover, tissue penetration typically doubles at wavelengths between 630 and 750 nm allowing larger tumours to be treated [Henderson & Dougherty, 1992; Wilson, 1989].

Most research suggests that, subsequent to irradiation, highly reactive singlet molecular oxygen ($^1\text{O}_2$) is the most damaging cytotoxic molecule *in vivo*, though other reactive oxygen species may also be involved [Weishaupt *et al.*, 1976]. Since the photophysics of PDT dictate that it is both a light- and oxygen-catalyzed process, the level of tissue oxygenation must therefore be adequate to sustain $^1\text{O}_2$ formation. PDT is dependent on both drug concentration (mg drug per kg body weight) and light dose (J cm^{-2}), with any tissue being susceptible to photodamage if the sensitizer concentration and light dose are sufficiently high. Since photosensitizers may be degraded (bleached) by light, a weaker response occurs at low drug concentrations [Section 1.2.3]. In order to obtain a PDT response at lower cellular drug concentrations, the light exposure must be increased. When the correct photosensitizer dose is used, differential uptake by the tumour allows destruction of tumour and protection of normal tissue even at very high light doses, because the level of photosensitizer in normal tissue is below the photodynamic threshold for necrosis. There are similarities between fluence rate effects

in PDT and dose rate effects in radiotherapy, in that repair of sublethal damage can occur at very low dose rates and oxygen depletion may decrease the efficacy of both therapies at very high dose rates. A variety of neoplasms respond to PDT, but the treatment is only efficient in cases where the entire tumour can be reached by light, and one of the problems with PDT is access of light to the tumour. Thus, PDT is not suitable for tumours thicker than between five and seven millimetres, unless the light is applied interstitially through fibres [Moan & Berg, 1992].

1.2.2 Advantages of Photodynamic Therapy

One major advantage of PDT over conventional surgical or radiotherapeutic regimes is its dual selectivity. This selectivity is obtained first by the preferential retention of the photosensitizer in target tissue. Secondly, since most photosensitizers exhibit very low toxicities in the absence of light, PDT is associated with minimal systemic toxicity. Photodynamic activity is confined to the illuminated area, thus ensuring a local response and sparing normal tissue. Chemotherapeutic drugs, in contrast, are toxic to cancerous and healthy cells alike although they can save lives. Previous treatment of tumours with radiation therapy and/or chemotherapy does not appear to reduce the efficacy of PDT, nor does PDT preclude the subsequent application of either regime. Unlike radiation therapy, PDT treatment can be repeated as often as necessary without danger to surrounding healthy tissue, as long as the light is focused only on the tumour. Moreover, tumour PDT does not in itself appear to be carcinogenic [Gomer *et al.*, 1988]. PDT is further favoured by a low incidence of complications and demonstrates excellent healing of affected areas, with regeneration of normal tissue and minimal scarring [Bown, 1993]. Although originally envisaged as a primary treatment for superficial lesions (particularly of the skin), PDT has since also proven effective, in conjunction with conventional cancer therapies, as an adjunct treatment for larger, bulkier tumours [Dougherty *et al.*, 1998]. PDT has a role to play in both palliation and complete local tumour eradication. A further application for PDT is as a diagnostic tool in tumour identification because, with a suitable imaging system, there is scope to exploit the fluorescent properties of photosensitizers that localise preferentially in tumour tissue [Peng *et al.*, 1996].

1.2.3 Light Dosimetry

Successful PDT requires homogeneous irradiation of the tumour region and light detection systems for dosimetry. Light dosimetry is a limiting factor in the application of PDT, yet most studies have failed to provide adequate and correct information on the total light output employed. The optimal dose of light used to activate a photosensitizer in human cancers is therefore not yet known. Since the distribution of photosensitizer concentration in tissue is often not known, the light dose absorbed by the photosensitizer cannot be calculated [Beyer, 1996].

Light dose is expressed as the delivered quantity in joules per square centimetre (J cm^{-2}), but the Grothus-Draper Law states that light must be absorbed by tissue in order for a clinical effect to take place [Dilkes, 1994]. The energy absorbed is referred to as the energy fluence (also measured in J cm^{-2}) and depends on several factors. These include the spectrum of the light source, irradiation geometry, depth of light penetration, light scattering in tissue (problematic in the brain), internal light reflection by normal tissue, photosensitizer concentration in tissue and haemorrhage within the tumour, all of which make the absorbed dose difficult to calculate [Anderson & Parrish, 1981]. Photobleaching of the photosensitizer must also be taken into account. Porphyrin molecules are photochemically unstable and cannot be activated an indefinite number of times to produce the desired therapeutic effect. Photobleaching in clinical PDT consists of one or more of the following: the photoinduced movement of porphyrins from one cellular location to another, photoinduced chemical modification of porphyrins without loss of the porphyrin ring, or photoinduced destruction of the porphyrin ring itself. Photobleaching occurs concurrently with the PDT effect and can be exploited to protect normal tissue [Potter *et al.*, 1987] [Section 1.2.1].

For accurate control of tissue destruction, dosimetry is required in order to plan each of the three components of PDT. Most clinical and preclinical studies find that, assuming adequate oxygen supply, minimum levels of combined light and photosensitizer doses must be delivered to the target tissue for effective PDT [Beyer, 1996]. Developments in fibre optic technology over recent years have provided various types of optical fibres that can be used simultaneously for light delivery and light fluence measurement in tissue. Tissue optical measurements are generally achieved by introducing a light-emitting source into the target tissue and mapping spatial distribution of light fluence

rates [Beyer, 1996]. The most common types for interstitial PDT treatment and light dosimetry measurement are cylindrical and isotropic diffusers, designed to provide more evenly distributed light emission patterns for irradiation. Cylindrical diffusers and microlenses have been used as light applicators in the bronchial tree during the PDT treatment of early stage lung cancer and in the surgical resection of pleural malignancies [Murrer *et al.*, 1997]. In order to obtain a good estimation of the actual light dose to the tissue, cylindrical diffusers are harnessed to an isotropic detector and an expander in a Teflon sheet and transported through the working channel of a bronchoscope into the target area. The diffuser, detector and expander are then pushed out of the Teflon sheet into a central position with the detector at the surface. Both incident and reflected light can be measured by this system, giving a good estimation of the actual light dose to the tissue.

1.2.4 Light Sources in Photodynamic Therapy

Irradiation to activate the photosensitizer is delivered usually from a laser although a number of non-laser systems have been used in both clinical and experimental PDT [Patterson *et al.*, 1991]. The light source is selected taking into consideration the absorption spectrum of the photosensitizer and the tissue transmission.

Non-laser Systems

Early PDT was performed mainly with non-laser systems such as xenon arc lamps, light-emitting diode arrays, fluorescent tubes and slide projectors [van Hillegersberg, 1994]. Non-laser light sources emit fluences across a broad spectrum of wavelengths along with the light required to activate the photosensitizer. Consequently, they are often fitted with filters to eliminate irrelevant wavelengths and infrared components. Infrared radiation should be filtered out to avoid significant heating of tissue, although some investigators find that mild hyperthermia (40°C to 42°C) acts additively or synergistically with PDT [Waldow & Dougherty, 1984]. Hyperthermia can be avoided by using a fluence rate lower than 150 mW/cm².

Laser Systems

The term 'laser' is an acronym for 'light amplification by the stimulated emission of radiation'. Lasers are classified according to the type of beam they emit [Rosenbach & Alster, 1996]. CW (continuous wave) lasers emit a constant beam of light for as long as

the operator depresses the foot pedal. Examples of CW lasers are the argon and CO₂ lasers. Pulsed lasers, on the other hand, emit high-energy light in short bursts in order to achieve selective photothermolysis. Examples of pulsed lasers are the Q-switched (QS) ruby, QS neodymium:yttrium-aluminium-garnet (Nd:YAG) and QS alexandrite lasers. Q switching is a technique that employs rotating mirrors and other devices to produce sudden bursts of stored high-energy light. Energy fluence is generally applied to lasers that emit short pulses of light, and irradiance used to describe output from CW lasers. It has been reported that pulsed light may have deeper penetration into tissue than CW light although some investigators find no difference at all [Cowed *et al.*, 1984].

A laser beam of light has certain unique characteristics that distinguish it from 'ordinary' light. It is monochromatic (has one narrow band of wavelengths), coherent (all the waves are in phase, in both time and space) and collimated (parallel, with very little divergence). It is also of high intensity in order to maximise its transmission through tissue. The parallel characteristics of a laser permit light to be focused to a fine point onto the end of a thin quartz fibre for interstitial insertion through endoscopes. For PDT, the monochromaticity of the laser beam permits selection of a single wavelength corresponding to the absorption maximum specific to the photosensitizer being used [Rosenbach & Alster, 1996]. This is in contrast to most natural and man-made light sources that produce light composed of many different wavelengths. PDT progressed with the development of tuneable dye lasers that can be set (tuned) to emit the appropriate wavelength of light [van Hillegersberg, 1994]. Unfortunately, current technology does not yet provide a single laser capable of transmitting all useful wavelengths at the energies needed for clinical efficacy.

The use of lasers in oncology began with high-power lasers acting as optical scalpels by thermal and ablative effects [Aronoff, 1997]. In contrast, PDT is carried out with low-power lasers since the fundamental purpose of lasers here is to serve as light sources for driving photochemical reactions in tissue. However, a laser offers significant advantages whenever fibre-optics are needed to reach a tumour and addresses the limitations of alternative systems of non-uniform light delivery, lack of precision and control, and poor intensity (typically about 50 mW cm⁻²) [Wilson & Patterson, 1986]. For porphyrin-sensitized tissue the helium-neon laser with a wavelength of 632.8 nm

was used first and proved to be a simple and reliable system despite its low power output. Nevertheless, it has since been superseded by a tuneable argon-dye laser, which delivers light of any wavelength between 350 and 700 nm. The energy for this is provided by a 5 to 25W continuous wave argon laser at 514.5/488 nm that optically pumps the dye laser containing a dye fluid fluorescent in the 630 nm region, such as rhodamine B or Kiton-red. This allows effective power levels of up to 3 or 4 W to be obtained, eighty to ninety per cent of which can be coupled into optical fibres of 200 to 600 μm core diameter. Unfortunately, the argon-dye laser is expensive and difficult to handle. It has been replaced by the gold vapour laser that is a cheaper and simpler model but which will only operate at a single fixed wavelength of 628 nm, making it unsuitable for a significant number of photosensitizers. It is expected that eventually more compact and less expensive semiconductor light-emitting diode dye lasers may be the light source of choice for clinical PDT [van Hillegersberg, 1994].

1.3 The Photochemical Reaction

1.3.1 Photosensitization

Light and oxygen are essential for life on earth, yet a combination of the two can be toxic. Alongside vital light-dependent processes occur simultaneous phototoxic reactions as a result of oxygen free radical formation [Spikes & Straight, 1967]. Molecular oxygen is a diradical that, in the absence of light, participates mainly in radical chain reactions. The peroxidic products formed as a result are potentially toxic to cells but these oxidation reactions in nature tend to have limited cytotoxicity, due to the protective effects of natural antioxidants such as tocopherol (vitamin E). The presence of light, however, creates many more reactive oxygen species, such as singlet oxygen and the superoxide anion radical, from which hydrogen peroxide and hydroxyl radicals can be derived [Singh, 1978]. Here again, natural cell components, such as the carotenoid pigments and the enzyme superoxide dismutase, offer protection from photocytotoxicity by respectively quenching singlet oxygen and converting the superoxide ion into hydrogen peroxide and water [Schaap, 1974].

Photosensitization is a widely occurring phenomenon in biological systems due to the ubiquitous nature of both visible light and a number of photosensitising pigments and

related compounds [Kamat, 1996]. Environmental chemicals and certain natural pigments contained in cells that are able to absorb light, can expose or “sensitize” organisms to photochemical damage by oxygen. A photosensitized reaction occurring in the presence of oxygen is referred to as a ‘photodynamic reaction’. Photocytotoxicity occurs as a consequence of oxygen free radical damage to certain cellular components. The main events are enzyme deactivation (from the destruction of specific amino acids) [Matheson *et al.*, 1975], nucleic acid oxidation (primarily of guanine residues) [Wang & Midden, 1983] and membrane damage (from the oxidation of unsaturated fatty acids and cholesterol) [Girotti, 1990].

Natural photosensitizers, such as the psoralens or hypericins found in plants, can induce photocytotoxicity if ingested or when deposited on the hands. Domestic cattle, for example, are liable to suffer hypericism from eating St John’s Wort (*Hypericum perforatum*) because the pigment hypericin then becomes transported in the bloodstream to the epidermal capillaries where it may subsequently be activated by sunlight [Wainwright, 1996]. Mammalian cells, however, generally contain few chromophores that absorb light in the visible range of the solar spectrum and which are thereby able to act as photosensitizers. Porphyrins, for instance, usually encountered in iron complexes such as haemoglobin, myoglobin and cytochrome, are essential for life and are active in all viable human cells. Nevertheless, photodynamic effects may result when exogenous photosensitizers are added to cells or in pathological conditions when endogenous photosensitizers are present at abnormally high levels. Unfortunately, in these circumstances, antioxidant and detoxifying defences and DNA repair systems may be insufficient to counter the effects of oxidative stress.

In humans, examples of photosensitization reactions are photosensitive porphyrias, drug-induced photosensitivity, and photoallergy. Related mechanisms may be responsible for the ageing of sun-exposed skin, cataract induction and some types of mutagenesis. In mammalian cells, endogenous photosensitization reactions commonly involve tetrapyrrolic derivatives. Porphyrias, for example, arise from enzymatic dysfunction in the haem biosynthetic and metabolic pathways. This leads to an accumulation of blood porphyrins in the skin and to a phototoxic response on exposure to UV or visible light.

1.3.2 Light Absorption

With the exception of oxygen, which exists as a ground state triplet molecule, all biological molecules in their unexcited ground state configurations are in the singlet state. On absorption of a photon of light, aromatic molecules are brought to their singlet excited states. These are extremely short-lived (less than one microsecond) and, from here, the photosensitizer may decay back to its original ground state and, for example, emit light in the form of fluorescence [Foote, 1990]. All excited singlet states have a corresponding lower energy triplet state. For the dynamic effect, the photosensitizer must undergo intersystem crossing to the excited triplet state of the molecule [Figure 1]. This triplet species is more stable, with a longer lifetime (millisecond range), which increases the probability of its interacting with ground state triplet oxygen [Takemura *et al.*, 1989].

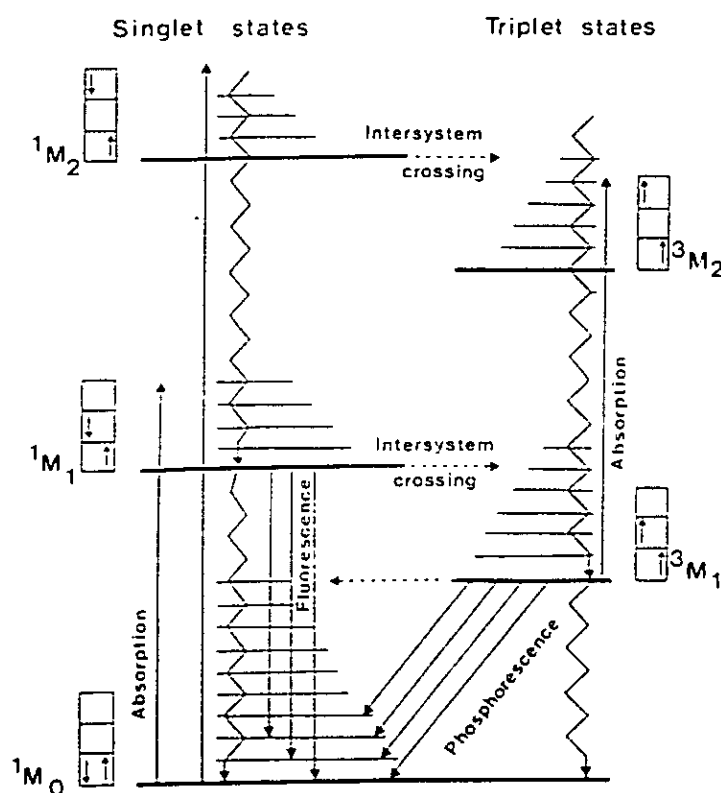


Figure 1. Jablonski Diagram showing possible transitions of aromatic molecules following light excitation [Taken from Kohen *et al.*, 1995]

In the presence of oxygen, two basic reactions can occur [Foote, 1991] [Figure 2]. The excited photosensitizer may undergo either a Type I photochemical reaction wherein it interacts directly with biomolecules by electron or hydrogen transfer, yielding radicals or radical ions. These in turn react with molecular oxygen to produce active species such as hydroxyl radicals, hydrogen peroxide and superoxide ion. Alternatively, and more commonly, the triplet photosensitizer undergoes a Type II mechanism and interacts with molecular oxygen, generating highly reactive singlet oxygen (half-life: 10^{-6} seconds [Truscott *et al.*, 1980]) by energy transfer. Occasionally, electron transfer from sensitizer to oxygen can occur generating oxidised sensitizer and superoxide ion [Athar *et al.*, 1989].

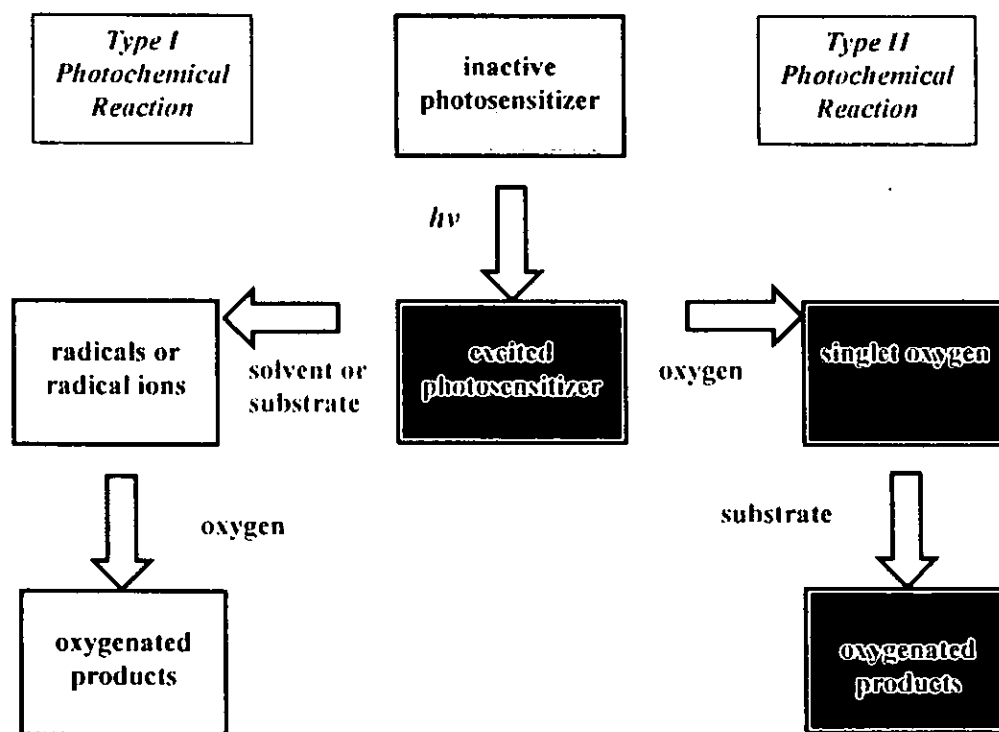


Figure 2. Chemical Mechanisms of Photosensitization [Adapted from Foote, 1990].

1.3.3 Cellular Effects

Singlet oxygen [1O_2] is highly electrophilic and reacts selectively with electron rich moieties, causing oxidative damage to essential cellular components. It has a lifetime of about 4 μ s in water and 50 to 100 μ s in lipid. In the cellular environment, this is reduced

to 0.6 μs , corresponding to a diffusion distance of about 0.1 μm due to quenching by cell constituents such as histidine, tryptophan, cholesterol or water [Moan *et al.*, 1990]. $^1\text{O}_2$ therefore reacts close to its site of origin but it may penetrate biological membranes [Thomas *et al.*, 1989; Girotti, 1990]. In fact, most observations have indicated that the cell membrane plays a critical role in porphyrin-sensitized photocytotoxicity. Certainly, $^1\text{O}_2$ generated from photosensitizers in the interstitial fluid is inefficient in inactivating cells compared to that generated by hydrophobic or cell-bound photosensitizers [Dougherty *et al.*, 1998].

Hydrophobic, anionic photosensitizers (such as porphyrins) attach to plasma membranes and to membranes of cellular organelles (mitochondria, lysosomes, endoplasmic reticulum and, to a lesser extent, the nuclear envelope). On illumination, they exert damage either by direct photoperoxidation of membrane phospholipids and cholesterol [Thomas & Girotti, 1989] or by inactivation of membrane-bound transport and receptor systems [Moan *et al.*, 1989]. PDT damage to the plasma membrane is detectable within minutes following light exposure and is indicated by oedema and bleb formation [Moan *et al.*, 1979], increased membrane permeability, leakage of enzymes (notably lactate dehydrogenase), cross-linking of amino acids [Reyftman *et al.*, 1986] and membrane depolarisation [Specht & Rodgers, 1990]. For porphyrin-based PDT, the inhibition of mitochondrial enzymes is considered to be a further key event [Salet & Moreno, 1989] with cytochrome *c* oxidase and succinate dehydrogenase serving as major early targets in cytotoxicity [Gibson *et al.*, 1989]. Depending on the type of photosensitizer, its concentration and distribution, these events will have far-reaching consequences. Photosensitizers that localise in mitochondria are likely to induce apoptosis and, indeed, this form of cell death following PDT has been described [Agarwal *et al.*, 1991]. However, unlike ionizing radiation that primarily affects the nucleus (causing double strand breaks in DNA), there is very little evidence for the nuclear uptake of hydrophobic photosensitizers [Moan, 1986]. The radius of a mammalian cell nucleus is approximately 5 μm so it is unlikely that photosensitizers located in the cytosol or plasma membrane could inflict major nuclear damage *via* a singlet oxygen mechanism. Nevertheless, there have been some unexplained reports of sister chromatid exchanges [Moan *et al.*, 1980] and chromosomal aberrations [Evenson *et al.*, 1982] being induced following porphyrin photosensitization.

For cationic and non-porphyrin photosensitizers, the order of cellular events may differ but is likely to reflect the pattern of their cellular distribution. Photosensitizers that are present in the cytosol can sensitize tubulin to photodamage causing an accumulation of mitotic cells and, in some cases, cell death [Berg & Moan, 1997]. Aggregated or hydrophilic photosensitizers are likely to be taken up by pinocytosis and/or endocytosis and to become localised in lysosomes or endosomes. These are permeabilized on exposure to light with the release of vast amounts of hydrolytic enzymes and culminating in necrotic cell death [Zdolsek, *et al.*, 1990]. Nevertheless, whatever the primary lethal insult, there follows a rapid loss of cell integrity that, for porphyrin-based PDT, is complete within four hours post-treatment [Bellnier & Dougherty, 1982].

1.3.4 Vascular Effects

Vascular damage is induced almost immediately upon light exposure and, with the exception of cationic compounds, is the most obvious acute effect of porphyrin-based PDT *in vivo* [Reed *et al.*, 1988; Nelson *et al.*, 1988]. The evidence for this has come from *in vitro* colony forming assays [Henderson *et al.*, 1985], sandwich observation chambers [Star *et al.*, 1986], measurements of blood flow [Selman *et al.*, 1986] and oxygen tension measurements within tissues [Hetzl & Farmer, 1984]. Porphyrin photosensitizers accumulate predominantly in the perivascular stroma [Peng *et al.*, 1991] with the endothelial cells of the vessel wall and red blood cells serving as major targets [Ben-Hur & Orenstein, 1991]. Endothelial cells accumulate high concentrations of porphyrin photosensitizers and have been found to be more sensitive than carcinoma cells to porphyrin-based PDT, supporting a vascular role in PDT-mediated toxicity [West *et al.*, 1990]. Monitoring of tissue oxygenation in transplanted tumours in rabbits has shown that tumour ischaemia is brought about in a three-phase process [Tromberg *et al.*, 1990]. First, molecular oxygen is expended during the photodynamic process for the generation of $^1\text{O}_2$. Then, endothelial cell damage triggers the first vascular events including platelet aggregation, transient vasoconstriction and vasodilation, vessel blanching, stasis and haemorrhage. These pathophysiological alterations in the microcirculation restrict the blood supply, reducing oxygen delivery to the tumour region. Total vascular collapse occurs ultimately therefore as a result of acute oxygen starvation (hypoxia) and nutritional deprivation [Reed *et al.*, 1989]. The first visible signs of photosensitization are oedema and erythema, prior to any detectable endothelial

or tumour damage. These are apparent usually within twenty-four hours of PDT, with maximum necrosis developing after a few days [Henderson & Dougherty, 1992].

1.3.5 Immunologic Effects

In addition to direct cell killing, a strong inflammatory reaction triggered by membrane damage is also an important post-PDT event that mediates further tumour destruction. Moreover, the immunologic effects generated are now no longer considered to be limited to the ischaemic effects caused by occlusion of the tumour vasculature. Rather, the antitumour activity of inflammatory cells and the existence of a tumour-sensitized immune reaction have now been demonstrated [Dougherty *et al.*, 1998]. At the membrane level, the liberation of membrane lipids activates membrane-bound phospholipases (A₁, A₂ and C) with concomitant acceleration of phospholipid degradation. This is accompanied by a massive local release of lipid fragments and arachidonic acid metabolites including cytokines such as prostaglandin E₂ (PGE₂), [Henderson & Donovan, 1989] and the immunomodulators, interleukin-2 (IL-2), interleukin-1 β (IL-1 β) and tumour necrosis factor- α (TNF- α) [Neyso & Dougherty, 1986]. Disruption of signal transduction pathways, also at the membrane level, triggers enhanced expression of stress proteins and early response genes [Luna *et al.*, 1994] and genes regulating apoptotic cell death [Oleinick *et al.*, 1993]. Consistent with a local response, tissues exposed to PDT ultimately become infiltrated by a wide range of fast-acting and potent mediators. They include lymphocytes, plasma cells, vasoactive peptides, complement and acute phase proteins, proteinases, peroxidases, radicals, leukocyte chemoattractants and cytokines. These act on capillaries to increase permeability, permitting leakage of fluids and causing perivascular oedema [Fingar *et al.*, 1992]. The inflammatory cascades themselves stimulate the recruitment of non-specific immune effector cells such as mast cells, monocytes/macrophages and neutrophils to the treated site.

The PDT drug, Photofrin® [Section 1.4.4], is found to concentrate not only in the vascular stroma but also in mast cells and macrophages within it [Korbelik *et al.*, 1991]. Neutrophils are particularly prolific and contribute to endothelial damage and destruction of the tumour parenchyma by their release of lysosomal enzymes and toxic oxygen radicals. Histamine release by mast cells has been observed *in vivo* [He *et al.*,

1989] and has been demonstrated in human and murine mast cells *in vitro* [Glover *et al.*, 1990] following porphyrin photosensitization. Histamine induces endothelial cells and other blood components to release large amounts of thromboxane and von Willebrand factor both of which mediate platelet adhesion to the subendothelium and may thus contribute to platelet thrombus formation that occurs after *in vivo* PDT. Neoplastic loci tend to be rich in macrophages, these accounting for between twenty and forty per cent of the total cell population in the majority of spontaneous, chemical-induced and transplantable tumours. Macrophages release TNF- α and are able to ingest invading agents as well as debris in necrotic regions. They have been shown to target PDT-treated tumour cells preferentially, with their tumouricidal action being potentiated both *in vitro* and *in vivo* [Korbelik & Krosi, 1994]. However, this is not likely to be an immediate post-PDT response since maximum levels of TNF- α are only noted three to six hours after light exposure. Long term prophylaxis of tumour recurrence in PDT may be the result of macrophage and lymphocyte stimulation. Studies show that cytokines such as IL-1 and TNF may be detected in the urine as long as four months after PDT even though the patient is asymptomatic [Korbelik & Krosi, 1994].

1.4 Development of Photodynamic Therapy

1.4.1 Early History

For centuries, man has been fascinated by the therapeutic properties of light. Heliotherapy (healing by the sun), first introduced in Ancient Greece by the renowned physician, Herodotus, was also practised by early civilisations from Egypt, China and India to treat diseases such as vitiligo, rickets, skin cancer and even psychosis [Epstein, 1990]. Modern phototherapy (the use of artificial light to treat disease) came into existence at the end of the nineteenth century. Its founder, the Dane, Niels Finsen, was awarded the Nobel Prize in 1903 for his pioneering work in the treatment of smallpox scarring and lupus vulgaris, in the wake of which came the phototherapy of rickets, certain dermatological lesions, neonatal hyperbilirubinaemia and, most recently, cancer [Bonnett, 1999]. The principle of dye-mediated photosensitization also has its roots in antiquity. Early recordings from India (1400 BC) and Egypt (12 AD), document the therapeutic application of psoralens containing preparations for the repigmentation of vitiliginous skin and leucoderma [Daniell & Hill, 1991].

The modern age of photodynamic therapy can be traced to the year 1900 when a young German student named Oskar Raab inadvertently discovered that the *in vitro* toxicity of acridine (a coal tar derivative), incubated with the malarial protozoan, *paramecium*, was significantly increased upon exposure to light. Although Raab himself failed to provide a complete explanation for his findings, he did propose a future therapeutic application for such material in dermatology [Raab, 1900]. In 1903, Raab's supervisor, Herman Von Tappeiner and the dermatologist, Jesionek, were first to apply the technique in oncology. They successfully treated skin conditions such as herpes, psoriasis and basal cell carcinoma, initially with eosin and then with a variety of photosensitizers, and employed either sunlight or an arc lamp as illumination [von Tappeiner & Jesionek, 1903]. Von Tappeiner, now regarded as probably the most important early pioneer of photodynamic therapy, continued to conduct experiments into the photodynamic effect and provided evidence for the essential role of oxygen in the process [von Tappeiner & Jodlbauer, 1904; 1907]. There followed a flurry of research activity using mammalian systems to study the mechanisms of photosensitization and it was noted that some dyestuffs could stain tumour tissue preferentially. However, no substantial work was done to follow up von Tappeiner's findings and it was to be over sixty years before the regime was again used to treat malignant disease.

The history of porphyrins and their role in medicine is, by contrast, very brief and linked to the search for fluorescence as a tumour localiser. In 1924, it was observed that certain tumours emitted a red-orange fluorescence when stimulated by ultra-violet light [Policard, 1924]. This was attributed to the presence of endogenous porphyrins and was later confirmed in tumour-bearing animals injected with haematoporphyrin [Auler & Banzer, 1942; Figge *et al.*, 1948]. Subsequently, the more purified haematoporphyrin derivative (HpD), synthesised by Schwartz in 1955, was used for the fluorescent detection of tumours in humans, opening the way for the use of PDT in patients with cancer [Lipson *et al.*, 1961].

1.4.2 First Generation Photosensitizers: the Porphyrins.

Porphyrins are cyclic compounds composed of a four-pyrrole ring linked through methylene bridges to form a planar macrocycle structure (a porphine). Porphyrins characteristically form complexes with metal ions that are able to bind to the nitrogen atom of the pyrrole rings. The electronic properties of the co-ordinated metal ion can, however, shorten the triplet lifetime of the porphyrin, thus reducing its photosensitising capabilities. Removal of the co-ordinately bound metal atom produces the free base porphyrin and a concomitant increase in photosensitising activity [Maillard *et al.*, 1980]. It is this free base porphyrin that is used in PDT.

The first photosensitizer tested in the clinic was a complex mixture of porphyrins, prepared originally by Schwartz in 1955, and known as haematoporphyrin derivative (HpD) [Schwartz, 1955] [Figure 3].

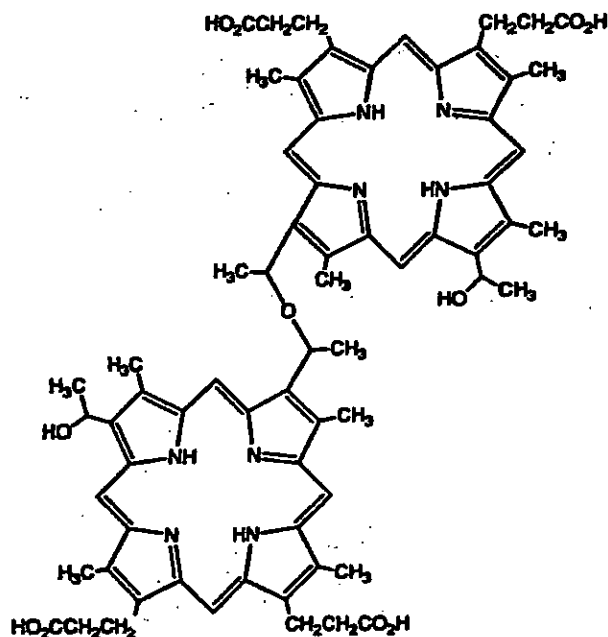


Figure 3. Chemical structure of haematoporphyrin derivative (HpD).

HpD is prepared by treating haematoporphyrin (Hp) with acetic acid, with the addition of a trace of sulphuric acid as a catalyst, then solubilization of the product in a dilute

base [Gomer & Dougherty, 1979]. The product contains several species including porphyrin monomers and oligomers, only some of which are clinically useful as photosensitizers. HpD was subsequently partially purified by gel filtration to obtain the enriched fraction of the active material. This is porfimer sodium or Photofrin II (Photofrin®, QLT Inc., Vancouver, Canada and Lederle Laboratories, Pearl River, NY, USA). Photofrin® is a red-coloured, lyophilized water-soluble mixture, almost always administered by the intravenous route. It is, despite purification, an aggregated mixture of monomers, dimers and oligomer porphyrin molecules and their dehydration products, linked by both ether and ester bonds [Dougherty, 1987]. It was originally believed that dihaematoporphyrin ether (DHE) was the active component of porfimer sodium, but it is now known that the important photosensitizers within this drug are the oligomers of haematoporphyrin consisting of two to eight subunits linked *via* ether bonds. Compounds similar to Photofrin® (Photosan, Photoheme, Photocarcinomin) have also been used in PDT [Wohrle *et al.*, 1998].

1.4.3 Modern History

The current era of clinical PDT dates therefore from the 1960s when Lipson and co-workers reported the first use of HpD for the PDT of metastatic breast cancer. Despite a positive response, Lipson did not pursue treatment beyond one patient [Lipson & Baldes, 1966]. Nevertheless, the resurgence of interest around this time marked the beginning of the current, expansive era of PDT, and owes much to the advent of laser technology and the development of fibre-optic delivery systems [Section 1.2.4]. This instigated experiments using HpD and laser light from several groups of workers, most notably Dougherty and co-workers, who came to initiate the first systematic human trials of PDT at the Rosewell Park Cancer Institute in Buffalo, U.S.A. Of a series of twenty-five patients, complete or partial response was found in one hundred and eleven out of one hundred and thirteen cutaneous or subcutaneous malignant lesions [Dougherty *et al.*, 1978]. From that time on, PDT has been the subject of many preclinical studies investigating its application as a treatment modality for a whole range of human cancers and with a multitude of papers published on the subject. See 'Table 1' for a summary of the main historical events that led to the establishment of current clinical PDT.

1841-1871	Haematoporphyrin (from the Greek 'porphuros' meaning 'purple') first synthesised by Scherer (Germany) as 'cruentin', a precipitate of sulphuric acid and dried blood, washed free of iron. Later described as 'iron-free haematin' by Mulder, then finally renamed 'haematoporphyrin' by Hoppe-Seyler in 1871. Spectrum, fluorescence and chemical properties defined by Thudichum in 1867 [Daniell & Hill, 1991].
1900	First photodynamic experiments performed by student, Oscar Raab under the supervision of Herman von Tappeiner (Germany) [Raab, 1900; von Tappeiner, 1900].
1900	First recorded incidence of photosensitization in humans. Neurologist, Prime (France), orally administered eosin for epilepsy and noted dermatitis in areas of the body exposed to light [Prime, 1990].
1903	Von Tappeiner and Jesionek (Germany) clinically exploited the photosensitized reaction, successfully treating herpes, psoriasis and skin carcinoma by topical application of eosin activated subsequently either by sunlight or arc lamp [von Tappeiner & Jesionek, 1903].
1905	Von Tappeiner and Jodlbauer (Germany) reported the oxygen-dependency of the photosensitized reaction and coined the term 'photodynamic action' [von Tappeiner & Jodlbauer, 1905; 1907].
1908-1911	Hausman (Austria) was first to study the biological properties of haematoporphyrin, showing that the destruction of <i>paramecium</i> and red blood cells by haematoporphyrin was accompanied by acute photosensitization in white mice and guinea pigs [Daniell & Hill, 1991].
1913+	Meyer-Betz (Germany) was first author to demonstrate photosensitization in humans when he self-administered 200 mg haematoporphyrin and exposed areas of his skin to light. The accompanying oedema and erythema persisted for over 2 months. Meyer-Betz and chemist, Fischer, continued to study porphyrin chemistry in tumour-bearing animals, Max Lemberg, later wrote the first book in English on porphyrins [Meyer-Betz, 1913; Fischer <i>et al.</i> , 1925].
1924	Policard (France) attributed spontaneous red fluorescence, induced by UV light in experimental tumours, to naturally occurring porphyrins in human tumours [Policard, 1924].
1942+	Auler and Banzer (Germany) were first to observe the photodynamic action of haematoporphyrin, confirming its selectivity for tumour tissue. They demonstrated haematoporphyrin-sensitized tumour necrosis in tumour-bearing animals but further experiments in humans were abandoned with the advent of the Second World War [Auler & Banzer, 1942].
1948	Figge and co-workers (U.S.A) demonstrated selective retention of haematoporphyrin <i>in vivo</i> in mice and recognised its potential as a diagnostic tool for cancer [Figge <i>et al.</i> , 1948].
1955	Rasmussen-Taxdal noted fluorescence of haematoporphyrin in a range of human tumours <i>in vivo</i> [Rasmussen-Taxdal <i>et al.</i> , 1955].
1955	Schwartz synthesized haematoporphyrin derivative (HpD) and demonstrated its enhanced localizing properties in experimental tumours [Schwartz <i>et al.</i> , 1955].
1961	Lipson and co-workers reported endoscopic fluorescence in 15 patients with endobronchial tumours using HpD as the photosensitizer [Lipson <i>et al.</i> , 1961].
1966	Lipson & Baldes were first to carry out PDT with HpD in humans. They treated a single chest wall recurrence of breast carcinoma that responded but was not cured. PDT in humans was abandoned for the second time [Lipson & Baldes, 1966].
1972-1974	Diamond <i>et al.</i> and Dougherty <i>et al.</i> demonstrated the long-term therapeutic effects of HpD on a variety of tumours in rats and mice [Diamond <i>et al.</i> , 1972; Dougherty <i>et al.</i> , 1974].
1975	Kelly & Snell (England) reported HpD uptake in malignant and pre-malignant bladder lesions and reported promising results of a single clinical treatment of bladder cancer with HpD using light from a mercury lamp [Kelly <i>et al.</i> , 1975].
1976	Singlet oxygen identified as the main cytotoxic agent [Weishaupt <i>et al.</i> , 1976].
1978	The first systematic human trials of PDT for skin tumours, using HpD and light from a xenon arc lamp, initiated at Roswell Park Cancer Institute in Buffalo, U.S.A. [Dougherty <i>et al.</i> , 1978].
1980	The first PDT treatment using HpD and 630 nm light from a tunable argon dye laser with a fibre optic delivery system [Dougherty <i>et al.</i> , 1980].

Table 1. Significant historical events leading to the development of photodynamic therapy

1.4.4 Photofrin®

The photosensitizer of choice over almost three decades and the only one currently registered for clinical use is the porphyrin-based porphyrin sodium or Photofrin II (Photofrin®). Photofrin® is an anionic, hydrophobic molecule and a purified form of its forerunner, haematoporphyrin derivative (HpD), manufactured by Quadra Logic Technologies Inc., Vancouver, Canada. In practice, intravenous injection of Photofrin® (1 to 5 mg kg⁻¹) is followed twenty-four to seventy-two hours later by local irradiation with long wavelength (red) light directed through single quartz fibres with a variety of speciality attachments [Henderson & Dougherty, 1992]. Photofrin® exhibits an intense characteristic porphyrin absorption peak in the blue region of the visible spectrum around 400 nm (termed the Soret band) and four additional absorption bands (of decreasing intensity) between 500 nm and 630 nm. The drug is illuminated at its weakest absorption band at about 630 nm [Gomer *et al.*, 1984] because light of this (red) wavelength has superior tissue penetrating properties [Section 1.2.1] [Wilson *et al.*, 1985]. Standard light dosimetry is 100 to 200 J cm⁻² [Schuitmaker *et al.*, 1996] although this and the method of light delivery may be varied according to the site and size of the tumour [Marijnissen & Star, 1987]. Photofrin® distributes well to all regions of the body, but is then cleared over the first twenty-four to seventy-two hours following infusion, from all tissues except the liver, spleen, kidneys, skin and malignant tumours [Gomer & Dougherty, 1979]. In mice, [¹⁴C] Photofrin® is cleared from the blood with kinetics fitting a triexponential equation with elimination half-lives of four hours, nine days and thirty-six days. Approximately one per cent of the total injected material remains in the circulation at twenty-four hours post-injection, with some material (approximately 0.01 per cent) still detectable at seventy-five days. Over sixty-five per cent of the drug is excreted in the faeces over an eight-day period [Bellnier *et al.*, 1989c].

Photofrin® demonstrates differential uptake and/or retention in malignant tissue such that after two to three days following administration there is a high concentration of the drug in the tumour relative to the surrounding normal tissue [Bugelski *et al.*, 1981]. The mechanisms by which porphyrins are taken up and retained, are not fully understood but are probably a combination of several factors. Once within the circulation, Photofrin® attaches to porphyrin-binding proteins in the blood, mainly

serum albumin and hemopexin that bind non-specifically to stromal elements and are found to accumulate in abnormal tissue such as tumours [Moan *et al.*, 1985]. A small amount (less than ten per cent) is also bound to erythrocytes. However, the most substantial proportion of the drug is bound to lipoproteins (and almost completely partitioned in the lipid moiety), although the concentration of these in the blood is less than five per cent that of albumin. Porphyrin-lipoprotein interaction is dependent upon the likelihood that low-density lipoprotein (LDL) receptor-mediated endocytosis activity is elevated in malignant cells [Korbelik, 1992]. Normal cells acquire cholesterol for membrane synthesis through the adsorptive endocytosis of plasma LDL. Since rapidly proliferating cancer cells require large amounts of cholesterol for the synthesis of new membranes, they also have higher LDL requirements and higher LDL receptor activities than normal cell types [Goldstein & Brown, 1977]. In fact, the distribution pattern of porphyrins is correlated with the relative number of LDL receptors in different normal tissues [Kessel, 1986]. However, the significance of the 'receptor hypothesis' in tumour selectivity is open to debate, since other porphyrin-based photosensitizers (such as *meso*-tetraphenylporphyrin tetrasulphonate and aluminium phthalocyanine tetrasulphonate [Section 1.5.1]) are excellent tumour localisers yet they do not bind to LDL. On the other hand, haematoporphyrin has a high affinity for LDL but, nevertheless, is a poor tumour localiser [Korbelik, 1992].

An alternative theory for preferential distribution of porphyrins may involve the abnormal structure of tumour stroma with its vast interstitial space, leaky vasculature, compromised lymphatic drainage and large content of collagen, elastin and lipid [Gullino, 1966]. Hydrophobic molecules such as Photofrin® are lipid-soluble [Freitas, 1990] and it has been observed that the affinity of such photosensitizers for neoplastic tissues increases upon increasing their degree of hydrophobicity [Berg *et al.*, 1995]. Porphyrins also bind to elastin, collagen and fibrin [Musser *et al.*, 1980], and newly synthesised collagen in tumours has a higher affinity for porphyrins than the acid-insoluble collagen in mature tissue [Musser *et al.*, 1982]. Consequently, the interstitial compartment of tumours, that comprises mainly a large collagen and elastic fibre network, may act as a 'reservoir' or 'sink' for circulating porphyrins. Furthermore, the interstitial fluid (which bathes cells and which is found between their plasma membranes and the vascular walls) has a pH value that is lower and a lactic acid

concentration that is higher in tumours (due to increased glycolytic activity) than in most normal tissues. (The intracellular pH, on the other hand, is identical or slightly higher in tumours than in normal tissue [Gerweck & Seetharaman, 1996]) A lowered pH results in neutralization of the negative charge of porphyrins, thereby increasing their hydrophobicity and favouring cellular uptake [Bohmer & Morstyn, 1985]. The fact that the pH of tumour tissue is lower than the blood supply that feeds it [Gullino *et al.*, 1965] may, at least in part, explain the selective retention of porphyrins in tumour tissue. Finally, there is a general recruitment of macrophages and inflammatory cells into tumour tissue and it has been shown that large amounts of Photofrin® are taken up by these cells in tumour-bearing animals [Korbelik *et al.*, 1991].

1.4.5 Current Status of Photodynamic Therapy

Since the first clinical experiments in the 1970s, several thousands of patients worldwide, both with early stage and advanced stage solid tumours, have been treated using PDT with Photofrin®. During that time, PDT has developed into a fully-fledged biomedical discipline with its own association, the International Photodynamic Association (IPA), and regular conferences devoted solely to this subject. Clinically, the regime has been used mainly for bladder cancer, lung cancer and in malignant disease of the skin and upper aerodigestive tract. The first health agency approval for PDT with Photofrin® was obtained in 1993 in Canada for the prophylactic treatment of recurrent papillary bladder cancer. Following this, the Canadians also approved its use for the reduction of obstruction and palliation of dysphagia in patients with completely or partially obstructing oesophageal cancer. In 1995, the Oncology Drugs Advisory Committee of the USA Food and Drug Administration (FDA) approved Photofrin® for palliative treatment of patients with totally obstructing tumours and partially obstructing oesophageal cancers and, in 1997, for tumour ablation of lung cancer patients who are unsuitable for thermal laser therapy. In countries such as the Netherlands, France, Germany and Japan, PDT is extensively used to treat lung and oesophageal cancer, superficial bladder cancer, cancers of the skin, gastric and cervical cancer, and cervical dysplasia [Schuitmaker *et al.*, 1996]. Although it is clearly evident that PDT can cause significant tumour necrosis, most clinical studies to date have involved patients who have failed conventional treatments. The likelihood of successful tumour control using PDT in these patients is therefore accordingly reduced. As a result, it is difficult to

assess the success and potential future benefit of PDT clearly. Nevertheless, most therapies have demonstrated at least a palliative effect of PDT, with reports generally of positive results [Dougherty *et al.*, 1998].

1.4.6 Disadvantages of Photofrin®

Despite attempts to purify the active components of haematoporphyrin, Photofrin® nevertheless remains a heterogeneous mixture of several porphyrin species, not all of which are involved in the photodynamic effect [Dougherty, 1987]. Variation between batches is therefore sometimes encountered in the clinic, making it difficult to predict the outcome of treatment. Furthermore, porphyrins do not readily undergo structural mono-substitution to allow investigation into changes in physico-chemical properties that might lead to increased drug activity. It has also become apparent, unfortunately, that the selectivity of Photofrin® for tumour tissue is less than originally reported and, on systemic administration, the drug is found also to localise in many normal tissues, especially those of the reticuloendothelial system, such as liver, kidneys and adrenals [Bugelski, 1981]. Drug accumulation reaches maximum levels more rapidly in normal tissues (< five to ten hours) than in tumour tissue (twenty-four to seventy-two hours). Consequently, illumination of the tumour region is carried out twenty-four to seventy-two hours after drug administration when the ratio of the drug concentrations favours malignant tissue. At this time, the photosensitizer shows minimal clearance from normal tissue, with about sixty per cent of peak levels in the spleen and about thirty per cent in lung still detectable seventy-five days after treatment. Particularly problematic is its accumulation in the skin, with slow clearance (half-life ca. nineteen days), necessitating that patients avoid exposure to bright light and sunlight for up to eight weeks post-treatment, in order to limit the risk of severe sunburn-type reactions [Dougherty *et al.*, 1990]. Although this is a minor inconvenience compared with the adverse effects of chemotherapeutic agents, it can lead to quite severe complications, especially when patient compliance is poor. Unlike true sunburn, which is the erythematous inflammation of the skin by ultraviolet radiation and which often develops over several hours, photodynamic reactions to the sun or bright lights may arise as soon as fifteen minutes following Photofrin® injection. The patient suffers acute stinging or itching, then oedema and blistering to the exposed area. If exposure is long enough, full thickness necrosis may be experienced.

The absorption spectrum of Photofrin® poses a further disadvantage for its use in PDT. Photofrin® (and similarly HpD) exhibits the characteristic intense porphyrin Soret band absorption peak around 400 nm (the blue region), with four weaker, Q bands at longer wavelengths (505, 540, 580 and 630 nm). However, this is not aligned with the therapeutic window (600 to 800 nm) [Section 1.2.2], so porphyrins are illuminated in the near infra red (around 630 nm) where their light absorption coefficients are very small ($\epsilon_{630 \text{ nm}} \approx 3500 \text{ l mol}^{-1} \text{ cm}^{-1}$) [Pottier *et al.*, 1986]. This permits maximum light penetration into tissue and overcomes problems of light scattering associated with shorter wavelength irradiation. Particularly disappointing, and of interest to this project, is the failure of porphyrin-based PDT to prove effective in the treatment of primary cutaneous melanotic melanoma, despite clear successes against a range of amelanotic metastatic lesions [Lui *et al.*, 1996]. This is thought to be a result of limited light penetration in pigmented lesions. The transmission of incident light increases up to about 700 nm in lightly pigmented tumours, whereas in the presence of extensive pigmentation (such as in melanotic melanoma), tissue transparency is observed only at wavelengths above 780 nm [Svaasand *et al.*, 1990]. Sensitivity of melanotic melanoma to PDT has only been observed in the presence of the porphyrin analogue, Si(IV)-naphthalocyanine which displays an intense absorbance ($\epsilon \approx 500\,000 \text{ l mol}^{-1} \text{ cm}^{-1}$) at 780 nm, thereby avoiding competition with melanin for light absorption [Biolo *et al.*, 1994].

1.5 Future directions

1.5.1 Second-generation Photosensitizers: Porphyrin-based Compounds

Second generation photosensitizers based on porphyrins are at various stages of pre-clinical and clinical evaluation. A vast array of new compounds has been produced either by synthetic modification of the parent molecule or by direct synthesis of *de novo* porphyrin analogues. Some of them are metal-free whilst others contain a diamagnetic metal complex. Derivatives of several groups, including the chlorins (also benzochlorins and bacteriochlorins), phthalocyanines (and the closely related naphthalocyanines), purpurins, benzoporphyrins, pheophorbides, porphycenes, verdins and texaphyrins, have been prepared and have proven preclinical efficacies. The phthalocyanines and naphthalocyanines are worthy of mention as a group since they are the most common family of hydrophobic photosensitizers. Following this only those

compounds that have entered clinical trials will be described further and these presented in order of extent of clinical use for cancer.

Phthalocyanines and Naphthalocyanines

Phthalocyanines (Pcs) (and the closely related naphthalocyanines (Ncs)) are structurally similar to porphyrins, with either a basic tetrabenz- or tetranaphtho-tetraazaporphyrin core, but show a strong absorption in the 650 to 750 nm range [Dougherty, 1984]. This is due to extended conjugation of the pyrrole moieties and replacement by nitrogen of the methine (-CH=) bridge [Figure 4].

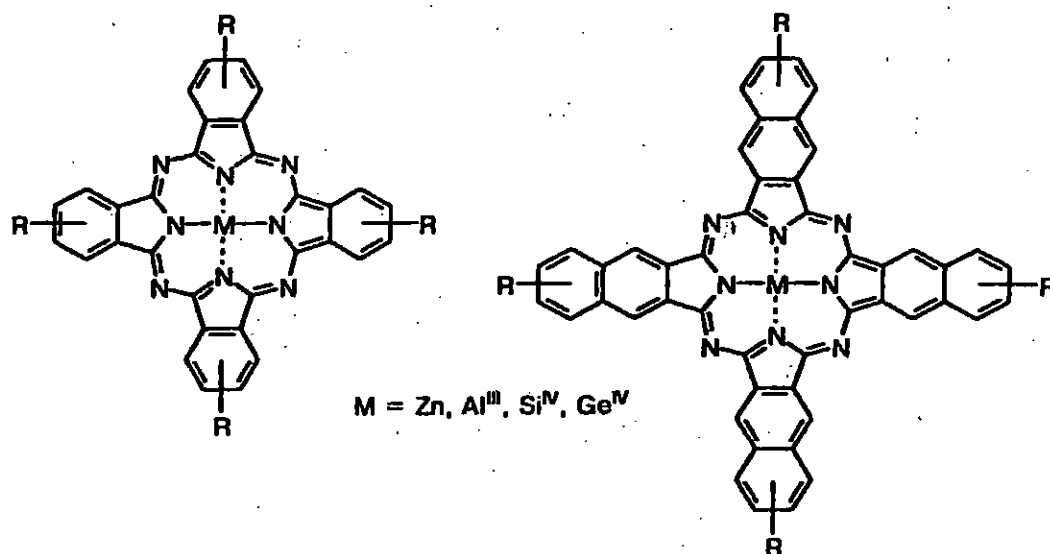


Figure 4. Chemical structures of phthalocyanine (left) and naphthalocyanine (right) molecules.

Substitution of these compounds is possible, either around the periphery of the molecule or within its central cavity, by chelation of metals bearing axial ligands. Both non-metallo and metallo derivatives have been studied but metal-free Pcs and Ncs show little photodynamic effect so, without exception, the Pcs and Ncs used in PDT contain a central metal atom. This is in contrast with porphyrin-based photosensitizers that tend to be non-metallated. The Pc (and Nc) macrocycle can combine with most metal and metalloid elements of the periodic table and be substituted at the periphery with a wide variety of substituents. However, the most potent photosensitizers of these classes are

reported to be the zinc- and aluminium-substituted Pcs, particularly the di-sulphonated Pc, AlPcS2 [Moan *et al.*, 1994]. AlPc is a particularly effective photosensitizer *in vitro* [Ben-Hur, 1989], whilst chloroaluminium sulphonated Pc has produced excellent responses in spontaneous tumours in animals [Roberts *et al.*, 1991]. Zinc extends the lifetime of the metastable triplet state [Rosenthal, 1991] and, for a series of four zinc(II)-substituted Ps, varying in charge and hydrophobicity, it was found that maximum tumour necrosis developed between nine and fourteen days in rats, with the cationic compound being the most potent photosensitizer [Cruse-Sawyer, J.E., 1998]. Of Ncs, Si(IV)-naphthalocyanine is the only photosensitizer to date that has proved effective against melanotic melanoma [Biolo *et al.*, 1994] [Section 1.4.6].

5-Aminolaevulinic acid/Protoporphyrin IX

A promising approach to PDT is the use of the five-carbon amino acid $\text{NH}_2\text{CH}_2\text{COCH}_2\text{CH}_2\text{COOH}$, 5-aminolaevulinic acid (5-ALA), to induce endogenous photosensitization in malignant tissue [Figure 5].

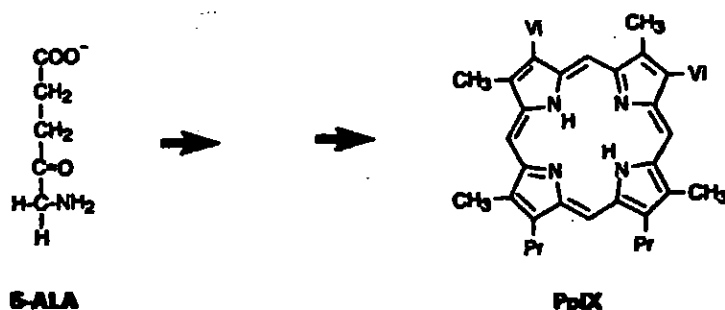


Figure 5. Chemical structures of 5-aminolaevulinic acid/Protoporphyrin IX

5-ALA is a naturally occurring precursor of haem that is produced in every nucleated cell. The technique exploits the haem biosynthetic pathway (which occurs in mitochondria) and, in particular, the immediate haem precursor, protoporphyrin IX (PpIX) [Kennedy *et al.*, 1990]. Exogenous 5-ALA acts as a prodrug that, upon local or oral administration, is absorbed locally or *via* the bloodstream and converted by cellular

enzymes to PpIX. Though an excellent photosensitizer, PpIX is not normally present within tissue at therapeutically useful concentrations since its production is subject to negative feedback inhibition, depending on the local concentration of haem [Figure 6].

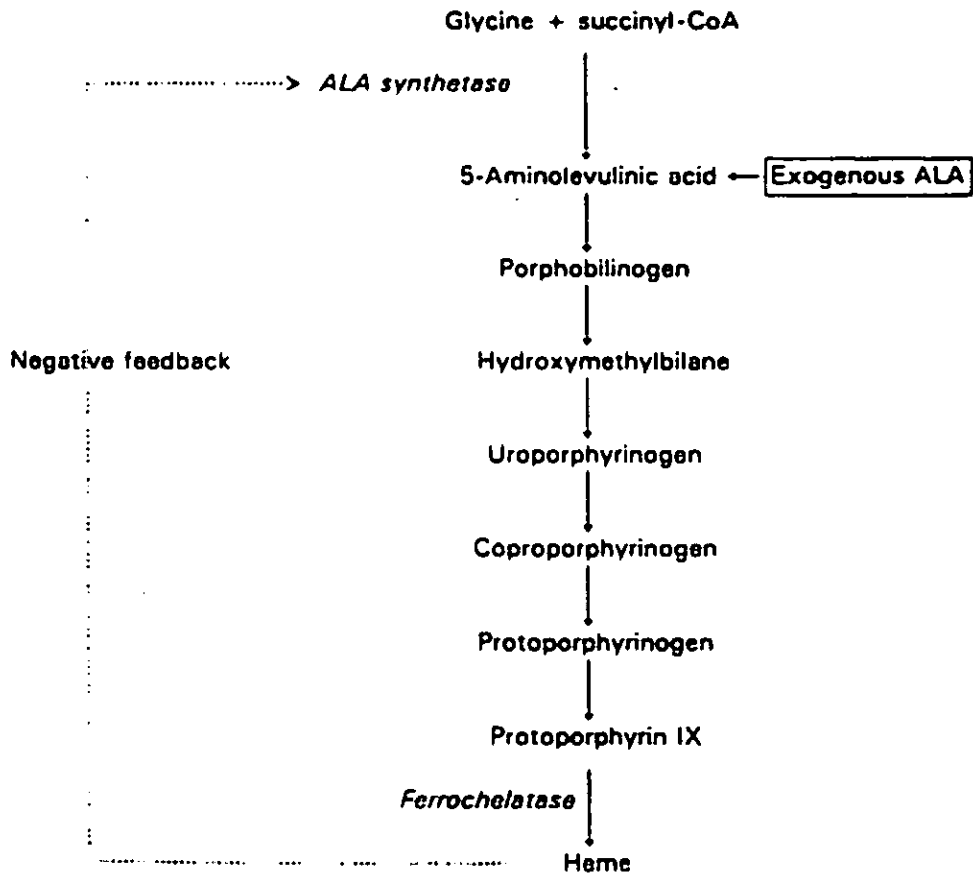


Figure 6. The haem biosynthetic pathway. [Taken from Kennedy *et al.*, 1990.]

Haem inhibits the activity of 5-ALA synthase, the first and rate-limiting enzyme of the biosynthetic pathway that catalyzes the production of 5-ALA from the condensation of glycine and succinyl CoA. Oral administration of 5-ALA bypasses this control in certain types of malignant (and regenerating) tissues. 5-ALA-PDT takes advantage of the fact that the activity of two particular enzymes is altered in some malignant cells [Leibovici *et al.*, 1988; El-Sharabasy *et al.*, 1992]. Ferrochelatase catalyzes the insertion of an iron atom into PpIX to form haem (which is not photoreactive), thereby inhibiting photodynamic activity. Porphobilinogen deaminase (PBGD) is the rate-limiting enzyme involved in precursory synthesis of PpIX. Some malignant cells have a relatively low activity of ferrochelatase but elevated activity of PBGD. High levels of

PBGD and low levels of ferrochelatase lead to overproduction of PpIX and its accumulation at photosensitizing concentrations in malignant tissue [Figure 6]. Following irradiation, 5-ALA-induced PpIX is photobleached very rapidly, leaving no detectable PpIX [Wessels *et al.*, 1992]. In fact, PpIX is almost completely cleared from the body within twenty-four hours of its induction whether orally, topically or intravenously administered, reducing the risk of prolonged skin photosensitivity [Bedwell *et al.*, 1992]. Moreover, since surrounding normal tissue contains very small amounts of PpIX, it runs no risk of serious photodamage, permitting the use of very large light doses, if necessary.

The first clinical results with 5-ALA appeared in 1990 from Kennedy *et al.*, who treated eighty basal cell carcinomas with 20 % (w/v) 5-ALA, applied topically in a proprietary oil-in-water emulsion. After an incubation time of three to six hours, lesions were exposed to light from a slide projector equipped with a 500 W lamp to give a range of light doses between 15 J cm^{-2} and 150 J cm^{-2} . Complete responses were found in ninety per cent of treated lesions two to three months post-treatment [Kennedy *et al.*, 1990]. At the same time, Kennedy and co-workers also reported on the use of ALA-PDT to treat early invasive squamous cell carcinoma and metastatic carcinoma of the breast. Further collaborative studies from the group using topically-applied 5-ALA found complete responses first in seventy-nine per cent (of three hundred lesions), and then in eighty-seven per cent (of over eight hundred cases) of basal cell carcinomas of the skin [Kennedy *et al.*, 1992; Kennedy *et al.*, 1996]. Other areas of investigation include the treatment of precancerous solar keratoses and various skin dysplasias [Peng *et al.*, 1997; Calzavara-Pinton, 1995; Cairnduff *et al.*, 1994; Wolf *et al.*, 1993], high-grade oesophageal dysplasia in Barrett's oesophagus [Barr *et al.*, 1996] and mucosal lesions in the gastrointestinal tract [Bown & Millson, 1997]. In June 1998, DUSA Pharmaceuticals, Inc. submitted to the US FDA the results of phase III clinical trials in which ninety-one per cent of lesions were cleared in patients using twenty per cent ALA plus blue light to treat multiple actinic keratoses of the face and scalp [McCaughan, 1999].

meso-tetra(m-hydroxyphenyl)chlorin (m-THPC, Temoporfin, Foscan®)

5,10,15,20-tetrakis(*meta*-tetrahydroxyphenyl)chlorin (*m*-THPC, temoporfin, Foscan®) was first synthesised at Queen Mary College, London, United Kingdom [Bonnett, *et al.*, 1989][Figure 7].

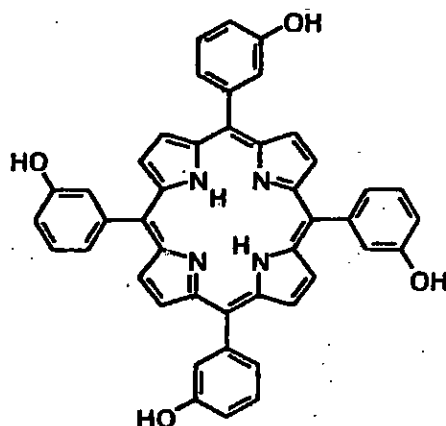


Figure 7. Chemical structure of *meso*-tetra(*m*-hydroxyphenyl)chlorin (*m*-THPC, Temoporfin, Foscan®)

Of all second-generation photosensitizers, chlorins have been most studied. They are derived from two sources, either by chemical synthesis or by modification of chlorophyll *a*, and have large molar extinction co-efficients above 650 nm [Spikes, 1990]. Foscan® itself is a stable compound, easily manufactured with a purity of over ninety-nine per cent and appears to date to be the most potent photosensitizer on a molar basis available for clinical PDT. Foscan® has a much stronger absorption peak in the red region of the visible spectrum than Photofrin® (at 652 nm compared with 630 nm, respectively) and consequently greater photoactivation and deeper tissue penetration. It also has a much higher $^1\text{O}_2$ yield and therefore relies on lower light doses for activation [Ma *et al.*, 1994]. Drug doses as little as 0.1 mg kg^{-1} and light doses as low as 10 J cm^{-2} with Foscan® are reported to be required for efficacy [Blant *et al.*, 1996]. Light doses with Photofrin® are generally above 100 J cm^{-2} [Schuitmaker *et al.*, 1996] [Section 1.2.2]. Skin photosensitization is less of a problem with Foscan® (two to three weeks compared with two to three months with Photofrin® [Dougherty *et al.*, 1990]), although

this varies greatly between individuals and is still longer than is found with other second generation photosensitizers [Savary *et al.*, 1994].

Interest in the *meso*-tetra(hydroxyphenyl)porphyrin series as clinical photosensitizers began in the 1980s because they, or their anions, were expected to show enhanced absorption at wavelengths in the red [Milgrom, 1983]. In the event, these compounds proved to be highly potent photosensitizers with favourable tumour selectivity [Berenbaum *et al.*, 1986]. Since then, Foscan has undergone extensive *in vivo* testing and cost-benefit analysis [Bonnett *et al.*, 1989; Berenbaum *et al.*, 1993], and appeared to be on the verge of commercialisation until non-approval by the FDA in early 2001. The first clinical reports appeared in 1991 and described the treatment of malignant mesothelioma using intraoperative PDT with Foscan®. Selective tumour uptake and tumour necrosis up to 10 mm in depth following surgery was reported [Ris *et al.*, 1991].

Most of the initial work with Foscan® focused on early-stage invasive cancers of the head and neck. Preliminary investigations from Savary *et al.* (1994) found a complete response in fourteen out of sixteen early-stage carcinomas of the upper aero-digestive tract without recurrence in a six-month follow-up period. In this case, skin photosensitivity was six weeks at most. Possibly the best results for early bronchial or oesophageal cancers have come from researchers in Lausanne, Switzerland, with seventy-seven per cent of tumours eradicated in twenty-eight patients using Foscan-mediated PDT. No recurrences occurred in a three to thirty-five month follow-up period. In contrast, late-stage tumours were controlled in only one out of four patients by this method. (In fact, none of the groups currently working with this photosensitizer now believes that it is an appropriate agent for palliating advanced malignant disease.) Skin photosensitivity here was seen only in the first week post-injection, although other complications (one oesophageal fistula, one bronchial stenosis and possibly two occult oesophageal perforations) occurred [Grosjean *et al.*, 1996]. As a result, it has been proposed that green light rather than red should be used for early lesions to minimise the risk of muscle damage and perforation [Monnier *et al.*, 1994]. Green light exhibits lower tissue penetration (and is less painful) than red [Fritsch, *et al.*, 1993] and Foscan® also absorbs in this part of the spectrum. The photosensitizer has a second, smaller absorption peak at 514 nm that can be used when treating superficial tumours in thin-walled organs such as the oesophagus. Consequent to these and other successful trials

[Dilkes & DeJode, 1995; Ris *et al.*, 1996; Baas *et al.*, 1997], a multicentre European evaluation study of Foscan-mediated PDT for head and neck cancers was carried out under the sponsorship of Scotia Pharmaceuticals, U.K. [Dilkes, *et al.*, 1997; Savary *et al.*, 1997]

Benzoporphyrin Derivative-Monoacid Ring A (BPD-MA, Verteporfin)

Derivatives of benzoporphyrins (BPDs) are of interest as clinical photosensitizers because they absorb light maximally at wavelengths around 690 nm and have low skin toxicity compared to Photofrin® [Pandey *et al.*, 1993].

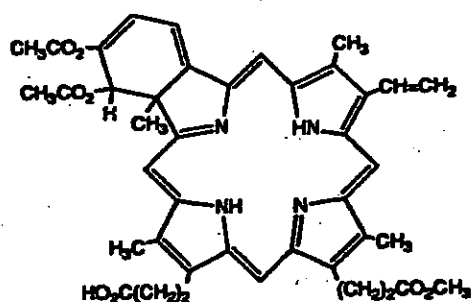


Figure 8. Chemical structure of benzoporphyrin derivative-monoacid ring A (BPD-MA, Verteporfin)

As they are hydrophobic molecules, BPDs must be formulated into liposomes for application. Monoacid forms of BPD share similar pharmacological properties but have greater PDT activity than their corresponding diacid analogues [Richter *et al.*, 1990]. Benzoporphyrin derivative-monoacid ring A (BPD-MA, Verteporfin) [Figure 8] is in fact a chlorin composed of two monomethyl esters and synthesised from protoporphyrin [Pangka *et al.*, 1986]. It has a strong molar absorption co-efficient at 690 nm where there is a “window” between the absorbance of haemoglobin and water. Further desirable features of the drug have led to its clinical use against a variety of cutaneous and extracutaneous targets. BPD-MA has, for instance, demonstrated good selectivity for tumour tissue. Drug concentrations five times greater in malignant tissue than in normal skin have been reported using fluorescence spectroscopy in patients with basal cell carcinoma [Lui *et al.*, 1996]. *In vitro* studies on various cell lines suggest that

uptake of BPD-MA is *via* receptor-mediated endocytosis through the LDL receptor [Kessel, 1989b; Allison *et al.*, 1994]. Accumulation of BPD-MA into malignant tissue following intravenous injection is rapid, permitting same-day irradiation of the tumour region. Furthermore, its short half-life and rapid clearance ensure that skin photosensitivity is only of very limited duration (seventy-two hours in humans is reported) [Levy *et al.*, 1994]. Consequently, Phase I/II trials with BPD-MA for the PDT of non-melanoma skin cancers, endometrial ablation and psoriasis have now been completed [Leung, 1994; Levy, 1995].

BPD-MA has also demonstrated potential in the treatment of atherosclerotic plaque [Allison *et al.*, 1997] illustrating the scope for PDT outside the field of neoplasia. Of particular interest though is the use of BPD-MA to treat choroidal melanomas [Allison *et al.*, 1997] and age-related macular degeneration (ARMD) [Husain *et al.*, 1996, 1997]. ARMD is the most common cause of blindness in people over fifty years of age. In certain patients, vision is impaired by leaky vasculature near the macula, but further loss may be incurred as a result of damage to the retina by the thermal lasers used in conventional treatment. Using PDT, BPD-MA is allowed to accumulate in the vessels as much as possible then activated at 690 nm through an ophthalmoscope generally using a diode laser. This allows selective closure of leaky vessels without damage to overlying tissue. A preliminary study of one hundred and seven patients showed that a single treatment was effective in forty-four per cent of patients though there was some recurrence of leakage after four to twelve weeks [Gragoudas *et al.*, 1997]. Multiple treatments may offer improved results and are being evaluated in further trials [Schmidt-Erfurth *et al.*, 1997]. BPD-MA has now moved into Phase III randomized trials involving four hundred patients in twenty-eight centres in North America and Europe for the treatment of ARMD.

mono-L-aspartylchlorin e₆ (Npe₆, MACE)

Mono-L-aspartyl chlorin e₆ (Npe₆, MACE) is a synthetic aspartyl derivative of chlorin-e6 [Figure 9]. It is a pure, monomeric compound with a major absorption peak at 664 nm, very short-lived phototoxicity and rapid clearance from tissues [Allen *et al.*, 1992].

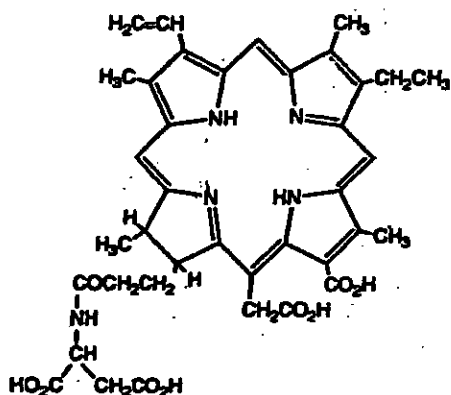


Figure 9. Chemical structure of mono-L-aspartylchlorin *e₆* (Npe₆, MACE)

Preliminary research in the late 1980s established that the aspartate esters of chlorin *e₆* could induce cell death *in vitro* and tumour control *in vivo* [Nelson *et al.*, 1987]. Mechanistic investigations revealed also the hydrophilic character of the molecule, demonstrating that MACE enters cells *via* endocytosis and becomes ultimately localised in lysosomes [Roberts & Berns, 1989]. In addition, it has been demonstrated in PTK2 cells that lysosomes are preferentially damaged following MACE-mediated PDT [Roberts *et al.*, 1989]. Subsequent *in vivo* and pharmacokinetic analysis confirmed the photodynamic action of MACE against transplanted mouse mammary carcinomas and suggested a major vascular component in the tumoricidal action of this photosensitizer [Gomer & Ferrario, 1990]. Further to this, MACE has been the subject of clinical trials for the treatment of endobronchial lung cancer and superficial malignancies of the skin and nasopharynx. Good response rates were seen with illumination four to eight hours following drug administration and skin photosensitivity was limited to the first two to four days [Allen *et al.*, 1992].

Tin ethyl etiopurpurin (SnET2, Purlytin®)

Purpurins were first synthesised in 1960 [Woodward, 1960] and metal derivatives of the free base purpurins prepared in 1986 by Morgan and Tertel at the University of Toledo [Morgan & Tertel, 1986].

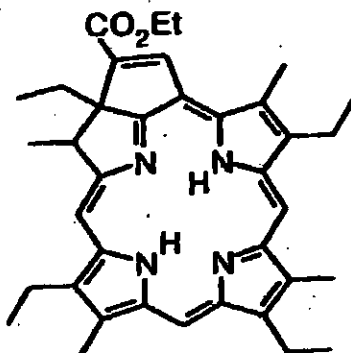


Figure 10. Chemical structure of tin ethyl etiopurpurin (SnET2, Purlytin®)

Tin ethyl etiopurpurin (SnET2, Purlytin®) is the major representative of the purpurin family [Figure 10]. It is a synthetic chlorophyll analogue (a metallochlorin) that can be activated by 664 nm visible red light *in vivo* [Garbo, 1996]. Since the molecule is hydrophobic, it must be formulated into a lipid emulsion or with the common solubilization agent, Cremophor EL, for clinical use [Razum *et al.*, 1996]. SnET2 has been shown to be selective for and retained by tumour but not normal tissue. The presence of the metal ligand alters intracellular targeting of the molecule so, whereas metal-free derivatives inhibit biosynthesis of DNA, SnET2 mediates photodamage at sites of membrane transport [Kessel, 1989c]. A pilot study on the canine prostate demonstrated tissue necrosis up to a depth of one centimetre following illumination twenty-four hours after administration of SnET2 [Selmen & Keck, 1994]. Preliminary Phase I/II clinical trials, carried out to evaluate drug and light doses and to assess the safety of the drug, found that ninety-five to one hundred per cent of basal cell carcinoma and all metastatic breast carcinoma lesions had responded twelve weeks following PDT treatment using SnET2. Of the breast carcinoma lesions, complete and partial responses were ninety-six per cent and four per cent respectively and, of basal cell nevus syndrome tumours, eighty-six per cent and fourteen per cent, respectively [Snyder *et al.*,

1996]. In a second study involving treatment of AIDS-related Kaposi's sarcoma, forty-five patients with four hundred and four tumours were treated. Complete responses were found in sixty per cent of lesions and partial responses in the remaining forty per cent [Razum *et al.*, 1996]. Side effects of PDT with SnET2 are reported to be minimal with mild, transient photosensitivity found only in a small percentage of patients. Furthermore, the rapid clearance of this drug is considered to be an advantage in dermatology. SnET2 has now moved into phase III clinical study with a view to U.S. FDA approval for its use in the PDT of various cutaneous metastases and AIDS related Kaposi's sarcoma [Razum, *et al.*, 1996; Rifkin *et al.*, 1997; Kaplan *et al.*; 1998].

Lutetium texaphyrin (PCI-0123, Lu-Tex)

The texaphyrins are a new class of "expanded porphyrins" which have a system that is not a tetrapyrrole, but does have an expanded co-ordination sphere that readily forms metal complexes [Sessler *et al.*, 1988; 1994]. Metallotexaphyrins substituted with lanthanum and lutetium form long-lived triplet states and are efficient generators of singlet oxygen [Harriman *et al.*, 1989; Grossweiner *et al.*, 1999]. Unfortunately, many of them have relatively poor solubility in aqueous solution and some only short stability in phosphate buffered saline or tissue culture media.

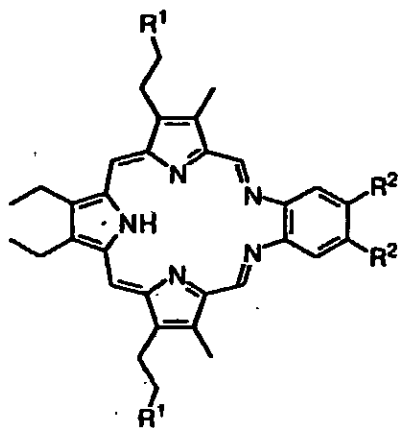


Figure 11. Chemical structure of a texaphyrin molecule

Lu(III) derivative PCI-0123 (lutetium texaphyrin) is one exception that is both stable and water-soluble [Figure 11]. Lu-Tex is highly fluorescent, acts both as a

photosensitizer and a magnetic resonance imaging contrast agent, and has a broad absorption peak at 732 nm, permitting maximum penetration (about six millimetres) into tissue [Young *et al.*, 1996]. Studies with Lu-TeX have progressed from cellular and bacterial [Ehrenberg *et al.*, 1991], then viral [Matthews *et al.*, 1992] systems, to mammalian tumour models [Woodburn *et al.*, 1996] and preliminary investigations involving various metastatic skin cancers [Wieman *et al.*, 1996; Renschler *et al.*, 1997]. Phase I clinical trials evaluated one hundred and sixty-three skin lesions from fifteen breast metastases, seven malignant melanomas, five Kaposi's sarcomas, two invasive basal cell and two squamous cell carcinomas and found a complete response in twenty-nine per cent and partial response in seventeen per cent of all cases. Unlike some other photosensitizers, Lu-TeX preferentially accumulates in malignant tissue (*via* an increased lipoprotein receptor mechanism) with no necrosis in the surrounding normal skin [Renschler *et al.*, 1997]. In fact, Lu-TeX is believed to be one of only a few photosensitizers to exert direct tumour cell toxicity, causing selective tumour necrosis with very little evidence of vascular-mediated damage. Woodburn *et al.* demonstrated intracellular localisation of Lu-TeX in lysosomes of EMT-6 neoplasms using confocal laser scanning microscopy and found an intense apoptotic response following illumination [Woodburn *et al.*, 1996]. PDT-induced apoptosis of vascular cells with Lu-TeX has recently also been reported [Simon *et al.*, 1999]. All *in vivo* studies to date have indicated that this drug is cleared rapidly from plasma with biphasic pharmacokinetics ($T_{1/2}$ 0.25 and 8.8 h in humans) and induces only mild, transient skin photosensitivity. This makes it a suitable agent for repeated PDT, which gives better results than single treatments in animal models [Miles & Young, 1997]. Lu-TeX is currently moving into Phase II/III clinical trials for various cutaneous cancers.

1.5.2 Second-generation Photosensitizers: Cationic Dyes

Cationic dyes represent an entirely different class of photosensitizers based on non-porphyrin compounds. Some vital dyes, used for over a century both in industry and histology, have long been known to act as photosensitizers and have attracted interest in PDT since they affect the mutation, metabolism and viability of mammalian cells, bacteria and viruses. Most dyes are organic compounds that contain a chromophore and an auxochromic group attached to at least one benzene ring. The colour of the dye is attributable to its chromophore and its dyeing property to the salt-forming auxochrome. Vital dyes are divided into two categories, basic and acid dyes, not terms that refer to

the hydrogen ion concentration, but that are indicative of whether the ionised auxochrome is respectively cationic or anionic [Gill *et al.*, 1981].

The earliest reports of vital dyes being used in histological staining came in 1642 from Grew, who used Cochineal extract to stain plant tissues, and shortly afterwards from Leeuwenhoek, who stained muscle fibres with Saffron [Barbosa and Peters, 1971]. One of the first reports of the use of a cationic dye in the treatment of human cancer, was presented in 1906 at the 57th Annual Meeting of the American Medical Association by Dr. Jacobi [Jacobi, 1906]. Over a period of fifteen years, Jacobi observed that the phenothiazinium dye, methylene blue, orally administered at 120 mg to 400 mg per day to one hundred and fifty patients with inoperable cancer, produced a palliative effect in most patients, especially women with uterine cancer. The treatment appeared to be particularly effective when patients were placed in bright sunlight for long periods of time. Methylene blue, along with several other cationic dyes, also demonstrated *in vivo* cytotoxicity against animal tumours in the 1940s, prior to the advent of modern PDT [Lewis *et al.*, 1946; Riley, 1948]. Later, in 1963, another phenothiazinium dye, toluidine blue (applied topically as a one per cent aqueous solution) was used for the *in vivo* delineation of dysplasia and carcinoma of the uterine cervix in two hundred women [Richart, 1963]. The degree of staining was found to correlate with the severity of the disease, which may explain the results obtained by Jacobi some sixty years before. Other examples of commercial photosensitizers that have been examined for photocytotoxicity include acridines [Iwamoto *et al.*, 1987], xanthenes [Melloni *et al.*, 1988], phenoxazines [Cincotta *et al.*, 1994], phenothiazines [Canete *et al.*, 1993] and triarylmethanes [Wadwa *et al.*, 1988].

Whilst cellular uptake of anionic compounds (such as Photofrin®) is strongly dependent upon their hydrophobicity [Moan *et al.*, 1987], uptake of cationic photosensitizers is thought to occur because of their attraction for the negatively-charged inside surface of cellular membranes. Whereas hydrophobic, anionic dyes generally localise in membrane structures (including plasma, mitochondrial, endoplasmic reticulum and nuclear membranes), hydrophilic compounds tend to localise in lysosomes. Hydrophobic, cationic photosensitizers are found to accumulate preferentially in mitochondria. Rhodamine 123, for example, is a mitochondria-specific cationic dye

[Bernal *et al.*, 1983] that has demonstrated photocytotoxicity in carcinoma cells *in vitro* [Nadakavukaren *et al.*, 1985; Meloni *et al.*, 1988] and antitumour activity in animal models *in vivo* [Herr *et al.*, 1988; Arcadi, 1990]. It is believed that their mitochondrial-localising property arises from an abnormally high electrochemical potential across the mitochondrial membranes of individual carcinoma cells [Davis *et al.*, 1985; Oseroff, 1986]. An observation of particular therapeutic interest is that light exposure seems to increase the retention of rhodamine derivatives in cells [Shea *et al.*, 1989]. However, although cationic, hydrophobic dyes (including rhodamine 123, triarylmethylmethane derivatives, chalcogenapyrylium dyes and cryptocyanins) appear to be selectively retained in certain types of carcinoma cells compared to normal cells *in vitro* [Modica-Napolitano *et al.*, 1990; Oseroff *et al.*, 1986], few demonstrate selective tumour accumulation *in vivo* [Kinsey *et al.*, 1989]. Furthermore, the photocytotoxicity of many commercial photosensitizers is not achieved without concomitant dark toxicity [Bernal *et al.*, 1983; Herr *et al.*, 1988; Arcadi, 1990], and few workers have thus far attempted to overcome this problem by the synthesis of specifically designed photosensitizers based on these compounds.

Nevertheless, some novel, cationic compounds based on phenoxazines and phenothiazines may hold promise for the future [Cincotta *et al.*, 1990]. Benzophenoxazines are derivatives of the tetracyclic dye, Nile blue, and possess several features required of an effective photochemotherapeutic drug *i.e.* they selectively stain tumours, are stable in physiological conditions, exhibit low systemic toxicity and absorb light within the therapeutic window. Unfortunately, these compounds are inefficient photosensitizers, both *in vitro* and *in vivo*, due to their inability to form long-lived triplet states [Section 1.3.2]. However, researchers found that use of the heavy atom effect to increase the spin-orbit coupling, and substitution of appropriate halogens (I, Br) to the benzo[*a*]phenoxazine nucleus, enhanced the photoactivity of several of the Nile blue derivatives thus created [Foley *et al.*, 1987]. *In vitro* photosensitization correlated with singlet oxygen yields for these compounds. Further studies using animal models demonstrated the selective retention of the derivatives *in vivo* [Lin, Schulok, Kirley *et al.*, 1991]. A preclinical evaluation of substituted benzo[*a*]phenothiazinium photosensitizers has demonstrated promising properties for their use in human skin cancer [Cincotta *et al.*, 1994]. The low systemic toxicity and an absorption peak at

around 650 nm are combined with a good tumour killing ability and lack of unwanted cutaneous toxicity.

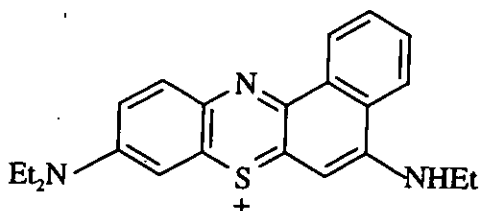


Figure 12. Chemical structure of 5-ethylamino-9-diethylaminobenzo[*a*]thiazinium chloride [EtNBS].

Replacement of the oxygen atom in benzophenoxazines with sulphur gives rise to the corresponding benzophenothiazinium chromophores [Cincotta *et al.*, 1987] [Figure 12]. Derivatives of benzo[*a*]phenothiaziniums are efficient absorbers of red light (620 to 660 nm) with molar extinction coefficients of about $75\,000\text{ l mol}^{-1}\text{ cm}^{-1}$, have more hydrophobic character than the parent compounds [Cincotta & Foley, 1988], and have demonstrated promising results *in vivo* [Cincotta *et al.*, 1990].

1.6 Aim of Project

The aim of the project was first to examine the effect of simple alkylation of the phenothiazinium chromophore on the cytotoxicity of the well-known biological stain and photosensitizer, methylene blue (MB). It was also proposed to investigate factors that might contribute to the observed patterns of cytotoxicity and to study the mechanisms by which the photosensitizers might bring about cell death. Ultimately, the project sought to assess the potential of MB and its derivatives, 1-methyl methylene blue (MMB), 1,9-dimethyl methylene blue (DMMB) and new methylene blue N (NMB) to be used in the PDT of both non-pigmented and pigmented lesions.

**CHAPTER TWO:
CYTOTOXICITY OF METHYLENE BLUE AND ITS
DERIVATIVES IN THE EMT-6 CELL LINE**

2.1 ABSTRACT

The cationic phenothiazinium dye, methylene blue (MB), has previously been investigated as a potential photosensitizer in clinical photodynamic therapy. Its apparent dismissal from mainstream PDT is likely to be as a result of an inherent (dark) toxicity and its rapid reduction *in vivo* to the inactive compound. The cytotoxic and photodynamic activities of MB and two other commercially-available stains, 1,9-dimethyl methylene blue (DMMB) and new methylene blue N (NMB), together with a newly synthesised compound, 1-methyl methylene blue (MMB), were measured here against the murine mammary tumour cell line, EMT-6, using a standard MTT assay. The three derivatives exhibited increased dark toxicity with concomitant higher phototoxicity compared to MB at a white light dose of 7.2 J cm^{-2} . Successive methylation also rendered the phenothiazinium chromophore more resistant to reduction to its inactive leuco form and led to increased levels of singlet oxygen production, increased hydrophobicity and improved cellular uptake, providing a possible explanation for the increased toxicities of the methylated derivatives. Of the four photosensitizers, NMB exhibited with the highest light:dark differential in this cell line and, in this respect, demonstrated the greatest clinical potential.

2.2 INTRODUCTION

The phenothiazinium dye, methylene blue (MB) (tetramethylthionin chloride), also known as Swiss blue, is a basic dye with a relative molecular mass of 319. As a member of the thiazine subgroup of the quinoneimine family of dyes, MB has typically a 2-benzene ring structure joined by one sulphur and one nitrogen atom [Figure 13]. Like most of the dyes in this group, the primary importance of MB is not within the textile industry but in several fields of biology including, amongst others, cytology, histochemistry, histology, microbiology, mycology, parasitology and virology. MB is one of the most widely used of all dyes, particularly in the field of histology, where it is used mainly as a nuclear stain. MB itself will stain a vast range of organisms, microorganisms, cellular and subcellular bodies and tissues including bacteria, leprosy organisms, yeast, diphtheria, rickettsiae, spirochaetes, algae, bone and cartilage, nervous tissue, splenic and lymphoid tissue, leukocytes, mitochondria, Nissl bodies, Negri bodies, pancreatic Paschen bodies and many others. In combination with acid dyes, MB is also an ingredient of staining formulations such as Giemsa and Leishman, which are used to study blood and parasites [Barbosa & Peters, 1971].

In addition to its long tradition as a vital stain, MB has played an important role in investigations of major biological processes *in vivo*. It has been used extensively in humans, for example, for the localisation of ureteral orifices, fistulae, and for the therapy of cystitis and urolithiasis [Gill *et al.*, 1981]. When the dye was found to stain injured urothelial surfaces but not normal urothelium, it was postulated that bladder tumours might also have abnormal surfaces that could be selectively targeted by vital dyes such as MB. Urothelial injury results in nucleation and crystal adhesion of calcium oxalate and magnesium ammonium phosphate (struvite) in experimental animals [Gill *et al.*, 1979]. Similarly, microscopic crystals of stone salts and gross crystalline masses are frequently found adherent to the surfaces of human bladder tumours. Consequently, MB was used to delineate tumour tissue in the management of patients with bladder cancer [Fukui *et al.*, 1983; Gill *et al.*, 1984] and as an adjunct to check cystoscopy in recurrent bladder tumours [Kaisary, 1986]. More recently, selective staining of intestinal metaplasia in Barrett's oesophagus has been demonstrated with MB [Canto, 1996].

MB is also a known bioactive photosensitizer and has several other features that would suggest its potential as an agent in clinical PDT. It is readily available and manufactured with a high level of purity. Very importantly, it absorbs light maximally in the red region of the spectrum (600 to 800 nm), which corresponds to the therapeutic window for PDT [Section 1.2.1]. To this end, several groups have tested the dye's toxicity against various cell lines [Gill *et al.*, 1987; Fowler *et al.*, 1990; Yu, D-S., 1990; Wang & Densmore, 1995] and in experimental animals, with promising results [Gill *et al.*, 1987; Yu, D-S, 1990; König *et al.*, 1987]. DNA is recognised as an important primary target for MB photosensitized biological damage, and mutagenic effects are found in living systems when cell destruction is incomplete [Bellin & Grossman, 1965; Tuite & Kelly, 1993; Antony *et al.*, 1995]. However, photoactivated MB will also oxidise lipids [Kamat & Devasagayam, 1996] and amino acids [Nilsson *et al.*, 1972], and cause damage to lysosomal membranes [Santus *et al.*, 1983; Yao & Zhang, 1996]. Recent research has implicated MB-induced microtubular photodamage in cell death [Stockart *et al.*, 1996]. As with porphyrin-based PDT, Type II photochemical reactions are believed to predominate in MB-induced photocytotoxicity, although Type I processes have also been observed [Kamat & Devasagayam, 1996] [Section 1.3.2]. The photochemistry of the phenothiazinium nucleus has been investigated extensively by several groups, particularly in the area of DNA-MB interactions. On illumination, intercalated MB causes the formation of oxidised guanine residues, notably 8-hydroxyguanosine, *via* the intermediacy of singlet oxygen [Tuite & Kelly, 1993]. This research has led to the use of MB in the eradication of viruses, such as HIV and Hepatitis C, from donated blood [Zeiler *et al.*, 1994; Bachmann *et al.*, 1995]. The technique involves mixing a small amount of photosensitizer with the blood and its subsequent illumination whilst still in the 'blood bag'. This is permitted because red blood cells, unlike viruses, do not contain DNA, and the long (red) wavelengths required to activate the photosensitizer do not cause collateral damage to other blood components. It has also been suggested that MB cytotoxicity includes the generation of hydroxyl radicals which effect changes to the homeostatic mechanisms of intracellular calcium [Lee & Würster, 1995].

Despite its extensive commercial applications, the use of MB as a photosensitizer in clinical PDT has been sparse. Nevertheless, MB has been used to treat several tumour types both in animals and in humans. One of the earliest publications of the use of MB

to treat cancer in humans dates back to 1906, when Jacobi treated patients suffering inoperable disease with pills containing MB. Although no cures were effected, the treatment was claimed to have prolonged lives [Jacobi, 1906]. In humans, MB has been used for the PDT of bladder carcinoma [Williams *et al.*, 1989] and inoperable oesophageal tumours [Orth *et al.*, 1995]. In the former case, direct instillation of the photosensitizer into the bladder cavity, and its local retention, reduces the possibility of systemic side effects. Using a topical application, MB, in combination with the photosensitizing pro-drug, 5-aminolaevulinic acid [Section 1.5.2], has been used in the PDT of psoriasis [Schick *et al.*, 1997]. MB has since also been tested alongside Zn-phthalocyanine and Photosan-3 in experimental colonic tumours in mice, comparing favourably with the other two photosensitizers, with seventy-five per cent of the tumours being destroyed by a single PDT treatment with MB [Orth *et al.*, 1998]. More recently, the effect of PDT using MB (free and combined with liposomes) as the photosensitizer for treating human ovarian malignant tumours cultivated on the chorioallantoic membrane has been evaluated. Two days after PDT, the treated implanted tumours were markedly decreased in size and areas of necrosis with black coloration, dryness and eschar formation were observed. Five days after PDT, tumour regression was clearly observed in all the treated tumours [Ismail *et al.*, 1999].

The hydrophilic/ hydrophobic character of any drug will influence its partitioning behaviour in the various pharmacological compartments in which it is subsequently found. The $\text{Log } P$ value is a simple *in vitro* measure of the partitioning behaviour of a compound and is taken as the logarithm of the partition coefficient of that compound between a two-phase mixture, normally water and 1-octanol, such that

$$\text{Log } P = \text{Log} \{c_{\text{Oct}} / c_w\}.$$

The more hydrophilic a compound, the greater its water solubility, and hence the more straightforward its systemic administration. On the other hand, the more hydrophobic (or lipophilic) a compound, the greater its affinity for the various lipids encountered (complexed to blood proteins or at the cell membrane, for example), and the greater the likelihood of cellular uptake. Normally, alkyl substitution of a compound will cause an increase in its hydrophobicity (positive $\text{Log } P$), promoting its binding to serum transport

lipoproteins, increasing cellular uptake and, possibly, altering its intracellular targeting and localisation.

Like most other phenothiazinium dyes, MB is a salt, with the dye chromophore being the cation. The dye cation is hydrophilic ($\text{Log } P = -0.9$) and this determines many aspects of its pharmacology and intracellular localisation. The presence of dimethylamino groups at positions 3- and 7- of the molecule, explains the fact that MB is cationic under normal physiological conditions, unlike other commercially available phenothiazinium dyes, such as toluidine blue O and new methylene blue *N* (NMB). These dyes contain primary and secondary amino functionality respectively, which can lead to the formation of neutral quinoneimines by deprotonation, thus allowing a greater variety of pharmacologically active species. In terms of biological activity, these dyes cannot be compared directly with true MB derivatives since, because of the presence of the two tertiary amino groups, MB derivatives are unable to form neutral quinoneimines.

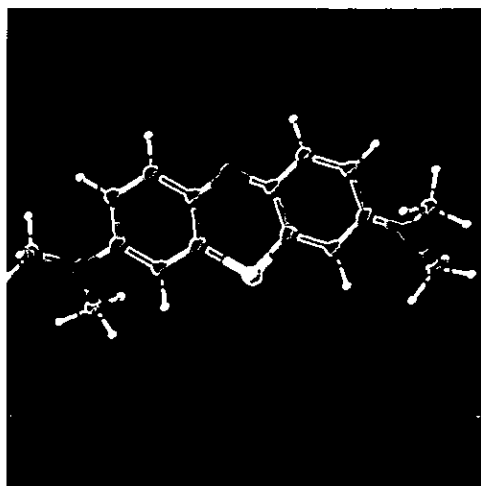
Once in the biological milieu, the metabolism of MB usually occurs rapidly *via* the reduction of the cation to the neutral leucobase (LMB) by the ubiquitous cellular coenzymes, NADH and FADH₂ [Bongard *et al.*, 1995]. The neutral species is highly hydrophobic ($\text{Log } P > +3$) and the difference in $\text{p}K_a$ of the two forms is sufficient to cause a considerable decrease in DNA binding affinity. Thus, although MB is cationic at physiological pH, LMB has a $\text{p}K_a$ of 5.8, resulting in only 3.8 per cent protonation at physiological pH. High ionisation is essential for efficient DNA intercalation, and photodamage to DNA is believed to be an important element of MB photocytotoxicity. In addition, LMB, in either its neutral or protonated form, absorbs only in the ultraviolet region of the spectrum, thus exhibiting negligible photodynamic activity at wavelengths in the region 600 to 800 nm, the therapeutic window for PDT [Section 1.2.1]. To some extent, this rapid metabolism might be useful in avoiding the current problem of prolonged skin photosensitivity that is a feature of porphyrin-based PDT. However, the short-lived pharmacological activity of MB, coupled with its inherent (dark) toxicity, may also explain the apparent dismissal of the photosensitizer as an agent in mainstream PDT.

Many of the vital stains, apart from MB, have been found to be either toxic to the target organism or to induce a number of subtle pathological symptoms in that organism [Barbosa & Peters, 1971]. Few workers have thus far attempted to eradicate this problem by the synthesis of specifically designed photosensitizers based on commercial dyes. Novel derivatives of MB are scarce, but arise mainly from changes in the amino substituents at positions 3- and 7- of the phenothiazine ring [Motsenbocker *et al.*, 1993; Strekowski *et al.*, 1993; Creed *et al.*, 1983]. One exception is a pentacyclic analogue, derived from a substituted tetrahydroquinoline, that has been prepared and investigated in rats [Peng *et al.*, 1993]. Commercial MB derivatives are available which have substituents in alternative positions in the ring, *e.g.* methylene green (4-nitro MB) or Taylor's blue (1,9-dimethyl MB) (DMMB) which has been used as a metachromatic stain. Recently, DMMB, like MB, has been found to photoinactivate viruses in red cell suspensions without significant loss of integrity of anucleate red cells [Wagner *et al.*, 1998]. There is no available literature on the effect of such substitution on the tumour-localising or photosensitizing abilities of the resulting compounds to enable quantitative structure-activity relationships to be derived, although such studies have been carried out on a series of benzo[*a*]phenothiazinium analogues [Foley & Cincotta, 1987; Cincotta *et al.*, 1987; Cincotta & Foley, 1988; Cincotta, 1990; Cincotta *et al.*, 1996]. Extra selectivity in anti-cancer drugs can be achieved using anti-tumour antibodies that bind to cancer cell surfaces. This has been attempted with MB by the synthesis of side chain maleimido- and succinimido-derivatives [Motsenbocker *et al.*, 1993]. The resulting MB-protein conjugates were reported to be slightly less photoactive *in vitro* than the parent compounds.

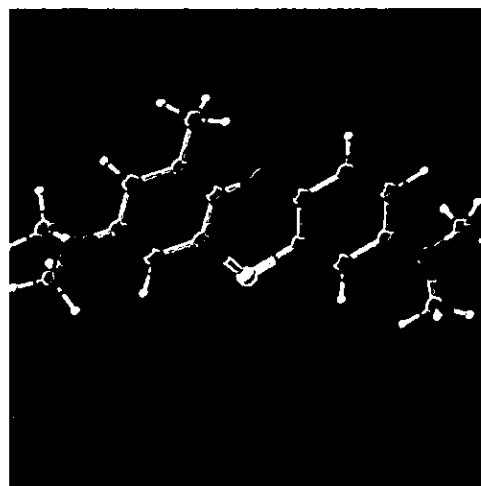
The purpose of this first study was to assess the effect of simple alkylation of the phenothiazinium chromophore using MB and two other known biological stains, 1,9-dimethyl methylene blue (DMMB) and new methylene blue *N* (NMB), together with a newly-synthesised intermediate compound, 1-methyl methylene blue, (MMB) [Figure 13]. In this way, it was intended that the weak electron-releasing and/or steric effects of the methyl group(s) would inhibit the cellular reduction of the chromophore, thus allowing a stronger photosensitizing effect to be exerted. Physicochemical characteristics (visible absorption, singlet oxygen efficiency, log *P*) were also established and the toxicity of MB and its three derivatives measured against the murine mammary tumour cell line, EMT-6, using a standard MTT assay [Carmichael *et al.*,

1987]. The cellular uptake of the photosensitizers (using methanol extraction) and the effect of variable illumination on toxicity were also investigated. The non-pigmented EMT-6 cell line is well characterised and was already in use within the university. It was chosen as a preliminary test system because it is an uncomplicated line that grows readily and rapidly in culture. A resistant sub-line of EMT-6 (EMT-6 (R)) had previously been used to demonstrate that treatment with MB and certain other cationic dyes, (such as Toluidine blue O and Victoria Blue BO), could overcome resistance in cells that over-express the P-glycoprotein (PgP) drug efflux pump. PgP is associated with resistance to conventional chemotherapeutic agents [Section 1.1.5] [Burrow, 1997].

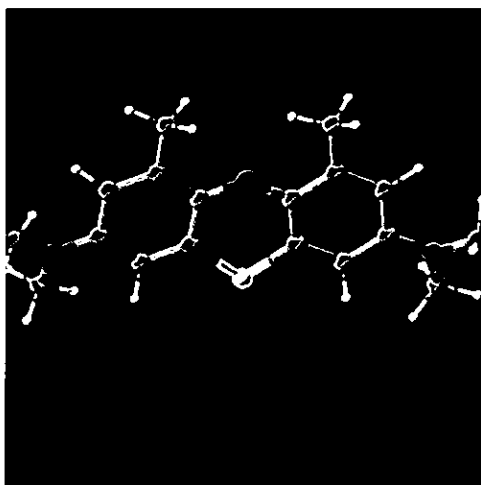
[a]



[b]



[c]



[d]

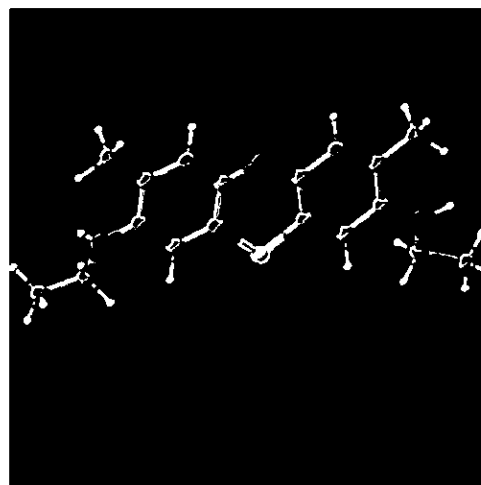


Figure 13. Schematic representations of the photosensitizers used in this study, [a] MB, [b] MMB, [c] DMMB and [d] NMB. MB has typically a 2-benzene ring structure joined by one nitrogen (blue) and one sulphur (yellow) atom. MMB has a substituted methyl (-CH₂-) group at position 1- of the basic phenothiazinium molecule. DMMB has substituted methyl groups at positions 1- and 9- of the molecule. NMB has methyl groups at positions 2- and 8- and the dimethylamino groups [(CH₃)₂N-] at positions 3- and 7- are replaced by ethylamino groups [CH₃CH₂NH-].

2.3 MATERIALS & METHODS

2.3.1 General Reagents

Methylene blue (MB), 1,9-dimethyl methylene blue (DMMB), new methylene blue N (NMB), 1,3-diphenylisobenzofuran (DPIBF), *N,N*-dimethylaniline, 3-(dimethylamino)toluene, methanol (spectrophotometric grade) and 1-octanol were purchased from Aldrich (Gillingham, UK) and used without further purification. Trypsin, MTT (3-[4,5-dimethylthiazol-2-yl]-2,5-diphenyl-2*H*-tetrazolium bromide) and DMSO (dimethyl sulfoxide) were obtained from Sigma (Poole, UK).

2.3.2 Photosensitizers

2.3.2.1 Preparation

MB, MMB and DMMB were recrystallised from methanol prior to use. 1-Methyl methylene blue (MMB) was synthesised from *N,N*-dimethylaniline and 3-(dimethylamino)toluene, using the oxidative method as described by Fiertz-David [1949]. The purity of the photosensitizers was ensured by thin layer chromatography (silica gel, eluent methanol/chloroform/acetic acid 85:10:5). The purity of MMB was further examined by high performance liquid chromatography: a 3.3 cm Perkin Elmer RPC-18 short column was employed with 10 % (v/v) methanol/water as the mobile phase. This gave a single peak with the same retention time (0.30 minutes) when monitored at either 656 nm or 290 nm. Proton magnetic resonance spectroscopy (Bruker WM250) gave the following peaks in D₂O: (3H, s CH₃-Ar), 2.7 (12H, s [CH₃]₂N), 6.2-6.9 (5H, m, Ar-H). Spectral measurements of stock solutions of the 4 photosensitizers (1 mg ml⁻¹ in methanol) were carried out on a Hewlett Packard 8452A diode array spectrophotometer.

2.3.2.2 Singlet Oxygen Measurements

The four photosensitizers were assayed for efficiency of singlet oxygen production using the decolourisation of DPIBF in methanol. Thus, the decrease in absorption at 410 nm was monitored spectrophotometrically with time as in the method of Cincotta *et al.* [1987]. The singlet oxygen yield for MB ($\Phi_{\Delta MB}$) is given as 0.443 [Cincotta *et al.*, 1987]. By assuming that the decrease in absorption of DPIBF at 410 nm is directly

proportional to its reaction with singlet oxygen, the time for a fifty per cent decrease in absorption of DPIBF at 410 nm is directly proportional to its reaction with singlet oxygen. The time for a fifty per cent decrease in absorption caused by each of the photosensitizers under identical conditions ($t_{1/2MBD}$) thereby gives a measure of its photosensitizing efficiency. Thus, the time for the DPIBF absorption to decrease by fifty per cent due to MB photosensitization ($t_{1/2MB}$) was taken as 1.0. To calculate the singlet oxygen yield for the methylated methylene blue derivatives ($\Phi_{\Delta MBD}$), the following formula was used.

$$\Phi_{\Delta MBD} = \Phi_{\Delta MB} \cdot \frac{t_{1/2MB}}{t_{1/2MBD}}$$

2.3.2.3 Hydrophobicity Values (Log *P*)

The hydrophobicities of the photosensitizers were calculated in terms of log *P*, the logarithm of their partition coefficients between phosphate-buffered saline and 1-octanol. The data were calculated using the standard spectrophotometric method [Pooler & Valenzano, 1979] based on the relationship

$$\text{Log } P = \text{Log} \left\{ \frac{(A - A^1) V_w}{A^1 V_o} \right\}$$

where *A* and *A*¹ are the absorption intensities before and after partitioning respectively, and *V*_w and *V*_o are the respective volumes of the aqueous and 1-octanol phases. Determinations were repeated five times.

2.3.2.4 Reduction Rates

Reduction rates for the four photosensitizers were determined by monitoring the diaphorase-catalysed conversion of NADH to NAD⁺ at 340 nm, using a spectrophotometer attached to a chart recorder. (Both forms of the coenzyme absorb light at 260 nm but only the oxidised form, NADH, absorbs at 340 nm). Diaphorase is probably a denatured lipoamide dehydrogenase and is the name loosely applied to

several enzymes which catalyse the oxidation of either β -NADH or β -NADPH in the presence of an electron acceptor such as methylene blue or 2,6-dichlorophenol-indophenol. Many different assay procedures and 'units' are used and diaphorases specific of β -NADH or β -NADPH are known. For this experiment, into a quartz cuvette were added 1 ml photosensitizer (20 μ M in HBSS) and 100 μ l NADH (2.5 mg ml^{-1} in HBSS), and the spectrophotometer set to zero. The reaction was initiated by the addition of 50 μ l diaphorase (from *Clostridium kuyven*, 13 BAEE units mg^{-1} solid, 1 mg ml^{-1} in HBSS) (Sigma) to the cuvette. Rates of reduction were calculated initially as absorption units/minute and converted to enzyme activity (μ moles/litre/minute) using the molar extinction coefficient (ϵ) for NADH, which is 6220 $\text{mol}^{-1} \text{cm}^{-1}$ at 340 nm.

2.3.3 Cell Culture

2.3.3.1 Maintenance of the EMT-6 Cell Line

The murine mammary tumour cell line (EMT-6) was originally obtained from Zeneca Pharmaceuticals, Macclesfield, Cheshire. Cultures of cells were grown routinely in 25 cm^2 tissue culture flasks (Falcon, Fahrenheit Laboratories, Rotherham, U.K.) in a 100 % humidified incubator (Napco, Model 5410, maintained at 37°C, 5 % CO_2 : 95 % air). They were cultured in RPMI 1640 culture medium (Life Technologies, Paisley, UK), supplemented with 10 % (v/v) foetal calf serum (Labtech International, Rigger, East Sussex, U.K.), 200 mM glutamine (Sigma) and penicillin (10 000 units ml^{-1}) / streptomycin (10 000 $\mu\text{g} \text{ml}^{-1}$) (Sigma). Subculture was performed every two to three days. For this, monolayer cultures of cells were dissociated using trypsin (activity 1200 BAEE units/mg solid) (Sigma) in 0.5 % (w/v) ethylenediaminetetraacetic acid (EDTA) (Sigma) in phosphate buffered saline (PBS) and resuspended at 5×10^4 cells per 10 ml medium.

Stock cultures were regularly frozen down at a rate of approximately $1^\circ\text{C} \text{min}^{-1}$ and preserved in 1 ml aliquots in liquid nitrogen at a density of $5 \times 10^6 \text{ml}^{-1}$ in RPMI 1640 medium containing 20 % (v/v) foetal calf serum and 10 % (v/v) DMSO (Sigma). When required, frozen stocks were thawed rapidly by immersion of the freezing vials (Sigma) in a 37°C water bath. The cells were then washed with RPMI 1640 medium, centrifuged at 150 g for five minutes, the medium aspirated and replaced with fresh

medium in order to remove the DMSO. The cell line was passaged at least twice prior to experimental use. All manipulations were carried out aseptically in a laminar air flow cabinet (Flow Gelaire BSB 4A).

2.3.3.2 Growth Kinetics of the EMT-6 Cell Line

Cultures of cells in the exponential phase of growth were dissociated using trypsin and resuspended at a cell density of 1×10^4 cells ml⁻¹. 2 ml aliquots of this suspension were seeded into 35 mm tissue culture plates and incubated in a humidified atmosphere at 37°C, 5 % CO₂: 95 % air. Three plates were removed at twenty-four-hour intervals and the cell number calculated by counting with an improved Neubauer haemocytometer. The medium was replaced on the remaining plates when necessary. A growth curve was constructed with growth of the cell line calculated as cell number per plate, with each point representative of three counts.

2.3.3.3 Cytotoxicity of the Photosensitizers against the EMT-6 Cell Line

A cell suspension of EMT-6 cells in RPMI 1640 was prepared at a density of 5×10^3 cells per ml and sufficient volume to seed eight 96-well microtitre plates (Falcon, Fahrenheit Laboratories, Rotherham, U.K.). Cells were seeded 1000 per well (in 200 µl medium) and incubated at 37°C, 5 % CO₂ and 95 % air for two days. Varying concentrations of each dye (0 to 160 µM) were added and the cells incubated, as previously, for three hours. The medium containing the drug was then aspirated and the cells rinsed twice with 200 µl RPMI 1640, before replacing with a further 200 µl RPMI 1640. Each plate was either illuminated for thirty minutes or kept dark. Light from a source of variable wavelength but with maximum emission in the 600 to 700 nm region and a fluence of 4 mW cm⁻² was used to illuminate plates of cells that had been exposed to the various dyes. The light dose was measured using a Skye SKP 200 light meter (Skye Instruments Ltd.). The temperature of the system was monitored constantly during irradiation but no heating effect was observed. Following this treatment, the cells were grown on again at 37°C, 5 % CO₂: 95 % air for a further three days. To evaluate cell viability and then calculate percentage toxicity, the MTT assay was adapted from Carmichael *et al.* [1987]. 25 µl MTT (5 mg ml⁻¹ in PBS) was added to each well and the plates returned to the incubator for five hours. The medium and MTT were subsequently aspirated, taking care not to disturb the formazan crystals. 100 µl DMSO was then added to each well to solubilise the crystals. The plates were shaken

for ten minutes and the absorbances read on a plate reader (Anthos HT111, measuring filter 540 nm; reference filter 620 nm). The various toxicities were calculated as a percentage of control.

2.3.3.4 Light Dose Study

EMT-6 cells were seeded into 35 mm petri dishes (1000 cells per ml in 2 ml of cell suspension), then grown on for two days in RPMI 1640 medium whilst being maintained at 37°C, 5 % CO₂ and 95 % air. After two days, the medium was removed and replaced by 2 ml of either 12 µM MB, 2.5 µM MMB, 0.2 µM DMMB or 0.4 µM NMB in RPMI 1640 (*i.e.* doses giving 5 % dark toxicity), with each experiment being carried out in triplicate. The cells were incubated in the presence of drug for a further three hours. Medium and drug were then removed, the cells rinsed with 2 ml of RPMI 1640 and finally 2 ml of medium replaced. The cells were illuminated with a fluence of either 9.8 mW cm⁻², 4.7 mW cm⁻², 3.3 mW cm⁻² or 2.0 mW cm⁻² for thirty minutes (corresponding to light doses of 17.6, 8.5, 5.9 or 3.6 J cm⁻², respectively), then grown on as above for a further three days. The cells in each petri dish were then counted microscopically using the improved Neubauer haemocytometer.

2.3.3.5 Uptake of the Photosensitizers in EMT-6 Cells

Spectral measurements on doubling dilutions of dye (0 to 20 µM in methanol) were carried out to check adherence to the Beer-Lambert law, and in order to construct a calibration curve expressed in picomoles dye/1000 cells.

Suspensions of EMT-6 cells were seeded into 75 cm² culture flasks at a cell density of 8 x 10⁴ cells ml⁻¹, in 20 ml RPMI 1640 medium, supplemented with 10 % (v/v) foetal calf serum, 200 mM L-glutamine and penicillin/streptomycin solution (at 1 × 10⁴ units and 10 mg ml⁻¹, respectively). The cells were then incubated at 37°C, 5 % CO₂: 95 % air and grown to confluence over five days. The medium was aspirated and replaced by doubling dilutions of each photosensitizer (0 to 10 µM) in 20 ml RPMI 1640 medium or by 20 ml RPMI 1640 medium for the control. Cultures of cells were also incubated in the presence of the photosensitizers (all at 5 µM) for 0.5, one, two or three hours under the same conditions.

Following incubation, the medium was aspirated from each flask and the cell monolayers rinsed twice with PBS to remove all traces of the photosensitizers. The cell monolayers were dissociated by the addition of 1 ml 0.25 % (w/v) trypsin (1200 BAEE units/mg solid) and 0.5 % (w/v) EDTA in PBS. The cells were resuspended in 10 ml RPMI 1640 to prevent further digestive action of the trypsin, and counted using an improved Neubauer haemocytometer. The cell suspensions were centrifuged for ten minutes at 150 *g* and the supernatants discarded. Each pellet was rinsed and resuspended twice in 2 ml PBS. The supernatant was aspirated and 1 ml methanol was added to each final pellet, mixed and left for ten minutes. The cell suspensions were then centrifuged at 2000 *g* for thirty minutes and the absorbances of the supernatants determined spectrophotometrically using λ_{max} values of 664 nm (MB), 656 nm (MMB), 648 nm (DMMB) and 630 nm (NMB) as determined previously [Section 2.2.2.1 and 2.3.1.1].

2.4 RESULTS

2.4.1 Photosensitizers

2.4.1.1 Absorption Spectra

The photosensitizers [for structures see Figure 13] were found to obey Beer's Law in the concentration range 10^{-5} to 10^{-7} M. In addition, the absorption spectra showed no change in the pH range 1 to 8. MB and its derivatives all have absorbance maxima at long (red) wavelengths, corresponding to the therapeutic window (600 to 800 nm) for PDT [Figure 14]. The three derivatives exhibited small hypsochromic shifts in long wavelength absorption compared to that of MB, and all of the methylated derivatives had slightly decreased intensities [Table 2].

2.4.1.2 Singlet Oxygen

Singlet oxygen yields, expressed as the relative rates of photosensitized oxidation of DPIBF in methanol at 279 K and measured as the decrease in absorption at 410 nm to half its original value, were elevated in all three derivatives compared to MB, following the order NMB>DMMB>MMB>MB [Table 2].

Table 2. Physicochemical data for the photosensitizers, MB, MMB, DMMB and NMB, and including data for the benzo[a]phenothiazinium, EtNBS, for comparison. (^aWavelength of maximum light absorbance, ^blogarithm of the extinction coefficient measured in aqueous buffer at pH 7.3, ^csinglet oxygen yield based on MB = 1.00 and ^dlogarithm of the partition coefficient between water and 1-octanol).

photosensitizer	λ_{\max} (nm) ^a	Log ϵ_{\max} ^b	¹ O ₂ ^c	Log P^d
MB	664	4.98	1.00	-0.10
MMB	656	4.78	1.11	+0.7
DMMB	648	4.91	1.22	+1.0
NMB	630	4.95	1.35	+1.2
EtNBS	652	4.84	0.06	+2.76

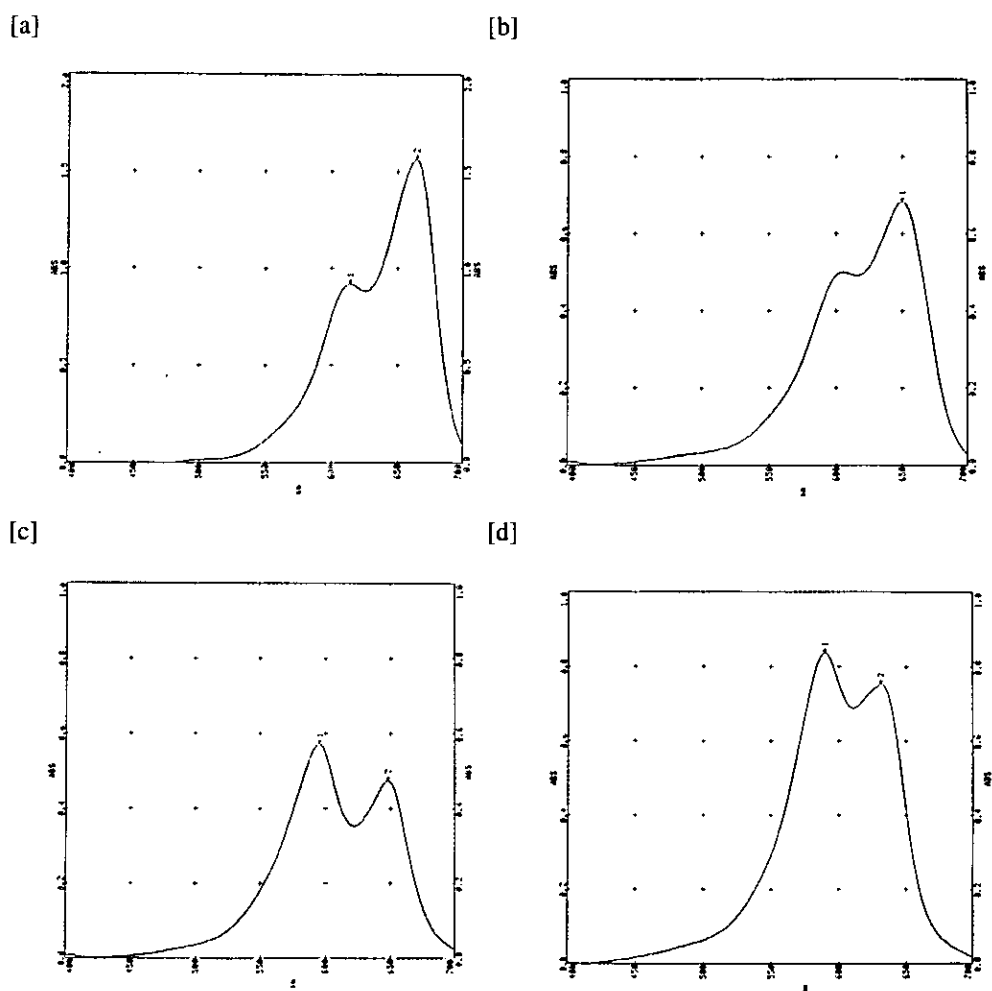


Figure 14. Absorption spectra of the photosensitizers in methanol, [a] MB, [b] MMB, [c] DMMB and [d] NMB. Values for λ_{max} are MB = 664 nm, MMB = 656 nm, DMMB = 648 nm and NMB = 630 nm.

2.4.1.3 Hydrophobicity Values (Log *P*)

The hydrophobicities of the methylated derivatives, calculated in terms of Log *P*, the logarithm of their partition coefficients between PBS and 1-octanol, were increased compared to the lead compound, MB, and followed the order NMB>DMMB>MMB>MB. The three derivatives have positive log *P* in contrast to that of MB itself, which is negative [Table 2].

2.4.1.4 Reduction Rates

Reduction rates were determined by monitoring spectrophotometrically the diaphorase-catalysed conversion of NADH to NAD⁺ in the presence of photosensitizers. By this method, chromophore methylation was found to decrease the reduction potential of the resulting compound and followed the order MB<NMB<MMB<DMMB. The order of the rates of reduction for MB, MMB and DMMB corresponded to the degree of methylation of the molecule, but the results for NMB deviated from the expected trend. NMB was less easily reduced than MB, with a value of almost half that of the parent compound, but was more readily reduced than both MMB and DMMB [Figure 15].

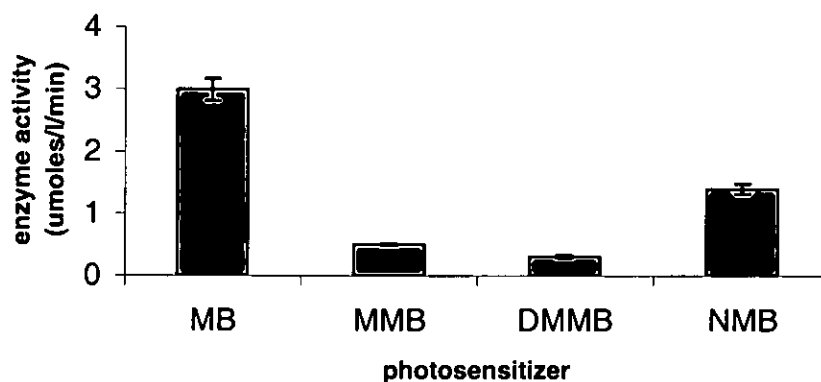


Figure 15. Rates of reduction for the photosensitizers, MB, MMB, DMMB and NMB, measured by monitoring the diaphorase-catalysed oxidation of NAD⁺ to NADH at 340 nm in the presence of each photosensitizer at 20 μ M concentrations. Each bar is the mean of ≥ 4 experiments \pm SEMs.

2.4.2 Cell Culture Experiments

2.4.2.1 Growth Kinetics of the EMT-6 Cell Line

The growth curve [Figure 16] was used to determine subculture regimes and experimental protocols involved in the testing of the photosensitizers on EMT-6 cells. After seeding, EMT-6 cells entered a characteristic lag period of two days, followed by a period of exponential growth over a further two to three days (the 'log' phase doubling time), before a final period of reduced or zero growth after they had become confluent.

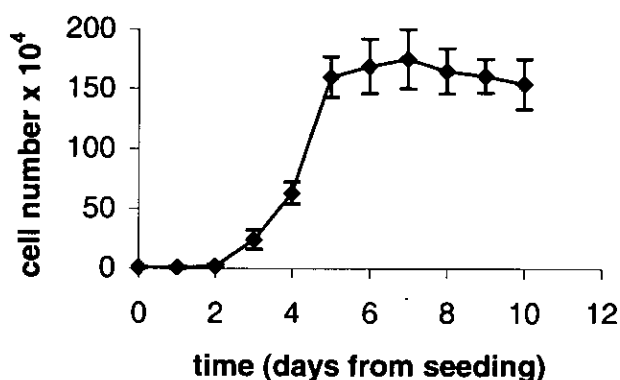


Figure 16. Growth kinetics of the murine, mammary tumour cell line, EMT-6, incubated in a humidified atmosphere at 37°C and in the presence of 95 % air, 5 % CO₂. Each point is the mean of 3 experiments carried out in triplicate ± SD.

2.4.2.2 Cytotoxicity of the Photosensitizers in EMT-6 Cells

Statistical analysis, using the Student's t-test, was carried out to confirm that exposure of EMT-6 cells to white light alone (7.2 J cm⁻²) did not produce cytotoxicity ($p < 0.05$) [Figure 17]. The methylated derivatives were more toxic against EMT-6 cells under dark conditions than was MB [Figure 18]. Using 7.2 J cm⁻² of white light, the associated photocytotoxic effects were also far greater with the derivatives than with MB. In terms of clinical application, the greater the ratio of light:dark toxicity, the more beneficial the photosensitizer. The IC₅₀ for MB at this light dose was 18.7 μM, with a corresponding dark toxicity of 7.9 %. Thus the toxicity ratio (light:dark) here was 50:7.9 = 6.3. The corresponding light:dark ratios for MMB, DMMB and NMB at their respective IC₅₀s are 11.9, 17.2 and 10.0. However, the IC₉₀ may give a more

useful clinical indication. For example, the IC_{90} value for DMMB on illumination at 7.2 J cm^{-2} is $0.27 \mu\text{M}$, and at this concentration the dark toxicity corresponded to a cell kill of 21.3 %, giving a ratio of 4.2. The corresponding ratios for NMB, MMB, and MB were 13.2, 6.3, and 3.2 respectively [Table 3].

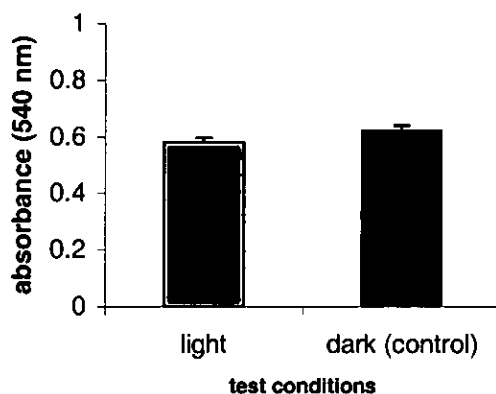
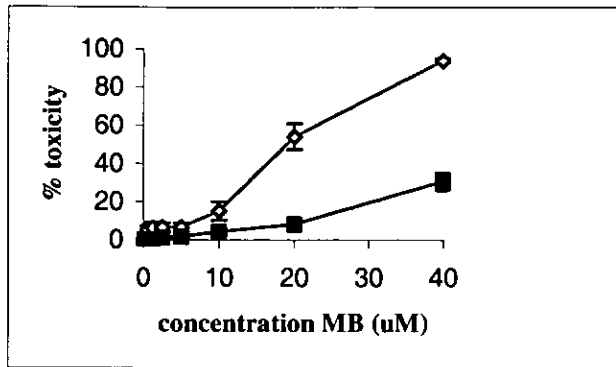
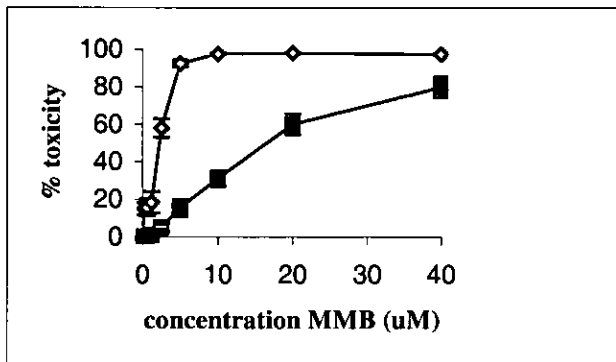


Figure 17. Effect of light (7.2 J cm^{-2}) on EMT-6 cells in culture. Cell viability was evaluated using the standard MTT assay adapted by Carmichael *et al.* (1987). MTT is a yellow tetrazolium dye that is reduced by the mitochondria of living cells to purple formazan crystals. The crystals are solubilised in DMSO and their absorbance read spectrophotometrically at 540 nm. Each point represents the mean of 8 experiments \pm SEMs.

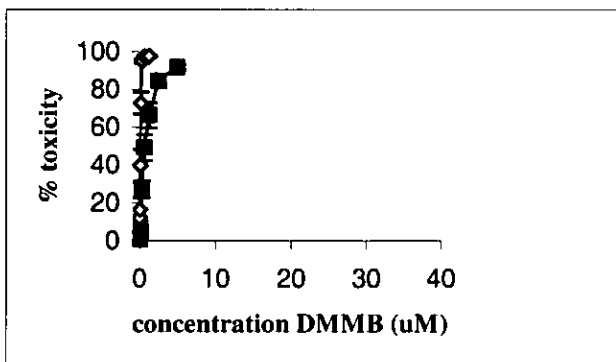
[a]



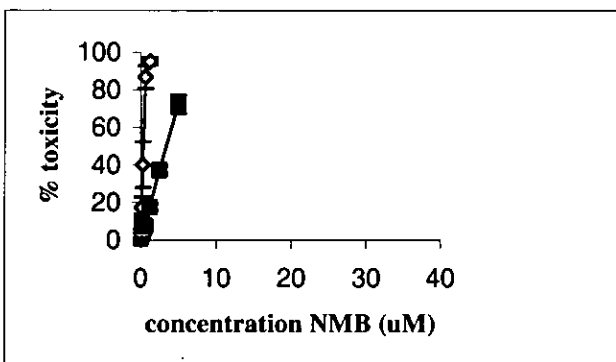
[b]



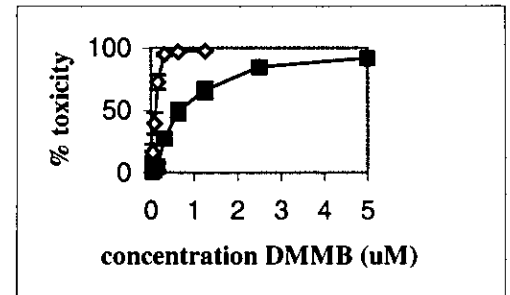
[c]



[d]



[e]



[f]

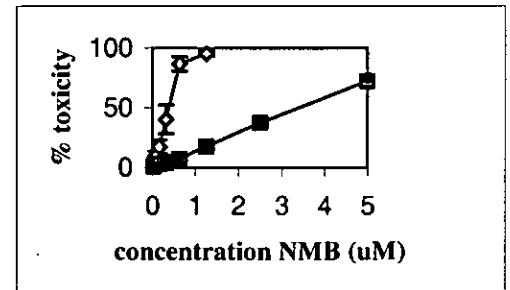


Figure 18. Photocytotoxicity [\blacklozenge] and dark toxicity [\blacksquare] of the photosensitizers [a] MB, [b] MMB, [c] DMMB and [d] NMB against the murine mammary tumour cell line, EMT-6. Responses at low concentrations of DMMB and NMB are represented in figures [e] and [f] respectively. Each point is the mean of at least 8 experiments \pm SEM.

Table 3. Toxicity data and light : dark ratios for the photosensitizers used in this study.

photosensitizer	dose (μM)	% light toxicity	% dark toxicity	light : dark toxicity
MB	18.7	50	7.9	6.3
MMB	2.20	50	4.2	11.9
DMMB	0.09	50	2.9	17.2
NMB	0.39	50	5.0	10.0
MB	37.7	90	27.9	3.2
MMB	4.80	90	14.2	6.3
DMMB	0.27	90	21.3	4.2
NMB	0.61	90	6.8	13.2

2.4.2.3 Light Dose Study

The light dose study was carried out at photosensitizer concentrations giving 5 % dark toxicity [Figure 19]. At this concentration, MB did not reach 100 % photocytotoxicity even at the highest light dose used (17.6 J cm^{-2}). This was considerably less than that used by Canete *et al.* who reported $\cong 100$ % cell death in HeLa cells at 90 J cm^{-2} with $10 \mu\text{M}$ MB [Canete *et al.*, 1993]. The methylated derivatives were already close to 100 % photocytotoxicity at the original light dose used (7.2 J cm^{-2}) and concentrations giving 5 % dark toxicity, so the increased light dose made little improvement on the photocytotoxicity in these cases. However, it was noticeable that the photocytotoxicity of MMB and NMB decreased slightly at light doses $< 7.2 \text{ J cm}^{-2}$ [Figure 19]. In terms of the light:dark differential, this was greatest ($78:5 = 15.6$) for MB at the highest light dose used (17.6 J cm^{-2}). The ratio for MMB and NMB approached 20 at the maximum light dose, whilst that for DMMB was $\cong 20$ across the light dose range. A maximum ratio of 20 light:dark toxicity may therefore be possible for MB at further increased light doses.

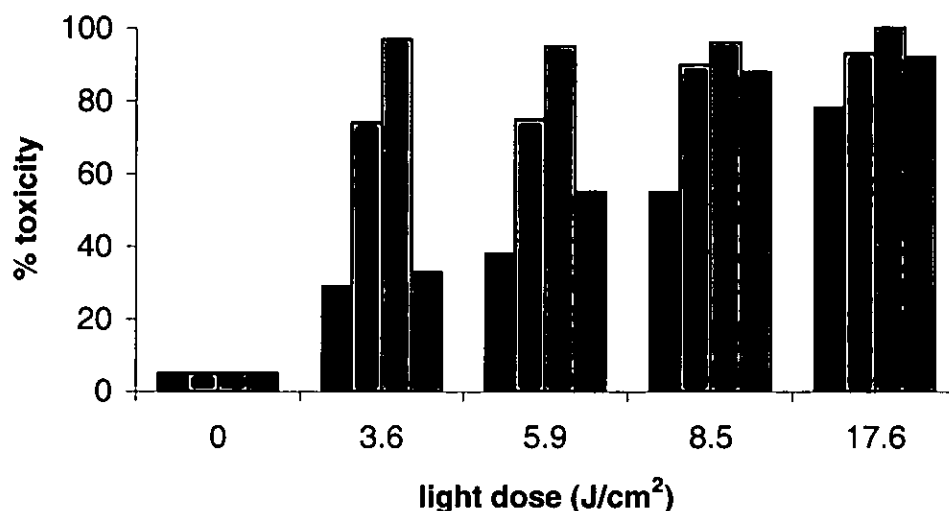


Figure 19. Photocytotoxicity of the photosensitizers, MB [■], MMB [■], DMMB [■] and NMB [■] against the EMT-6 cell line as a function of the light dose. Photosensitizer concentration in each case was that giving 5 % dark cytotoxicity. Each bar is the mean of μ 9 experiments and standard error was less than 5 % in all cases.

2.4.2.4 Uptake of the Photosensitizers in EMT-6 Cells

For calibration curves of photosensitizers in methanol, see Appendix 1. The three derivatives, MMB, DMMB and NMB showed good correlation between extracellular photosensitizer concentration and cellular uptake after three hours incubation [Figure 20]. The parent compound, MB, showed a concentration-dependent increase only up to a concentration of 2.5 μ M. At concentrations of 2.5 to 10 μ M uptake of MB almost levelled. The order of concentration-dependent uptake of the dyes over three hours was MB<MMB<DMMB<NMB [Figure 20].

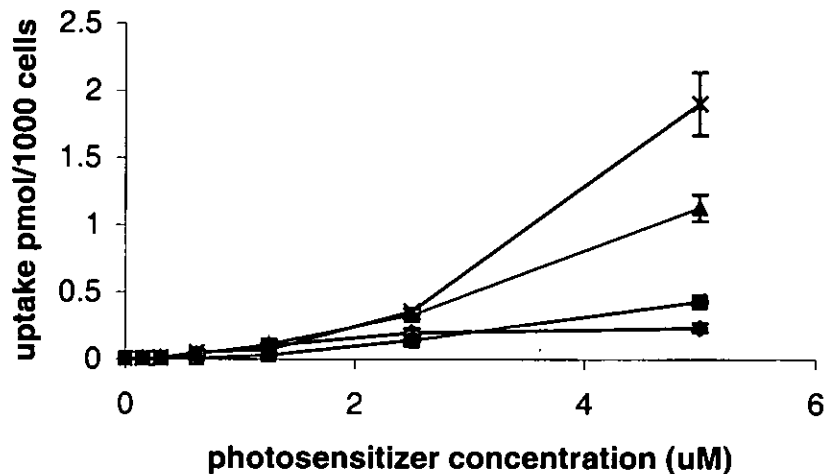


Figure 20. Uptake of the photosensitizers MB [◆], MMB [■], DMMB [▲] and NMB [x] into EMT-6 cells over a range of concentrations. Each point is the mean of 4 experiments carried out in triplicate ! SEM.

Evidence of cellular uptake of all the photosensitizers was apparent after only thirty minutes of incubation with a significant amount present after one hour [Figure 21]. The degree of uptake after thirty minutes was MB=MMB<NMB<DMMB. At one to three hours the pattern of uptake was MB<MMB<DMMB<NMB [Figure 21].

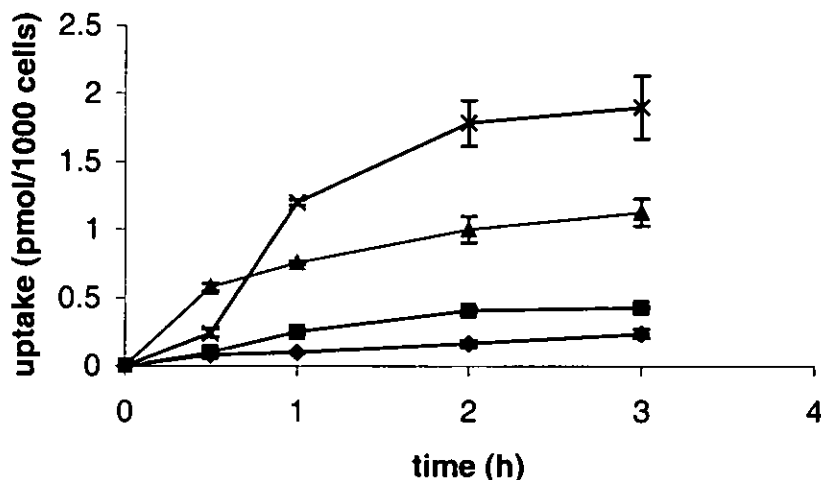


Figure 21. Uptake of the photosensitizers MB [◆], MMB [■], DMMB [▲] and NMB [x] at 5 μM concentrations into EMT-6 cells over a period of 3 hours. Each point is the mean of 4 experiments carried out in triplicate ! SEM.

2.4 DISCUSSION

We have shown that, at a white light dose of 7.2 J cm^{-2} , substitution of the established photosensitizer, methylene blue, at various positions of the phenothiazinium chromophore leads to both increased photocytotoxicity and increased dark toxicity in the murine mammary tumour cell line, EMT-6, compared to that of MB itself. However, the ratios for light:dark toxicity were also higher at lower light doses for the methylated derivatives and their levels of photocytotoxicity are comparable to that of the benzo[*a*]phenothiazinium compounds investigated by Cincotta *et al.* [Section 1.5.2] [Cincotta *et al.*, 1993]. For example, against EMT-6 cells, the promising photosensitizer EtNBS gave an IC_{50} of $0.1 \mu\text{M}$. This is comparable with the value of $0.09 \mu\text{M}$ obtained in the present work for DMMB. Moreover, DMMB gave > 90 per cent photocytotoxicity at a concentration of $0.2 \mu\text{M}$ and a light dose of 3.6 J cm^{-2} which is comparable to the 3.3 J cm^{-2} employed with EtNBS. Although the dark toxicity for EtNBS is reportedly much lower for a $0.5 \mu\text{M}$ dose (six per cent compared to forty-one per cent for DMMB), no IC_{90} was reported for the photocytotoxicity [Cincotta *et al.*, 1993]. The IC_{90} value may, in fact, give a more useful indication of clinical potential, particularly when considered alongside the light:dark ratio. The greater the light:dark differential, the greater the clinical potential of the photosensitizer, since a high degree of photosensitizing activity can be achieved with little or no toxicity in the dark, thus minimizing the possibility of systemic side effects. From the present study using the EMT-6 cell line, it is clear that of the four photosensitizers, NMB is more effective as far as light:dark differential is concerned at both the IC_{50} and IC_{90} levels. However, this is most apparent at the IC_{90} since here the light:dark differential for NMB is more than four-fold that of MB, more than double that of MMB and at least three-fold that of DMMB.

The higher dark toxicities and photocytotoxicities of the methylated derivatives may be explained by several factors. As discussed earlier, it is apparent from the literature that phenothiazinium photosensitizers and their benzologues are prone to cellular reduction [Bongard *et al.*, 1995]. Indeed this may be advantageous in the clinic as the rate of reduction of EtNBS in mice is reportedly higher in healthy tissue than in tumours, thus increasing the apparent tumour selectivity and decreasing the probability of skin

photosensitization [Cincotta *et al.*, 1996]. The *in vitro* reduction of MB, MMB and DMMB was examined prior to this study in aqueous media with a gold microdisc electrode using the method of Svetlicec *et al.* [1987] (data not shown) and followed the order MB>MMB>DMMB. In the present study, the *in vitro* reduction of MB and its derivatives was examined by monitoring the diaphorase-catalysed conversion of NADH to NAD⁺ at 340 nm and supported the previous observations, following the order MB>NMB>MMB>DMMB. Thus, from a cellular point of view, it can be argued that the derivatives, particularly MMB and DMMB, will be present in their oxidised (cationic) forms for a longer period of time than MB. There will therefore be higher concentrations of the photoactive form of the methylated derivatives present. The increased stability to reduction, at least in the *in vitro* electrochemical system used, may be explained by the weak electron-releasing effect of the methyl groups. This would make the chromophore more electron rich and thus less amenable to reduction. In cell culture this could contribute to the increased levels both of dark toxicity and photocytotoxicity exhibited by the methylated derivatives.

Methylation of the phenothiazinium chromophore resulted in considerable increases in the hydrophobicity of the system. This was expected, since the non-polar character of the methyl group is well established [Hansch & Leo, 1979]. Indeed, Hansch and Leo give a guideline figure for Log *P* supplement of +0.65 for the addition of one -CH₂-unit. A degree of hydrophobic character (log *P*) is necessary for uptake into cells and will influence, to some extent, intracellular targeting and localisation. The three derivatives have positive log *P* values, whereas that for MB is negative. All three derivatives demonstrated improved and concentration-dependent uptake into EMT-6 cells compared to MB. Uptake of MB was relatively poor with little increase in uptake at concentrations above 2.5 μM. Evidence of cellular uptake of all four photosensitizers was apparent after thirty minutes with a significant amount present after one hour of incubation. Improved cellular uptake and the lower reduction rates are expected to give higher viable intracellular concentrations of the methylated photosensitizers. Taken with the higher singlet oxygen efficiencies, this provides a feasible explanation for the much improved photocytotoxicities encountered, relative to MB. The lower reduction rates, together with potential variation in intracellular localisation may also explain the increased dark toxicities of the methylated derivatives.

As already mentioned, changes in hydrophobicity also bear influence on intracellular localisation and it may be possible that increased hydrophobicity leads to increased mitochondrial targeting. It has been shown previously in fibroblasts that vital stains bearing a unipositive charge and having $0 < \log P < 5$ tend to localise in the mitochondria [Raschid & Horobin, 1990]. It has also been found that the mitochondria of malignant cells preferentially accumulate and retain certain hydrophobic, cationic compounds, such as rhodamine 123 [Summerhayes *et al.*, 1982] and dequalinium chloride [Rashid & Horobin, 1990] to a much greater extent than the mitochondria of most normal cells. MB itself is thought to localise mainly in the cell nucleus [Tuite & Kelly, 1993; Yu *et al.*, 1990]. This could indicate that a different cellular localisation pattern for the methylated derivatives is responsible for their greater observed cytotoxicities.

Phenothiazinium dyes are already established as efficient photosensitizing compounds. However, this efficiency is affected by the substitution pattern in the periphery of the chromophore. For example, the presence of a fused benzene ring lowers the singlet oxygen efficiency as in the benzo[*a*]phenothiazinium series [Lin *et al.*, 1991], as does the inclusion of alkylamino groups at positions 3- and 7- in place of alkylamino [Wainwright *et al.*, 1999]. In the current study, the presence of extra methyl groups in the ring system led to increased singlet oxygen efficiencies in the spectrophotometric assay employed. It is also interesting to note that the singlet oxygen efficiencies of the MB derivatives used in the present study were increased approximately 20-fold compared to that of the promising benzo[*a*]phenothiazinium derivative, EtNBS [Table 2; Figure 12]. In terms of inherent ability to photosensitize the production of singlet oxygen, as measured spectrophotometrically, the order was NMB>DMMB>MMB>MB. Taken with the increased resistance to reduction and the possibility of more critical intracellular localisation, this may explain the greater photocytotoxicity of the methylated derivatives against EMT-6 cells relative to that of MB. Ionisation data for MB, MMB and DMMB is not included as each is fully ionised in the pH range 1-8. Such behaviour separates these three compounds from NMB and other phenothiazinium photosensitizers such as toluidine blue O and the benzo[*a*]phenothiaziniums, such as EtNBS. In NMB, the presence of *N*-ethylamino instead of *N,N*-dimethylamino groups at positions 3- and 7- of the phenothiazinium chromophore facilitates deprotonation of the N-H group, leading to a neutral quinoneimine species. This can be shown

spectrophotometrically in alcohol, the maximum absorption wavelength (λ_{max}) for the NMB cation being 630 nm at neutral pH, the quinoneimine being formed at higher pH with the λ_{max} shifting to 540 nm. Both cationic and neutral forms exist in equilibrium ($[\text{cation}] \gg [\text{quinoneimine}]$) at neutral pH, allowing the possibility of differing uptake mechanisms for this class of compounds. The importance of such behaviour has been reported previously in studies on benzo[*a*]phenothiazinium photosensitizers. The presence of the neutral species as part of an equilibrium may have important ramifications in terms of *in vitro* uptake and *in vivo* pharmacology and may explain the high light:dark differential found with NMB. Such equilibria are not formed by the other photosensitizers in the present study, since the dimethylamino group does not allow deprotonation. In this respect, the presence of the tertiary dimethylamino groups in positions 3- and 7- of the phenothiazine ring system makes the MB system somewhat simpler.

**CHAPTER THREE:
CYTOTOXICITY OF METHYLENE BLUE AND ITS
DERIVATIVES AGAINST THE SK-23 AND SK-MEL-28
MELANOMA CELL LINES.**

3.1 ABSTRACT

The cytotoxicity and photocytotoxicity of methylene blue (MB) and three of its derivatives, 1-methyl methylene blue (MMB), 1,9-dimethyl methylene blue (DMMB) and new methylene blue N (NMB) against two pigmented melanoma cell lines (SK-23, murine melanoma and SK-MEL-28, human melanoma) were investigated in culture. The derivatives were all more effective photosensitizers than MB in both cell lines over a range of light doses (3.6 to 17.6 J cm⁻²). In fact, the patterns of cytotoxicity for the four photosensitizers were very similar to those found earlier against the murine mammary tumour cell line, EMT-6. The increased activity correlated with increased cellular uptake and inherent photosensitizing efficacy. The photosensitizers also showed varying levels of interaction with the biopolymer melanin and, although this appeared to affect uptake and activity, there was no direct correlation with toxicity. Of the four photosensitizers, NMB exhibited with the highest light:dark differential in the SK-23 and SK-MEL-28 cell lines, as was found earlier in the EMT-6 line. In this respect, NMB again demonstrated the greatest clinical potential.

3.2 INTRODUCTION

Melanoma is the most rapidly increasing malignancy in humans and poses the greatest risk in terms of mortality. The two most common forms are superficial spreading melanoma (SSM) and lentigo malignant melanoma (LMM). Early malignant melanomas are usually variegated in colour (ranging from shades of tan and brown to black, sometimes red and white), asymmetrical with irregular borders and generally greater than six millimetres in diameter. As such, they are distinct from benign pigmented lesions that are more uniform in colour and shape. A malignant melanoma is diagnosed on the basis of any significant change in a preexisting melanocytic nevus or in the skin surrounding it, or the development of any new pigmented lesion in patients over forty years of age [Steiner *et al.*, 1987]. Various factors influence the risk of developing malignant melanoma including family history, blond or red hair, freckled skin, excessive solar exposure and/or over three sunburns before the age of twenty years [Clark *et al.*, 1978]. The disease frequently afflicts comparatively young people, with one child in a million under the age of ten developing the disease each year. By the mid-teens this incidence is increased one hundred-fold to one in ten thousand per year. In addition to this, certain benign pigmented lesions pose an added clinical dilemma since they are associated with an increased risk of developing malignant melanoma. These include congenital melanocytic nevi, dysplastic nevi, dysplastic nevus syndrome and common melanocytic nevi, all of which are themselves disfiguring, becoming more difficult to treat with time.

If detected early, skin cancer is easily treatable with a minimum amount of discomfort and scarring. However, melanomas in particular are aggressive tumours and, in the majority of cases, cannot be cured by any of the conventional therapies, once metastasis has taken place. The usual treatment is surgical excision but adjuvant chemotherapy may be employed, particularly decarbazine (DTIC) [Ho, 1995] or limb perfusion involving the nitrogen mustards (*e.g.* melphalan) [Krementz *et al.*, 1994]. Radiotherapy is also an option. Depending on the progress of the tumour at diagnosis, lymphadenectomy may be indicated, although a more conservative approach to dissection may be possible *via* the use of sentinel node demarcation [Rivers, 1996]. With the traditional therapies, there remains the problem of side effects, either due to disfigurement in surgery or to systemic toxicity and immunosuppression following

chemotherapy or radiotherapy. Both in terms of morbidity and patient compliance, the minimization of such side effects is obviously highly desirable. However, even with the increased sophistication of modern cancer treatments, the degree of further improvement of these therapies is limited, mainly due to a fundamental lack of selectivity for tumour tissue. The ongoing search for new drugs and novel therapeutic approaches to cancer treatment, which offer greater selectivity, thus remains important.

A therapeutic approach offering lower toxicity and invasiveness is photodynamic therapy (PDT) [Section 1.2]. Over recent years, dermatology has taken advantage of PDT for the treatment of skin cancer and other skin diseases. In fact, modern PDT was first envisaged as a treatment for cutaneous disease and originates from the first published study of clinical PDT in 1903 by the dermatologist, Jesionek, who successfully treated skin cancer with eosin and light [Section 1.4.1]. The skin has significant advantage over other organs for the application of PDT, in having accessibility to all of its three essential requirements (photosensitizer, visible light and oxygen). Another major benefit is the ability to assess the clinical response visually and the relative ease in obtaining biopsies for analysis. Unfortunately, prolonged acute skin photosensitization limits the application of PDT using the conventional photosensitizer, Photofrin®, in the treatment of cutaneous disease. Nevertheless, in exceptional circumstances, this therapy provides a useful and seemingly effective alternative mode of treatment, yielding high response rates and excellent cosmetic results. PDT has been most extensively studied for the treatment of malignant non-melanotic cutaneous lesions, particularly basal cell carcinoma (BCC), squamous cell carcinoma (SCC) and Bowen's Disease, using either systemic or topical administration of a photosensitizer (or photosensitizer precursor), coupled with a superficial light delivery system [Calzavara-Pinton *et al.*, 1996]. BCC of the skin is the single most common malignancy seen today and its incidence continues to increase. It has been the most commonly treated skin tumour using PDT, with a complete response rate of eighty-three to eighty-eight per cent [Wilson *et al.*, 1989]. Good palliation has also been achieved using PDT for patients with primary and secondary breast carcinomas who have failed one or more of the conventional therapies. Preliminary results in the treatment of advanced classic and AIDS-related Kaposi's Syndrome appear to indicate that PDT may replace ionizing radiation and chemotherapy as the treatment of choice, because it is

very effective and may be repeated several times without causing cumulative side-effects. Unfortunately, results using PDT for SCC have so far been poor and lower than those found with surgery and radiotherapy [Calzavara-Pinton *et al.*, 1996].

Unlike the amelanotic melanomas mentioned above, it is generally believed that pigmented (melanotic) melanomas in humans do not respond well to PDT, due to the presence of the pigment melanin in tumour cells. In fact, there is found to be a correlation between the degree of tumour pigmentation and the PDT response, with a better response found in lighter tumours than darker ones [Calzavara-Pinton *et al.*, 1996]. The situation is further complicated in the case of metastasizing tumours, such as malignant melanoma, since it may be difficult to trace the secondary foci. Natural melanins are biological pigments that can be found in humans in the skin, hair, eyes, and also in the midbrain and inner ear. In mammals, melanins are formed as intracellular granules and are then transferred from melanocytes to epithelial cells where they form the predominant pigment of hair and the epidermis. In the skin and eye, their main role is to afford protection from photodamage as a result of exposure to solar radiation. The capacity of melanins to bind both exogenous and endogenous substances in a dynamic fashion may bring about various, possibly pathogenic, effects in the organism involved. These effects may be implicated in the pathogenesis of certain disease states linked to some long-term drug regimes, for example in the case of chlorpromazine and chloroquine which both induce chorioretinopathy by binding to and subsequent release from retina melanin [Knoerle *et al.*, 1998]. As complex biopolymers with free radical centres that can bind multivalent metal ions, melanins are capable of absorbing light quite strongly even at long, visible wavelengths. They are also able to scavenge reactive oxygen species and to participate in electron-exchange reactions. In lightly pigmented mammalian tissues, light scattering limits the efficacy of PDT in the far-red region (700 to 850 nm) of the spectrum, whilst in heavily pigmented tissues, light absorption by melanin at these wavelengths is still significant. Melanin absorbs light even at the long visible wavelengths used in PDT, thus decreasing the amount of light available to the photosensitizer and possibly reducing the efficacy of the regime [Herd *et al.*, 1997]. In addition, the antioxidant properties of melanin might interfere with the cell killing processes involving oxygen radicals that are commonly associated with PDT [Corsaro *et al.*, 1995]. Such protective effects have been reported against hydrogen peroxide and hydroxyl radicals during Rose Bengal photosensitization (Type I

photosensitization) [Rozanowska *et al.*, 1995], whilst the perylenequinone hypericin exhibited significantly higher photocytotoxicity against amelanotic melanoma cell lines than against a melanin producing melanoma cell line [Hadjur *et al.*, 1996]. In order to circumvent any likely effects of melanin, the use of long-wavelength absorbing photosensitizers, outside the absorption spectrum of melanin, is a logical initial step. Photodamage has been demonstrated in the presence of silicon naphthalocyanine derivatives which display intense absorbances ($\epsilon \approx 500\,000 \text{ l mol}^{-1} \text{ cm}^{-1}$) at 780 nm, although they are significantly less effective against melanotic than amelanotic melanoma cell lines [Soncin *et al.*, 1998]. Benzoporphyrin derivative (BPD-MA) is also reported to be effective *in vivo* against pigmented melanoma in mice, the efficacy being increased by pre-illumination with 1064 nm (near infrared) light in order selectively to break down melanosomes [Busetti *et al.*, 1999]. Finally, the effectiveness of several treatment strategies in metastasizing melanotic melanoma may be severely compromised by the immunosuppressive [Wick, 1983] and mutagenic potential of melanogenesis [Miranda *et al.*, 1984]. Melanin synthesis can, in some cases, induce resistance in melanoma cells to radiotherapy [Hill, 1989], chemotherapy [Slominski *et al.*, 1993] and PDT [Favilla *et al.*, 1995].

Several photosensitizers have been used in dermatology including haematoporphyrin derivative (HpD), Photofrin®, 5-aminolaevulinic acid (5-ALA), benzoporphyrin derivative (BPD), tin ethyl etiopurpurin (SnET2) and monoaspartyl chlorin e6 (MACE). The use of the well-known phenothiazinium photosensitizer, methylene blue (MB), and its congeners in clinical PDT remains sporadic, mainly because PDT has developed from porphyrin-derived drugs [Wainwright, 1996]. However, PDT using topically applied MB (10 % ointment) has been used in dermatology for the treatment of psoriasis and compared with 5-ALA (also 10 % ointment). The responses of the lesions were similar for both drugs although those treated with ALA-PDT were accompanied by a burning sensation, whereas none occurred with MB-PDT [Schick *et al.*, 1997]. Logically, the widespread application of MB and the related phenothiazinium dye, toluidine blue O, in surgical demarcation (such as the tracing of sentinel lymph nodes [Rivers, 1996]), in addition to their widespread use in the clinical staining of carcinomata [Creagh *et al.*, 1995], underlines the low toxicity of the compounds. The efficient photosensitizing behaviour of the phenothiazinium dyes is also well

established [Tuite & Kelly, 1993]. However, in terms of its use in clinical malignancy, MB is utilised locally, mainly against accessible tumours such as superficial bladder cancer [Williams *et al.*, 1989] and has been used against inoperable oesophageal tumours [Orth *et al.*, 1995]. Unlike Rose Bengal, which is an anionic dye and does not bind to melanin, MB is known to have a high affinity for the polymer, as do other cationic compounds [Potts, 1964; Knoerle *et al.*, 1998]. The mechanism behind this is not fully understood, though it could involve the formation of charge-transfer complex and van der Waals' forces between the aromatic rings of MB and the aromatic indole-nucleus of melanin [Foster & Hanson, 1966; Larsson & Tjälve, 1979]. In recent work, Link *et al.* demonstrated high affinity and stable binding of radiolabelled MB to pigmented melanomas in both athymic mice and humans [Link *et al.*, 1996]. The group subsequently reported the use of radiolabelled MB as a tracer for metastatic melanoma in humans. Melanoma secondaries are often less pigmented than the primary lesions due to a 'depigmentation' process that accompanies tumour growth proportionally with the growth rate. Since random dissemination of melanoma makes it virtually impossible to predict the localisation of its metastases, the diagnostic potential of radioiodinated MB in the detection and treatment of small secondaries has been evaluated [Link *et al.*, 1998].

The increased efficacy of MB derivatives having successive chromophore methylation has already been established in the murine mammary tumour cell line, EMT-6 [Chapter 2; Wainwright *et al.*, 1997]. Various physico-chemical characteristics that are pertinent to an efficient photosensitizer and that may be responsible for the increased efficacy (absorption spectra, singlet oxygen efficiency, Log *P*, reduction rates, cellular uptake) have also been investigated. The present study is an investigation into the activity of MB and the same phenothiazinium derivatives against a murine melanoma cell line (SK-23) and a human melanoma cell line (SK-MEL-28). The ability of the photosensitizers to bind to melanin was also examined.

3.3 MATERIALS & METHODS

3.3.1 Reagents and Photosensitizers

3.3.1.1 Preparation

The photosensitizers, methylene blue (MB), 1-methyl methylene blue (MMB), 1,9-dimethyl methylene blue (DMMB) and new methylene blue N (NMB), and various reagents were purchased and/or prepared as previously described [Sections 2.3.1 and 2.3.2.1]. Synthetic melanin was purchased from Sigma.

3.3.2 Cell culture

3.3.2.1 Maintenance of the SK-23 and SK-MEL-28 Cell Lines

The melanoma cell lines (murine SK-23 and human SK-MEL-28) were originally obtained from the Cancer Research Centre (Patterson Institute), Christie Hospital, Manchester. Both cell lines were cultured routinely in 25 cm² tissue culture flasks (Falcon, Fahrenheit Laboratories, Rotherham, U.K.) in a 100 % humidified incubator (Napco, Model 5410, maintained at 37°C, 5 % CO₂: 95 % air). They were grown in RPMI 1640 culture medium (Life Technologies, Paisley, UK), supplemented with 10 % (v/v) foetal calf serum (Labtech International, Rigmer, East Sussex, U.K.), 200 mM L-glutamine (Sigma) and penicillin (10 000 units ml⁻¹) / streptomycin (10 000 µg ml⁻¹) (Sigma). Subculture was performed every five to six days (SK-23 cells) or every six to seven days (SK-MEL-28 cells) as previously described [Section 2.3.3.1]. Stock cultures were regularly frozen down and stored in liquid nitrogen, also as previously described [Section 2.3.3.1].

3.3.2.2 Growth kinetics of the SK-23 and SK-MEL-28 Cell Lines

Growth kinetic analysis of the SK-23 and SK-MEL-28 cell lines was carried out as previously described [Section 2.3.3.2].

3.3.2.3 Cytotoxicity of the Photosensitizers against SK-23 and SK-MEL-28 Cells

Toxicity testing of the four photosensitizers, in both the SK-23 and SK-MEL-28 cell lines, was carried out as in Section 2.3.3.3, with the following amendments, taking into account the different growth characteristics of the cells [Section 3.4.1.1]:

[1] Cells were seeded with 1000 cells per well (in 200 μl RPMI 1640) and incubated for three to four days in a humidified atmosphere at 37°C, 5 % CO₂: 95 % air.

[2] Following photodynamic treatment, cultures of cells were grown on for a further four to five days, prior to MTT assay.

3.3.2.4 Light Dose Study

SK-23 or SK-MEL-28 cells were seeded at 1000 cells per well (in 200 μl medium) into 96-well microtitre plates and grown on for three to four days in a humidified atmosphere at 37°C, 5 % CO₂: 95 % air. The cells were then incubated for three hours with the relevant photosensitizers at a dose giving 15 % dark toxicity in the initial toxicity test [Section 3.4.1.2]. The medium containing the drug was then aspirated and the cells rinsed twice with 200 μl RPMI 1640, before replacing with a further 200 μl RPMI 1640. The cells were illuminated with a fluence rate of either 9.8 mW cm⁻², 4.7 mW cm⁻², 3.3 mW cm⁻², or 2 mW cm⁻², for thirty minutes (*i.e.* light dose = 17.6, 8.5, 5.9 or 3.6 J cm⁻²), then grown on as above for a further four to five days. Toxicity was measured as previously described using a standard MTT assay [Section 2.3.3.3].

3.3.2.5 Uptake of the Photosensitizers in SK-23 and SK-MEL-28 Cells

Cellular uptake into SK-23 and SK-MEL-28 cells was carried out for the four photosensitizers as previously described [Section 2.3.3.5].

3.3.3 Melanin Binding Studies

3.3.3.1 Absorption Spectrophotometry

The photosensitizers were assayed for melanin binding following the method of Potts [1964]. Most natural melanins are particulate in nature and not soluble in most solvents so, for conventional spectrophotometric methods, certain synthetic polymers can serve

as reasonable models for analysis. Briefly, the light absorption of 5 μM solutions of the photosensitizers in buffer was measured at the relevant λ_{max} value. The solutions were then stirred vigorously with 10 μg of synthetic melanin (Sigma) for fifteen minutes, centrifuged at 600 g and the absorption of the supernatants re-read on the spectrophotometer. The percentage binding to melanin was thus calculated by difference. Measurements were carried out four times.

3.3.3.2 Absorption Spectra

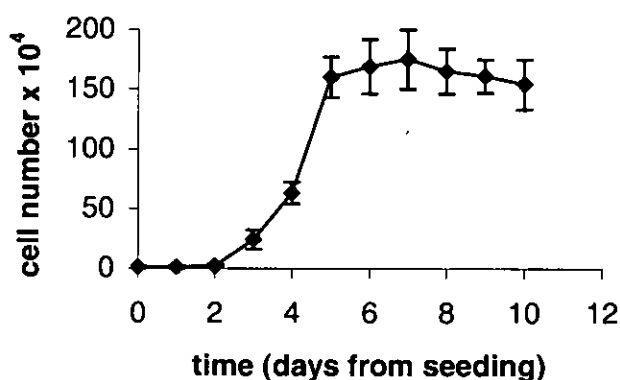
The photosensitizers were prepared as in Section 3.3.3.1 and their absorption spectra recorded both in the presence and absence of melanin.

3.4 RESULTS

3.4.1 Cell Culture Experiments

3.4.1.1 Growth Kinetics

[a]



[b]

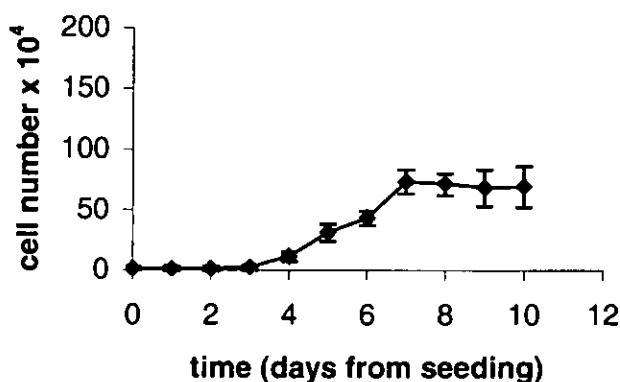


Figure 22. Growth kinetics of [a] the murine, melanoma cell line, SK-23 and [b] the human melanoma cell line, SK-MEL-28, incubated in a humidified atmosphere at 37°C and in the presence of 95 % air, 5 % CO₂. Each point is the mean of 3 experiments carried out in triplicate ± SD.

The growth curves [Figure 22] were used to determine subculture regimes and experimental protocols involved in the testing of the photosensitizers on SK-23 and SK-MEL-28 cells. After seeding, cells entered a characteristic lag period of three days (SK-23 cells) and four days (SK-MEL-28 cells). This was followed by a period of

exponential growth over a further five to six days (SK-23 cells) or six to seven days (SK-MEL-28 cells), before a final period of reduced or zero growth after they had become confluent. The log phase doubling time of these cell lines was therefore considerably longer than that of the EMT-6 cells used in the previous study [Section 2.3.2].

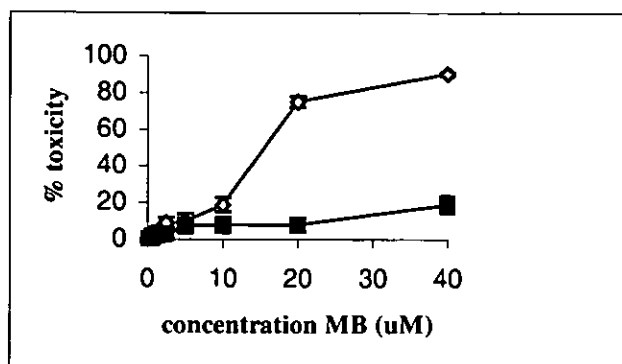
3.4.1.2 Cytotoxicity of the Photosensitizers against SK-23 and SK-MEL-28 Cells

At the standard light dose of 7.2 J cm^{-2} , each of the compounds exhibited higher photosensitising efficacies in both melanoma cell lines compared to the lead compound, MB [Figures 23 & 24]. As in the previous cell culture study using the murine mammary tumour cell line, EMT-6, DMMB was highly photoactive at very low concentrations. The IC_{90} values for DMMB were 0.1 and $0.4 \text{ }\mu\text{mol}$ for the human and murine melanoma cell lines, respectively, and compared with those for the EMT-6 line in the previous study [Table 4]. NMB also performed well against both melanoma cell lines (SK-MEL-28; $\text{IC}_{90} = 0.5 \text{ }\mu\text{mol}$; SK-23; $\text{IC}_{90} = 1.1 \text{ }\mu\text{mol}$) [Table 4]. MMB was less effective in both cell lines than either of the dimethylated photosensitizers, but was considerably more active than MB [Table 4].

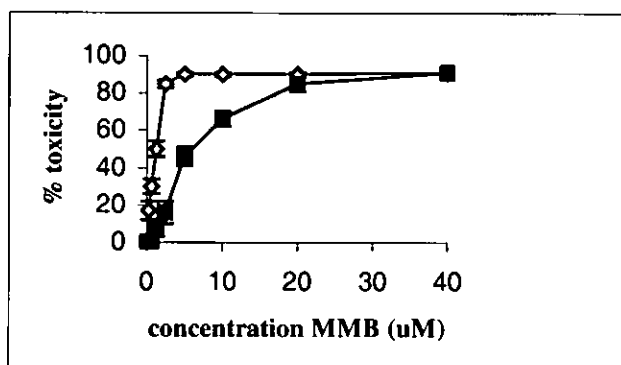
When tested against the SK-MEL-28 human melanoma cell line at the standard light dose (7.2 J cm^{-2}), it was evident that the dark (inherent) toxicities of MB and MMB were appreciable relative to their phototoxicities, even at high phototoxicity values. Thus, $38.8 \text{ }\mu\text{M}$ MB caused 80 % phototoxicity and 52.6 % dark toxicity, while MMB at $9.7 \text{ }\mu\text{M}$ gave 90 % photo- and 43.2 % dark toxicity. The corresponding light:dark ratios were 1.5 and 2.1. In the SK-MEL-28 cell line, DMMB and NMB both exhibited high levels of photocytotoxicity at relatively low corresponding dark toxicities, thus having higher light:dark toxicity ratios than the lead compound, MB. NMB was particularly interesting in this respect, having by far the highest ratio at 7.5 [Table 5].

The behaviour of the photosensitizers against the SK-23 murine melanoma cell line was broadly similar to that in the human melanoma cell line. At the standard light dose, MMB exhibited higher dark toxicity than MB which had a much improved light:dark toxicity ratio. In this cell line, the activity of DMMB was higher than that of NMB, although both showed improved light:dark toxicities (10.2 and 8.0, respectively).

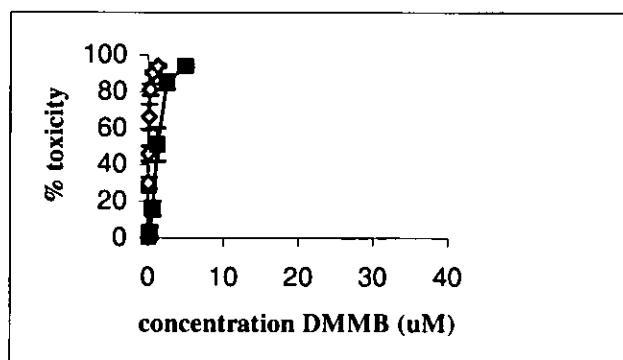
[a]



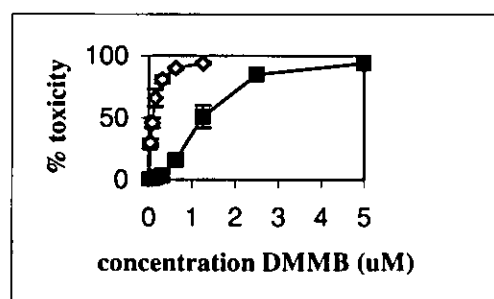
[b]



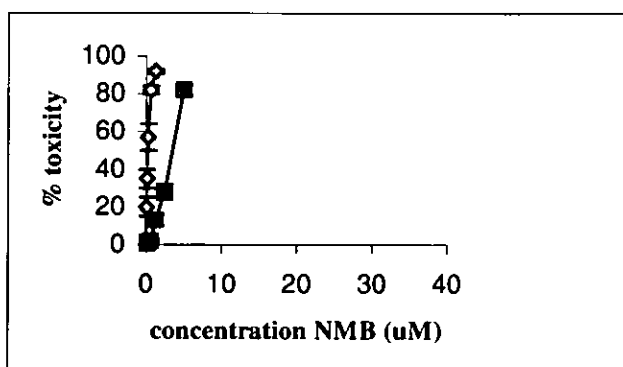
[c]



[e]



[d]



[f]

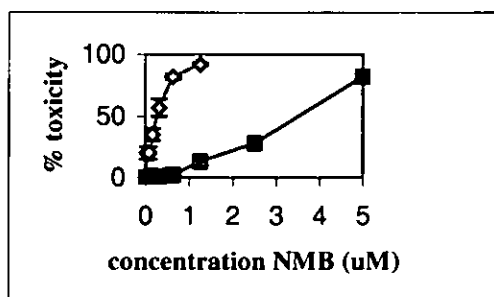
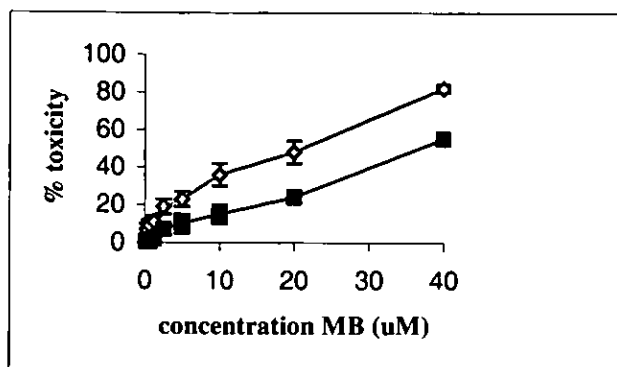
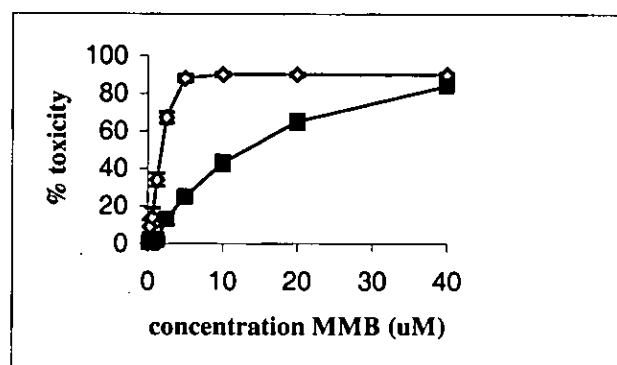


Figure 23. Photocytotoxicity [♦] and dark toxicity [■] of the photosensitizers, [a] MB, [b] MMB, [c] DMMB and [d] NMB, against the murine melanoma cell line, SK-23. Responses at low concentrations of DMMB and NMB are represented in figures [e] and [f] respectively. Each point is the mean of at least 14 experiments \pm SEM.

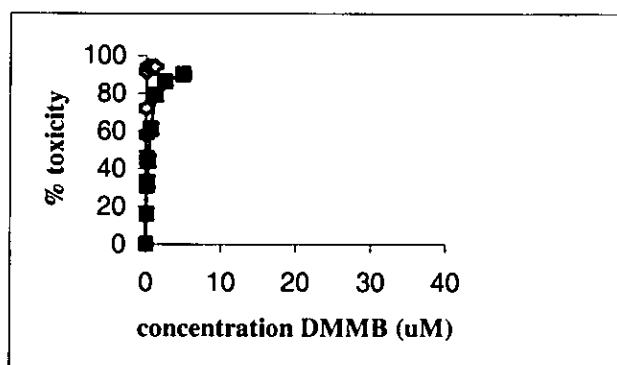
[a]



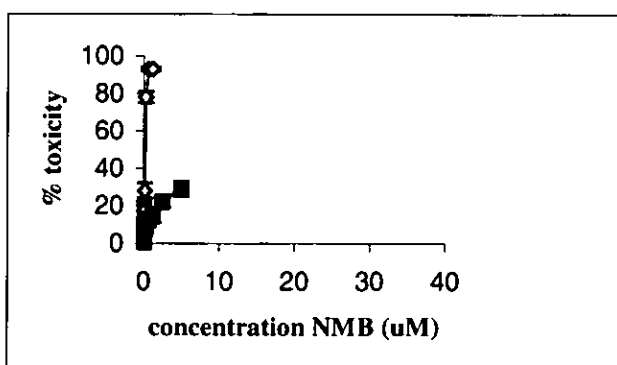
[b]



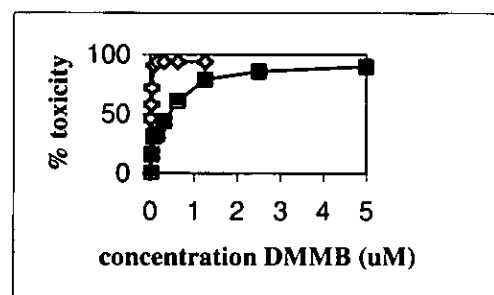
[c]



[d]



[e]



[f]

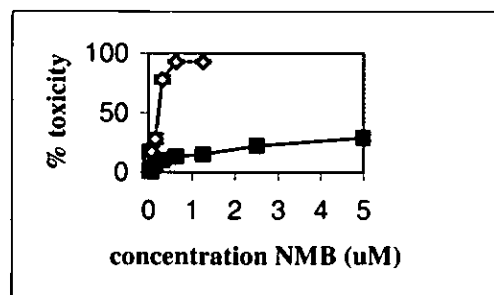


Figure 24. Phototoxicity [♦] and dark toxicity [■] of the photosensitizers, [a] MB, [b] MMB, [c] DMMB and [d] NMB, against the human melanoma cell line, SK-MEL-28. Responses at low concentrations of DMMB and NMB are represented in figures [e] and [f] respectively. Each point is the mean of at least 10 experiments \pm SEM.

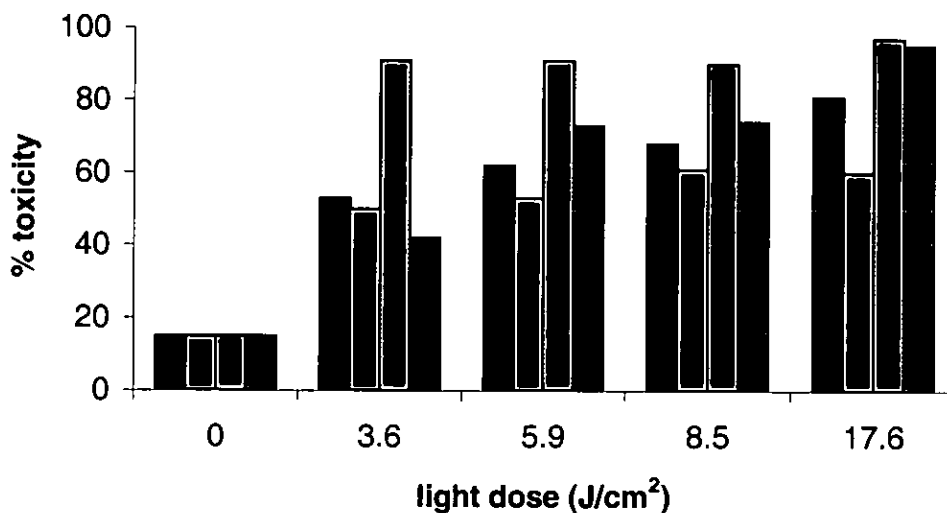
Table 4. Toxicity data and light:dark ratios in the SK-23 cell line for the photosensitizers at a light dose of 7.2 J cm^{-2} .

photosensitizer	dose (μM)	% light toxicity	% dark toxicity	light : dark toxicity
MB	15.2	50	7.8	6.4
MMB	1.6	50	7.0	7.1
DMMB	0.05	50	0	-
NMB	0.3	50	1.0	50
MB	39.6	90	17.6	5.1
MMB	5.0	90	46.0	2.0
DMMB	0.4	90	8.8	10.2
NMB	1.1	90	11.2	8.0

Table 5. Toxicity data and light:dark ratios in the SK-MEL-28 cell line for the photosensitizers at a light dose of 7.2 J cm^{-2} .

photosensitizer	dose (μM)	% light toxicity	% dark toxicity	light : dark toxicity
MB	21.0	50	25.5	2.0
MMB	2.2	50	10.1	5.0
DMMB	-	50	-	-
NMB	0.3	50	9.1	5.5
MB	38.8	80	52.6	1.5
MMB	9.7	90	43.2	2.1
DMMB	0.1	90	31.8	2.8
NMB	0.5	90	12.0	7.5

[a]



[b]

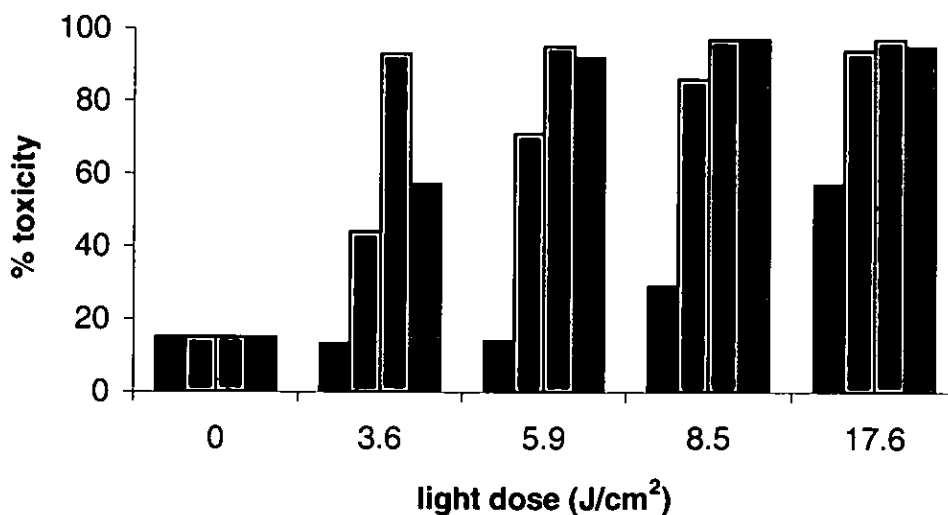


Figure 25. Photocytotoxicity of the photosensitizers, MB [■], MMB [■], DMMB [■] and NMB [■], against [a] SK-23 and [b] SK-MEL-28 cell lines as a function of the light dose. Photosensitizer concentration in each case was that giving 15 % dark cytotoxicity. Each bar is the mean of μ 4 experiments and standard error was less than 5 % in all cases.

3.4.1.3 Light Dose Study

Using a series of light doses (ranging from 3.6 to 17.6 J cm⁻²), and photosensitizer concentrations giving 15 % dark toxicity in the previous experiments [Section 3.4.1.2], MB was clearly the least effective photosensitizer in the human melanoma cell line (SK-MEL-28). The photosensitizer did not, in fact, achieve a complete cell kill even at the highest light dose used in this cell line [Figure 25b]. Here, DMMB demonstrated the highest degree of photocytotoxicity, achieving almost 100 per cent cell kill at all the light doses used, whilst similar results were achieved with NMB at light doses of 5.9 J cm⁻² and above, and with MMB at the highest light dose of 17.6 J cm⁻². In the SK-23 cell line, and with lower light doses, MB and MMB exhibited similar activity [Figure 25a]. However, the light:dark toxicity ratios for these two photosensitizers in this cell line were increased at higher light doses, more so for MMB than for MB [Figure 25a]. Here too, DMMB demonstrated the highest level of photocytotoxicity, again achieving almost 100 per cent cell kill at all the light doses used. NMB achieved 100 per cent kill only at the highest light dose of 17.6 J cm⁻², whereas MB and MMB failed to achieve this at any of the light doses used.

3.4.1.4 Uptake of the Photosensitizers in SK-23 and SK-MEL-28 Cells

The four photosensitizers showed a concentration- and time-dependent uptake into both murine (SK-23) and human (SK-MEL-28) cell lines. Alkyl substitution of the phenothiazinium chromophore influenced cellular uptake in both cell lines, with successive methylation corresponding to successive improvements in cellular uptake [Figures 26 & 27]. The doubly methylated compounds, DMMB and NMB, exhibited the greatest cellular uptake in both cell lines, although their pattern of uptake was reversed. In SK-23 cells, the pattern of uptake was MB<MMB<NMB<DMMB whilst in the SK-MEL-28 line, it was MB<MMB<DMMB<NMB. The relative uptakes of the DMMB and NMB in the SK-23 cell line were similar at the IC_{90s}. At 5 μM concentrations, a significant amount of all four photosensitizers was present within the cells after only one hour of incubation and it also appeared that, after two hours, uptake began to level. Cellular uptake of the photosensitizers was considerably greater into SK-23 cells than into the human (SK-MEL-28) melanoma line. The low dark toxicity of NMB is underlined by the greater uptake of this photosensitizer compared with the more dark toxic DMMB in the human melanoma cell line.

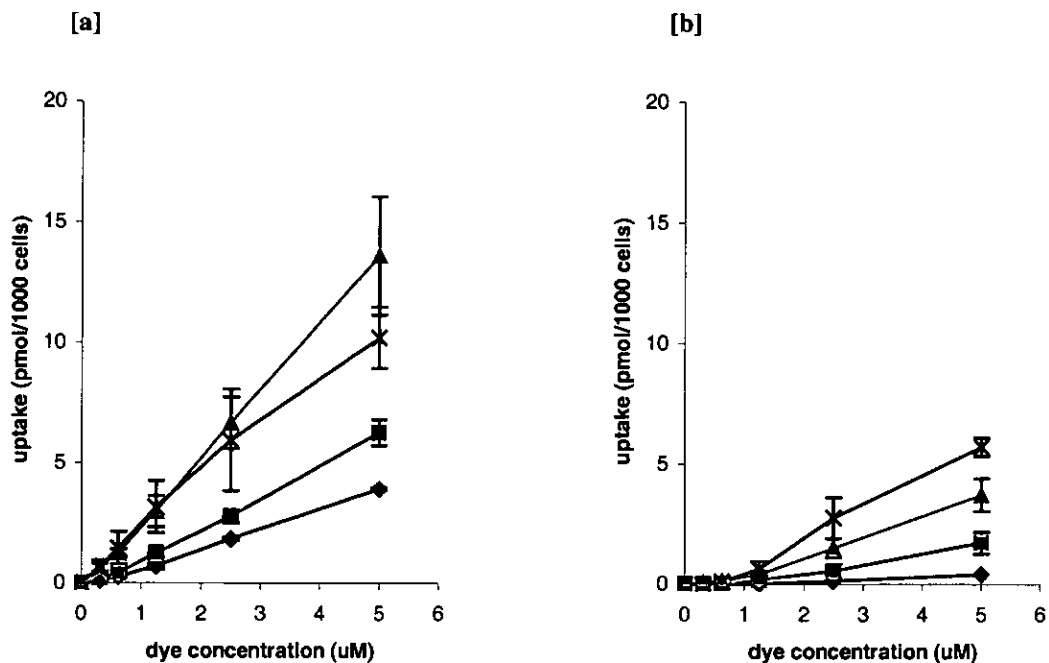


Figure 26. Uptake of the photosensitizers into [a] SK-23 cells and [b] SK-MEL-28 cells of the photosensitizers, MB [◆], MMB [■], DMMB [▲], NMB [×] over a range of concentrations. Each point is the mean of 3 experiments carried out in triplicate \pm standard deviation.

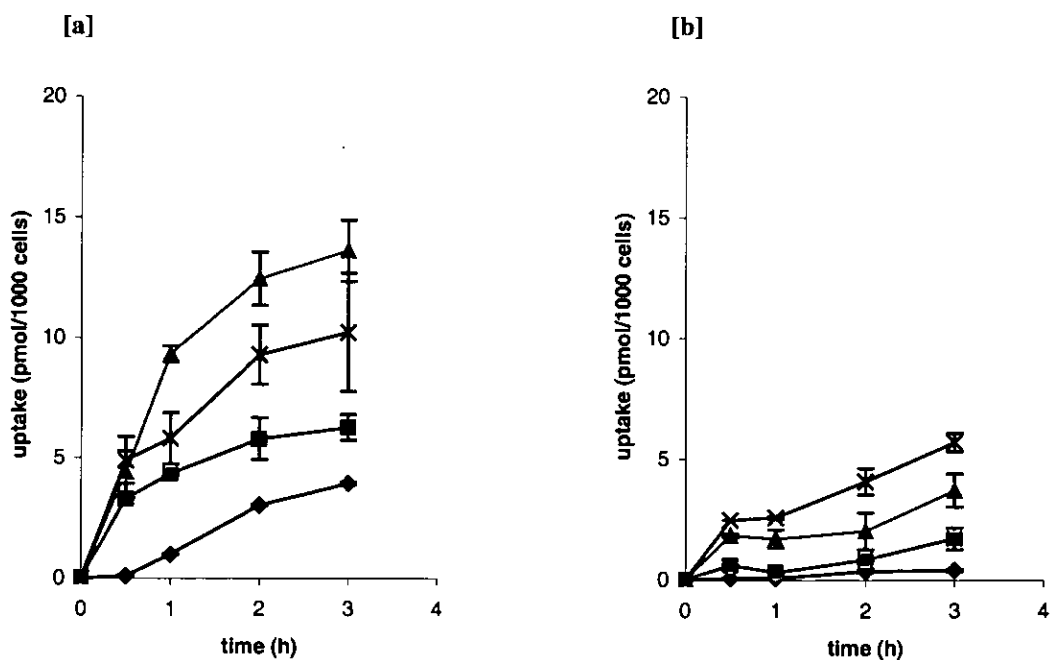


Figure 27. Uptake of the photosensitizers into [a] SK-23 cells and [b] SK-MEL-28 cells of the photosensitizers, MB [◆], MMB [■], DMMB [▲], NMB [×] (all 5 µM) over a period of 3 hours. Each point is the mean of 3 experiments carried out in triplicate \pm standard deviation.

3.4.1 Melanin Binding Experiments

3.4.2.1 Absorption Spectrophotometry

Using the method of Potts [1964] and calculated as percentage binding, the melanin affinities of the photosensitizers were found to follow the order: MB>MMB>NMB>DMMB [Figure 28].

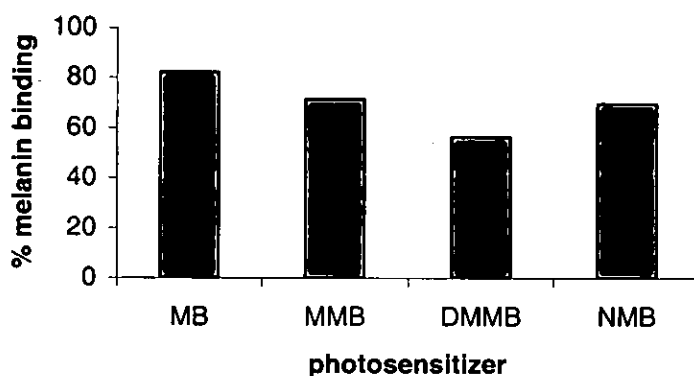
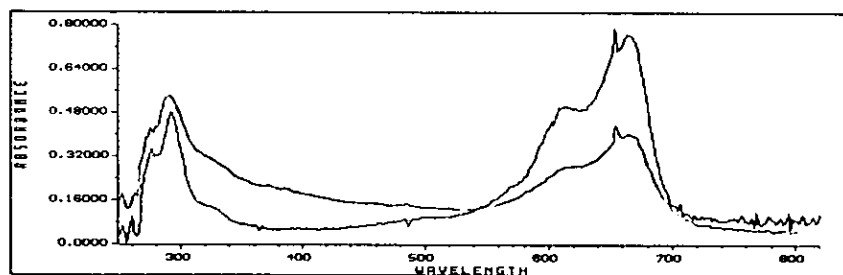


Figure 28. Percentage binding of the four photosensitizers to melanin. The value of 82.2 % for MB compares favourable with a value of 87 % from previously published literature [Potts, 1964]. Each bar is the mean of 4 experiments. SEMs were less than 5 per cent in all cases.

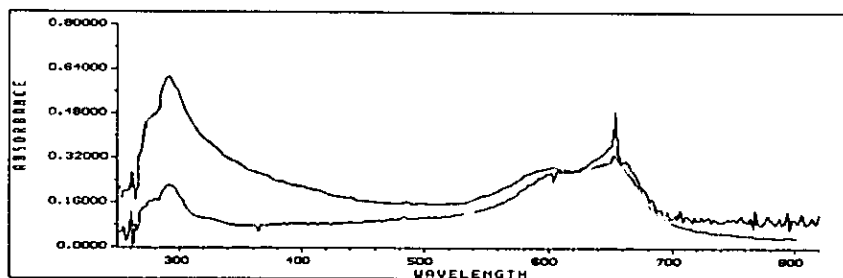
3.4.2.2 Absorption Spectra

Absorption spectra in the region of 250 to 820 nm for the four photosensitizers and their compositions with synthetic melanin are presented in Figure 29. The absorption peaks of the photosensitizers were decreased in the presence of melanin, indicative of binding to the biopolymer. Particularly of note is the absorption spectrum of DMMB, which is shifted hypsochromically (to lower wavelength) on binding to melanin. This suggests that the interaction between DMMB and the biopolymer is significant, as there has been a change in the electron cloud of the phenothiazinium chromophore, moreso than the other photosensitizers investigated in this work.

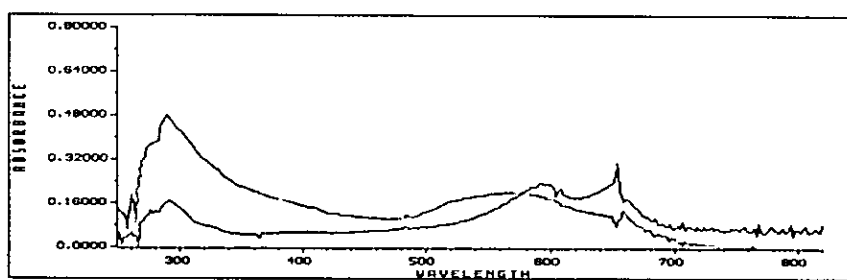
[a]



[b]



[c]



[d]

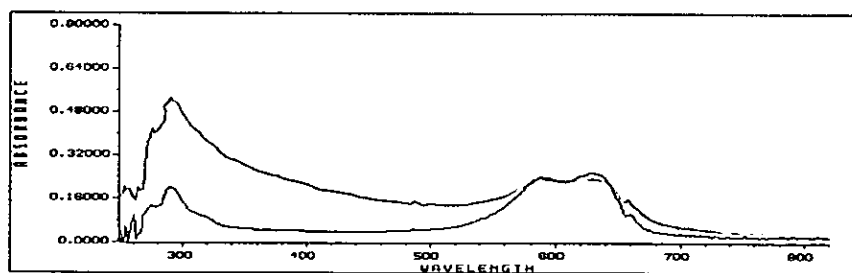


Figure 29. Absorption spectra in the region of 250 nm to 820 nm for the photosensitizers, [a] MB, [b] MMB, [c] DMMB and [d] NMB and their compositions with synthetic melanin. Black line is photosensitizer alone, red line is photosensitizer plus synthetic melanin.

3.5 DISCUSSION

The photosensitizers used in the present study were selected on evidence obtained in the earlier work using the non-pigmented mouse, mammary tumour cell line, EMT-6 [Wainwright *et al.*, 1997][Chapter 2]. The patterns of both photocytotoxicity and dark toxicity mirrored those found in the previous experiments, with successive methylation of the phenothiazinium chromophore corresponding to increased photosensitizing efficacy in both cell lines. Patterns of cellular uptake were also similar although the amount of each photosensitizer present in the cells, following the three-hour incubation period, varied between the two cell lines and differed also from the previous experiments using EMT-6.

The sites of action of the phenothiazinium photosensitizers in melanoma cells are, as yet, unknown. As suggested earlier, they may be various and time-dependent, although Link *et al.* found a fourfold increase in the uptake of radiolabelled MB in melanotic B16 melanoma cells compared to the amelanotic sub-line and also reported that radiolabelled MB is localised in melanosomes [Link *et al.*, 1996 & 1998]. Using the method of Potts [1964], the melanin affinities of the photosensitizers were found to follow the order: MB>MMB>NMB>DMMB which, taken with the photocytotoxicity data, suggests that melanin may have had an inhibitory effect on their photodynamic action. This is in agreement with comparative studies utilizing other types of photosensitizer, *e.g.* naphthalocyanines, in melanotic and amelanotic strains [Soncin *et al.*, 1998]. However, uptake in the murine melanoma cell line (SK-23) was considerably higher for each of the photosensitizers, which contained visibly higher levels of melanin. This suggests that melanin is important in cellular uptake, but that intracellular redistribution is probable for the MB derivatives. Since cellular uptake data suggest that NMB and DMMB exhibit greater uptake in both cell lines than do MB or MMB, it is suggested that different sites of action exist for the photosensitizers. Thus, for example, DMMB, which showed the least affinity for melanin, might be expected to show cellular localisation other than in the melanosomes, *e.g.* mitochondria as suggested in the previous work [Chapter 2]. This, coupled with a high photosensitizing efficacy, would explain the high levels of photocytotoxicity encountered. NMB showed similar melanin binding to MMB [Figure 28] but exhibited higher uptake than the mono-methylated derivative in both cell lines and gave the highest yield of singlet oxygen [Section

2.4.1.2]. It was thus more phototoxic than MMB. The variation in dark toxicities encountered in both cell lines for the different photosensitizers also indicates localisation at sites other than melanosomes, which are not vital to cell viability.

The toxicity levels and ratios encountered in the SK-23 and SK-MEL-28 melanoma cell lines were expected to differ from those in the earlier study on a murine mammary carcinoma line, EMT-6 [Chapter 2], due to the presence of the photoprotective and antioxidant melanin. That the toxicity trends were similar indicates that, with phenothiazinium photosensitizers, at least, the protective effect of melanin against photodynamic action in cell culture is limited. In addition, cellular uptake of the phenothiaziniums by the melanin-expressing cells exhibited a gross correlation with melanin content, indicating that the biopolymer may be important in the uptake mechanism. This has been demonstrated previously in studies on melanotic and amelanotic sub-lines.

In terms of the possible clinical application of the current work, PDT employing phenothiazinium photosensitizers is not suggested procedurally for the removal of primary melanoma, since this is routinely performed by excision. However, due to the demonstrated efficacy of MB in tracing microsattelites and its use in sentinel lymph node tracing, it may be of use in the photodynamic treatment of local metastatic lymph infiltration immediately post-surgery, *i.e.* as an alternative to lymphadenectomy. At present, MB is used routinely in various tracing or demarcation procedures, either visible or scintillographic, without reported toxicity. The derivatives used in the present *in vitro* study were all more effective in terms of the photodynamic effect and it is thus suggested that future clinical developments in this direction may be feasible.

**CHAPTER FOUR:
SUBCELLULAR LOCALISATION OF METHYLENE BLUE AND
ITS DERIVATIVES IN PIGMENTED AND NON-PIGMENTED
CELLS IN CULTURE**

4.1 ABSTRACT

The cationic photosensitizer, methylene blue (MB) has been exploited as an alternative agent in clinical PDT with some success. MB is disadvantaged, however, by an inherent (dark) toxicity and its rapid reduction *in vivo* to the neutral leucobase. It was found earlier that the derivatives of MB, 1-methyl methylene blue (MMB), 1,9-dimethyl methylene blue (DMMB) and new methylene blue N (NMB) have increased photosensitizing efficacies in the murine mammary tumour cell line (EMT-6), the murine melanoma cell line (SK-23) and the human melanoma cell line (SK-MEL-28) in culture. These were related to increased resistance to reduction and elevated levels of singlet oxygen production by the derivatives. In addition, methyl substitution was expected to lead to an increase in the hydrophobicity of the system and indeed this was found for the methylated derivatives. Increased hydrophobicity ($\log P$) generally leads to improved cellular uptake and possibly alternative intracellular targeting and localisation. MB is known to target the nucleus but it was expected that structural changes to the derivatives and increased $\log P$ would favour mitochondrial targeting. In this study, fluorescence microscopy indicated that, upon incubation, DMMB and NMB form a punctate pattern in the cytoplasm of cells, but are absent from the nucleus. However, from scanning laser confocal microscopy it was seen that none of the photosensitizers was present in the nucleus following a three-hour incubation period. Nevertheless, all four photosensitizers rapidly relocated from the cytoplasm to the nucleus upon illumination. In addition, the effect of three of the photosensitizers on isolated rat mitochondria was examined. Oxygen utilisation in the presence of the photosensitizers followed the order MMB>MB>DMMB.

4.2 INTRODUCTION

Photodynamic therapy (PDT) is dependent upon the administration of a tumour-localising, photosensitive dye and its subsequent activation by red wavelength light that, in the presence of molecular oxygen, produces a cytotoxic effect in targeted (malignant) cells. However, the sole photosensitizer currently registered for clinical use, the porphyrin-based Photofrin®, is associated with several drawbacks. Most notable are its poor light absorption properties at the activating wavelength (~630 nm) and a prolonged skin photosensitization, persisting in patients for up to eight weeks post-treatment. The predominant mechanism of porphyrin-mediated cell death is believed to be a Type II process with the formation of singlet oxygen ($^1\text{O}_2$) and its subsequent action on key components of the cell.

The cationic dye, methylene blue (MB), important primarily as a nuclear stain in histology, is also known to have photosensitizing properties [Section 2.2]. As a result, MB has been tentatively exploited as one of many second-generation photosensitizers in clinical photodynamic therapy (PDT). MB has been used to treat carcinoma of the bladder [Williams *et al.*, 1989] and inoperable oesophageal tumours [Orth *et al.*, 1995], with some success. In a related field, the photosensitizer has been used for the elimination of viruses from samples of donated whole blood [Zeiler *et al.*, 1994]. MB itself is known to target the nucleus of cells and to intercalate with DNA whereupon, following illumination, it causes the formation of oxidised guanine residues, notably 8-hydroxyguanosine, also *via* the intermediacy of $^1\text{O}_2$ [Tuite & Kelly, 1993]. Despite the need for alternative, more efficacious photosensitizers, the use of MB in PDT has been sparse, due possibly to its rapid reduction *in vivo* to the neutral (colourless) leucobase and to an inherent (dark) toxicity [Section 2.2].

Whilst the majority of compounds under investigation as clinical photosensitizers have tended to be derivatives of first-generation, porphyrin-based compounds, it is similarly possible to produce more efficacious derivatives of second-generation compounds (including the cationic dyes) by chemical substitution of the molecule. Since the diffusion length of $^1\text{O}_2$ is 0.1 μm or less in its intracellular lifetime [Moan, 1990], it is reasonable to assume, given an adequate oxygen supply and light intensity, that the site

of photodamage will be close to the location of the photosensitizer at the time of its irradiation. It is not yet clear whether the total drug distribution to neoplastic tissue or its concentration in specific sub-cellular sites is the important factor in the cell death mechanism. Nevertheless, it might be expected that the efficacy of PDT could be enhanced by the use of photosensitizers that localise within critical components of the cell. Several subcellular sites have been identified as major targets for photosensitizing drugs, although the nucleus itself is not believed to be a primary target for porphyrin-based compounds. HpD and Photofrin® are hydrophobic, anionic molecules and localise in the mitochondria, endoplasmic reticulum, cytoplasmic and nuclear membrane, and perinuclear region of the cytoplasm of cells *in vitro* and, to a lesser extent, in lysosomes or nuclei [Moan *et al.*, 1989]. Many second-generation porphyrin drugs with enhanced photosensitizing capabilities show significant differences in their patterns of subcellular localisation when compared to Photofrin®. Depending on the photosensitizer, overall dose and experimental protocol, photodamage has been observed in microtubules, membranous organelles, plasma membrane and the nucleus.

The synthesis of new, more efficacious photosensitizers has involved huge efforts by researchers to identify specific features that might be involved in toxicity. Studies have sought to correlate photosensitizer structure with the biodistribution and intracellular targeting (and hence photodynamic activity) of a compound, but the picture is complicated by the wide variety of photosensitizers, different methodologies, experimental conditions and biological systems that have been used. The specific localisation and the kinetics of the intracellular distribution of an individual photosensitizer depend upon its hydrophobicity, the type and number of its charges, the charge-mass ratio, the type and number of ring and core substituents, and its mode of entry (diffusion or endocytosis) into the cell [Peng *et al.*, 1996].

A determinant of major importance in both cellular uptake and intracellular targeting is the hydrophilic/hydrophobic character of a molecule. Hydrophilic photosensitizers are generally defined as those having three or more charged substituents. They are freely soluble in water at physiological pH. Hydrophobic photosensitizers are those bearing no charged peripheral substituents and which have negligible solubility in water or alcohol. An increase in the hydrophobicity of the system generally increases the affinity

of a photosensitizer for the various lipids encountered (complexed to blood proteins or at the cell membrane, for example), improves cellular uptake and alters intracellular targeting and localisation. In the case of Photofrin® and similar hydrophobic photosensitizers, the $^1\text{O}_2$ quantum yield for cell killing is found to be ten times greater than that of some hydrophilic compounds [Moan *et al.*, 1987]. Since these particular photosensitizers have similar yields of $^1\text{O}_2$, the data demonstrates the importance of the intracellular distribution pattern and the availability of molecular oxygen in PDT. However, the situation for hydrophobic photosensitizers is complicated by the fact that, due to lack of water solubility, they must be injected into suitable delivery vehicles such as liposomes, emulsions or nanoparticles. It has also been observed that the positions of the hydrophilic and/or hydrophobic substituents play an important role in the localisation of photosensitizers in tumours [Ressler & Pandey, 1998]. For instance, the insertion of two polar substituents (such as carboxylate, sulphonate or hydroxyl groups) on two adjacent rings of a phthalocyanine-type macrocycle and the consequent presence of a hydrophobic matrix on the opposite side of the molecule (two unsubstituted rings) makes the photosensitizer an amphiphilic species. Amphiphilic photosensitizers are difficult to define precisely but are usually recognized to be compounds with both a hydrophilic and a hydrophobic region. Although they generally have no more than two hydrophilic substituents, the spacial distribution of these is important, in order for the molecule to be soluble in water or alcohol at physiological pH. The photosensitizer is then sufficiently water-soluble to allow its systemic injection *in vivo*, whilst retaining its ability to cross the lipid barrier of cellular and/or intracellular membranes and localise at intracellular sites [Kessel, 1982]. For porphyrin-based PDT agents, amphiphilic character often arises from an asymmetric distribution of charge groups around the periphery of the molecule with the region most distant from the charged groups becoming the hydrophobic component [Peng *et al.*, 1996]. Photosensitizers of the amphiphilic class include two of the most potent PDT agents, *meta*-tetrahydroxyphenylchlorin (*m*-THPC) and benzoporphyrin derivative monoacid ring A (Verteporfin, BPD-MA).

The intracellular distribution of a photosensitizer is further influenced by the type and number of its charges, and by the charge-mass ratio. Studies of cellular distribution in V-79 Chinese hamster cells using the anionic dyes, AIPcS4 and AIPcS3, suggest a

relationship between the number of negatively charged groups attached to the photosensitizing 'core' and the mode of entry into the cell. The exact amount of negative charge that prevents diffusion across the cell membrane and allows endocytosis to become the dominant mode of entry has been found to be around -2 . This, in turn, determines the intracellular distribution pattern of the molecule [Paquette *et al.*, 1988]. A further study by Woodburn *et al.* [1991] found that, of a series of hydrophobic porphyrin derivatives, bearing either anionic or cationic residues at physiological pH, those with a net cationic profile became localised in mitochondria, whilst those with net anionic profile localised in lysosomes. As all the anionic porphyrins in this second study bore two negative charges, these results are in accord with those of the earlier work. Additional factors relate to the consequences of drug-delivery systems, and their properties. Different anionic photosensitizers do not necessarily have the same subcellular localisation pattern due mainly to the fact that they have different hydrophobic character.

Mitochondria are believed to be important targets in PDT-induced cytotoxicity. Studies using Photofrin® have demonstrated, both in intact cells and in isolated mitochondria, an immediate post-PDT inhibition of respiration and inhibition of electron transport components, such as succinate dehydrogenase and cytochrome *c* oxidase, and disturbance of the mitochondrial electrochemical gradient. With PDT using the metabolic precursor, 5-ALA [Section 1.5.1], to stimulate production of PPIX by mitochondria, mitochondrial damage is most apparent when cells are irradiated soon after drug exposure (approximately four hours). Since PPIX can diffuse out of mitochondria, photodamage is also found at other sites [Peng *et al.*, 1996]. Many cationic dyes that have been introduced as photosensitizers for PDT are also found to be distributed in mitochondria [Oseroff, 1986]. Cationic, hydrophobic compounds (such as the kryptocyanine dye, EDKC, and rhodamine 123) accumulate in mitochondria due to the highly negative electrochemical potential of the active inner mitochondrial membrane. However, some negatively charged (such as Photofrin®) or neutral porphyrins (Pc4) also accumulate due, possibly, to binding to specific mitochondrial constituents (possibly cardiolipins of the inner mitochondrial membrane). It has been shown that those photosensitizers that bind to mitochondria induce apoptosis upon

irradiation, whilst those that bind to elements other than mitochondria, kill cells less efficiently and by a mechanism not involving apoptosis [Kessel *et al.*, 1997].

Four main factors appear to be involved in the uptake of photosensitizers by lysosomes. Highly hydrophobic photosensitizers (including Photofrin®, benzoporphyrins and phthalocyanines) become more or less solubilised in lipoproteins, particularly low-density lipoproteins (LDLs) in the serum, and taken into cells by LDL receptor-mediated endocytosis [Section 1.2.2]. LDL catabolism involves the endocytotic pathway and lysosomal degradation of the lipoprotein carrier. This implies that hydrophobic photosensitizers become associated with the lysosomal membrane during this process. Photosensitization of the membrane by subsequent light activation of the photosensitizer would likely cause rupture of the membrane with the release of cryptic lysosomal hydrolases. In the intracellular space these would cause cell death, but in the extracellular matrix they would act as powerful mediators of the inflammatory response. Of course, lysosomal enzyme release following cell lysis would be expected irrespective of the cellular target of photosensitization. A second class of compounds that tends to localise in lysosomes includes the negatively charged and very polar photosensitizers, such as aluminium phthalocyanine and the sulfonates of tetraphenylporphine. It is believed that, for negatively charged molecules, their anionic character prevents binding to the predominant anions in the cell surface coat, thus facilitating cellular uptake. Furthermore, the action of organic anion transporters may also play a part. Mono-aspartyl chlorin e6 (MACE) is a hydrophilic photosensitizer that is reported to localise in lysosomes following its ingestion by endocytosis. MACE has four ionizable carboxyl groups in an asymmetric arrangement around a central chlorin ring, making it sufficiently polar to avoid passive diffusion into the cytoplasm and subsequent migration to the mitochondrion [Robert & Berns, 1989]. Representatives of the third group of lysosome-locating molecules are lysosotropic photosensitizers, such as the Nile Blue derivatives synthesized by Lin *et al.* [1991] and a tetraphenylporphine derivative linked to chloroquine [Morlière *et al.*, 1990]. These are weak bases that enter cells as uncharged species but the proton gradient between the cytosol and the lysosome interior permits them to become incorporated as protonated species within the organelle. A final method of inducing specific lysosomal targeting is by phagocytosis of photosensitizers covalently linked to microspheres [Bachor *et al.*, 1991].

As already mentioned, hydrophobic photosensitizers (including Photofrin®) tend to target membrane structures, including that of the nucleus, but seldom reach DNA unless it is sited close to the nuclear membrane [Moan *et al.*, 1989]. PDT-induced photodamage has also been observed in cytoskeletal elements, in particular non-polymerised tubulin [Sporn & Foster, 1992]. Subsequent illumination of the photosensitizer prevents polymerisation of tubulin, and instead induces the formation of micronuclei and giant cells, and the accumulation of cells in mitosis. Alternatively, DNA damage may be induced as a consequence of the relocation of photosensitizers to the nucleus during illumination. Several photosensitizers have been reported to act in this manner [Wood *et al.*, 1997; Peng *et al.*, 1991; Berg *et al.*, 1991]. Various types of lesions have been reported including single-strand breaks, DNA-protein crosslinking, chromosome aberrations and sister chromatid exchanges, although the mutagenic potential of PDT varies with photosensitizer and cell line, and also the target gene. It is important, therefore, to avoid exposure of normal cells to PDT and to exercise extreme caution in the treatment of benign conditions using this regime.

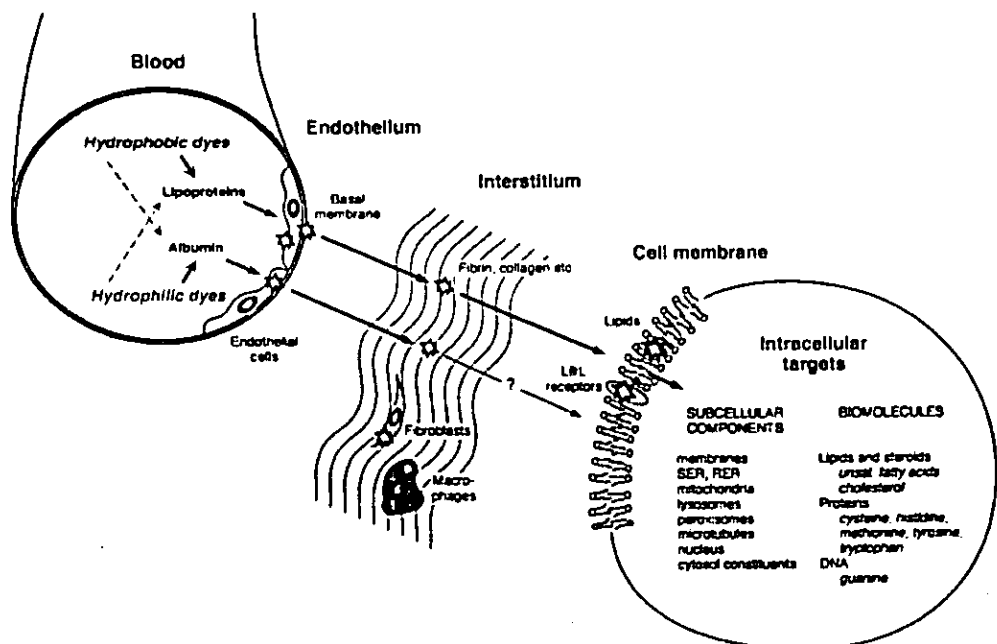


Figure 30. Intracellular targets for hydrophilic and hydrophobic photosensitizers. [Taken from Peng *et al.*, 1996].

The effect of chemical substitution on the photodynamic activity of MB was previously investigated by toxicity testing the photosensitizer alongside two commercial (doubly-methylated), related dyes, 1,9-dimethyl methylene blue (DMMB) and new methylene blue (NMB), and a third (singly-methylated), newly-synthesized intermediate, 1-methyl methylene blue (MMB). It was found that both the photocytotoxicity and dark toxicity are significantly enhanced by successive methylation of the parent molecule in non-pigmented and pigmented cells in culture, and that this corresponds generally to increased $^1\text{O}_2$ quantum yields, increased resistance to reduction, increased Log *P* and improved cellular uptake. The increased Log *P* was not unexpected, since a common effect of substitution is to increase the hydrophobicity of a compound, giving it a greater affinity for lipid. As with other cationic photosensitizers, lysosomal targeting and localisation in extranuclear granules has also been observed with MB. However, it is believed that the presence of bulky methyl substituent groups on the three derivatives is likely to make DNA intercalation of these molecules highly improbable. Taken with their altered physicochemical characteristics, the enhanced toxicities of the derivatives may therefore ultimately be due to different intracellular localisation patterns at the time of their activation by light. The increases in Log *P*, which confer greater hydrophobic character on the derivatives, together with their positive charge, make mitochondrial targeting extremely likely, particularly for the doubly-methylated compounds, DMMB and NMB. A number of different methods have been used to study the intracellular localisation of photosensitizers. For instance, the porphyrin content of specific organelles has been examined using a method that combines homogenization and ultracentrifugation to produce fractions of nuclear, mitochondrial and microsomal material, in addition to a supernatant fraction, that can be individually assessed [Cozzani *et al.*, 1981]. Alternatively, there are several studies that have used electron, fluorescence and confocal microscopy to provide detailed information of cells exposed to light in the presence of photosensitizers. Fluorescence microscopy can be used with living cells and has wide applications since most photosensitizers fluoresce. Conventional fluorescence microscopy, however, has severe limitations because many dyes are rapidly photodegraded by light exposure in the microscope. This present study proposed to examine the subcellular localisation of MB and the aforementioned derivatives, using both fluorescence and confocal microscopy. In addition, the effect of three of the compounds (MB, MMB and DMMB) on respiration in isolated rat mitochondria was examined.

4.3 MATERIALS AND METHODS

4.3.1 Localisation Studies

4.3.1.1 Fluorescence Microscopy

EMT-6 cells in 'complete' RPMI 1640 medium [Section 2.3.3.1] were seeded into 35 mm petri dishes, 2 ml of cell suspension per dish @ 1000 cells per ml, and grown on for two days. After two days, the medium was removed and replaced by 2 ml of photosensitizer at their respective IC_{50} s. [In the EMT-6 cell line, MB = 18.7 μ M, MMB = 2.2 μ M, DMMB = 0.09 μ M and NMB = 0.39 μ M. In the SK-23 line, MB = 15.2 μ M, MMB = 1.6 μ M, DMMB = 0.05 μ M and NMB = 0.3 μ M. In the SK-MEL-28 line, MB = 21.0 μ M, MMB = 2.2 μ M, DMMB = 0.01 μ M and NMB = 0.3 μ M]. The cells were incubated in the presence of the photosensitizers for three hours. After three hours, medium plus photosensitizer was poured off and the cells rinsed twice in PBS. A Leitz diaphan microscope with a removable rhodamine filter was used to obtain light and fluorescence images in order to gain an indication of intracellular localisation patterns for the photosensitizers.

4.3.1.2 Scanning Laser Confocal Microscopy

EMT-6, SK-23 or SK-MEL-28 cells were seeded at a cell density of 1×10^4 cells ml^{-1} into 35 mm petri dishes (Falcon, Fahrenheit Laboratories, Rotherham, U.K.) in RPMI 1640 medium, supplemented with 10 % (v/v) foetal calf serum, 200 mM L-glutamine and penicillin/streptomycin solution (at 1×10^4 units and 10 mg ml^{-1} , respectively), as previously described [2.3.3.1]. Circular glass coverslips, size 0 or 1.5, diameter 22 mm (Merck), were placed into each petri dish and the cells allowed to attach for three days (EMT-6 cells) or four days (SK-23 and SK-MEL-28 cells), whilst incubating at 37°C, 5 % CO_2 : 95 % air. The medium was then aspirated and replaced with medium plus, either MB, MMB, DMMB or NMB and incubated for three hours, as previously described. Photosensitizers were added to cells at both 5 μ M concentrations and at their IC_{50} values, also as previously described [Section 2.4.2.2]. Following three hours' incubation, the cells were examined with a scanning laser confocal fluorescence microscope, using a helium/neon laser at 633 nm. Untreated cells were also examined for autofluorescence, under the same conditions.

4.3.1.3 Image Processing

Black and white images produced from the scanning laser confocal microscopy were superimposed with colour using the 'Photostyler' computer package. Images were converted first to 8-bit greyscale and thence to 256-bit pseudocolour before printing. In this way, the order of increasing fluorescence (indicative of increasing concentration) is represented by a colour scale such that blue<green<yellow<red<white.

4.3.2 Effect of Photosensitizers on Mitochondrial Respiration

4.3.2.1 Preparation of Liver Homogenates

Liver mitochondria were isolated from male Sprague-Dawley rats into ice-cold isolation medium (0.25 M sucrose, 10 mM Tris-HCl, 0.5 mM EDTA, at pH 7.4). The tissue was homogenised in fresh, ice-cold, isolation medium with added bovine serum albumin (BSA) (5 mg ml⁻¹), then centrifuged at 600 g for ten minutes at 4°C. The supernatant was centrifuged at 8000 g for ten minutes also at 4°C. The resulting pellet was washed twice in isolation medium and resuspended in 4 ml of respiratory medium (225 mM sucrose, 10 mM KCl, 1 mM EDTA, 10 mM K₂HPO₄, 5 mM MgCl₂, 10 mM Tris-HCl at pH 7.4) and left on ice for one hour.

4.3.2.2 Protein Estimation

Protein was estimated using a BIO-RAD protein assay kit and BSA as standard. To create a calibration curve for BSA, dilutions of BSA standards, (0.2 to 1.6 mg ml⁻¹ protein) were prepared in clean, dry test tubes. The various reagents were added as per manufacturers' instructions and the tubes then immediately vortexed. After fifteen minutes, the absorbances were read spectrophotometrically at 750 nm. The protein concentrations of the various samples were determined using the 'Minitab' computer package, by plotting the calibration curve data for BSA and entering the absorbance value of each unknown. Absorbance was plotted against protein concentration (mg ml⁻¹). All data are expressed as mean ± standard error of the mean (SEM).

4.3.2.3 Mitochondrial Respiration

Mitochondrial respiration was measured polarographically using an oxygen electrode in a 3 ml water-jacketed chamber maintained at 30°C. The electrode was set to zero using

3 ml air-saturated distilled water at 30°C. This was removed and liver mitochondria (1 to 2 mg protein) were added to the chamber to a final volume of 3 ml. A substrate, (either 50 mM pyruvate/50 mM L-malate or 100 mM succinate/ 500 ng ml⁻¹ rotenone) was added and the respiratory rate recorded as basal respiration. An addition of 100 nmol ADP was then made and the rapid rate of oxygen utilization that ensued was recorded, and used to elicit the coupled respiratory rate. Only healthy, “well-coupled” mitochondria were retained in the chamber. The degree of coupling was determined by calculating the acceptor control ratio (ACR) for each sample addition made to the chamber [See Appendix 2]. ACR values varied even within samples. An ideal ACR would be about 4 although values above 2 were considered acceptable in most cases. Finally, 10 µl additions of drug (1 mg ml⁻¹) were made and the respiratory rate measured, up to a final concentration of about 50 µM.

4.3.2.4 Calculation of Data

The oxygen content of air-saturated water at 30°C is 230 µmol l⁻¹. If the oxygen electrode is first calibrated with air-saturated distilled water, this fact can be used to calculate oxygen utilization for each experiment. Oxygen utilization by the individual photosensitizers was calculated as a percentage of the recorded basal mitochondrial respiratory rate before additions of ADP or photosensitizer were made.

4.4 RESULTS

4.4.1 Localisation Studies

The patterns of cellular uptake and intracellular localisation of the photosensitizers, MB, MMB, DMMB and NMB at their IC₅₀ values were studied using both fluorescence and confocal microscopy.

4.4.1.1 Fluorescence Microscopy

Using fluorescence microscopy, the localisation of MB and MMB remained obscure, as certain cells appeared to show evidence of nuclear targeting, whilst in others, the photosensitizers appeared as a particulate pattern in the cytoplasm [Figure 31a and 31b]. There were also areas of dense blue staining and an absence of fluorescence in these regions. For DMMB and NMB, however, the pattern of intracellular localisation was more defined, with no evidence of nuclear targeting and the photosensitizers appearing as a clearly defined punctate pattern within the cytoplasm [Figure 31c and 31d]. The images presented are light images of the four photosensitizers incubated at IC₅₀ values for three hours with EMT-6 cells. They are generally representative of images also taken with SK-23 and SK-MEL-28 cells under the same conditions.

4.4.1.2 Confocal Microscopy

Using confocal microscopy and following three hours' incubation, there was no evidence of nuclear targeting for any of the compounds tested in any of the cell lines. In some cases, it was possible to record a clearly particulate pattern of distribution of the photosensitizers within the cytoplasm [Figure 35j]. However, during the process of visualisation (*i.e.* with progressive exposure to the laser beam), all four photosensitizers initially became spread more diffusely throughout the cytoplasm and eventually relocalised to the nucleus [Figures 32 to 39]. When the laser beam was left running in between image capture (continuous illumination), progression into the nucleus was more rapid than when it was shut down (discontinuous illumination) [compare for MMB, Figure 35h and Figure 37c]. The photosensitizers were also incubated at concentrations of 5 μ M, in order to establish whether intracellular targeting varied with photosensitizer concentration. In fact, there was no difference in the pattern of uptake

and subcellular localisation for any of the photosensitizers in any of the cell lines, whether incubated at 5 μM concentrations or at their IC_{50} values. However, it was found that the rate of uptake and progression into the nucleus was more rapid (and the fluorescence far greater) at higher concentrations of photosensitizer than at lower concentrations [compare for MB, Figure 32a and Figure 34].

To test whether the action of the laser beam alone could provoke relocation of the photosensitizers, the protocol was repeated, but with omission of the incubation procedure. In this case, coverslips containing cells of the various lines were loaded into the incubation chamber in RPMI 1640 medium and onto the microscope stage. Medium containing various concentrations of each photosensitizer allowed to flow into the incubation chamber *via* capillary tubing and with the aid of a syringe. Using this method, uptake of the photosensitizers from the surrounding medium and into the cells was immediate and clearly visible [Figures 33, 37, 38 and 39]. With continuous exposure to the laser beam, relocation of all four photosensitizers from the cytoplasm to the nucleus was rapid, and occurred within minutes of uptake. Again, cellular uptake and nuclear relocation were more rapid and fluorescence signals greater at higher concentrations of photosensitizer.

The images presented are generally representative of events that were recorded for all four photosensitizers in the EMT-6, SK-23 and SK-MEL-28 cell lines. However, only those results for the melanoma (SK-23 and SK-MEL-28) lines are presented here. The clearest images were usually obtained using the SK-23 murine melanoma cell line that tends to have a more regular shape and a more distinct and visible profile in culture than the SK-MEL-28 line. It was also noted that fluorescence in the SK-23 cell line was generally greater than in the human SK-MEL-28 line, possibly confirming earlier data that demonstrates greater cellular uptake of the photosensitizers in this line [Section 3.4.1.4].

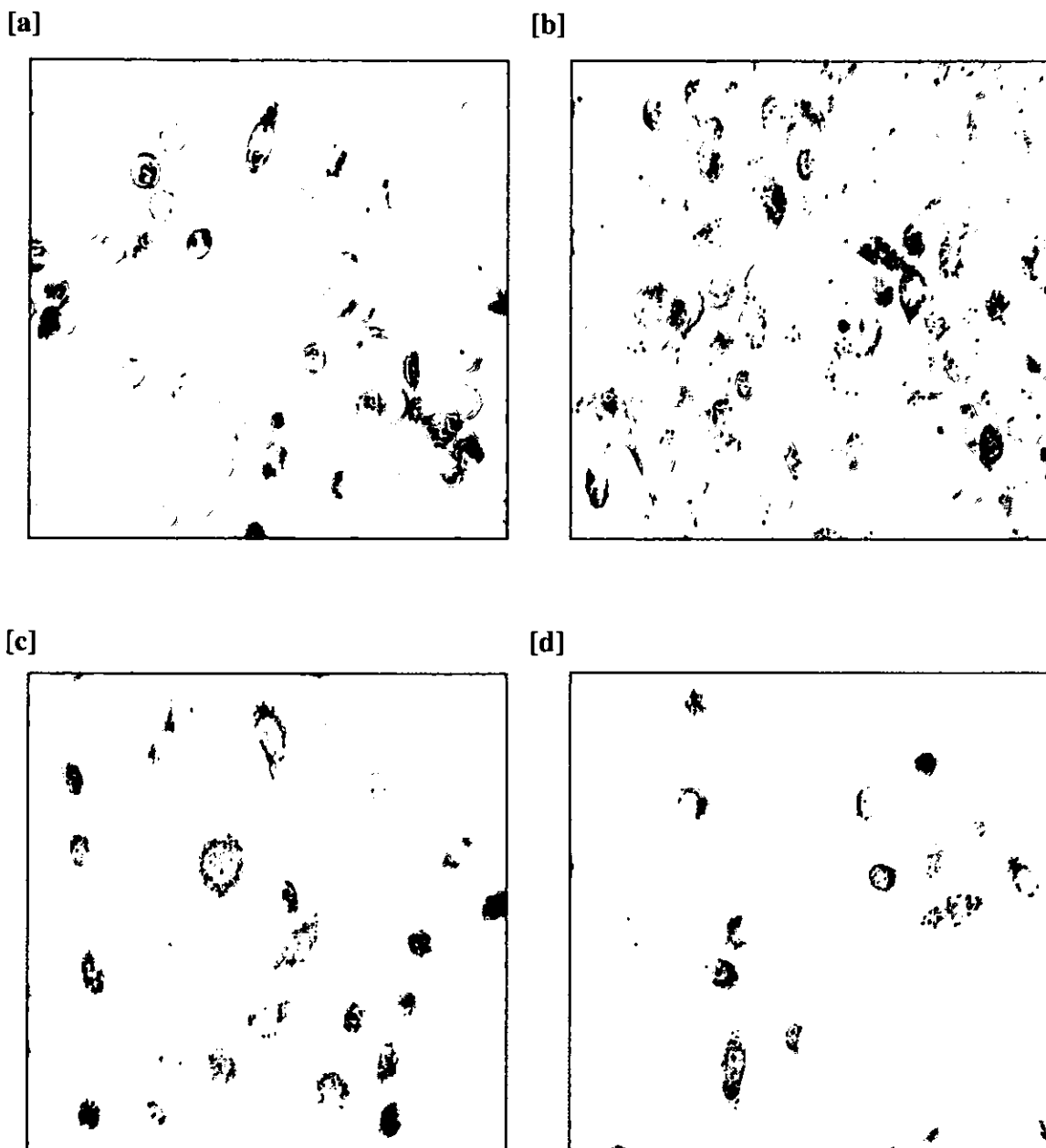


Figure 31. Fluorescent images of EMT-6 cells following incubation for three hours with [a] MB, [b] MMB, [c] DMMB and [d] NMB at their IC_{50} values, *i.e.* MB = 18.7 μM , MMB = 2.2 μM , DMMB = 0.09 μM and NMB = 0.39 μM . Cellular uptake of MB does not appear to be uniform, with the photosensitizer apparent in some cells but absent in others [a]. Intracellular localisation of MB also appears to be random with evidence of both nuclear and cytoplasmic targeting. Uptake and distribution of MMB are also ambiguous, although much of the photosensitizer appears to be located in the cytoplasm [b]. Aggregation by these two photosensitizer molecules seems likely. Uptake of both DMMB and NMB appears uniform throughout the cell population and both photosensitizers are well distributed in a punctate pattern throughout the cytoplasm. There is no evidence of nuclear targeting [c & d].

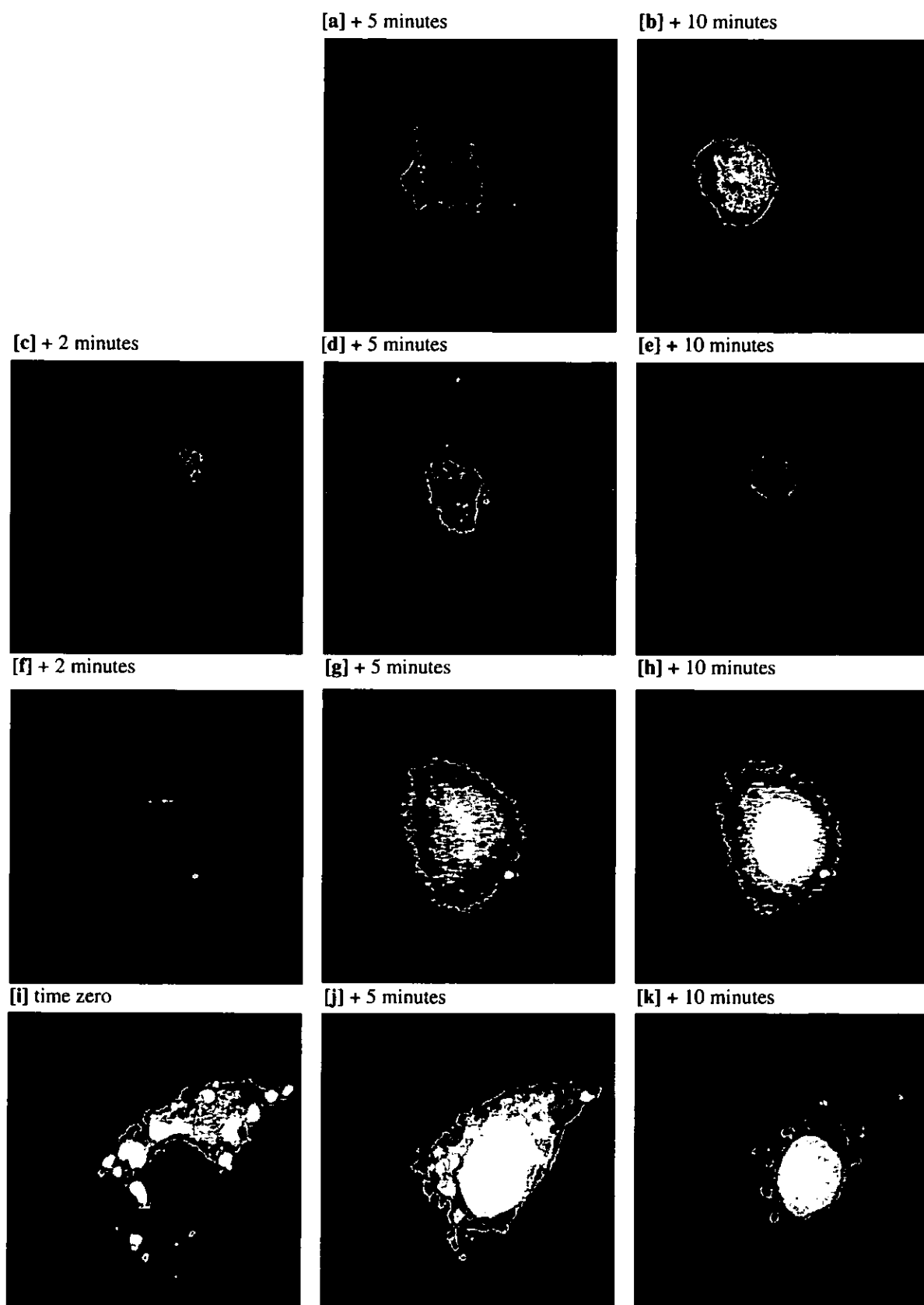


Figure 32. Subcellular localisation of [a, b] 21 μM MB, [c-e] 2.2 μM MMB, [f-h] 0.01 μM DMMB and [i-k] 0.3 μM NMB in typical SK-MEL-28 cells using confocal microscopy over a period of 10 minutes following 3 hours pre-incubation. Cells were visualised using continuous illumination with the laser beam.

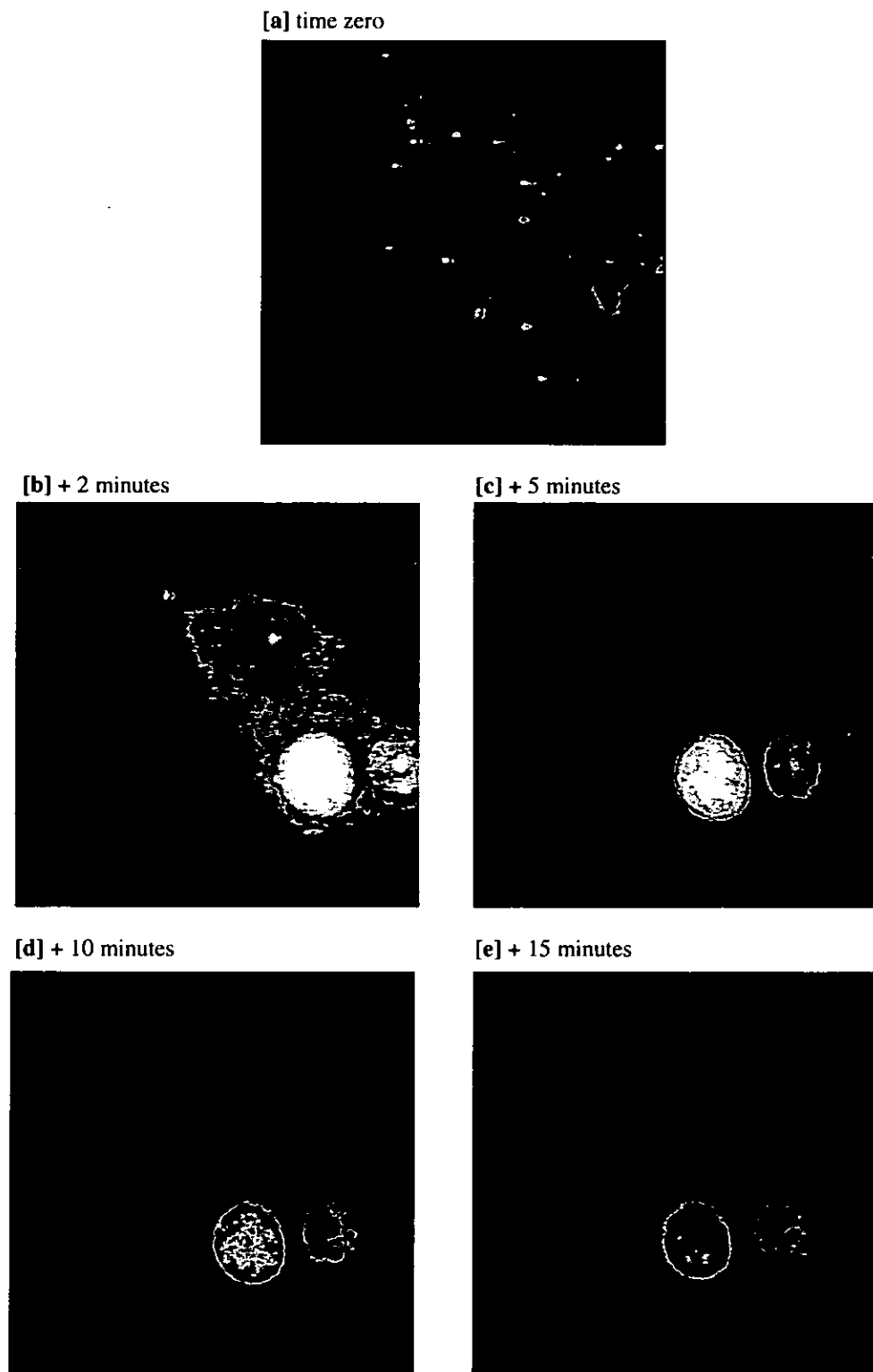


Figure 33. Subcellular localisation of 5 μM MMB in a typical SK-MEL-28 cell using confocal microscopy with the flow-through method and continuous illumination with the laser beam. The photosensitizer can be seen in the medium at time zero [a] and after 2 minutes [b]. At this point, the incubation chamber is flushed through with fresh medium in order to rinse the cells. (Subsequent to this experiment, the protocol was carried out with the rinsing step immediately prior to exposure to the laser beam). Cellular uptake of MMB is immediate and uptake into the nucleus at a maximum after 2 minutes. The nucleus on the right of the image is believed to be that of a second cell lying in a different plane of visualisation.

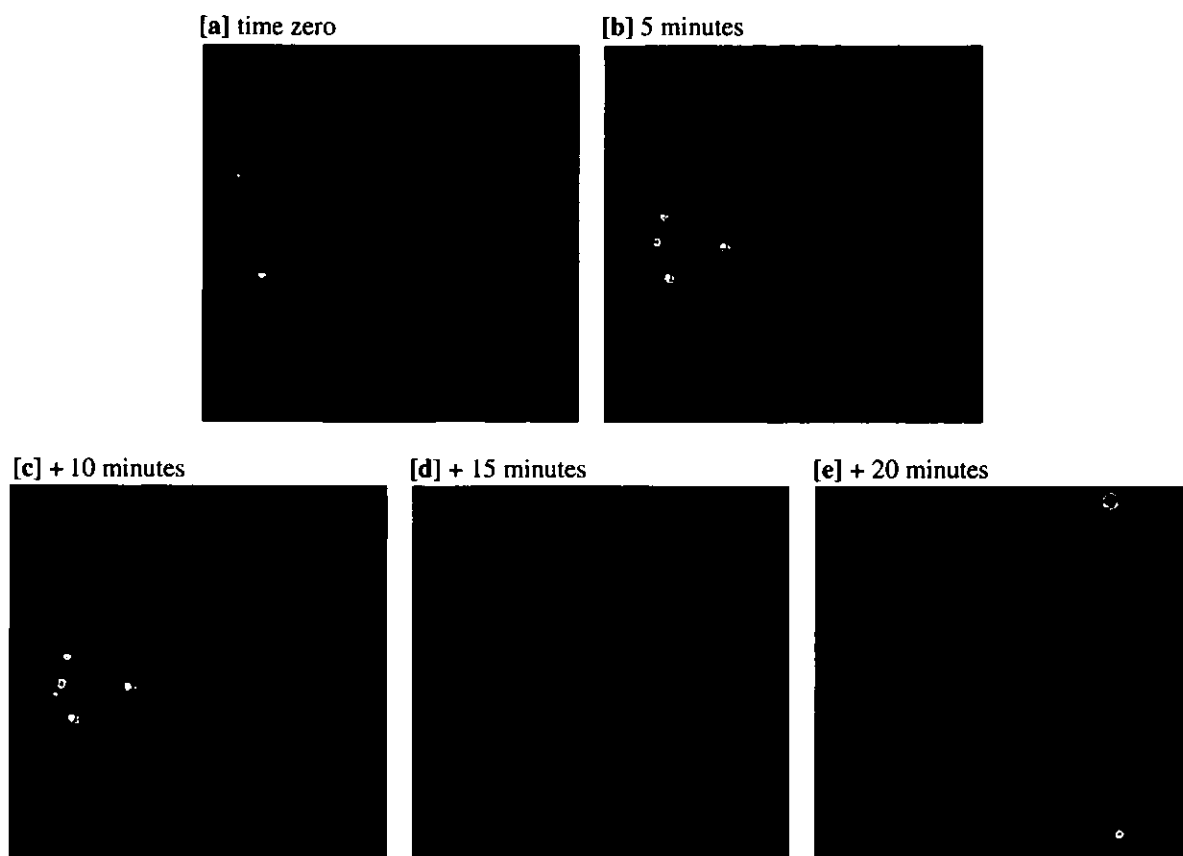


Figure 34. Subcellular localisation of 5 μM MB in a group of typical SK-MEL-28 cells as shown by confocal microscopy following 3 hours pre-incubation and over a period of 20 minutes. The cells were visualised using discontinuous illumination with the laser beam.

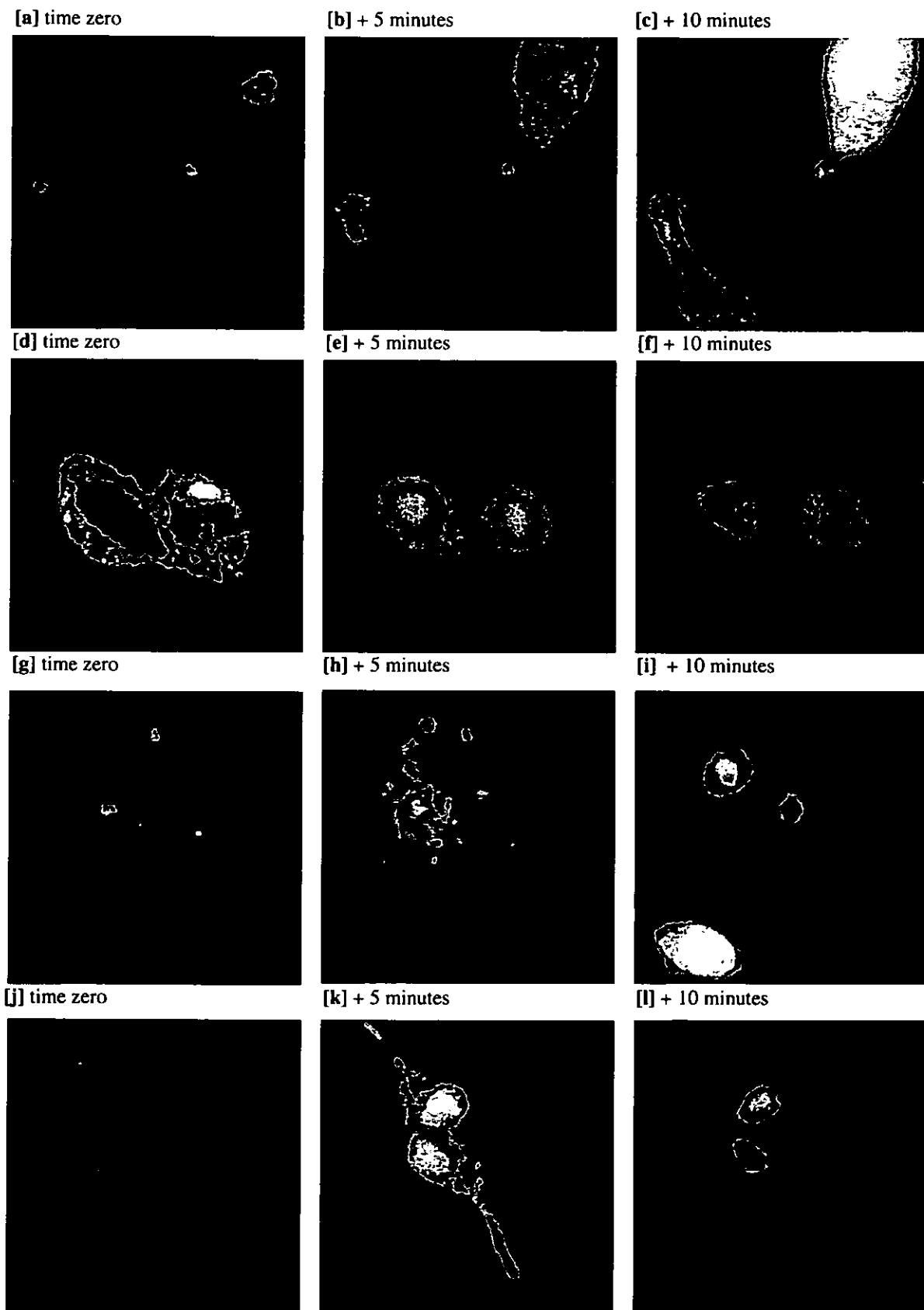


Figure 35. Subcellular localisation of [a-c] 15.2 μM MB, [d-f] 1.6 μM MMB, [g-i] 0.05 μM DMMB and [j-l] 0.3 μM NMB in SK-23 cells, as shown by confocal microscopy following 3 hours pre-incubation. The cells were visualised using continuous illumination with the laser beam.

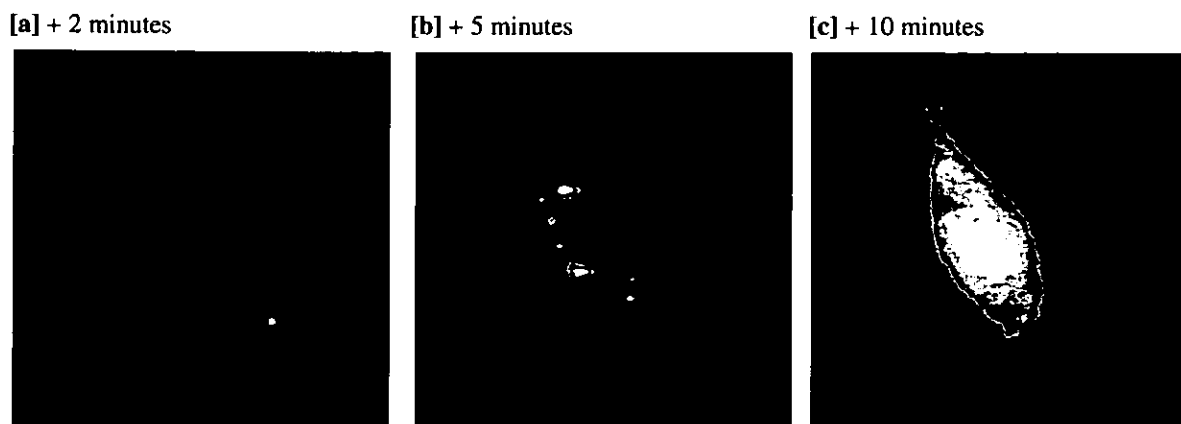


Figure 36. Subcellular localisation of 15.2 μM MB into a typical SK-23 cell over a period of 10 minutes using confocal microscopy with a flow-through method and a rinsing procedure. Cells were visualised using discontinuous illumination with the laser beam

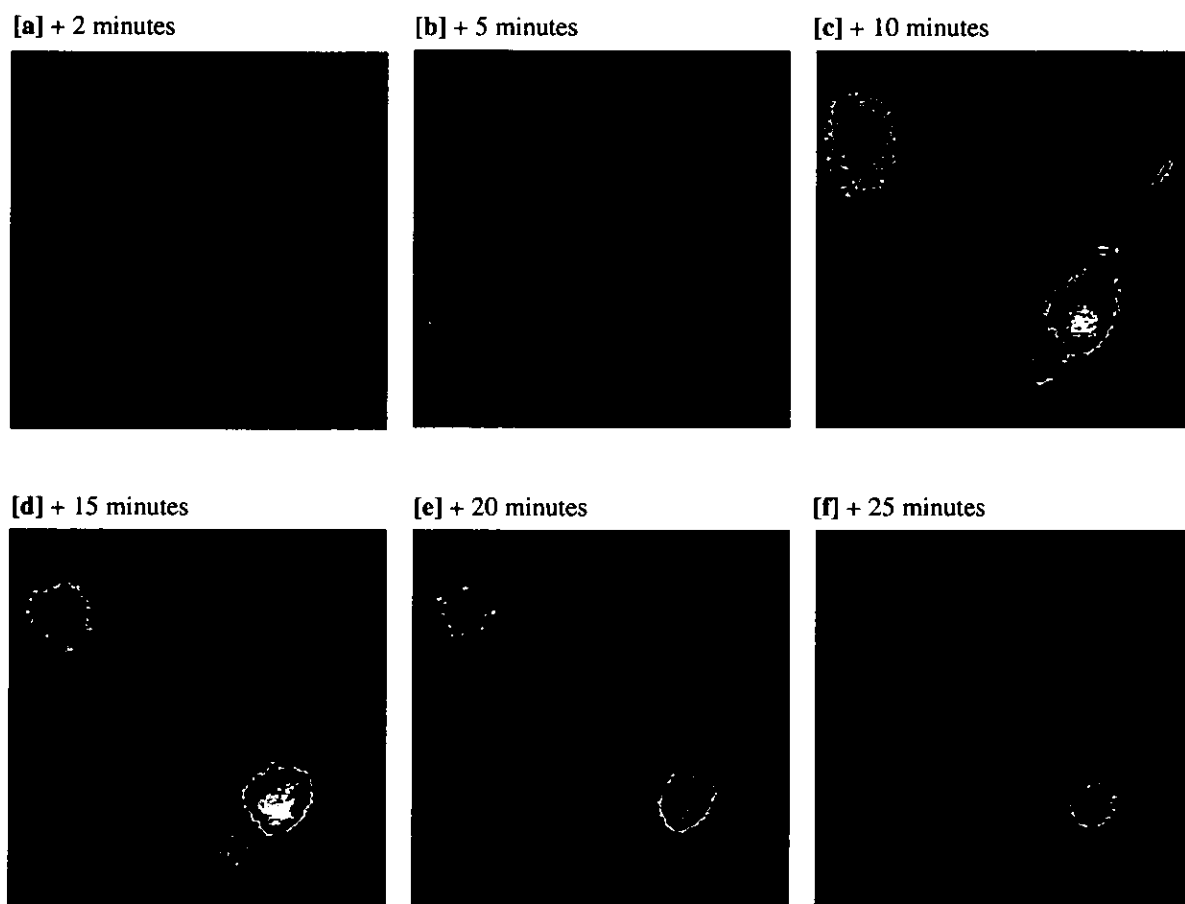


Figure 37. Subcellular localisation of 1.6 μM MMB into a pair of typical SK-23 cells over a period of 25 minutes using confocal microscopy with a flow-through method and a rinsing procedure. Cells were visualised using discontinuous illumination with the laser beam.

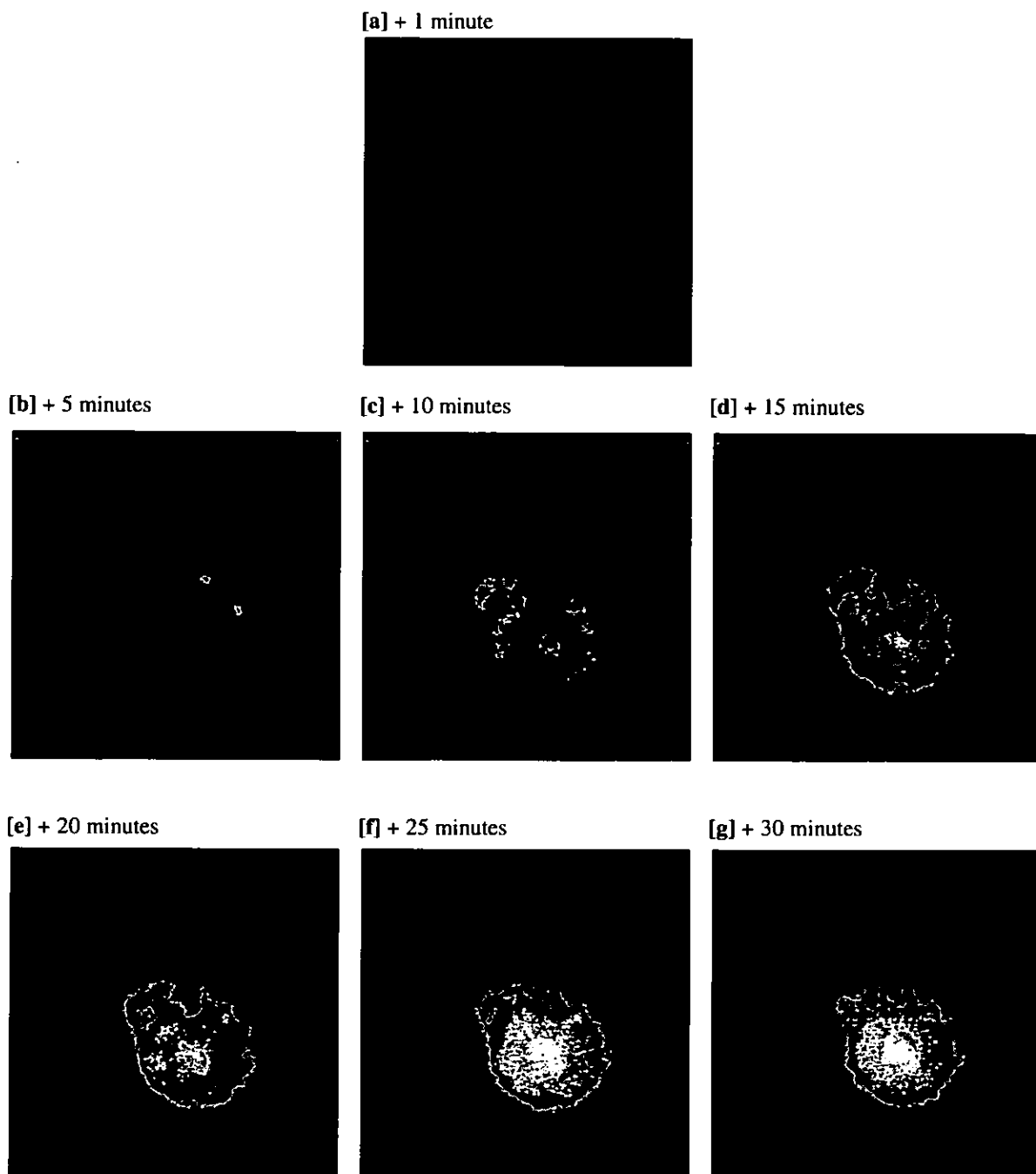


Figure 38. Subcellular localisation of 0.05 μM DMMB in a typical SK-23 cell using confocal microscopy with a flow-through method and a rinsing procedure over a period of thirty minutes. Cells were visualised using discontinuous illumination with the laser beam.

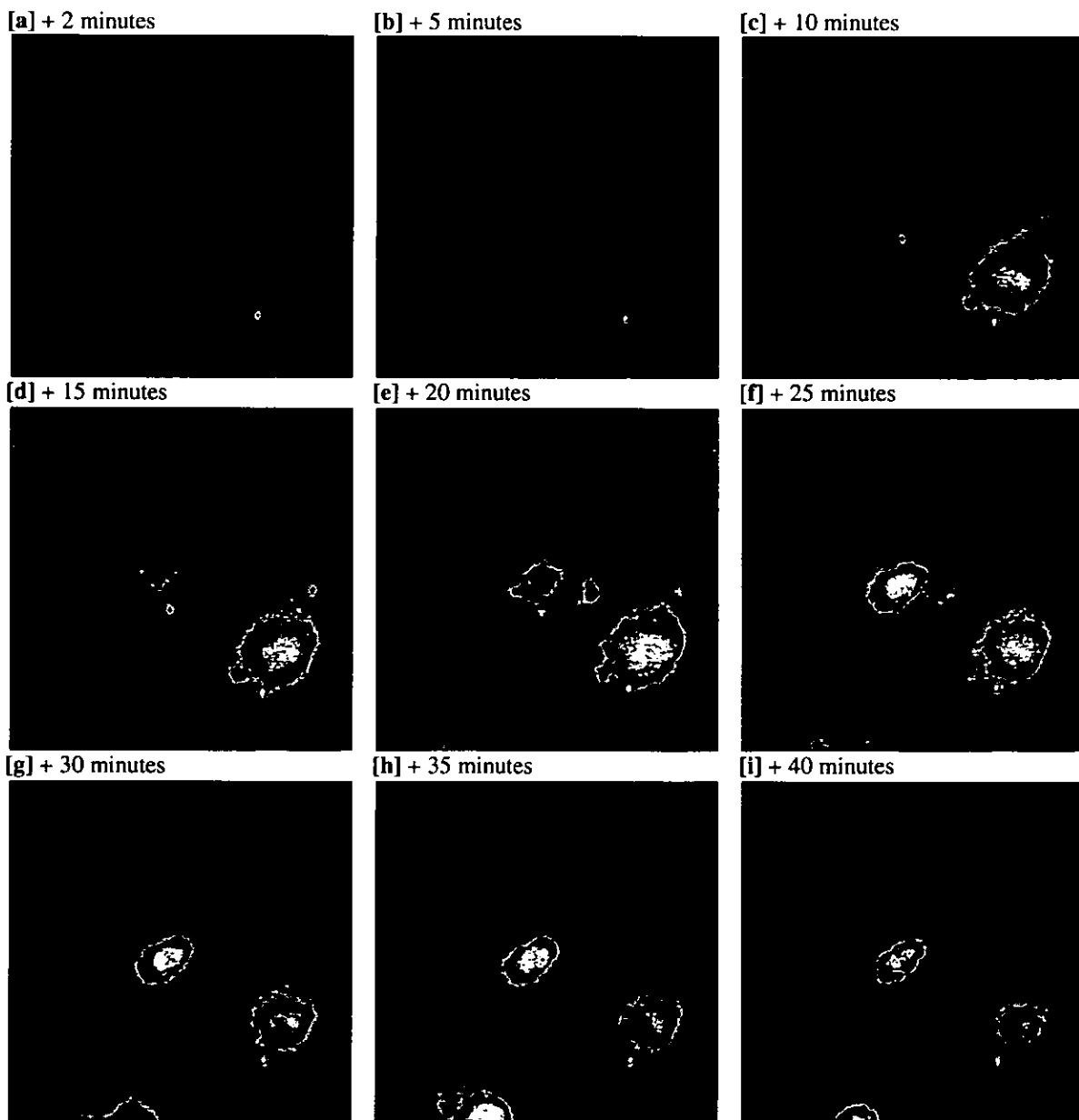


Figure 39. Subcellular localisation of 0.3 μM NMB in a group of typical SK-23 cells over a period of forty minutes using confocal microscopy and a flow-through method with a rinsing procedure. Cells were visualised using discontinuous illumination with the laser beam.

4.4.2 Effect of Photosensitizers on Mitochondrial Respiration

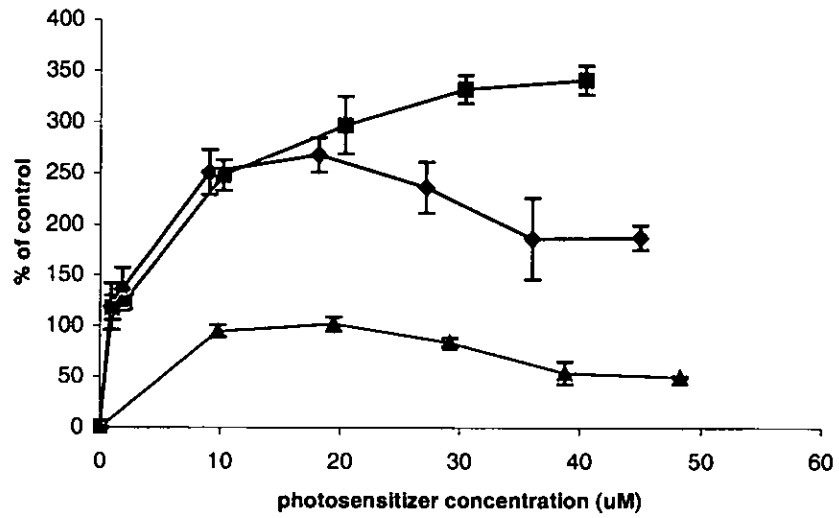
4.4.2.1 Protein Estimation

Mitochondrial protein was determined from the BSA calibration curve and fell within the concentration range 0 to 0.6 mg ml⁻¹ protein [Appendix 3].

4.4.2.2 Mitochondrial Respiration

The effect of three of the photosensitizers (MB, MMB and DMMB) on respiration was determined in isolated rat mitochondria, using either L-malate/pyruvate or succinate as substrates. In the presence of L-malate/pyruvate, additions of MB caused an increase in oxygen utilization up to a maximum level of 2.5 × basal rate at approximately 10 μM MB, after which, levels were seen to plateau, then decline. With added MMB, oxygen utilization mirrored that with added MB, up to 10 μM MMB. However, oxygen utilization continued to increase to a maximum level of over 3 × basal rate, at a concentration of 30 μM MMB, before declining. In contrast, with added DMMB, oxygen utilization never rose significantly above the basal rate, and, in fact, declined at concentrations over 20 μM DMMB [Figure 40]. Similarly, in the presence of succinate/rotenone, oxygen utilization was greatest with added MMB (a maximum level of approximately 2.5 × basal rate), approximately twice basal rate with added MB, and only slightly above basal with DMMB [Figure 40].

[a]



[b]

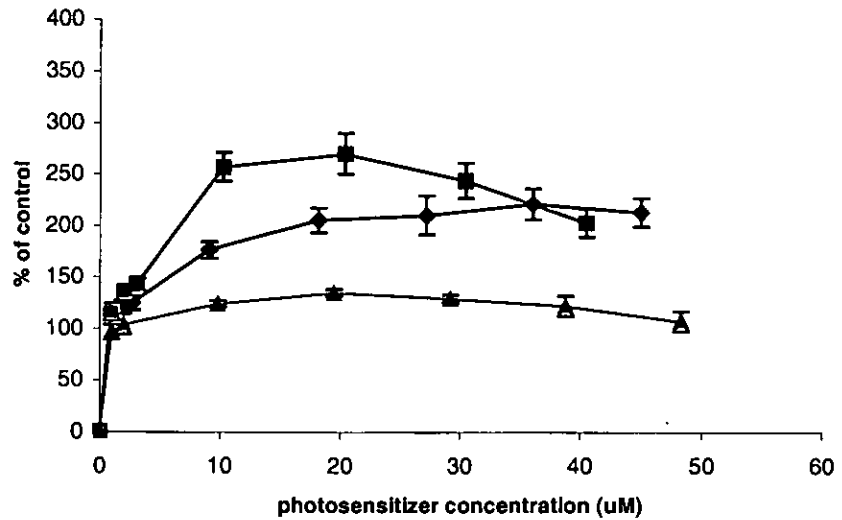


Figure 40. Effect of photosensitizers on oxygen utilisation in isolated rat mitochondria using [a] L-malate/pyruvate as substrate [b] succinate/rotenone as substrate; \blacklozenge = MB, \blacksquare = MMB, \blacktriangle = DMMB.

4.5 DISCUSSION

Fluorescence microscopy is an adequate method of studying the subcellular localisation of PDT photosensitizers, due to the fact that many are reasonably fluorescent in the red region of the visible spectrum. Despite this, the images obtained for MB and MMB in the EMT-6 cell line using this method are difficult to interpret clearly as, in either case, the photosensitizers appear to accumulate in the nucleus of certain cells, yet remain cytoplasmic in others. There also appear to be areas of dense blue staining with absence of fluorescence due, possibly, to aggregation of the dye molecules. Dye aggregation is a problem, particularly at high concentrations of photosensitizer, that reduces the efficacy of PDT. MB and MMB were incubated with the various cell lines at higher concentrations than both DMMB and NMB, in accordance with their IC_{50} values. However, the fluorescence images for DMMB and NMB are much more conclusive. Here, fluorescence microscopy demonstrates consistently that, in EMT-6, SK-23 and SK-MEL-28 cells, following three hours incubation at their IC_{50} values, these two compounds are distributed uniformly throughout the cytoplasm as a particulate pattern, but are absent in the nucleus.

Subsequent to this, from images of fluorescence captured using confocal microscopy, it is observed that, following three hours' incubation at their IC_{50} values, none of the four photosensitizers, MB, MMB, DMMB and NMB, is located in the nucleus in any of the three cell lines, EMT-6, SK-23 or SK-MEL-28. Rather, fluorescence is limited to small, subcellular bodies located in the cytoplasm of the various cells. In order to ascertain the primary localisation of the photosensitizer prior to light activation, it was necessary to capture images without delay, since the laser beam used to excite fluorescence in the cells for visualisation purposes, would also initiate the photodynamic reaction. Moreover, continued exposure to the laser beam would lead to photobleaching of the photosensitizer and a reduction in fluorescence. Another possible consequence of light exposure is the redistribution of the photosensitizer from its primary localisation in the cell to other cellular components. In fact, soon after exposure to the laser beam, the fluorescence signal increased and changed from a particulate pattern within the cytoplasm and generally spread diffusely throughout the cytoplasm. Within minutes of light exposure, all four photosensitizers were localised within the nucleus. Fluorescence signals faded with continued exposure to the laser. In

order to confirm that nuclear localisation was dependent upon illumination, image capture was also later performed without prior incubation of the photosensitizers and by using a flow-through method to deliver the photosensitizers to cells that had been preloaded onto the microscope stage. It was clearly demonstrated using this method, that uptake of the four photosensitizers into the three cell lines is rapid and that nuclear localisation of the photosensitizers follows within minutes of light exposure. The observed patterns of subcellular localisation were not unexpected since studies by other groups of workers have also reported light-induced redistribution of photosensitizers. In cervical carcinoma cells (NHIK 3025), for example, light doses that inactivate twenty per cent of cells also result in a relocation of TPPS4 from lysosomes to the nucleus, and of TPPS2 from lysosomes to the cytoplasm in general. This behaviour is attributed to photodynamic permeabilization of the lysosomal membrane, thus allowing small molecules, including the photosensitizers, to leak out [Berg *et al.*, 1991]. Similarly, Peng *et al.* [1991] observed the light-induced subcellular relocation of several sulfonated aluminium phthalocyanines in the LOX human melanoma cell line. Whilst Al-PcS₁ and Al-PcS₂ localise diffusely throughout the cytoplasm, Al-PcS₃ and Al-PcS₄ exhibit a granular pattern throughout the cytoplasm, which corresponds to the red fluorescence of lysosome-located acridine orange. Subsequent laser exposure of the cells incubated with high concentrations of Al-PcS₃ and Al-PcS₄ results generally in a relocation of the two photosensitizers to the cytoplasm, with a small fraction taken up into nuclei [Peng *et al.*, 1991]. The experiments in the present work were also carried out using constant concentrations of photosensitizer (5 μ M) to see if different concentrations would affect the observed patterns of intracellular targeting. The patterns of localisation were in fact the same whether photosensitizers were added at 5 μ M concentrations or added at their IC₅₀ value. This was true both following the three-hour incubation procedure and when using the flow-through method of drug delivery. However, higher concentrations of the photosensitizers appeared to favour more rapid uptake into the cells and to prolong the fluorescence signal. This permitted the capture of images over a longer period of time.

Although all four photosensitizers clearly did not target the cell nucleus prior to illumination, it was not possible to confirm their specific intracellular localisation from these studies. Their punctate pattern of distribution did, however, suggest that they do

become bound to subcellular organelles rather than remaining free within the cytosol. To gain insight into the likelihood of mitochondrial targeting by the photosensitizers, the effect of three of the compounds on respiration in isolated rat mitochondria was also examined. Here, the rates of oxygen utilization, using either L-malate/pyruvate or succinate/rotenone as substrates, are different for the three photosensitizers, yet do not mirror the pattern of methylation as might be expected. In this case the trend of oxygen utilization was DMMB<MB<MMB. The reason for this pattern may be linked to changes in hydrophobicity and to the ability of the photosensitizers to be reduced in their surrounding media. MB is known to be an artificial electron acceptor which draws off electrons from the respiratory chain at a point of interception after Complex I (redox potential [E'_0] = +0.01). Cycling of electrons between the reduced photosensitizer and oxygen at this point would explain the increased oxygen utilization in mitochondria with added MB. Furthermore, increased hydrophobicity could also be aiding the interaction of MMB with the respiratory chain, thereby increasing the rate of reduction of the agent, with concomitant increase in the rate of oxygen utilization, compared with MB. The succinate/rotenone system shows exactly the same pattern of oxygen utilization as with L-malate/pyruvate. Since rotenone blocks electron transport beyond the points of MB and MMB interaction, but before Complex I, oxygen utilization must be *via* interaction of the photosensitizers with oxygen, and not due to use of oxygen by the respiratory chain. Since it did not appear possible to assess the direct effect of the photosensitizers on oxygen utilization (*i.e.* respiration) using this system, experiments to examine the fourth compound, NMB, were abandoned.

Although the traditional cationic dye, MB, is known primarily to target the nucleus, the localisation studies described above indicate that its derivatives, MMB, and DMMB and NMB, are likely to follow different cellular localisation patterns due to the presence of substituent methyl moieties at various positions of the molecule. The physicochemical character of both the doubly-methylated molecules, DMMB and NMB, in particular, is indicative of mitochondrial targeting. In fact, it is known that the mitochondria of malignant cells preferentially accumulate and retain certain, hydrophobic, cationic compounds, such as rhodamine 123 and dequalinium chloride [Oseroff *et al.*, 1986]. The levels of these compounds accumulated, and their retention times, are much greater than those found in the mitochondria of most normal cells. This is likely to be due to differences in morphology, membrane and matrix compositions, and to a high negative

potential across the mitochondrial membrane. The use of carcinoma cell-specific, cationic dyes as photochemotherapeutic agents suggests that mitochondria may therefore serve as targets for highly selective photochemotherapy.

Although these studies failed to establish the primary subcellular localisation of the four photosensitizers, it was clear, nevertheless, that, upon illumination, they each become redistributed from small subcellular bodies, first to the cytoplasm in general and then almost immediately to the nucleus. Since PDT is mainly dependent upon the generation of $^1\text{O}_2$ as the damaging species and since singlet oxygen diffuses intracellularly only about $0.1\ \mu\text{m}$ in its lifetime [Moan, 1990], the cellular structures close to high sensitizer concentration will be preferentially damaged by the activating light. Consequently, the sites of photodynamic action of a photosensitizer ought therefore to be closely related to its pattern of subcellular/intratumoral localisation. If DMMB and NMB should relocate to the nucleus from mitochondria, then the overall PDT response (and the greatly enhanced toxicities of these two agents) may be a combination of both sublethal and lethal insults to cells. For instance, gene induction that occurs many hours after PDT would be unlikely if the cells had already undergone apoptosis within two hours of mitochondrial damage.

CHAPTER 5:
EVIDENCE FOR INDUCTION OF APOPTOSIS BY METHYLENE
BLUE AND ITS DERIVATIVES IN EMT-6, SK-23 AND SK-MEL-28
CELLS IN CULTURE

5.1 ABSTRACT

The photosensitizing capabilities of the cationic photosensitizer, methylene blue (MB), have been investigated by several groups of workers. However, the potential of MB to be used in clinical PDT is limited by an inherent toxicity and by its rapid reduction *in vivo* to the neutral leucobase. The derivatives of MB, however, 1-methyl methylene blue (MMB), 1,9-dimethyl methylene blue (DMMB) and new methylene blue N (NMB) are found to have increased photosensitizing efficacies compared to MB itself. Several factors may be responsible for this. Of particular interest in this study was an increase in the hydrophobic character of the derivatives that not only improved cellular uptake but was also expected to favour their mitochondrial targeting. The doubly methylated derivatives, DMMB and NMB, in particular, were expected to target mitochondria, although this was not confirmed during the course of this study. Photosensitizers that localise in mitochondria are found to be more efficient inducers of apoptosis than photosensitizers that target other subcellular sites. The ability of the photosensitizers, MB, MMB, DMMB and NMB, to induce apoptosis in EMT-6, SK-23 and SK-MEL-28 cells in culture was investigated in this study. From examination of cell morphology, by use of the cyanine dye, JC-1, and the use of the FluorAce® Apopain Assay Kit from Biorad, it was concluded that apoptosis may be an important cell killing mechanism in the photocytotoxicity of the photosensitizers, moreso for DMMB and NMB.

5.2 INTRODUCTION

Photodynamic therapy (PDT) is an alternative treatment regime for malignant and pre-malignant disease based on the administration of a tumour-specific, photosensitizing drug (usually the porphyrin-based Photofrin®) and its subsequent local activation by long (red) wavelength light [Section 1.2]. In the presence of molecular oxygen this produces a cytotoxic response in targeted cells [Henderson & Dougherty, 1992]. Cell killing is brought about mainly *via* Type II photochemical processes with the generation of highly reactive singlet oxygen ($^1\text{O}_2$) and its subsequent lethal action on key cellular components [Weishaupt *et al.*, 1976]. Responses to PDT vary according to the photosensitizer, cell type, illumination conditions and the oxygenation status of the tissue. Cellular structures having both high photosensitizer and high oxygen concentrations will be vulnerable to photodynamic activity. For energy transfer reactions (Type I), the photosensitizer must interact directly with its target [Foote, 1991] [Section 1.3]. Similarly, for electron transfer reactions (Type II), the sites of photodamage will be close to the location of the photosensitizer at the time of its activation by light, because $^1\text{O}_2$ has a diffusion distance of up to only 0.1 μm in its intracellular lifetime [Moan 1990]. Consequently, it might be expected that the efficacy of PDT could be enhanced by the use of photosensitizers that localise within critical components of the cell [Section 4.2]. Hydrophobicity and charge are important determinants of the subcellular localisation of a particular photosensitizer, as too are its mode of entry (diffusion or endocytosis) or, in some cases, special delivery system (liposomes or antibodies) into the cell.

PDT-treated cells may undergo a rescue response and/or die by either a necrotic or an apoptotic mechanism, depending on the dose, cell line and photosensitizer used [He & Oleinick, 1996]. Necrosis is a passive, uncontrolled process involving swelling of the cell and its intracellular organelles, loss of membrane integrity, and culminating in cell lysis and the generation of a localised inflammatory response [Boobis *et al.*, 1989]. Cells that suffer irreparable damage are more likely to die by necrosis. In contrast, apoptosis or 'cell suicide' is a highly regulated, evolutionary conserved mechanism that is executed by cellular proteins [Wylie *et al.*, 1980]. Both necrosis and apoptosis can occur simultaneously in tissues or cell cultures exposed to the same stimulus [Shimizu

et al., 1996], but it is often the intensity of the initial insult that decides the prevalence of either mechanism. Lesser doses of the same agent that produces necrosis can lead to apoptosis [Bonfoco *et al.*, 1995].

Cells undergoing apoptosis are characterised by distinct morphological alterations, including a specific pattern of DNA fragmentation, chromatin condensation, membrane blebbing, cell shrinkage and disassembly into membrane-delineated vesicles called apoptotic bodies [Arends & Wylie, 1991]. These are subsequently phagocytosed by macrophages or neighbouring cells with the lack of an inflammatory response in the affected tissue. Apoptotic changes occur as a two-phase (commitment followed by execution) process in a predictable, reproducible sequence and are usually complete within thirty and sixty minutes. Various death receptors belonging to the tumour necrosis factor (TNF) receptor gene superfamily and present on the cell membrane play a pivotal role in apoptosis. Death receptors have a characteristic cysteine-rich, extracellular domain and an additional homologous cytoplasmic sequence called the 'death domain' [Ashkenazi & Dixit, 1998]. The propensity of death domains to associate with one another facilitates both pro- and anti-apoptotic communication between death receptors and the cell's apoptotic machinery.

Genetic regulation of apoptosis has been studied extensively in the nematode, *Caenorhabditis elegans*, since it contains a similar enzymatic system that initiates apoptosis upon activation [William & Smith, 1993]. In *C. elegans*, apoptosis is dependent upon three specific gene products; Ced-3 and Ced-4 that promote apoptosis [Yuan & Horvitz, 1990], and Ced-9 that inhibits it [Hengartner & Horvitz, 1994]. Ced-3 shares homology with the mammalian cysteine protease, interleukin-1-converting enzyme (ICE), one of a family of at least fourteen other cysteine proteases that have been renamed 'caspases'. Caspases operate as a cascade mechanism and are commonly described as the 'executioners' of apoptosis [Thornberry & Lazebnik, 1998]. The only Ced-4 homologue so far identified is Apaf-1, involved mainly in caspase activation. Ced-9 shares homology with the mammalian Bcl-2 family proteins that are generally regarded as central regulators of apoptosis. Bcl-2 proteins integrate signal transduction pathways and modulate the apoptotic response to DNA damage. Whilst some Bcl-2 members serve to inhibit apoptosis (Bcl-2 itself, Bcl-X_L, A1/Bfl-1, Bcl-w, Nr13 and Mcl-1), others (Bax, Bik, Bak, Bad and Bcl-X_S) are involved in its promotion [Nagata,

1997]. Resistance to PDT is demonstrated consistently in cell lines that overexpress Bcl-2 [He *et al.*, 1996].

Cell death mechanisms are commonly associated with mitochondrial damage and loss of electron transport, with subsequent decline in levels of ATP [Green & Reed, 1998]. Apoptosis, however, is a form of cell death that requires energy [Richter *et al.*, 1996]. Consequently, intracellular ATP levels are believed to be a major determinant of the mechanism of cell death, since apoptosis is dependent upon high levels of ATP. Apoptosis may be induced when ATP levels start to decline, as long as a certain level of ATP is maintained to fuel various downstream apoptotic processes such as hydrolysis of macromolecules, nuclear condensation and bleb formation. Consequently, although levels of ATP have been observed to fall during apoptosis, this often occurs relatively late in the process. Thus, although loss of mitochondrial ATP production can kill a cell, it is unlikely that this is the mechanism of induction of apoptosis. Only when ATP levels are severely depleted, is necrotic cell death induced [Richter *et al.*, 1996; Eguchi *et al.*, 1997; Leist *et al.*, 1997].

Cell death following PDT was originally believed to be induced solely *via* a necrotic mechanism [Henderson & Dougherty, 1992]. However, evidence continues to accumulate that apoptosis also plays a major role in photocytotoxicity. The first observations of apoptosis following PDT were made in murine L5178Y (LY-R and LY-S) cells *in vitro* [Agarwal *et al.*, 1991] and in RIF-1 tumours in C3H mice *in vivo* [Zaida *et al.*, 1993]. Since then, PDT has been shown to be an efficient inducer of apoptosis in various carcinoma cell lines [He *et al.*, 1994], in human squamous epithelial cells *in vitro* and in biopsies of PDT-treated human skin tumours [Oseroff, 1993]. The degree of the apoptotic response depends upon the photosensitizer [He *et al.*, 1994], the cell line [Lauka *et al.*, 1994] and the doses of PDT [Luo & Kessel, 1997]. Apoptosis following PDT with Photofrin® appears to be restricted mainly to lymphoma and epithelial cells lines [Dellinger, 1996].

The initiation and rate of progression of apoptosis is highly dependent upon the site of photodynamic action. Mitochondria are considered to be important targets for PDT-induced photodamage [Salet & Moreno, 1990] and photosensitizers that localise in

mitochondria are found to be more efficient inducers of apoptosis than photosensitizers that target other subcellular sites [Kessel *et al.*, 1997]. This is most likely to be as a result of the induction of specific signalling pathways.

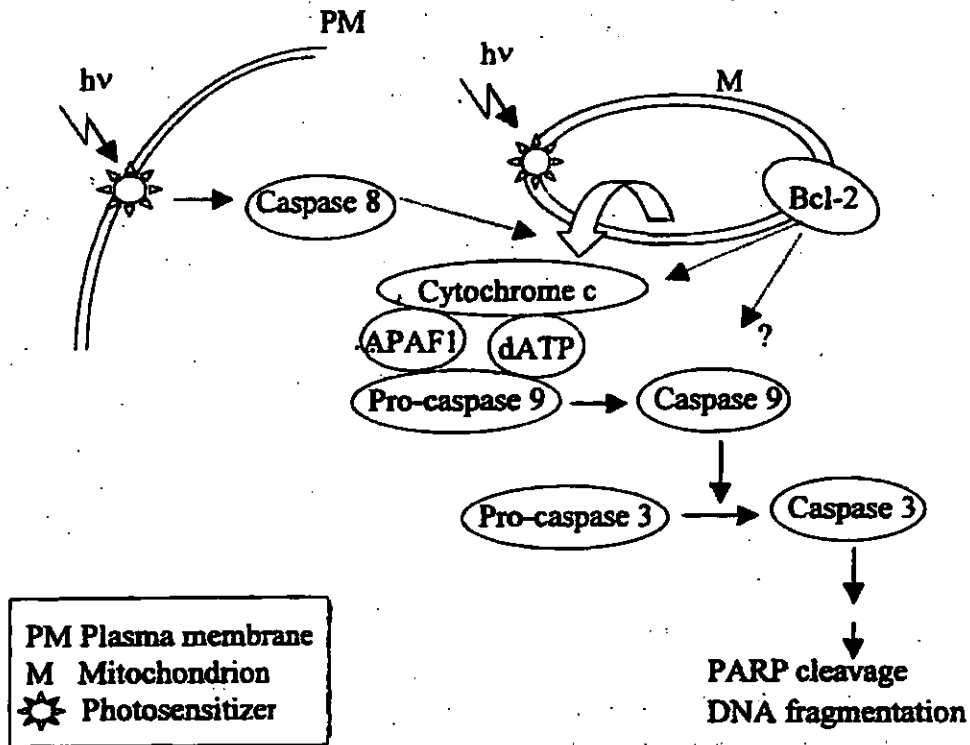


Figure 41. Apoptosis induction *via* caspase activation for mitochondria-specific and plasma membrane bound photosensitizers [Taken from Moor, 2000]

A primary event in PDT following illumination is release of the electron-transfer protein, cytochrome *c*, from mitochondria into the cytosol of damaged cells. This has been demonstrated in HeLa cells treated with benzoporphyrin derivative monoacid ring A (BPD) [Granville *et al.*, 1998] in L5178-R cells with Pc4 [Varnes *et al.*, 1999] and in P388 leukaemia cells using a porphycene monomer or capronyloxy porphycene [Kessel & Luo, 1999]. In the latter study, a rapid loss of mitochondrial membrane potential was also observed. Collapse of the mitochondrial inner transmembrane potential during apoptosis often leads to the opening of a large non-selective, conductance channel known as the mitochondrial permeability transition pore (MPTP) [Green & Reed, 1998]. MPTP is located in the inner mitochondrial membrane. It is normally fully closed but opens in the presence of high calcium plus oxidants or high phosphate, *via* a conformational change of the adenine nucleotide translocase (ANT) bound to matrix cyclophilin-D. Opening of MPTP allows leakage of protons and the equilibration of

ions within the mitochondrial matrix and intermembrane space. It is believed that calcium release might play a role in the observed loss of cytochrome *c* [Green & Reed, 1998]. The H⁺ gradient across the inner membrane is rapidly dissipated with uncoupling of the respiratory chain and rapid hydrolysis of cellular ATP. Without closure, this sequence of events results in necrosis. Apoptosis is more likely to arise from transient opening of MPTP that results in a volume dysregulation of mitochondria due to the hyperosmolality of the matrix. This causes the matrix space to expand and, because the inner membrane has a larger surface area than the outer membrane, this swelling eventually causes rupture of the outer mitochondrial membrane with release into the cytosol of caspase-activating proteins (including cytochrome *c*) located within the intermembrane space. Reclosure of MPTP maintains levels of ATP. However, it is not yet certain whether opening of MPTP is critical in PDT-induced release of cytochrome *c*, since PDT with haematoporphyrin on isolated rat mitochondria has been shown to degrade critical histidines with loss of function of MPTP [Salet *et al.*, 1997].

Cytochrome *c* functions as an early signalling molecule in apoptosis that, along with other mitochondrial components (such as procaspase-3 and apoptosis-inducing factor) activates caspase 3 *via* cleavage of CPP32 at the onset of apoptosis [Green & Reed, 1998]. Depending on cell type, it is believed that cytochrome *c* release causes rapid apoptotic cell death involving Apaf-1-mediated caspase activation, or slow necrotic demise, due to loss of electron transport, decreased production of ATP and generation of oxygen free radicals. (Generation of oxygen free radicals is also increased during apoptosis though is likely to be a relatively late event.) In cells where cytochrome *c* is available in excess, apoptosis *via* caspase activation can occur whilst sufficient amounts of cytochrome *c* remain bound to cytochrome *b-c₁* and cytochrome *c* oxidase to maintain electron transport and ATP production. Alternatively, in cells containing large quantities of endogenous caspase inhibitors, cytochrome *c* release may fail to induce caspase-dependent apoptosis and instead necrotic demise may ensue as a result of the eventual loss of electron chain transport [Green & Reed, 1998]. Varnes *et al.*, (1999) found that cytochrome *c* release following PDT with Pc 4 caused an inhibition of respiration that was reversed on addition of exogenous cytochrome *c*, implying only a subtle effect of PDT on the mitochondrial membrane. The effect of cytochrome *c* release here was an increase in caspase 3 activity. Similarly, Granville *et al.* (1998) found increases in the activity of caspases 3, 6 and 7 following PDT with BPD.

Furthermore, this latter study showed delayed activation of caspase 8 that mediates the CD95/FAS apoptotic pathway [Ashkenazi & Dixit, 1998], indicating a secondary apoptotic mechanism for ensuring cell demise. The caspase 8 substrate, Bid, itself known to induce release of cytochrome *c*, was cleaved by BPD-induced PDT, yet was also preceded by cytochrome *c* release, confirming the secondary role of the caspase 8-Bid pathway under these conditions [Granville *et al.*, 1999]. In a separate study by Zhuang *et al.* (1999), the photosensitizer, Rose Bengal that localises in the plasma membrane was found to induce apoptosis by direct activation of caspase 8, with subsequent release of cytochrome *c* and activation of caspase 3. This clearly illustrates the importance of photosensitizer localisation at the time of illumination in determining ultimately the pathway of cell death. Loss of cytochrome *c* is prevented by the Bcl-2 protein, located in mitochondrial membranes, that can impair or prevent the apoptotic response to many stimuli [He *et al.*, 1996]. Furthermore, PDT-resistant cells have mitochondria that are relatively smaller, stain more densely and display a higher cristae density than the parental line [Sharkey *et al.*, 1993].

Mitochondrial targeting is not, however, necessarily a prerequisite for the induction of apoptosis. Hydrophobic photosensitizers also localise in the plasma membrane and a number of signalling pathways can be induced as a result of photodamage to this site [Moor, 2000]. The exact roles of these pathways have not yet been elucidated but it is believed that inhibition of calcium regulation plays a major role on cell death. The activities of certain second messengers are increased following PDT with Photofrin® [Agarwal *et al.*, 1993]. Calcium may be responsible for induction of prostaglandin E₂ and leukotriene synthesis that would lead to the increased levels of molecules such as phospholipase A₂, phospholipase C, cAMP, adenylyl cyclase and protein kinase C (PKC), that have been observed with PDT. In T24 cells treated with PDT using HPD, phospholipases initiate a rescue response [Penning *et al.*, 1993], whilst in L5178 cells using PDT with ALPc, phospholipases trigger apoptotic cell death [Agarwal *et al.*, 1993]. The role of PKC is unclear, although studies using various inhibitors indicate that PKC activation initiates a rescue response by cells undergoing PDT-induced apoptosis [Zwang *et al.*, 1998; Luo & Kessel, 1996]. Photosensitizers localised in lysosomes may trigger cell death either by release of lysosomal enzymes into the cytosol or by relocalisation of the photosensitizers to secondary subcellular sites [Peng

et al., 1991]. Apoptosis induced by photosensitizers localised in lysosomes has been reported, but it is a much slower and less efficient process than that induced by agents that target mitochondria [Noodt *et al.*, 1999]. Ceramide is a potential mediator of apoptosis that is generated from its precursor, sphingomyelin, by a family of isoenzymes called sphingomyelinases (Smases). The acid form of Smase (aSmase) is found in lysosomes or is secreted into the extracellular space. Apoptosis associated with rapid generation of ceramide was found following PDT with Pc 4 in LY-R, CHO and U937 cell lines, although in RIF-1 cells, which also accumulate ceramide upon PDT, no apoptosis was observed [Separovic *et al.*, 1997; 1998; 1999]. Apoptosis following PDT with Pc 4 was also studied in cells deficient in aSMase. Ceramide generation (and thence apoptosis) was restored following treatment of the cells with bacterial Smase, suggesting that aSmase might be a target for induction of apoptosis with Pc 4 [Separov *et al.*, 1999]. The mechanism behind this is not known since Pc 4 preferentially targets mitochondria, although it might also be present in lysosomal membranes.

Methylene blue (MB) is one of a multitude of agents investigated as alternatives to Photofrin®, the sole photosensitizer currently registered for clinical use, that is associated with several drawbacks. MB has found success in treating inoperable oesophageal tumours [Orth *et al.*, 1995] and carcinoma of the bladder [Williams *et al.*, 1989], but its own use is limited by its rapid reduction *in vivo* and by an inherent (dark) toxicity [Section 2.1]. The derivatives of MB, 1-methyl methylene blue (MMB), 1,9-dimethyl methylene blue (DMMB) and new methylene blue N (NMB) have significantly enhanced dark and photocytotoxicities in non-pigmented and pigmented cells in culture, compared to MB itself [Chapter 2; Chapter 3]. These correspond generally to increases in singlet oxygen quanta, increased resistance to reduction, increased hydrophobicities and improved cellular uptake. It is also believed that the derivatives may follow different intracellular localisation patterns to MB and that this might be a further contributory factor to the enhanced photodynamic activity of these compounds. MB is recognised traditionally as a nuclear stain [Tuite & Kelly, 1993] but may also target lysosomes [Santus *et al.*, 1983; Yao & Zhang, 1996] and microtubules [Stockart *et al.*, 1996]. The substitution of bulky methyl groups to its structure and the increased hydrophobic character of the derivatives are indicative of mitochondrial

targeting, although this was not confirmed during this study [Chapter 4]. Photosensitizers that localise in mitochondria are rapid inducers of apoptosis upon irradiation [Kessel *et al.*, 1997]. A hydrophobic derivative of MB, MBD, is reported to localise in mitochondria and to induce cell death by apoptosis [Noodt *et al.*, 1998] and the methylene blue analogue, DO15, also yields mitochondrial photodamage during apoptosis, whilst membrane and lysosomal integrity are maintained [Ball *et al.*, 1998]. The aim of this part of the project was to examine the evidence for apoptosis in cultures of cells (EMT-6, SK-23 and SK-MEL-28 lines) incubated with the cationic dyes, MB, MMB, DMMB and NMB, and subjected to photodynamic treatment. The methods chosen for this were microscopic examination of cellular morphology pre- and post-PDT, fluorometric analysis using the fluorescent dye, JC-1, to detect changes in mitochondrial membrane potential, and use of the FluorAce® Apopain Assay for detection of caspase 3 activity, (both in cell cultures subjected to PDT).

5.3 METHODS & MATERIALS

5.3.1 Cell Morphology

Cultures of EMT-6, SK-23 and SK-MEL-28 cells growing in RPMI 1640 culture medium and in 35 mm petri dishes were incubated with MB, MMB, DMMB and NMB at their IC_{50} concentrations. [In the EMT-6 cell line, MB = 18.7 μ M, MMB = 2.2 μ M, DMMB = 0.09 μ M and NMB = 0.39 μ M. In the SK-23 line, MB = 15.2 μ M, MMB = 1.6 μ M, DMMB = 0.05 μ M and NMB = 0.3 μ M. In the SK-MEL-28 line, MB = 21.0 μ M, MMB = 2.2 μ M, DMMB = 0.01 μ M and NMB = 0.3 μ M]. The cells were visualised under a standard light microscope and photographed at 1-hour, 2-hour and 3-hour intervals, and finally, following a further thirty minute period of illumination.

5.3.2 Detection of Apoptosis using JC-1

5.3.2.1 JC-1

5,5',6,6'-tetrachloro-1,1',3,3'-tetraethylbenzimidazolylcarbocyanine iodide (JC-1; CBIC₂(3)) is a green fluorescent dye (supplied as a red orange solid) that is used as a fluorescent probe for monitoring mitochondrial membrane potential. JC-1 belongs to the 'slow' class of cyanine dyes that are hydrophobic, cationic compounds with a delocalised positive charge. As such, JC-1 will respond within minutes or seconds to changes in membrane potential, mostly in accordance with the Nernst equation. It has been known for over fifty years that some of the 'slow' dyes form aggregates in certain environments, accompanied by dramatic shifts in both absorption and fluorescence maxima, leading to violations of Beer's Law [Jelley, 1937; Scheibe, 1937]. The absorption spectrum of a monomer usually consists of a broad peak with a vibrational shoulder at the side of the shorter wavelength. This peak is referred to as the M-band (for monomer). The absorbance and fluorescence maxima of the monomeric dye species are 510 nm and 520 nm, respectively. Dye aggregation may cause a shift of the absorption maximum to either a shorter wavelength (called H-aggregates or H-bands, for hypsochromic) or to a longer wavelength (called J-aggregates after their discoverer, Jelley). Whilst H-aggregates do not emit fluorescence, J-aggregates are often intensely fluorescent, a feature that can be exploited for the measurement of membrane potentials. J-aggregates have absorption and fluorescence wavelengths that are similar (*i.e.* 585

nm) and this lack of a Stoke's shift is termed 'resonance fluorescence'. The factors most important for the formation of J-aggregates in living cells are the concentration of the dye, and the pH and ionic strength of the environment [Kay *et al.*, 1964]. JC-1 forms J-aggregates at an ionic strength and pH that are compatible with the intramitochondrial environment, and at a concentration that can readily be attained by mitochondria in response to the Nernst potentials. The propensity of cyanine dyes to form J-aggregates locally and instantaneously has proved a useful tool in the study of cell biology. JC-1 is used to detect apoptosis-induced changes in mitochondrial transmembrane activity because it exists as a monomer at low concentrations and in regions of low membrane potential, and forms J-aggregates at higher concentrations or in regions of high membrane potential. JC-1 emits either green fluorescence (under blue excitation) or red fluorescence (under green excitation), green fluorescence being indicative of the uptake of JC-1 monomers and red fluorescence indicative of J-aggregates. Orange fluorescence may be visualised in regions where both green and red fluorescence co-exist. The characteristics of JC-1 under various conditions were examined according to the fluorometric method developed by Chen & Smiley (1994). Subsequently, JC-1 in its monomeric form was added to cultures of cells that had been exposed to the photosensitizers, MB, MMB, DMMB and NMB, and the fluorescence spectra of these cell suspensions also recorded.

5.3.2.2 Effect of Concentration on the Fluorescence Spectrum of JC-1

JC-1 ($10 \mu\text{g ml}^{-1}$, $50 \mu\text{g ml}^{-1}$, $100 \mu\text{g ml}^{-1}$ and $200 \mu\text{g ml}^{-1}$) in 50 mM Tris HCl (pH 8.2) containing 1 % DMSO was placed in a 1 cm quartz cuvette, equipped with a magnetic stirrer. The fluorescence spectrum of the dye under these conditions was examined in a Perkin Elmer LS50B Luminescence Spectrophotometer set to read wavelengths from 480nm to 640 nm (excitation wavelength: 514 nm, slit width: 5 nm).

5.3.2.3 Effect of Ionic Strength on the Fluorescence Spectrum of JC-1

JC-1 ($10 \mu\text{g ml}^{-1}$) in 40 % dimethylsulphoxide (DMSO) in double distilled water at pH 7.2 or in 1 % DMSO in high K^+ buffer (3.6 mM NaCl, 137 mM KCl, 0.5 mM MgCl_2 , 1.8 mM CaCl_2 , 4 mM HEPES, 1 mg ml^{-1} dextrose and 1 % modified Eagles' medium amino acid solution (100 ×, GIBCO), pH 7.2) was placed in a 1 cm quartz cuvette, equipped with a magnetic stirrer. The fluorescence spectrum of the dye under these

conditions was examined in a Perkin Elmer LS50B Luminescence Spectrophotometer set to read wavelengths from 480nm to 640 nm (excitation wavelength: 514 nm, slit width: 5 nm).

5.3.2.4 Effect of pH on the Fluorescence Spectrum of JC-1

JC-1 ($10 \mu\text{g ml}^{-1}$) in 50 mM Tris-HCl containing 1 % DMSO at pH 7.2 and similarly at pH 8.2 (the intramitochondrial pH) was placed in a 1 cm quartz cuvette, equipped with a magnetic stirrer. The fluorescence spectrum of the dye under these conditions was examined in a Perkin Elmer LS50B Luminescence Spectrophotometer set to read wavelengths from 480nm to 640 nm (excitation wavelength: 514 nm, slit width: 5 nm).

5.3.2.5 Fluorescence Microscopy with JC-1 to detect Apoptosis in Cell Cultures

EMT6, SK-23 and SK-MEL-28 cells were grown to approximately fifty per cent confluence on 12 mm square glass coverslips in 35 mm petri dishes as described in Sections 2.2.3.1 and Section 3.2.2.1. Cultures were incubated three hours with the four photosensitizers (MB, MMB, DMMB and NMB) at their IC_{50} concentrations [In the EMT-6 cell line, MB = $18.7 \mu\text{M}$, MMB = $2.2 \mu\text{M}$, DMMB = $0.09 \mu\text{M}$ and NMB = $0.39 \mu\text{M}$. In the SK-23 line, MB = $15.2 \mu\text{M}$, MMB = $1.6 \mu\text{M}$, DMMB = $0.05 \mu\text{M}$ and NMB = $0.3 \mu\text{M}$. In the SK-MEL-28 line, MB = $21.0 \mu\text{M}$, MMB = $2.2 \mu\text{M}$, DMMB = $0.01 \mu\text{M}$ and NMB = $0.3 \mu\text{M}$]. The flasks were subsequently rinsed twice and replaced with fresh medium, then illuminated for thirty minutes with light from a bank of fluorescent tubes at a dose of 7.2 J cm^{-2} . Subsequently, cells were rinsed twice and incubated for a further ten minutes with fresh RPMI 1640 containing $10 \mu\text{g ml}^{-1}$ JC-1. Cells were again rinsed in fresh culture medium and coverslips of cells mounted onto warmed 76×26 mm glass micro cavity slides filled with fresh culture medium at 37°C . Cells were viewed immediately under a Leitz diaphan microscope using optical rhodamine and fluorescein filters.

5.3.2.6 Fluorometric Determination of Apoptosis in Cell Cultures using JC-1

EMT6, SK-23 and SK-MEL-28 cells were grown to confluence in 25 cm^2 tissue culture flasks as described in Section 2.2.3.1 and Section 3.2.2.1. Cultures were incubated for three hours with the four photosensitizers (MB, MMB, DMMB and NMB) at their IC_{50} concentrations [In the EMT-6 cell line, MB = $18.7 \mu\text{M}$, MMB = $2.2 \mu\text{M}$, DMMB = 0.09

μM and NMB = 0.39 μM . In the SK-23 line, MB = 15.2 μM , MMB = 1.6 μM , DMMB = 0.05 μM and NMB = 0.3 μM . In the SK-MEL-28 line, MB = 21.0 μM , MMB = 2.2 μM , DMMB = 0.01 μM and NMB = 0.3 μM]. The flasks were subsequently rinsed twice and replaced with fresh medium, then illuminated for thirty minutes with light from a bank of fluorescent tubes at a dose of 7.2 J cm⁻². Subsequently cells were incubated for a further ten minutes with fresh RPMI 1640 containing 10 $\mu\text{g ml}^{-1}$ JC-1. Cells were washed three times with and incubated in (5 ml) low K⁺ buffer (137 mM NaCl, 3.6 mM KCl, 0.5 mM MgCl₂, 1.8 mM CaCl₂, 4 mM HEPES, 1 mg ml⁻¹ dextrose and 1 % modified Eagles' medium amino acid solution (100 ×, GIBCO), pH 7.2) for ten minutes. Cells were then washed three times with (2 ml each) and left in (1 ml) trypsin (Sigma) in low K⁺ buffer for five minutes. Finally, 0.8 ml of cell suspension was mixed with 1.2 ml of low K⁺ buffer and placed into a quartz cuvette equipped with a magnetic stirrer. Fluorescence signals were recorded on a Perkin Elmer LS50B Luminescence Spectrophotometer set to read wavelengths from 480nm to 640 nm (excitation wavelength: 514 nm, slit width: 5 nm).

5.3.3 The FluorAce® Apopain Assay

5.3.3.1 Apopain/Caspase 3

Apopain/Caspase 3 is derived from the proenzyme CPP32 at the onset of apoptosis. Apopain/Caspase 3 exhibits the highest similarity to Ced-3 (*C. elegans* cell death gene) [Section 5.2] in both sequence homology and substrate specificity. Apopain activity therefore appears to be a suitable indicator of critical apoptosis biochemistry. Activity is monitored *in vitro* using the fluorogenic peptide substrate carbobenzoxy-Asp-Glu-Val-Asp-7-amino-4-trifluoromethyl coumarin (Z-DEVD-AFC), a variation of the substrate described by Nicholson *et al.* [1995]. This peptide-dye conjugate produces a blue fluorescence upon exposure to near-UV light. Apopain enzymatically cleaves the AFC from the peptide and releases free AFC, which then produces a blue-green fluorescence. The AFC substrate is both chromogenic (*i.e.* yellow-green colour is visible to the naked eye) and fluorogenic (detectable at 500 to 550 nm with a fluorometer). The reaction is selectively inhibited by the peptide chloromethyl ketone, Ac-DEVD-CMK, a potent inhibitor of apopain.

5.3.3.2 The FluorAce® Apopain Assay Kit

The Apopain Assay Kit from Bio-Rad contains reagents for one hundred one ml reactions and was used to detect apoptosis in cell cultures subjected to PDT, with some minor adjustments to the recommended schedule. After preparation, stock solutions were apopain substrate (Z-DEVD-AFC) (4.9 mM in DMSO), apopain inhibitor (Ac-DEVD-CMK) (4.4 mM in DMSO), apopain (120 µl in distilled water), 7-amino-4-trifluoromethyl coumarin (AFC) (200 µM in DMSO), 25× Reaction buffer (250 mM PIPES, pH 7.4, 50 mM EDTA, 2.5 % CHAPS, 125 mM DTT). All reagents were stored as instructed and used within six months of stock preparation.

5.3.3.3 Cell Cultures

EMT-6, SK-23 and SK-MEL-28 cells were grown in 75 cm² tissue culture flasks as detailed in Section 2.2.3.1 and Section 3.2.2.1 in order to obtain approximately 10⁷ cells.

5.3.3.4 Preparation of Cell Extracts

Floating cells were removed from prepared cultures into 15 ml disposable centrifuge tubes, pelleted and the supernatant removed. The attached cells were rinsed twice with 10 ml PBS (10 mM sodium phosphate, pH 7.2-7.4, 150 mM NaCl) and this added to the pellet of floating cells in the centrifuge tubes. The cells were re-pelleted and the supernatant removed. The attached cells were lysed by adding 500 µl Apopain Lysis Buffer (10mM HEPES, pH 7.4, 2 mM EDTA, 0.1 % CHAPS, 5 mM DTT, 1 mM PMSF, 10 µg ml⁻¹ pepstatin A, 10 µg ml⁻¹ aprotinin, 20 µg ml⁻¹ leupeptin) and dislodged by shaking the flasks. Buffer and cell debris were then also transferred to the centrifuge tube. The sample was subjected to four or five rapid freeze-thaw cycles by transferring successively from dry ice at -80°C to a 37°C water bath.

5.3.3.5 Apopain Assay

Cuvettes were prepared with 40 µl 25× Reaction Buffer, 10 µl Z-DEVD-AFC (substrate), 100 µl of sample (dye-treated cell extract) and made up to 1 ml with distilled water. To ensure positive detection of apoptosis, the following controls were also run:

- [a] blank (40 μ l 25 \times Reaction Buffer, 10 μ l Z-DEVD-AFC, 950 μ l distilled water)
- [b] sample of non-treated cell lysate
- [c] positive control (40 μ l 25 \times Reaction Buffer, 10 μ l Z-DEVD-AFC, 10 μ l apopain and 940 μ l distilled water)
- [d] negative control (inhibition of apopain activity) (see below)

Cuvettes containing the blank, positive control, photosensitizer-treated samples and non-treated control sample were mixed and the time and fluorescence signal recorded. The cuvettes were sealed with Parafilm and incubated at 30°C. Fluorescence signals were recorded at one-hour intervals for three hours on a Perkin Elmer LS50B Luminescence Spectrophotometer set to read wavelengths from 510 nm to 550 nm (excitation wavelength: 360 nm, slit width: 5 nm).

5.3.3.6 Inhibition of Apopain Activity (Negative Control)

To test for interference from non-specific protease activity, samples with and without the apopain specific inhibitor, Ac-DEVD-CMK were compared. Cuvettes were prepared and, in all cases made up to 990 μ l with distilled water, for the blank (40 μ l 25 \times Reaction Buffer), sample (40 μ l 25 \times Reaction Buffer, 100 μ l sample) and negative control (40 μ l 25 \times Reaction Buffer, 10 μ l Ac-DEVD-CMK, 100 μ l same sample). Any activity measured for the negative control would be from enzymes other than apopain. The cuvettes were mixed, sealed with Parafilm and incubated at 20°C for thirty minutes. 10 μ l of substrate (Z-DEVD-AFC) were added to each cuvette, mixed and the fluorescence measured and recorded immediately (t=0). The cuvettes were resealed and incubated again at 30°C. Fluorescence readings were taken at thirty-minute intervals for two hours.

5.4 RESULTS

5.4.1 Cell Morphology

There was evidence of cell rounding and shrinkage (characteristic of cells undergoing apoptosis) in cultures of the three cell lines, EMT-6, SK-23 and SK-MEL-28, subjected to photodynamic treatment with MB, MMB, DMMB and NMB, compared to controls, when visualised under a standard light microscope [Figure 42]. This morphology was only evident following illumination of the cells and was not seen immediately following the three-hour incubation period with the photosensitizers. Apoptosis was not conclusive, however, since cell lysis in cultures was also observed.

5.4.2 Detection of Apoptosis using JC-1

5.4.2.1 JC-1

The characteristics of JC-1 under various conditions were examined using fluorescence spectrophotometry. The emission maxima for the JC-1 monomer and the J-aggregate as defined by Chen & Smiley (1994) [Section 5.2.1.1] were shifted slightly using this particular machine and appeared at 516 nm and 599 nm, respectively. The importance of dye concentration and the pH and the ionic strength of the environment on J-aggregate formation were clearly demonstrated using this method [Figure 43].

5.4.2.2 Effect of Concentration on the Fluorescence Spectrum of JC-1

JC-1 existed as the monomeric form at a concentration of $10 \mu\text{g ml}^{-1}$. There was a successive increase in J-aggregate formation at concentrations between $50 \mu\text{g ml}^{-1}$ and $200 \mu\text{g ml}^{-1}$. J-aggregate formation was strongly favoured at concentrations above $100 \mu\text{g ml}^{-1}$ [Figure 43].

5.4.2.3 Effect of Ionic Strength on the Fluorescence Spectrum of JC-1

JC-1 remained in the monomeric form in a low ionic environment but formed J-aggregates in high potassium buffer that has an ionic strength comparable to that of the intracellular environment [Figure 43].

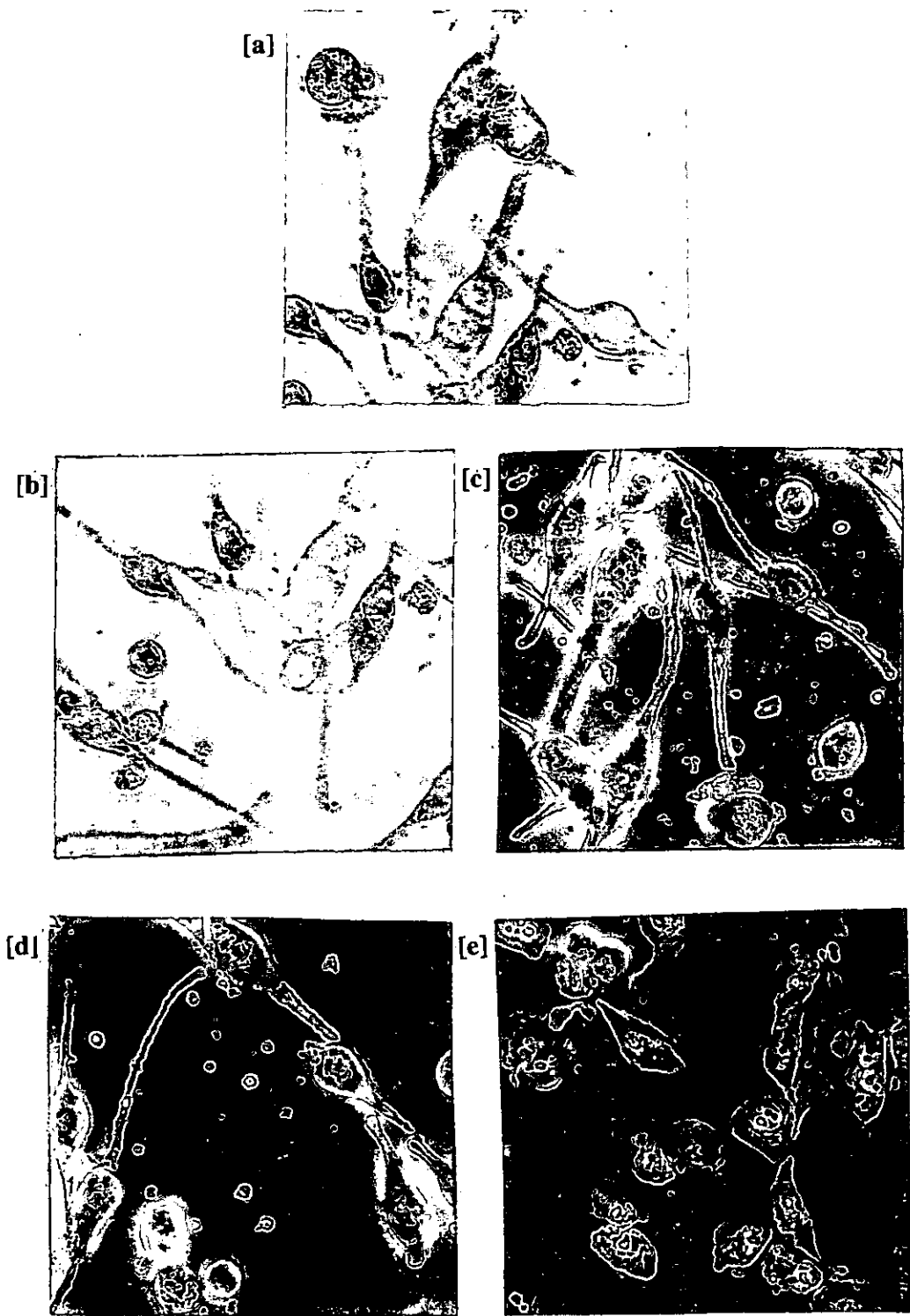


Figure 42. Light microscope images of SK-23 cells incubated with DMMB ($0.05 \mu\text{M}$) and subjected to PDT. Images are cells with [a] no photosensitizer, [b] light alone [c] DMMB plus 2-hour incubation, [d] DMMB plus 3-hour incubation and [e] DMMB plus 3-hour incubation and 30 minutes illumination.

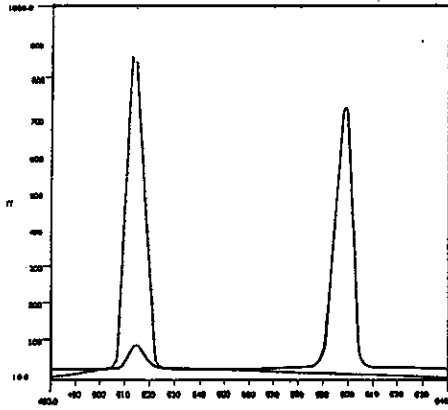
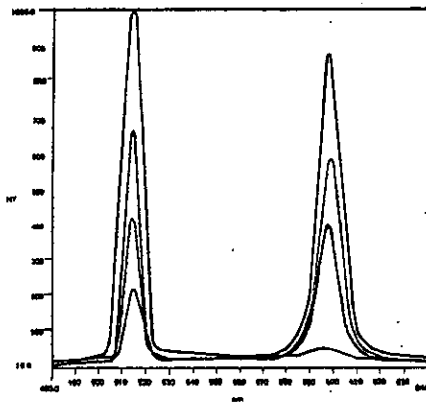
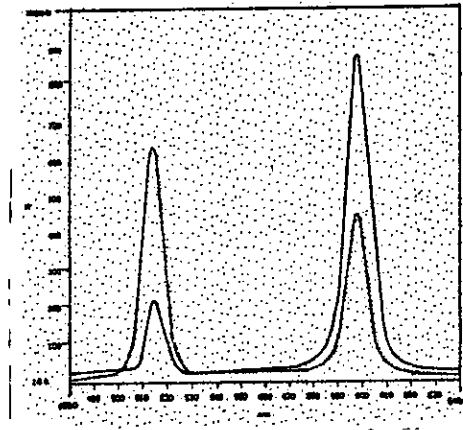


Figure 43. Effect of [a] pH, [b] concentration and [c] ionic strength on the fluorescence spectrum of JC-1. For [a] red line is JC-1 in 50 mM Tris-HCl containing 1 % DMSO at pH 7.2. Black line is JC-1 in 50 mM Tris-HCl containing 1 % DMSO at pH 7.2. As shown, J-aggregate formation is strongly favoured by the intramitochondrial pH of 8.2. For [b], for JC-1 in 50 mM Tris HCl (pH 8.2) containing 1 % DMSO, green line is JC-1 at $10 \mu\text{g ml}^{-1}$, blue line at $50 \mu\text{g ml}^{-1}$, red line at $100 \mu\text{g ml}^{-1}$ and black line, JC-1 at $200 \mu\text{g ml}^{-1}$. As shown, J-aggregate formation is highly concentration dependent. For [c], red line is JC-1 ($10 \mu\text{g ml}^{-1}$) in 40 % DMSO in double distilled water at pH 7.2. Black line is JC-1 ($10 \mu\text{g ml}^{-1}$) in 1 % DMSO in high potassium buffer. J-aggregate formation is favoured by a buffer with ionic strength comparable to that of the intracellular environment.

5.4.2.4 Effect of pH on the Fluorescence Spectrum of JC-1

At a pH of 7.2, JC-1 existed mainly as the monomeric species although there was evidence of J-aggregate formation. However, J-aggregate formation was strongly favoured by a pH of 8.2 that is compatible with the intramitochondrial environment [Figure 43].

5.4.2.5 Fluorescence Microscopy with JC-1 to detect Apoptosis in Cell Cultures

Cultures of cells from the three cell lines, EMT-6, SK-23 and SK-MEL-28, previously exposed to the photosensitizers, MB, MMB, DMMB and NMB, and subsequently incubated with $10 \mu\text{g ml}^{-1}$ JC-1 were examined using fluorescence microscopy. Using this method, regions of both green (the monomeric species) and orange (predominance of J-aggregates) fluorescence were detected in all cultures examined including control samples. It was impossible using this method to quantify the ratio of the different patterns of fluorescence or to establish whether there were any real differences between treated samples and controls. Examples of typical images captured both in both treated cells and in controls are found in Figure 44, which shows patterns of fluorescence in SK-23 cells exposed to NMB.

5.4.2.6 Fluorometric Determination of Apoptosis in Cell Cultures using JC-1

In EMT-6 cells, there were no differences in J-aggregate formation between treated cells and controls up to two hours of incubation with the photosensitizers [Figure 45a & 45b]. After three hours, J-aggregate formation was increased in all treated cell samples compared to controls [Figure 45c]. Following a further period of illumination of thirty minutes, whilst there appeared to be no further increases in J-aggregate formation in MB- and MMB-treated cells, J-aggregate formation in DMMB- and NMB-treated cells was significantly enhanced [Figure 45d]. In SK-23 cells, there were no differences in J-aggregate formation between MB- and MMB-treated cells and controls up to two hours of incubation with the photosensitizers, yet J-aggregate formation in DMMB- and NMB-treated cells appeared to be slightly enhanced [Figure 46a & 46b]. After three hours, J-aggregation was increased in all treated cell samples except for MB, compared to controls [Figure 46c]. Following a further period of illumination of thirty minutes, J-aggregate formation was enhanced in all treated cell samples, and particularly in DMMB- and NMB-treated cells, compared to controls [Figure 46d]. In SK-MEL-28

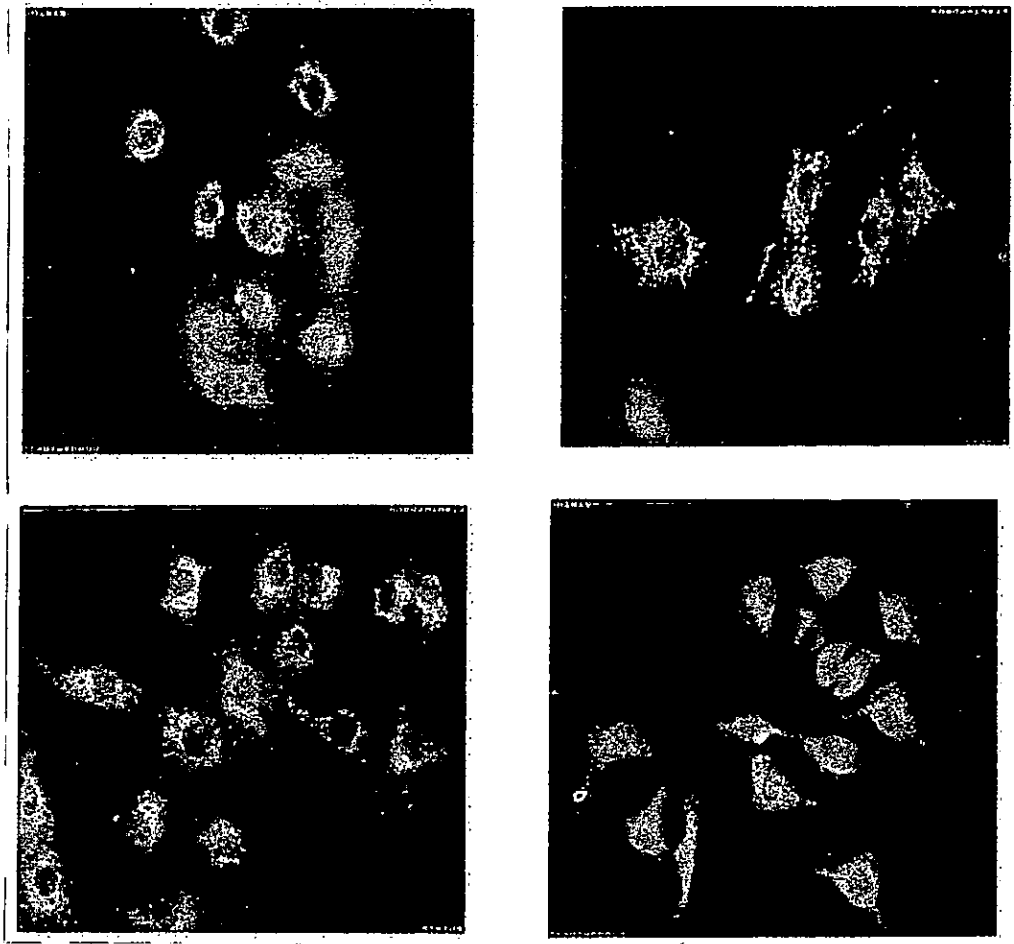
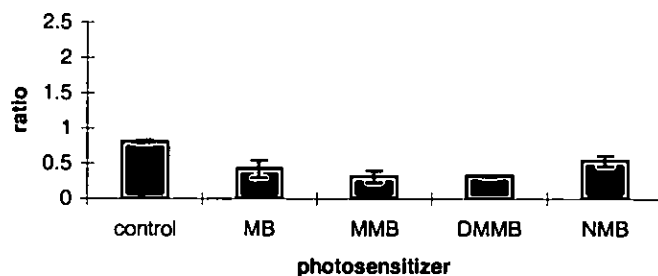
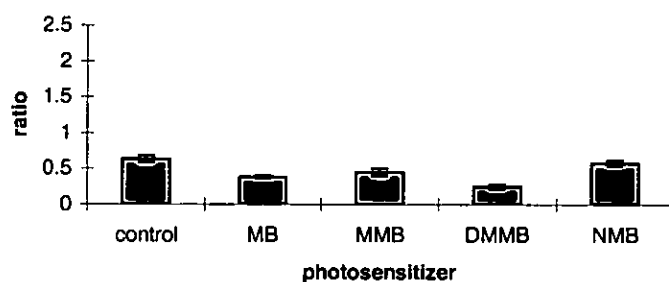


Figure 44. Fluorescence microscopy with JC-1 to detect apoptosis in cell cultures. Images are for SK-23 cells incubated with 0.3 μM NMB but are also typical of images found for MB, MMB and DMMB in this cell line and of images for the four photosensitizers in EMT-6, SK-23 and SK-MEL-28 cells.

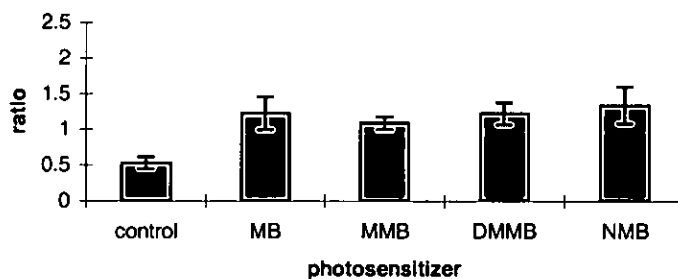
[a]



[b]



[c]



[d]

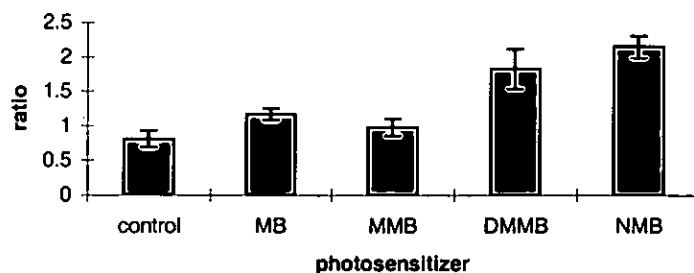
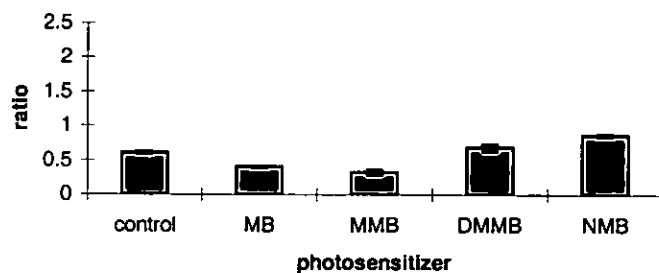
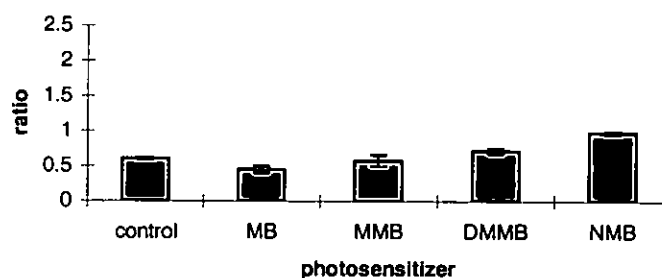


Figure 45. J-aggregate formation in EMT-6 cells following various exposures to phenothiazinium photosensitizers, [a] 1-hour incubation, [b] 2-hour incubation, [c] 3-hour incubation, [d] 3-hour incubation plus 30 minutes illumination. The results are the mean of two experiments \pm SD and are expressed as the ratio of J-aggregates to the monomeric species of JC-1. J-aggregate formation occurs in response to increases in intramitochondrial membrane potential brought about by events involved in apoptotic pathways.

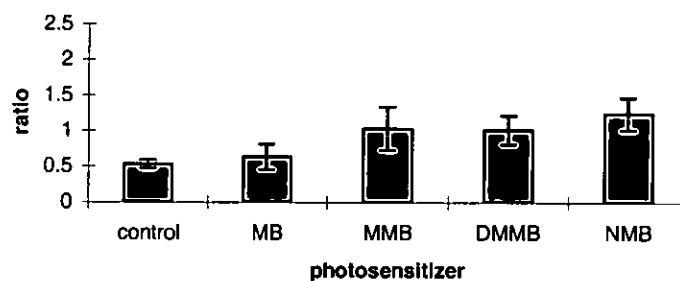
[a]



[b]



[c]



[d]

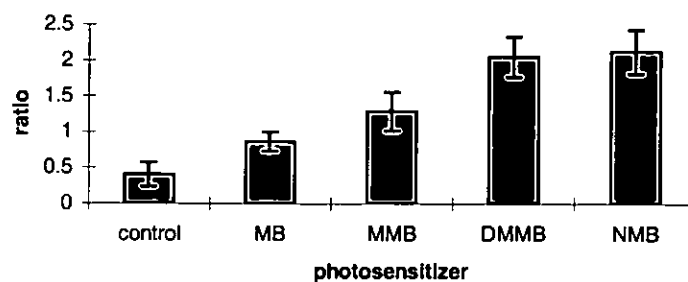
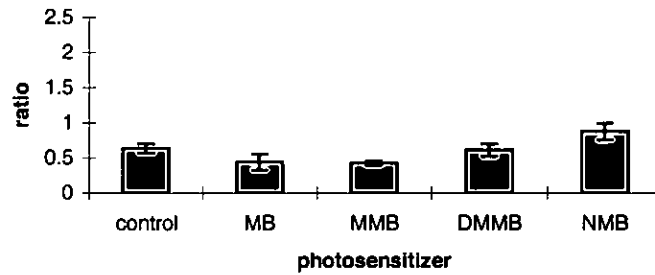
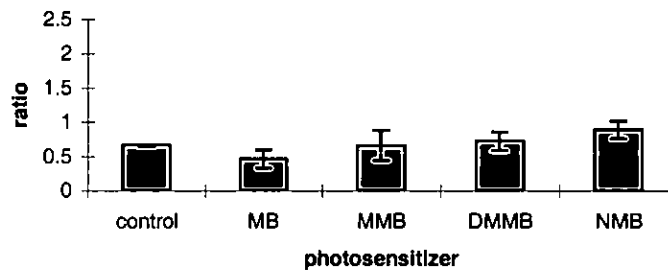


Figure 46. J-aggregate formation in SK-23 cells following various exposures to phenothiazinium photosensitizers, [a] 1-hour incubation, [b] 2-hour incubation, [c] 3-hour incubation, [d] 3-hour incubation plus 30 minutes illumination. The results are the mean of two experiments \pm SD and are expressed as the ratio of J-aggregates to the monomeric species of JC-1. J-aggregate formation occurs in intramitochondrial membrane potential brought about by events involved in apoptotic pathways.

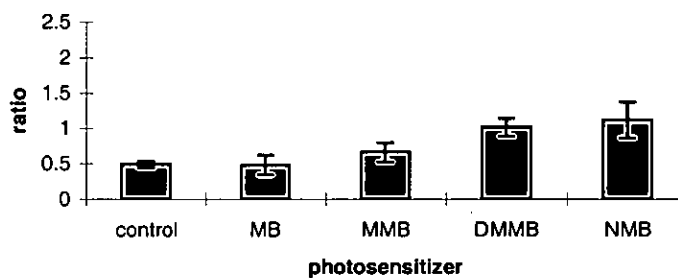
[a]



[b]



[c]



[d]

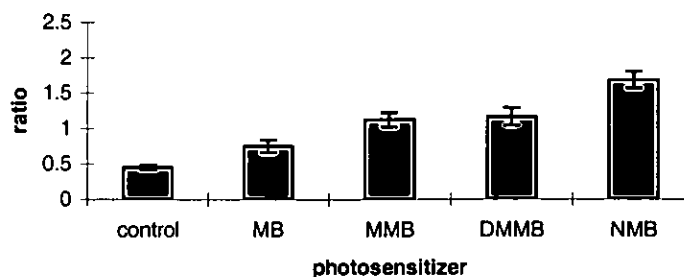
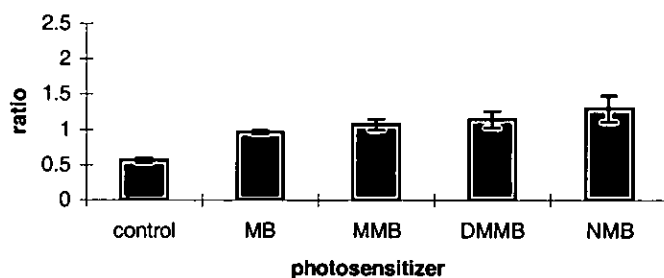
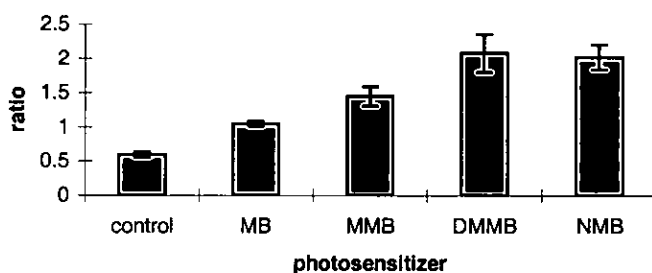


Figure 47. J-aggregate formation in SK-MEL-28 cells following various exposures to phenothiazinium photosensitizers, [a] 1-hour incubation, [b] 2-hour incubation, [c] 3-hour incubation, [d] 3-hour incubation plus 30 minutes illumination. The results are the mean of two experiments \pm SD and are expressed as the ratio of J-aggregates to the monomeric species of JC-1. J-aggregate formation occurs in response to increases in intramitochondrial membrane potential brought about by events involved in apoptotic pathways.

[a]



[b]



[c]

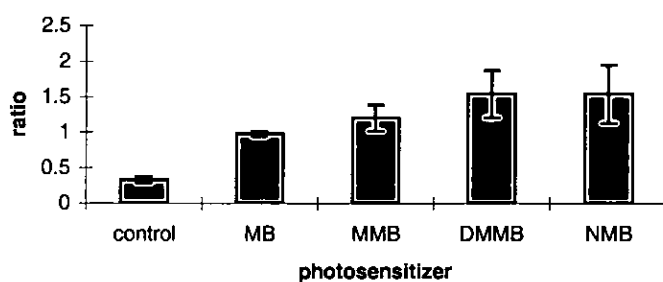


Figure 48. J-aggregate formation in [a] EMT-6 cells, [b] SK-23 cells and [c] SK-MEL-28 cells after 1-hour incubation with phenothiazinium photosensitizers following 30 minutes illumination. The results are the mean of two experiments \pm SD and are expressed as the ratio of J-aggregates to the monomeric species of JC-1. J-aggregate formation occurs in response to increases in intramitochondrial membrane potential brought about by events involved in apoptotic pathways.

cells, there were no differences in J-aggregate formation between MB-, MMB-, or DMMB-treated cells and controls up to two hours of incubation with the photosensitizers, yet J-aggregate formation in NMB-treated cells appeared to be slightly enhanced [Figure 47a & 47b]. After three hours, J-aggregate formation was increased only in DMMB- and NMB-treated cell samples, compared to controls [Figure 47c]. Following a further period of illumination of thirty minutes, J-aggregate formation was enhanced in all treated cell samples, moreso in MMB- and DMMB-than MB-treated cells, but particularly in NMB-treated cells, compared to controls [Figure 47d]. To test whether illumination *per se* is a determinant in the rate/degree of the apoptotic response, cultures of cells subjected to photodynamic treatment after only one hour of incubation with the photosensitizers, were incubated with JC-1 as previously described [Section 5.2.2.6] and examined for J-aggregate formation. In this instance, the rate (and, in some cases, the degree) of J-aggregate formation was significantly enhanced in all treated cell samples in the three cell lines, compared to controls [Figure 48a, 48b, 48c].

5.4.3 Detection of Apoptosis using the FluorAce® Apopain Assay Kit

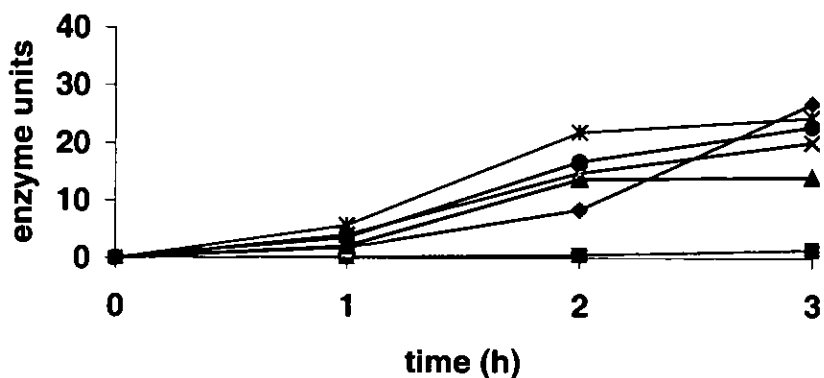
5.4.3.1 Apopain Assay

Apopain/Caspase 3 activity was detected in all treated cell samples after three hours of incubation with the photosensitizers followed by thirty minutes illumination, but not in controls. The pattern of apopain activity was MB<MMB<DMMB<NMB in all three cell lines. In EMT-6 and SK-23 cells, activity was greatest between one and two hours following preparation [Figures 49a & 49b], whilst in SK-MEL-28 cells activity was greatest between two and three hours following preparation [Figure 49c]. Enzyme activity increased steadily in the positive control but not in a linear fashion.

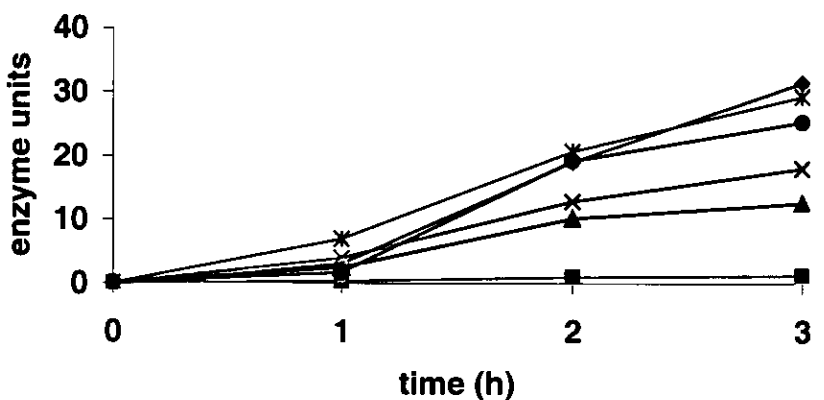
5.4.3.2 Inhibition of Apopain Activity (Negative Control)

Apopain/Caspase 3 activity was not detected in any of the treated cell samples that had been incubated in the presence of the apopain specific inhibitor, Ac-DEVD-CMK

[a]



[b]



[c]

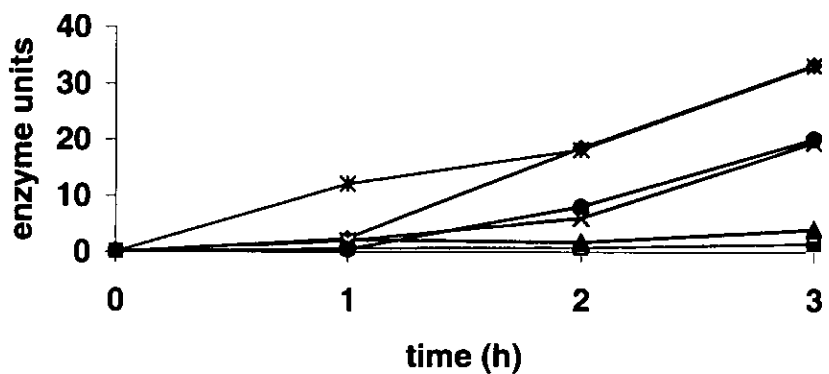


Figure 49. Detection of apoptosis in cultures of [a] EMT-6 cells, [b] SK-23 cells and [c] SK-MEL-28 cells preincubated with phenothiazinium photosensitizers for three hours followed by thirty minutes illumination. Apopain/caspase 3 activity was monitored using the fluorogenic peptide-dye conjugate, Z-DEVD-AFC, as substrate. Apopain/caspase 3 enzymatically cleaves AFC to produce blue-green fluorescence that can be monitored fluorometrically at 550 nm. Results are for two experiments, with ○ = control; □ = MB; x = MMB; x = DMMB; • = NMB; ◆ = positive control.

5.5 DISCUSSION

Evidence for an apoptotic mechanism of cell death was found in cultures of EMT-6, SK-23 and SK-MEL-28 cells that had been exposed to photodynamic treatment with, either MB, MMB, DMMB or NMB. This evidence came from morphological examination of cell cultures, by use of the cyanine dye, JC-1, to detect changes in mitochondrial membrane potential, and by monitoring apopain/caspase 3 activity using the FluorAce® Apopain Assay Kit from Biorad.

From examination of cellular morphology using the light microscope, there was no evidence for apoptosis prior to illumination, for any of the photosensitizers in any of the cell lines. However, following a thirty-minute period of illumination, cell rounding was strikingly evident in many cells. Since morphological changes in the cell (seen microscopically as cell rounding and nuclear condensation) can be a consequence of apoptosis, this suggests that, in the absence of illumination, apoptosis is still incomplete following three hours of incubation with the photosensitizers. This was true for all four photosensitizers and in all three cell lines. These results are not conclusive since observations are subjective and evidence of necrosis (visualised as cell lysis) was also present.

Using JC-1, evidence for apoptosis was detected post-illumination in all cases, but also prior to illumination in some cases and in certain cell lines. JC-1 is used to detect changes in mitochondrial membrane potentials, forming J-aggregates in regions of high membrane potentials, this being indicative of apoptotic activity [Chen & Smiley, 1994]. High membrane potentials are associated with high intracellular levels of ATP and hence apoptosis, since apoptosis is a mechanism that requires energy [Richter *et al.*, 1996]. Intracellular levels of ATP are believed to be a major determinant of the cell death mechanism, acting as a switch in the decision between apoptosis and necrosis [Leist *et al.*, 1997]. High mitochondrial membrane potentials are clearly, therefore, a very early marker for apoptotic events. Here, increases in mitochondrial membrane potential were seen to occur as soon as one hour following incubation with NMB in the SK-23 and SK-MEL-28 cell lines. However, increases in mitochondrial membrane potential were most apparent following a three-hour period of incubation and were particularly pronounced in the three cell lines for DMMB and NMB. In the case of MB

and MMB in EMT-6 cells, illumination made no difference to the formation of J-aggregate following the three-hour incubation period, whilst those for DMMB and NMB were greatly enhanced. In SK-23 cells, the ratios were slightly increased for MB and MMB but again significantly enhanced for DMMB and NMB. In SK-MEL-28 cells, only the ratio for NMB was significantly enhanced. When cell cultures were illuminated following only a one-hour period of incubation with the photosensitizers, increases in mitochondrial membrane potential were detected for all the photosensitizers in the three cell lines.

JC-1 was also used to stain cultures of cells that had been exposed to various periods of incubation with the photosensitizers without illumination, and to a three-hour incubation period plus thirty minutes illumination, for the purpose of microscopic visualisation. In all cases, regions of both green and orange fluorescence were seen to co-exist, and it was impossible to assess the ratios of the different fluorescence signals. JC-1 at $10 \mu\text{g ml}^{-1}$ has been used to stain a variety of cell types and cell lines in culture and these findings are typical of those described by other researchers. In the presence of JC-1, mitochondria with low membrane potentials ($< 100 \text{ mV}$) exhibit green fluorescence, whilst mitochondria with high membrane potential (140 to 160 mV) exhibit mostly orange fluorescence [Chen & Smiley, 1994]. Different cell lines have mitochondria with widely differing membrane potentials. Human bladder epithelial cells, for instance, tend to have mitochondria with low membrane potentials, whilst mitochondria with high membrane potentials have been found in a human bladder cell carcinoma cell line [Reers *et al.*, 1995]. Very high mitochondrial membrane potentials ($> 190 \text{ mV}$), indicated by red fluorescence, have been detected in cardiac muscle cells incubated with JC-1 [Reers *et al.*, 1995], which is not surprising, given the very high metabolic requirements of these cells. Most other cell types and cell lines fall between these two extremes and have two populations of mitochondria. In addition, many cells in culture exhibit both intercellular and intracellular heterogeneity. Not only are there differences in fluorescence between individual cells and between the mitochondria of the same cell, but even within a single mitochondrion, there may be regions of either only green or only orange fluorescence. This implies that different mitochondria in the same cell and different regions of the same mitochondrion have different membrane potentials.

The FluorAce® Apopain Assay Kit was used subsequent to JC-1 analysis to identify apoptosis mainly in cell cultures that had been subjected to a complete photodynamic treatment since, using the JC-1 protocol, it appeared that illumination was important in enhancing the apoptotic response. Apopain/caspase 3 activity is initiated *via* cleavage of CPP32 at the onset of apoptosis [Green & Reed, 1998] and, as such, is another early marker for apoptotic events. Using this method, cultures of EMT-6, SK-23 and SK-MEL-28 cells that had been incubated for three hours with the four photosensitizers, MB, MMB, DMMB or NMB, followed by thirty minutes illumination, all produced evidence of apoptosis. Here, too, the apoptotic response was greatest in DMMB- and NMB-treated cells and followed the pattern MB<MMB<DMMB<NMB in all cases. However, these results were difficult to reproduce, and attempts to detect apoptosis in non-illuminated cells failed. Moreover, the Apopain® Assay Kit was by far the more laborious method and, on reflection, it was probably not suitable for the large amount of samples that could have been tested.

In conclusion, these results strongly implicate the role of an apoptotic mechanism in the photocytotoxicity of MB and its derivatives, MMB, DMMB and NMB in the EMT-6, SK-23 and SK-MEL-28 cell lines. There is also evidence to suggest that apoptosis is induced even in the absence of illumination in some cases, indicating a subsidiary role for the mechanism under these conditions. However, it is also apparent that illumination of the photosensitizers, pre-incubated with the various cell lines, enhances both the rate and perhaps also the degree of the apoptotic response in these cell lines. Apoptosis is more likely to be the predominant mechanism of cell death in DMMB- and NMB-mediated photocytotoxicity than it is MB- and MMB-mediated photocytotoxicity, and may depend on several factors.

The initiation and rate of progression of apoptosis in PDT is highly dependent upon the localisation of the photosensitizer at the time of its activation by light. Photosensitizers that localise in mitochondria are more efficient inducers of apoptosis than photosensitizers that target other subcellular sites [Kessel *et al.*, 1997]. Hydrophobic, cationic molecules preferentially target mitochondria [Oseroff, 1986] and it is possible that DMMB and NMB, in particular, are likely to follow this type of intracellular distribution pattern. MB is known to target the nucleus [Tuite & Kelly, 1993],

microtubules [Stockart *et al.*, 1996] and lysosomes [Santus *et al.*, 1983]. Photosensitizers that localise in lysosomes may trigger cell death either by release of lysosomal enzymes into the cytosol or by relocalisation of the photosensitizers to secondary subcellular sites [Peng *et al.*, 1991]. In fact, relocalisation to the nucleus was observed for all four photosensitizers in all three cell lines using confocal microscopy [Chapter 4]. Furthermore, apoptosis induced by photosensitizers localised in lysosomes is a much slower and less efficient process than that induced by mitochondrial agents and may explain the small detection of apoptosis in MB-treated cells. The induction of apoptosis in PDT is also dependent upon the photosensitizer dose [Luo & Kessel, 1997], and it must be remembered that DMMB and NMB exert their lethal photodynamic effects at much lower concentrations than do MB and MMB [Chapter 2]. Although both necrosis and apoptosis can occur simultaneously in cells exposed to the same stimulus [Shimizu *et al.*, 1996], the predominant mechanism is usually decided by the intensity of the insult, such that lesser doses of the same agent that produces necrosis can lead to apoptosis [Bonfoco *et al.*, 1995].

CHAPTER SIX.
CLOSING DISCUSSION

CLOSING DISCUSSION

The initial aim of this project was to assess the effect of chemical substitution on the photosensitizing capabilities of the well-known cationic phenothiazinium dye, methylene blue (MB). The effect of simple alkylation of the phenothiazinium chromophore using MB and two other known biological stains, 1,9-dimethyl methylene blue (DMMB) and new methylene blue N (NMB), together with a newly synthesised intermediate compound, 1-methyl methylene blue (MMB), was investigated in three cell lines. For the work described, the synthesis of MMB was straightforward. The purity of the four photosensitizers was ensured first using thin layer chromatography, then the purity of MMB further examined by high performance liquid chromatography. The use of a single substance in PDT is clearly advantageous in order to reduce the risk of systemic side effects, and because this facilitates mono-substitution of the molecule to identify those parts of the molecule that may be involved in toxicity. Purification may be difficult if the molecule has two or more peripheral substituents and/or chiral centres.

It was found that MB is inherently toxic to murine mammary (EMT-6), murine melanoma (SK-23) and human melanoma (SK-MEL-28) cells in culture. In addition, the levels of toxicity of MB in the three cell lines following three hours of incubation were significantly enhanced by a period of illumination for a further thirty minutes. This was not surprising since MB has already been used experimentally as a photosensitizer including, in humans, for the treatment of carcinoma of the bladder [Williams *et al.*, 1989] and inoperable oesophageal tumours [Orth *et al.*, 1995]. It was also found that both the photocytotoxicity and the inherent (dark) toxicity of MB are increased by methylation of the molecule. The patterns of toxicity encountered corresponded to the degree of methylation and mirrored increased singlet oxygen yields, increased hydrophobic character and the increased resistance to reduction of the three derivatives.

The apparent dismissal of MB in mainstream PDT is likely due not only to its inherent (dark) toxicity, but also because its photosensitizing capacity is curtailed by its rapid reduction *in vivo* to the neutral leucobase. Leuco-MB is colourless and therefore incapable of being further activated by light, although reoxidation is possible.

Nevertheless, there are many possibilities for overcoming problems associated with the various second-generation photosensitizers so far evaluated, since predetermined characteristics may be introduced into a photosensitizer molecule by chemical synthesis and substitution. Unfortunately, the inherent (dark) toxicity of MB was similarly enhanced by methyl substitution. Nevertheless, it is possible to assess the potential clinical usefulness of the photosensitizers by examination of the light:dark differential. In fact, the light:dark differential was improved for all the derivatives of MB in all three cell lines. In this respect, NMB consistently performed the best, achieving maximum photocytotoxicity at concentrations that caused very little toxicity in the dark. The problem of dark toxicity could in fact be overcome if, in the case of skin lesions, the photosensitizers were incorporated into a topical application. This would have the added advantage in that it would reduce the long drug to light interval that is currently required with Photofrin® and allow treatment to be carried out on an outpatient basis.

Several groups of researchers are working to develop new, more efficacious photosensitizers for PDT. The photosensitizing capacity of a compound is of course important but the success of the regime also requires an optimal interplay among a number of several different parameters. For efficient PDT, a photosensitizer should possess a large molar extinction coefficient in the red part of the visible spectrum where transmission of light through mammalian tissues is most effective. Photofrin®, the sole agent currently registered for clinical use, is highly disadvantaged in this respect because its maximum absorption peak lies in the blue region of the spectrum at around 400 nm (the Soret band). For PDT, Photofrin® must therefore be illuminated at its weakest absorption band of 630 nm, where its light absorption properties are very poor. However, it is possible to overcome this problem by careful manipulation and fine-tuning of the chemical structure of the molecule. It is found, for example, that the inclusion of an extended chromophore or the insertion of additional double bonds, enhances molar absorptivity and shifts light absorption bands of second generation photosensitizers to wavelengths in the red [Jori, 1992]. Light penetration into mammalian tissue increases with wavelength and typically doubles between 630 nm and 750 nm allowing larger tumours to be treated [Wilson *et al.*, 1985]. However, there is likely to be a 'photochemical limitation' to the long wavelength for new photosensitizers of around 800 nm because of the need to generate significant amounts

of singlet oxygen ($^1\text{O}_2$) [Truscott, 1980]. One potential problem with intensely absorbing drugs is that the effective depth of light penetration through tissue may decrease owing to light attenuation by the photosensitizer itself. [Wilson, 1989]. In the case of Photofrin®, its low extinction coefficient at 630 nm does not really cause any important clinical dilemma since it is accompanied by low toxicity. In the case of MB and its derivatives, the absorption properties of the photosensitizers are not an issue since all four compounds absorb light maximally within the therapeutic window (600 to 800 nm) for PDT. These are 664 nm for MB, 656 nm for MMB, 648 nm for DMMB and 630 nm for NMB.

The photosensitizing capacity of a photosensitizer is partly based on its power to generate singlet oxygen ($^1\text{O}_2$) that, in turn, is highly dependent on its triplet lifetime (τ_T) *in vivo*. τ_T is defined as the average time a molecule spends in its first excited triplet state and determines the time available for transfer of the triplet state excitation energy to molecular oxygen or for redox reactions with other cellular substrates. The slower the decay of this triplet state, the more time available for the photosensitizer to interact with its environment. It has been shown that the longer τ_T ($\tau_T \geq 500$ ns) and the greater the triplet state quantum yield, the more enhanced is the photocytotoxic effect of a given photosensitizer [Takemura *et al.*, 1989]. These findings are consistent with the fact that the diverse porphyrins existing in the human body (Fe-, Cu- and Mn-chelating compounds), which have very short lifetimes, have never been observed to cause sunlight-induced photosensitivity in healthy individuals. Compounds that have a triplet state energy lower than the excitation energy of $^1\text{O}_2$ (7900 cm^{-1}) are generally unable to generate $^1\text{O}_2$ because they are unable to transfer their excitational energy to molecular oxygen. In order to promote $^1\text{O}_2$ quantum efficiency and therefore a type II mechanism, the energy of the first excited triplet state of a photosensitizer should be in the range 7900 to 18000 cm^{-1} . Nevertheless, compounds having a triplet state energy below 7900 cm^{-1} , but possessing a high triplet quantum yield and high absorbance in the red, may alternatively be effective type I photosensitizers, if they also possess long-lived excited singlet and/or triplet states with a strong tendency to induce electron transfer. Subsequently, it has been found that porphyrin-type molecules containing a diamagnetic central metal ion within the macrocycle have a prolonged τ_T and are the most efficient photosensitizers for clinical PDT. Analogous compounds containing a paramagnetic

metal ion have a significantly shortened τ_T and are better suited for diagnosis where photodamage to tissues must be avoided [Rosenthal & Ben-Hur, 1989]. 1O_2 quantum efficiency has often been achieved by introduction of the internal heavy atom effect, *i.e.* replacement of an atom in a lead structure with one of higher atomic number. Initially, an iodinated analogue of MB was included in the series of photosensitizers that were tested for toxicity against the EMT-6 cell line in order to examine here the ‘heavy atom’ effect on MB [Section 2.2]. 4-iodo-MB was synthesised and purified by the UCLan Chemistry Department. The results obtained in EMT-6 cells were comparable to those for MMB. Unfortunately, purification of subsequent batches proved unsuccessful, so further investigations were abandoned. Future studies would prove useful for an apparently promising photosensitizer. 1O_2 quanta (and hence photosensitizing capacity) for the three derivatives used in this study were measured relative to that of MB and were found to be elevated in all cases, compared to the parent compound. The three derivatives were also more resistant to reduction than is MB, so are likely to be present in the cell as the cation, and thus to exert their photodynamic effects, for longer.

For PDT, it is also advantageous to use a photosensitizer with a high molar extinction co-efficient so that a lower drug dose can be used, thus avoiding internal shielding effects and reducing systemic toxicity. A lower drug dose is also useful in preventing the formation of aggregates at higher concentrations that would significantly inhibit the photosensitizing activity. In the case of porphyrins, the insertion of electrically charged functional groups protruding from the pyrrole rings, or bulky axial ligands perpendicular to the plane of the molecule, generates electrostatic repulsion and steric hindrance, thereby reducing the tendency of the drug to aggregate in aqueous milieu [Jori, 1992]. In the present work, it was believed that the doubly-methylated derivatives, DMMB and NMB, form aggregates at concentrations above 5 μM . In cellular uptake, this manifests as deviations from Beer’s Law, and in fluorescent imaging, as regions of dense blue staining that are generally accompanied by a lack of fluorescence [data not shown]. Nevertheless, for the purposes of PDT, this should not be a problem since these two photosensitizers exert cell photokilling at very low concentrations (*i.e.* < 1 μM).

An essential requirement of an ideal photosensitizer, and one that is lacking in all conventional cancer treatments, is efficient and preferential killing of malignant cells. For PDT, pure photosensitizers with high specificity for target tissues, have low systemic toxicity and may be administered in higher doses without fear of unwanted side effects. The potential selectivity of the photosensitizer for malignant tissue can be assessed from the ratio of its concentration in the tumour and the tissue from which the tumour originates or into which the tumour grows. As with most pharmacological approaches, drug specificity can also be achieved by taking advantage of intrinsic features of malignant cells that are different from those of their normal counterparts. Examples of these that are under investigation for PDT are the incorporation of the photosensitizer into serum LDL and the covalent binding of photosensitizers to monoclonal antibodies. Malignant tumour cells have cell surface antigens that are different from those of normal cells and that can be targeted by monoclonal antibodies [Woehrle *et al.*, 1998]. For the present work, it is already established that MB has some specificity for tumour tissue. The dye has been used extensively in the demarcation of human bladder tumours due to its affinity for the microscopic crystals of stone salts and crystalline masses that are commonly found adherent to their surfaces [Fukui *et al.*, 1983; Gill *et al.*, 1984]. Indeed, it was this specificity that led to its first use as a photosensitizer for the treatment of carcinoma of the bladder [Williams *et al.*, 1989]. It is not known whether the derivatives of MB would have similar specificity for tumour tissue *in vivo*.

It is important that new systemic drugs should have minimal accumulation in the skin in order to avoid the acute cutaneous photosensitivity that is an unacceptable feature of the current regime. An ideal anti-cancer drug should, therefore, apart from efficiently and selectively targeting tumour tissue, be cleared rapidly from normal tissues and/or metabolised to an inactive form following treatment. One of the limitations of MB is its rapid reduction *in vivo* to the inactive form, leuco-MB, and although the derivatives demonstrate a greater resistance to reduction, it is unlikely that they would persist systemically for as long as does Photofrin®. A photosensitizer that has a high affinity for serum proteins involved in transport to the liver is more likely to be cleared rapidly from serum and healthy tissues. In general, favourable pharmacokinetic behaviour may

be bestowed upon a photosensitizer by increasing its degree of hydrophobicity or by imparting amphiphilic properties to the molecule [Kessel, 1982]. An amphiphilic photosensitizer is sufficiently water-soluble to allow its systemic injection *in vivo*, whilst retaining its ability to cross the lipid barrier of cellular and/or intracellular membranes and localise at intracellular sites [Kessel, 1982]. One effect of methylation of the phenothiazinium chromophore was an increase in the hydrophobicity of the system. This was not unexpected, since the non-polar character of the methyl group is well established, with a guideline figure for Log *P* supplement of +0.65 for the addition of one $-CH_2-$ unit [Hansch & Leo, 1979]. An increase in hydrophobicity was expected to improve on the cellular uptake of MB and affect the intracellular targeting of its derivatives. This was manifest with all three methylated derivatives of MB.

PDT is a treatment regime that has dual selectivity since it is dependent upon a combination of both photosensitizer and light for cytotoxicity. The use of a photosensitizer that is non-toxic in the absence of light gives PDT an added advantage over other anti-cancer regimes, since then no effect is seen in the presence of either photosensitizer or light alone. Unfortunately, MB suffers from an inherent toxicity and this problem was not overcome by methyl substitution of the phenothiazinium chromophore. Methylation increased both the photocytotoxicity and the dark toxicity of MB, and the patterns of toxicity for the four photosensitizers were the same in all three cell lines. Nevertheless, the advent of elaborate endoscopic laser systems has made it possible to restrict illumination only to the target area. However, since PDT always involves taking a margin of surrounding normal tissue, it is important that there is a large concentration difference of the photosensitizer between tumour and peritumoural tissue and that there is rapid healing of photodamaged healthy tissue. As already mentioned, this is possible with MB because the ability of the photosensitizer to act as a tumour marker is already established. The potential of the derivatives also to stain tumour tissue selectively could form the basis for future studies. As far as illumination is concerned, it has been found that irradiation of tissues with wavelengths longer than 600 nm causes no adverse effect, provided the fluence rate is kept below about 150 mW cm^{-2} to avoid heating of tissue and consequent thermal damage [Jori, 1996].

The practical use of any drug requires that its mutagenic and carcinogenic properties be taken into consideration. PDT with Photofrin® is not believed to be carcinogenic

[Gomer *et al.*, 1988] presumably because, except in a very few exceptional cases [Moan *et al.*, 1980; Evenson *et al.*, 1982], porphyrin-mediated singlet oxygen damage never penetrates beyond the nuclear membrane [Moan *et al.*, 1986]. However, MB is known to intercalate with DNA, even prior to illumination [Tuite & Kelly, 1993], and mutagenic effects with MB have been found in living systems when cell destruction is incomplete [Bellin & Grossman, 1965]. Since most evidence from this project suggests that the derivatives of MB localise only within the cytosol (with mitochondrial targeting possible, particularly for DMMB and NMB) and show no evidence at all of nuclear targeting prior to illumination, then the risk of damage to the DNA of normal cells from these photosensitizers ought to be negligible. However, confocal microscopy showed that, upon illumination, all four photosensitizers underwent relocalisation to the nucleus. Nevertheless, the risk of mutagenic effects in normal tissue from this should be minimal since, because PDT is a selective regime, a combination of photosensitizer and light is required for toxicity, with no appreciable effect produced from either photosensitizer or light alone.

Ultimately, the aim of this study was to assess the potential of MB and the derivatives, MMB, DMMB and NMB to be used in the photodynamic therapy of both non-pigmented and pigmented lesions. Certainly for cells in culture there was no difference in the patterns of toxicity exhibited by the photosensitizers between non-pigmented and pigmented cells. In this case, the presence of melanin did not inhibit the photodynamic effect. In terms of a clinical application of the current work, PDT employing phenothiazinium photosensitizers is not suggested procedurally for the removal of primary melanoma, since this is routinely performed by excision. However, due to the demonstrated efficacy of MB in tracing microsattellites and its use in sentinel lymph node tracing, it may be of use in the photodynamic treatment of local metastatic lymph infiltration immediately post-surgery, as an alternative to lymphadenectomy. At present, MB is used routinely in various tracing or demarcation procedures, either visible or scintillographic, without reported toxicity. The derivatives used in the present *in vitro* study were all more effective in terms of the photodynamic effect and it is thus possible that future clinical developments in this direction may be feasible.

CHAPTER SEVEN.
REFERENCES.

- Agarwal, M.L., Clay, M.E., Harvey, E.J., Evans, H.H., Antunez, A.R. & Oleinick, N.L. (1991) Photodynamic therapy induces rapid cell death by apoptosis in L5178Y mouse lymphoma cells. *Cancer Res* **51**: 5993-5996
- Agarwal, M.L., Larkin, H.E., Zaidi, S.I., Mukhtar, H. & Oleinick, N.L. (1993) Phospholipase activation triggers apoptosis in photosensitized mouse lymphoma cells. *Cancer Res* **53**: 5897-5902
- Allen, R.P., Kessel, D., Tharratt, R.S. & Volz, W. (1992) Photodynamic therapy of superficial malignancies with Npe₆ in man. In: Photodynamic therapy and biomedical lasers. Spinelli P., Dal Fante M., Marschesini, R., editors. International Congress Series 1011, Excerpta Medica, Amsterdam, pp. 441-445
- Allison, B.A., Pritchard, P.H. & Levy, J.G. (1994) Evidence for low-density lipoprotein receptor-mediated uptake of benzoporphyrin derivative. *Br J Cancer* **69**: 833-839
- Anderson, R.R. & Parrish, J.A. (1981) The optics of human skin. *J Invest Dermatol* **77**: 13-19
- Antony, T., Atreyi, M. & Rao, M.V.R. (1995) Interaction of methylene blue with transfer RNA-a spectroscopic study. *Chemico-Biological Interactions* **97**: 199-214
- Arends, M.J. & Wylie, A.H. (1991) Apoptosis. Mechanisms and role in pathology. *Int Rev Exp Pathol* **32**: 223-254
- Arcadi, J.A. (1990) Use of rhodamine 123 in the treatment of the Pollard III rat prostate adenocarcinoma. *J Surg Oncol* **44**: 103-108
- Aronoff, B.L. (1997) Lasers: Reflections on their evolution. *J Surg Oncol* **64**: 84-92
- Ashkenazi, A. & Dixit, V.M. (1998) Death receptors: signaling and modulation. *Science* **281**: 1305-1308
- Athar, M., Elmets, C.A., Bickers, R. & Mukhtar, H. (1989) A novel mechanism for the generation of superoxide anions in haematoporphyrin derivative-mediated cutaneous photosensitization. Activation of the Xanthine Oxidase Pathway. *J Clin Invest* **83**: 1137-1143
- Auler, H. & Banzer, G. (1942) (cited in Daniell & Hill, 1991) Untersuchungen über die Rolle der Porphyrine bei geschwulstkranken Menschen und Tieren. *Z Krebsforsch* **53**: 65-68
- Baas, P., Murrer, L. & Zoetmulder, F.A. (1997) Photodynamic therapy as adjuvant therapy in surgically treated pleural malignancies. *Br J Cancer* **76**: 819-826
- Baas, P (1997) Laser therapy in pulmonary medicine: review article. *Lasers Med Sci* **13**: 86-97

- Bachor, R., Shea, C.R., Gillies, R. & Hassan, T. (1991) Photosensitized destruction of human bladder carcinoma cells treated with chlorin e_6 -conjugated microspheres. *Proc Natl Acad Sci USA* **88**: 1580-1584
- Bachmann, B., Knüver-Hopf, J., Lambrecht, B. & Mohr, H. (1995) Target structures for HIV-1 inactivation by methylene blue and light. *J Med Virol* **47**: 172-178
- Ball, D.J., Luo, Y., Kessel, D., Griffiths, J., Brown, S.B. & Vernon, D.I. (1998) The induction of apoptosis by a positively charged methylene blue derivative. *J Photochem Photobiol B: Biology* **42**: 159-163
- Barbosa, P. & Peters, M.T. (1971) The effects of vital dyes on living organisms with special reference to methylene blue and neutral red. *Hist J* **3**: 71-93
- Barr, H., Shepherd, N.A., Dix, A., Roberts, D.J.H., Tan, W.C. & Frasner, N. (1996) Eradication of high-grade dysplasia in columnar-lined (Barrett's) oesophagus by photodynamic therapy with endogenously generated protoporphyrin IX. *Lancet* **348**: 584-585
- Bedwell, J., MacRobert, A.J. & Phillips, D. (1992) Fluorescence distribution and photodynamic effect of ALA-induced PPIX in the DMH rat colonic tumour model. *Br J Cancer* **65**: 818-824
- Bellin, J.S. & Grossman, L.I. (1965) Photodynamic degradation of nucleic acids. *Photochem Photobiol* **4**: 33-44
- Bellnier, D., Ho, K., Pandey, R.K., Missert, J. & Dougherty, T.J. (1989c) Distribution and elucidation of the tumour-localising component of haematoporphyrin derivative in mice. *Photochem Photobiol* **50**: 221-228
- Ben-Hur, E. & Rosenthal, I. (1985) The phthalocyanines: a new class of mammalian cell photosensitizers with a potential for cancer phototherapy. *Int J Radiat Biol* **47**: 145-147
- Ben-Hur, E. & Orenstein, A. (1991) The endothelium and red blood cells as potential targets in PDT-induced vascular stasis. *Int J Radiat Biol* **60**: 293-301
- Berenbaum, M.C., Akande, S.L., Bonnett, R. (1986) *Meso*-tetra(hydroxyphenyl) porphyrins, a new class of potent tumour photosensitizer with favourable selectivity. *Br J Cancer* **54**: 717-725
- Berenbaum, M.C., Bonnett, R., Chevretton, E.B., Akande-Adebakin, S.L. & Ruston, M. (1993) Selectivity of *meso*-tetra(hydroxyphenyl) porphyrins and chlorins and of Photofrin II in causing photodamage in tumour, skin, muscle and bladder. The concept of cost-benefit in analysing the results. *Lasers Med Sci*: **8**: 235-243
- Berg, K., Madslie, K., Bommer, J.C., Oftebro, R., Winkelman, J.W. & Moan, J. (1991) Light-induced relocalisation of sulphonated *meso*-tetraphenylporphyrins in NHIK 3025 cells and effects of dose fractionation. *Photochem Photobiol* **53**: 203-210

- Berg, K., Anholt, H., Moan, J., Ronnestad, A. & Rimington, C. (1995) Photobiological properties of haematoporphyrin diesters: evaluation of possible applications in photochemotherapy. *J Photochem Photobiol B: Biol* **20**: 37-45
- Berg, K. & Moan, J. (1997) Lysosomes and microtubules as targets for photochemotherapy of cancer. *Photochem Photobiol* **65**: 403-409
- Bernal, S.D., Lampidis, T.J., McIsaac, R.M. & Chen, L.B. (1983) Acticarcinoma activity of rhodamine 123, a mitochondria specific dye. *Science* **222**: 169-172
- Beyer, W. (1996) Systems for light application and dosimetry in photodynamic therapy. *J Photochem Photobiol B: Biology* **36**: 153-156
- Biolo, R., Jori, G., Soncin, M., Pratesi, R., Vanni, U., Rihter, B., Kennedy, M.E. & Rodgers, M.A.J. (1994) Photodynamic therapy of B16 pigmented melanoma with liposome-delivered Si(IV)-naphthalocyanine. *Photochem Photobiol* **59**: 362-365
- Blant, S.A., Woodtli, A., Fontollet, C., van den Bergh, H & Monnier, P. (1996) *In vivo* fluence rate effect in photodynamic therapy of early cancers with tetra(m-hydroxyphenyl)chlorin. *Photochem Photobiol* **64**: 963-968
- Bohmer, R.M. & Morstyn, G. (1985) Uptake of haematoporphyrin derivative by normal and malignant cells: effect of serum, pH, temperature and cell size. *Cancer Res* **45**: 5328-5334
- Bonfoco, E., Kraine, D., Ankarcona, P., Nicotera, P & Lipton, S.A. (1995) Apoptosis and necrosis: two distinct events induced respectively by mild and intense insults with NMDA or nitric oxide/superoxide in cortical cell cultures. *Proc Natl Acad Sci USA* **92**: 7162-7166
- Bongard, R.D., Merker, M.P., Shundo, R., Okamoto, Y., Roerig, D.L., Linehan, J.H. & Dawson, C.A. (1995) Reduction of thiazine dyes by bovine arterial cells in culture. *Am J Physiol* **269**: L78-L84
- Bonnett, R., White, R.D., Winfield, U-J. & Berenbaum, M.C. (1989) Hydroporphyrins of the *meso*-tetrahydroxyphenyl porphyrin series as tumour photosensitizers. *J Biochem* **261**: 277-280
- Bonnett, R. (1999) Photodynamic therapy in historical perspective. *Rev Contemp Pharmacother* **10**: 1-17
- Boobis, R.A., Fawthrop, D.J. & Davis, D.S. (1989) Mechanisms of cell death. *Trends Pharmacol Sci* **10**: 275-280
- Bown, S.G. (1993) Photodynamic therapy in gastroenterology: current status and future prospects. *Endoscopy* **25**: 683-786
- Bown, S.G. & Millson, C.E. (1997) Photodynamic therapy in gastroenterology. *Gut* **41**: 5-7

- Bugelski, P.J., Porter, C.W. & Dougherty, T.J. (1981) Autoradiographic distribution of haematoporphyrin derivative in normal and tumour tissue of the mouse. *Cancer Res* **41**: 4606-4612
- Burrow, S.M. (1997) The membrane as a barrier or target in cancer chemotherapy. *PhD Thesis*: University of Central Lancashire
- Busetti, A., Soncin, M., Jori, G. & Rodgers, M.A.J. (1999) High efficiency of benzoporphyrin derivative in the photodynamic therapy of pigmented malignant melanoma. *Br J Cancer* **79**: 821-824
- Cairnduff, F., Stringer, M.R., Hudson, E.J., Ash, D.V. & Brown, S.B. (1994) Superficial photodynamic therapy with topical 5-aminolaevulinic acid for superficial primary and secondary skin cancer. *Br J Cancer* **133**: 282-288
- Calzavara-Pinton, P.G. (1995) Repetitive photodynamic therapy with topical 5-aminolaevulinic acid as an appropriate approach to the routine treatment of superficial non-melanoma skin tumours. *J Photochem Photobiol B: Biol* **29**: 53-57
- Calzavara-Pinton, P.G., Szeimies, R-M., Ortel, B. & Zane, C. (1996) Photodynamic therapy with systemic administration of photosensitizers in dermatology. *J Photochem Photobiol B* **36**: 225-231
- Canete, M., Villanueva, A. & Juarranz, A. (1993) Uptake and photoeffectiveness of two thiazines in HeLa cells. *Anti-Cancer Drug Design* **8**: 471-477
- Canto, M. I F., Setrakian, S., Petras, R.E., Blades, E., Chak, A. & Sivak, M.V.Jr. (1996) Methylene blue selectively stains intestinal metaplasia in Barrett's oesophagus. *Gastrointest Endosc* **44**: 1-7
- Carmichael, J., DeGraff, W.G., Gazdar, A.F., Minna, J.D. & Mitchell, J.B. (1987) Evaluation of a tetrazolium-based semiautomated colourimetric assay: assessment of chemosensitivity testing. *Cancer Res* **47**: 936-942
- Chen, L.B. & Smiley, S.T. (1994) Probing mitochondrial membrane potential in living cells by a J-aggregate-forming dye. In *Fluorescent and Luminescent Probes for Biological Activity*. W.T.Mason (ed.), Academic Press, pp 124-132
- Cincotta, L., Foley, J.W. & Cincotta, A.H. (1987) Novel red absorbing benzo[a]phenoxazinium and benzo[a]phenothiazinium photosensitizers: *in vitro* evaluation. *Photochem Photobiol* **46**: 751-758
- Cincotta, L. & Foley, J.W. (1988) Novel phenothiazinium photosensitizers for photodynamic therapy. *SPIE* **997**: 145-153
- Cincotta, A.H., Cincotta, L., & Foley, J.W. (1990) Novel benzophenothiazinium photosensitizers: Preliminary *in vivo* results. *Proc SPIE "Photodynamic therapy: Mechanisms II"* **1203**: 202-210

- Cincotta, L., Foley, J.W. & Cincotta, A.H. (1993) Phototoxicity, redox behaviour and pharmacokinetics of benzophenoxazine analogues in EMT-6 murine sarcoma cells. *Cancer Res* **53**: 2571-2580
- Cincotta, L., Foley, J.W., Maceachern, T., Lampros, E. & Cincotta, A.H. (1994) Novel photodynamic effects of the benzophenoxazine on two different murine sarcomas. *Cancer Res* **54**: 1249-1258
- Cincotta, L., Szeto, D., Lampros, E., Hasan, T. & Cincotta, A.H. (1996) Benzophenothiazine and benzoporphyrin derivative combination phototherapy effectively eradicates large murine sarcomas. *Photochem Photobiol* **63** (2): 229-237
- Clark, W.H., Jr., Reimer, R.R. & Greene, M. (1978) Origin of familial malignant melanomas from heritable melanocytic lesions: "The B-K mole syndrome." *Arch Dermatol* **117**: 732-738
- Corsaro, C., Scalia, M., Blanco, A.R., Aiello, I. & Sichel, G. (1995) Melanins in physiological conditions protect against lipoperoxidation. A study on albino and pigmented *Xenopus*. *Pigment Cell Res* **8**: 279-282
- Cowed, P.A., Grace, J.R. & Forbes, I.J. (1984) Comparison of the efficacy of pulsed and continuous-wave red laser light in induction of photocytotoxicity by haematoporphyrin derivative. *Photochem Photobiol* **39**: 115-117
- Cozzani, I., Jori, G. & Reddi, E. (1981) Distribution of endogenous and injected porphyrins at the subcellular level in rat hepatocytes and in ascites hepatoma. *Chem-Biol Interact* **37**: 67-75
- Creagh, T.A., Gleeson, M., Travis, D., Grainger, R., McDermott, T.E.D. & Butler, M.R. (1995) Is there a role for *in vivo* methylene blue staining in the prediction of bladder tumour recurrence? *Br J Urol* **75**: 477-479
- Creed, D., Burton, W.C. & Fawcett, N.C. (1983) Ground and excited state properties of some new, highly water soluble *N*-substituted thiazine dyes for photogalvanic applications. *J Chem Soc Chem Commun*: 1521-1523
- Cruse-Sawyer, J.E., Griffiths, J., Dixon, B. & Brown, S.B. (1998) The photodynamic response of two rodent tumour models to four zinc(II)-substituted phthalocyanines. *Br J Cancer* **77** (6): 965-972
- Daniell, M.D. & Hill, J.S. (1991) A history of photodynamic therapy. *Aust N Z J Surg* **61**: 340-348
- Davis, S., Weiss, M.J., Wong, J.R., Lampidis, T.J. & Chen, L.B. (1985) Mitochondria and plasma membrane potentials cause unusual accumulation and retention of rhodamine 123 by human breast adenocarcinoma derived MCF-cells. *J Biol Chem* **260**: 13844-13850
- Dellinger, M. (1996) Apoptosis or necrosis following Photofrin® photosensitization: influence of the incubation protocol. *Photochem Photobiol* **64** (1): 182-187

- Diamond, I., Granelli, S.G., McDonagh, A.F., Nielsen, S.F., Wilson, C.B. & Jaenicke, R. (1972) Photodynamic therapy of malignant tumours. *Lancet* **ii**: 1175-1177
- Dilkes, M.G. (1994) Lasers in otolaryngology. Invited review. *Lasers Med Sci* **9**: 71-79
- Dilkes, M.G. & DeJode, M.L. (1995) *m*-THPC mediated PDT. Experience and thoughts after 17 treatments, in D.A.Cortese (ed.) *5th Int Photodynamic Association Biennial Meeting, Proc SPIE* **2371**: 256-261
- Dilkes, M.G., DeJode, M.L., Rowntree-Taylor, A., McGilligan, J.A., Kenyon, G.S. & McKelvie, P. (1997) *m*-THPC photodynamic therapy for head and neck cancer. *Lasers Med Sci* **11**: 23-30
- Dougherty, T.J., Grindey, G.B., Weishaupt, K.R. & Boyle, D.G. (1974) Photoradiation therapy II. Cure of animal tumours with haematoporphyrin and light. *J Natl Cancer Inst* **55**: 115-121
- Dougherty, T.J., Kaufman, J.E., Goldfarb, A., Weishaupt, K.R., Boyle, D. & Mittleman, A. (1978) Photoradiation therapy for the treatment of malignant tumours. *Cancer Res* **38**: 2628-2635
- Dougherty, T.J. (1984) Photodynamic therapy (PDT) of malignant tumours. *Crit Rev Oncol Hematol* **2**: 83-116
- Dougherty, T.J. (1987) Studies on the structure of porphyrins contained in Photofrin® II. *Photochem Photobiol* **46** (a): 569-573
- Dougherty, T.J., Cooper, M.T. & Mang, T.S. (1990) Cutaneous phototoxic occurrences in patients receiving Photofrin. *Lasers Surg Med* **10**: 485-488
- Dougherty, T.J., Gomer, C.J., Henderson, B.W., Jori, G., Kessel, D., Korbélik, M., Moan, J. & Peng, Q. (1998) Photodynamic therapy (Review) *J Natl Cancer Inst* **90** (12): 889-905
- Eguchi, Y., Shimizu, S. & Tsujimoto, Y. (1997) Intracellular ATP levels determine cell death fate by apoptosis or necrosis. *Cancer Res* **57**: 1835-40
- Ehrenberg, B., Malik, Z., Nitzan, Y., Ladan, H., Johnson, F.M., Hemmi, G. & Sessler, J.L. (1991) Photosensitization of bacterial and animal cells with the photosensitizer benzoporphyrin and texaphyrin [abstract A43]. *Fourth Congress of the European Society for Photobiology*. Amsterdam, September 1991
- El-Sharabasy, M.M.H., El-Waseef, A.M. & Hafez, M.M. (1992) Porphyrin metabolism in some malignant diseases. *Br J Cancer* **65**: 109-141
- Epstein, J.M. (1990) Phototherapy and photochemotherapy. *N Engl J Med* **32**: 1149-1151

- Evans, S., Matthews, W., Perry, R.R., Fraker, D., Norton, J. & Pass, H.I. (1990) Effect of photodynamic therapy on tumour necrosis factor production by murine macrophages. *J Natl Cancer Inst* **82**: 34-39
- Evensen, J.F. & Moan, J. (1982) Photodynamic action chromosomal damage: A comparison of haematoporphyrin derivative (HpD) and light with x-irradiation. *Br J Cancer* **45**: 456-465
- Fadok, V.A., Savill, J.S., Haslett, C., Bratton, D.L., Doherty, D.E., Campbell, P.A. & Henson, P.M. (1992) Different populations of macrophages use either the vitronectin receptor or the phosphatidylserine receptor to recognise and remove apoptotic cells. *J Immun* **149**: 4029-4035
- Favilla, I., Favilla, M.L., Gosbell, A.D., Barry, W.R. Ellims, P., Hill, J.S. & Byrne, J.R. (1995) Photodynamic therapy: a 5-year study of its effectiveness in the treatment of posterior uveal melanoma, and evaluation of haematoporphyrin uptake and photocytotoxicity of melanoma cells in tissue culture. *Melanoma Res* **5**: 355-364
- Fiertz-David, H.E. & Blangey, L (1949) in *Fundamental Processes in Dye Chemistry*, Interscience, NY. Pp. 311-313
- Figge, F.H.H., Weiland, G.S. & Manganiello, L.O.J. (1948) Cancer detection and therapy: Affinity of neoplastic, embryonic and traumatised tissues for porphyrins and metalloporphyrins. *Proc Soc Exp Biol Med* **68**: 640-641
- Fingar, V.H., Wieman, T.J., Wiekle, S.A. & Cerrito, P. (1992) The role of microvascular damage in photodynamic therapy: The effect of treatment on vessel constriction, permeability and leukocyte adhesion. *Cancer Res* **52**: 4919-4921
- Fischer, H., Hilmer, H., Linder, F. & Putzer, B. (1925) (cited in Daniell & Hill, 1991) *Z Physiol Chem* **150**: 44
- Fischer, A.M.R., Murphree, A.L. & Gomer, C.J. (1995) Clinical and preclinical photodynamic therapy. *Lasers Surg Med* **17**: 2-31
- Foley, J.W., Cincotta, L. & Cincotta, A.H. (1987) Structures and properties of novel benzo[a]phenoxazinium photochemotherapeutic agents. *SPIE* **847**: 90-95
- Foote, C.S. (1990) Chemical mechanisms of photodynamic action. *Proc SPIE Institute "Advanced Optical Technologies on Photodynamic Therapy IS"* **6**: 115-126
- Foote, C.S. (1991) Definition of type I and type II photosensitized oxidation. *Photochem Photobiol* **54**: 659
- Foster, R. & Hanson, P. (1966) Electron-donor-acceptor complex formation by compounds of biological interest. I. Optical absorption spectra of mixtures of phenothiazines and related compounds with electron acceptors. *Biochim Biophys Acta* **112**: 482-489

- Foster, T.H., Primavera, M.C., Marder, V.J., Hilf, R. & Sporn, L.A. (1991) Photosensitized release of von Willebrand factor from cultured human endothelial cells. *Cancer Res* **51**: 3261-3266
- Fowler, G.J.S., Rees, R.C. & Devonshire, R. (1990) The photokilling of bladder carcinoma cells *in vitro* by phenothiazine dyes. *Photochem Photobiol* **52** (3): 489-494
- Freitas, I. (1990) Lipid accumulation: the common feature to photosensitizer-retaining normal and malignant tissues. *J Photochem Photobiol B: Biol* **7**: 359-361
- Fritsch, C., Stege, H., Saalman, G., Goerz, G., Ruzicka, T. & Krutmann, J. (1993) Green light is effective and less painful than red light in photodynamic therapy of facial solar keratoses. *Photodermatol Photoimmunol Photomed* **13**: 181-185
- Fukui, I, Yokokawa, M., Mitani, G., Ohwada, F., Wakui, M., Washizuka, M., Tohma, T., Igareshi, K. & Yamada, T. (1983) *In vivo* staining test with methylene blue for bladder cancer. *J Urol* **130**: 252-255
- Garbo, G.M. (1996) Purpurins and benzochlorins as sensitizers for photodynamic therapy. *J Photochem Photobiol* **34**: 109-116
- Gerweck, L.E. & Seetharaman, K. (1996) Cellular pH gradient in tumour versus normal tissue: potential exploitation for the treatment of cancer. *Cancer Res* **56**: 1194-1198
- Gibson, S.L., Murand, R.S., Chasen, M.D., Kelly, M.E. & Hilf, R. (1989) *In vitro* photosensitization of tumour cell enzymes by Photofrin II administered *in vivo*. *Br J Cancer* **59**: 47-53
- Gill, W.B., Jones, K.W. & Schoenberg, H.W. (1981) Deleterious effects of certain intravesical urological solutions on the urothelium of rat bladders (Abstr). *Proc Am Urol Assoc*: 76-78
- Gill, W.B., Huffman, J.L., Lyon, E.S., Bagley, D.H., Schoenberg, H.W. & Straus, F.H. (1984) Selective surface staining of bladder tumours by intravesical methylene blue with enhanced endoscopic identification. *Cancer* **53**: 2724-2727
- Gill, W.B., Taja, A., Chadbourne, D.M., Roma, M. & Vermeulen, C.W. (1987) Inactivation of bladder tumour cells and enzymes by methylene blue plus light. *J Urol* **138**: 1318-1320
- Girotti, A.W. (1990) Photodynamic lipid peroxidation in biological systems. *Photochem Photobiol*: **51**: 497-509
- Glover, R.A., Bailey, C.S., Barrett, K.E., Wasserman, S.I. & Gigli, I. (1990) Histamine release from rodent and human mast cells induced by protoporphyrin and ultraviolet light: studies of the mechanism of mast-cell activation in erythropoietic protoporphyria. *Br J Dermatol* **122**: 502-512
- Goldstein, J.L. & Brown, M.S. (1977) The low-density lipoprotein pathway and its relation to atherosclerosis. *Annu Rev Biochem* **46**: 897-930

- Gomer, C.J & Dougherty, T.J. (1979) Determination of [³H]- and [¹⁴C]-haematoporphyrin derivative distribution in malignant and normal tissue. *Cancer Res* **39**: 146-151
- Gomer, C.J., Doiron, D.R. & Rucker, N. (1984) Action spectrum (620-640 nm) for haematoporphyrin derivative induced cell killing. *Photochem Photobiol* **39**: 365-368
- Gomer, C.J., Rucker, N. & Murphree, A.L. (1988) Transformation and mutagenic potential of porphyrin photodynamic therapy in mammalian cells. *Int J Radiat Biol* **53**: 651-659
- Gomer, C.J. (1989) Photodynamic therapy in the treatment of malignancies. *Sem Hematol* **26**: 27-34
- Gomer, C.J. & Ferrario, A. (1990) Tissue distribution and photosensitizing properties in mono-L-aspartyl chlorin *e*₆ in a mouse tumour model. *Cancer Res* **50**: 1985-1990
- Gomer, C.J., Luna, M., Ferrario, A., Wong, S., Fisher, A. & Rucker, N. (1996) Cellular targets and molecular responses associated with photodynamic therapy. *J Clin Laser Med Surg* **14**: 315-321
- Gragoudas, E., Schmidt-Erfurth, U. & Sickenkey, M. (1997) Results and preliminary dosimetry of photodynamic therapy for choroidal neovascularization in age-related macular degeneration in a phase I/II study. Abstract. *Assoc Res Vision Ophthalmology* **38**: 73
- Granville, D.J., Carthy, C.M., Jiang, H., Shore, G.C., McManus, B.M. & Hunt, D.W. (1998) Rapid cytochrome *c* release, activation of caspases 3, 6, 7 and 8 followed by Bap31 cleavage in HeLa cells treated with photodynamic therapy. *FEBS Lett* **437**: 5-10
- Granville, D.J., Shaw, J.R., Leong, S., Carthy, C.M., Margaron, P., Hunt, D.W. & McManus, B.M. (1999) Release of cytochrome *c*, Bax migration, Bid cleavage, and activation of caspases 2, 3, 6, 7, 8 and 9 during endothelial cell apoptosis. *Am J Pathol* **155**: 1021-1025
- Green, D.R & Reed, J.C. (1998) Mitochondria and apoptosis. *Science* **281**: 1309-1312
- Grosjean, P., Savary, J.F. & Mizeretet, J. (1996) Tetra(*m*-hydroxyphenyl) chlorin clinical photodynamic therapy of early bronchial and oesophageal cancers. *Lasers Med Sci* **11**: 227-235
- Grossweiner, L.I., Bilgin, M.D., Berdusis, P., Mody, T.D. (1999) Singlet oxygen generation by metallotexaphyrins. *Photochem Photobiol* **70** (2): 138-145
- Gullino, P.M., Grantham, F.H., Smith, S.H., & Haggerty, A.C. (1965) Modification of the acid-base status of the internal milieu of tumours. *J Natl Cancer Inst* **34**: 857
- Gullino, P.M. (1966) The interstitial milieu of tumours. *Tumour Res* **8**: 1

- Hadjur, C., Richard, M.J., Parat, M.O., Jardon, P. & Favier, A. (1996) Photodynamic effects of hypericin on lipid peroxidation and antioxidant status in melanoma cells. *Photochem Photobiol* **64**: 375-381
- Hansch, C & Leo, A. (1979) Substituent Constants for Correlation Analysis in Chemistry and Biology. Wiley, New York, pp 18-43
- Harriman, A., Maiya, B.G., Murai, T., Hemmi, G., Sessler, J.L. & Mallouk, T.E. (1989) Metallotetrapyrin: a new family of photosensitizers for efficient generation of singlet oxygen. *J Chem Soc Chem Commun*: 314-316
- He, D., Soter, N.A. & Lim, H.W. (1989) The late phase of haematoporphyrin derivative-induced phototoxicity in mice: release of histamine and histologic changes. *Photochem Photobiol* **50**: 91-95
- He, J. & Oleinick, N.L. (1996) Cell death mechanisms vary with photodynamic therapy dose and photosensitizer. *SPIE* **2371**:92-96
- He, J., Agarwal, M.L., Larkin, H.E., Friedman, L.R., y-Xue, L. & Oleinick, N.L. (1996) The induction of partial resistance to photodynamic therapy by the protooncogene, *bcl-2*. *Photochem Photobiol* **64** (5): 845-852
- He, X.-Y., Sikes, R., Thomsen, S., Chung, L.W.K. & Jacques, S.L. (1994) Photodynamic therapy with photofrin II induces programmed cell death in carcinoma cell lines. *Photochem Photobiol* **59**: 468-473
- Hellman, S. & Vokes, E.E. (1996) Advancing current treatments for cancer. *Scientific American* **275** (3): 84-89
- Henderson, B.W. & Donovan, J.M. (1990) Release of prostaglandin E₂ from cells by photodynamic treatment *in vitro*. *Cancer Res* **49**: 6896-6900
- Henderson, B.W. & Dougherty, T.J. (1992) How does photodynamic therapy work? *Photochem Photobiol* **55**(1): 145-157
- Henderson, B.W, Waldow, S.M., Mang, T.S., Potter, R.W., Malone, PB. & Dougherty, T.J. (1985) Tumour destruction and kinetics of tumour cell death in two experimental mouse tumours following photodynamic therapy. *Cancer Res* **45**: 572-576
- Hengartner, M.O. & Horvitz, H.R. (1994) *C. elegans* cell survival gene *ced-9* encodes a functional homolog of the mammalian proto-oncogene *bcl-2*. *Cell* **76**: 665-676
- Herd, R.M., Dover, J.S. & Arndt, K.A. (1997) Basic laser principles. *Dermatol Clin* **15**: 355-374
- Herr, H.W., Huffman, J.L., Huryk, R., Heston, W.D.W., Melamed, M.R. & Whitmore, W.F. (1988) Anticarcinoma activity of rhodamine 123 against a murine renal adenocarcinoma. *Cancer Res* **48**: 2061-2063

- Hill, H.Z. (1989) The relationship of the photobiology of skin cancer and melanins to the radiation biology of melanoma: a selective review. *Comments Mol Cell Biophys* **6**: 141-174
- Ho, R.C.S. (1995) Medical management of stage IV malignant melanoma. *Cancer* **75**: 735-741
- Ismail, M.S., Torsten, U., Dressler, C., Diederichs, J.E., Huske, S., Weitzel, H., Berlien, H.P. (1999) Photodynamic therapy of malignant ovarian tumours cultivated on CAM. *Laser Med Sci* **14** (2): 91-96
- Iwamoto, Y., Yoshioka, H. & Yanagihara, Y. (1987) Singlet oxygen producing activity and photodynamic biological effects of acridine compounds. *Chem Pharm Bull* **35**: 2478-2483
- Jacobi, A. (1906) Methylthionin hydrochloride in inoperable cancer. *J Amer Med Assoc* **47**: 1545-1546
- Jori, G. (1992) Far-red absorbing photosensitizers-their use in the photodynamic therapy of tumours. *J Photochem Photobiol: A* **62** (3): 371-378
- Jori, G. (1996) Tumour photosensitizers: approaches to enhance the selectivity and efficiency of photodynamic therapy. *J Photochem Photobiol B: Biology* **36**: 87-93
- Kaisary, A.M. (1986) Assessment of radiotherapy in invasive bladder carcinoma using *in vivo* methylene blue staining technique. *Urology* **28** (2): 100-102
- Kane, D.J., Sarafian, T.A., Anton, R., Hahn, H., Gralla, E. B., Valentine, J.S., Ord, T. & Bredesen, S.E. (1993) Bcl-2 inhibition of neural death: decreased generation of reactive oxygen species. *Science* **262**: 1274-1277
- Kaplan, M.J., Somers, R.G., Greenberg, R.H. & Ackler, J. (1998) Photodynamic therapy in the management of metastatic cutaneous adenocarcinomas: case reports from phase 1/2 studies using tin ethyl etiopurpurin (SnET2). *J Surg Oncol* **67**(2): 121-125
- Kartner, N. & Ling, V. (1989) Multidrug resistance in cancer. *Scientific American* **231**: 26-34
- Kelly, J.F., Snell, M.E. & Berenbaum, M.C. (1975) Photodynamic destruction of human bladder carcinoma. *Br J Cancer* **31**: 237-244
- Kennedy, J.C., Pottier, R.H. & Pross, D.C. (1990) Photodynamic therapy with endogenous protoporphyrin IX: basic principles and present clinical experience. *J Photochem Photobiol B: Biol* **6**: 143-148
- Kennedy, J.C. & Pottier, R.H. (1992) Endogenous protoporphyrin IX, a clinically useful photosensitizer for photodynamic therapy. *J Photochem Photobiol B: Biol* **28**: 275-292

- Kennedy, J.C., Marcus, S.L. & Pottier, R.H. (1996) Photodynamic therapy (PDT) and photodiagnosis (PD) using endogenous photosensitization induced by 5-aminolaevulinic acid (ALA): mechanisms and clinical results. *J Clin Laser Med Surg* **14**: 289-304
- Kerdel, F.A., Soter, N.A. & Lim, H.W. (1987) *In vivo* mediator release and degranulation of mast cells in haematoporphyrin derivative-induced phototoxicity in mice. *J Invest Derm* **88**: 277-280
- Kessel, D. (1982) Determinants of haematoporphyrin-catalyzed photosensitization. *Photochem Photobiol* **36**: 99-101
- Kessel, D. (1986) Porphyrin-lipoprotein association as a factor in porphyrin localisation. *Cancer Lett* **33**: 183-188
- Kessel, D. (1989b) *In vitro* photosensitization with a benzoporphyrin derivative. *Photochem Photobiol* **49**: 579-582
- Kessel, D. (1989c) Determinants of photosensitization by purpurins. *Photochem Photobiol* **50**: 169-174
- Kessel, D. Luo, Y., Deng, Y. & Chang, C.K. (1997) The role of subcellular localisation in initiation of apoptosis by photodynamic therapy. *Photochem Photobiol* **65**: 422-426
- Kessel, D. & Luo, Y. (1999) Photodynamic therapy: a mitochondrial inducer of apoptosis. *Cell Death Differ* **6**: 28-35
- Kinsey, B.M., Van den Abbeele, A.D., Adelstein, S.J. & Kassis, A.I. (1989) Absence of preferential uptake of [¹²⁵I] iododihydrorhodamine 123 by four human tumour xenografts. *Cancer Res* **49**: 5986-5988
- Knoerle, R., Schnitz, E. & Feuerstein, T.J. (1998) Drug accumulation in melanin: an affinity chromatographic study. *J Chromatog B* **714**: 171-179
- Kohen, E., Santus, R. & Hirschberg, J.G. (1995) Photochemotherapy (PUVA Therapy) and UVB Phototherapy in "Photobiology", Academic Press, UK., pp 447-468
- Kohen, E., Santus, R. & Hirschberg, J.G. (1995) Pathways of molecular excitation and deactivation in "Photobiology". Academic Press, UK., pp 23-32
- König, K., Bockhorn, V., Dietel, W. & Schubert, H. (1987) Photochemotherapy of animal tumours with the photosensitizer methylene blue using a krypton laser. *J Cancer Res Clin Oncol* **113**: 301-303
- Korbelik, M., Krosol, G., Olive, P.L. & Chaplin, D.J. (1991) Distribution of Photofrin between tumour cells and tumour associated macrophages. *Br J Cancer* **64**: 508-512
- Korbelik, M. (1992) Low-density lipoprotein pathway in the delivery of Photofrin: how much is it relevant for selective accumulation of the photosensitizer in tumours. *J Photochem Photobiol B: Biol* **12**: 107-119

- Korbelik, M. & Krosi, G. (1994) Enhanced macrophage cytotoxicity against tumour cells treated with photodynamic therapy. *Photochem Photobiol* **60**: 497-502
- Krementz, E.T., Carter, R.D. Sutherland, C.M., Muchmore, J.H., Ryan, R.F. & Creech, O. (1994) Regional chemotherapy for melanoma: a 35-year experience. *Ann Surg* **220**: 520-535
- Lam, M., Dubyak, G., Chen, L., Nunez, G., Miesfeld, L. & Distelhorst, C.W. (1994) Evidence that Bcl-2 represses apoptosis by regulating endoplasmic reticulum-associated Ca²⁺ fluxes. *Proc Natl Acad Sci USA* **91**: 6569-6573
- Larsson, B. & Tjälve, H. (1979) Studies on the mechanism of drug binding to melanin. *Biochem Pharmacol* **28**: 1181-1187
- Lauka, M.A., Wang, K.K. & Bonner, J.A. (1994) Apoptosis occurs in lymphoma cells but not in hepatoma cells following ionizing radiation and photodynamic therapy. *Dig Dis Sci* **39**: 2467-2475
- Lee, Y.S. & Wurster, R.D. (1995) Methylene blue induces cytotoxicity in human brain tumour cells. *Cancer Lett* **88**: 141-145
- Leibovici, L., Schönfeld, N. & Yehoshua, H.A. (1988) Activity of porphobilinogen deaminase in peripheral blood mononuclear cells of patients with metastatic cancer. *Cancer* **62**: 2297-2300
- Leist, M., Single, B., Castoldi, A.F., Koehnle, S. & Nicotera, P. (1997) Intracellular adenosine triphosphate (ATP) concentration: A switch in the decision between apoptosis and necrosis. *J Exp Med* **185** (8): 1481-1486
- Leung, J. (1994) Photosensitizers in photodynamic therapy. *Semin Oncol* **21**: 4-10
- Levi, J.G., Waterfield, E. & Richter, A. (1994) Photodynamic therapy of malignancies with benzoporphyrin derivative monoacid ring A. *Proc Soc Photo-Opt Instrum Eng* **2078**: 99-101
- Levi, J.G. (1995) The preclinical and clinical development of Photofrin® and benzoporphyrin derivative: a reflection on opportunities and changes. *J Photochem Photobiol B: Biol* **30**: 79-82 (ESP newsletter)
- Lewis, M. R., Slovirer, N. A. & Goland, P.P. (1946) *In vivo* staining and retardation of sarcomata in mice. *Anat Rec* **95**: 89-96
- Lin, C.W., Shulok, J.R., Wong, Y.K., Schanbacher, C.F. & Cincotta, L. (1991) Photosensitization, uptake and retention of phenoxazine Nile blue derivatives in human bladder carcinoma cells. *Cancer Res* **51**: 1109-1116
- Lin, C.W., Schulock, J.R., Kirley, S.D., Cincotta, L. & Foley, J.W. (1991) Lysosomal localization and mechanism of uptake of Nile Blue photosensitizers in tumour cells. *Cancer Res* **51**: 2710-2719

- Link, E.M., Costa, D.C., Lui, D., Ell, P.J., Blower, P.J. & Spittle, M.F. (1996) Targeting disseminated melanoma with radiolabelled methylene blue. *Acta Oncologica* **35** (3): 331-341
- Link, E.M., Blower, P.J. & Costa & D.C. (1998) Early detection of melanoma metastases with radioionated methylene blue. *Eur J Nucl Med* **25**: 1322-1329
- Lipson, R.L. & Baldes, E.J. & Olsen, A.M. (1961) The use of a derivative of haematoporphyrin in tumour detection. *J Natl Cancer Inst* **26**: 1-11
- Lipson, R.L., Baldes, E.J. & Gray, M.J. (1966) Haematoporphyrin derivative for detection and management of cancer. *Cancer* **20**: 2255-2257
- Liu, L. (1989) DNA topoisomerase poisons as antitumour drugs. *Ann Rev Biochem* **58**: 351
- Lui, H., Zeng, H. & McLean, D.I. (1996) *In vivo* fluorescence spectroscopy monitoring of BPD verteporfin concentration changes in skin tissue during photodynamic therapy of cancer. *J Dermatol Sci* **12**: 87
- Luna, M.C., Wong, S. & Gomer, C.J. (1994) Photodynamic therapy mediated induction of early response genes. *Cancer Res* **53**: 1374-1380
- Luo, Y., Chang, C.K. & Kessel, D. (1994) Rapid initiation of apoptosis by photodynamic therapy. *Ibid.* **63** (4): 528-534
- Luo, Y. & Kessel, D. (1996) The phosphatase inhibitor calyculin antagonizes the rapid initiation of apoptosis by photodynamic therapy. *Biochem Biophys Res Commun* **221**: 72-76
- Luo, Y. & Kessel, D. (1998) Initiation of apoptosis versus necrosis by photodynamic therapy with chloroaluminium phthalocyanine. *Photochem Photobiol* **66**: 479-483
- Ma, L., Moan, J. & Berg, K. (1994) Evaluation of a new photosensitizer, *meso*-tetrahydroxyphenyl chlorin for use in photodynamic therapy: a comparison of its photobiological properties with those of two other photosensitizers. *Int J Cancer* **57**: 883-888
- Maillard, P., Krausz, P., Sianotta, C. & Garpard, S. (1980) Photoinduced activation of molecular oxygen by various porphyrins, bisporphyrins, phthalocyanines, pyridinoporphyrazines and their metal derivatives. *J Organomet Chem* **197**: 285-290
- Marijnissen, J.P.A. & Star, W.M. (1987) Quantitive light dosimetry *in vitro* and *in vivo*. *Lasers Med Sci* **2**: 235-241
- Matheson, I.B.C., Etheridge, R.D., Kratowich, N.R. & Lee, J. (1975) The quenching of singlet oxygen by amino acids and proteins. *Photochem Photobiol* **21**: 165-171

- Matthews, J.L., Sogandares-Bernal, F., Judy, M., Gulliya, K., Newman, J., Chanh, T. & Marengo-Rowe, A. (1992) Inactivation of viruses with photoactive compounds. *Blood cells* **18**: 75-88
- Meloni, E., Dasdia, T., Fava, G., Rocca, E., Zucrino, F. & Marchesini, R. (1988) *In vitro* photosensitizing properties of rhodamine 123 on different human tumour cell lines. *Photochem Photobiol* **48**: 311-314
- Meyer-Betz, F. (1913) (cited in Daniell & Hill, 1991) Untersuchungen über die biologische (photodynamische) Wirkung des haematoporphyrins und anderer Derivative des Blut-und Gallenfarbstoffs. *Dtsch Arch Klin Med* **112**: 476-503
- Miles, D.R. & Young, S.W. (1997) Repeated treatment of RIF-1 tumours with photodynamic therapy (PDT) using lutetium texaphyrin (PCI-0123). *Photochem Photobiol* **65**: 47s
- Milgrom, L.R. (1983) Synthesis of some new tetraarylporphyrins for studies in solar energy conversion. *J Chem Soc., Perkin Trans I*: 2535
- Miranda, M., Botti, D. & Di Cola, M. (1984) Possible genotoxicity of melanin synthesis intermediates: tyrosinase reaction products interact with DNA *in vitro*. *Mol Gen Genet* **193**: 395-399
- Moan, J., Petterson, E.O. & Christensen, T. (1979) The mechanism of photodynamic inactivation of human cells *in vitro* in the presence of haematoporphyrin. *Br J Cancer* **39**: 398-407
- Moan, J., Waksvik., H. & Christensen, T. (1980) DNA single-strand breaks and sister chromatid exchanges induced by treatment with haematoporphyrin and light or by x-rays in human NHIK 3025 cells. *Cancer Res* **40**: 2915-2918
- Moan, J., Rimington, C., Evensen, J.F. & Western, A. (1985) Binding of porphyrins to serum proteins. In: Kessel, D., ed.. *Methods in porphyrin photosensitization*, Plenum Publ Corp., pp 193-205
- Moan, J. (1986) Porphyrin photosensitization and phototherapy. *Photochem Photobiol* **43**: 681-690
- Moan, J., Peng, Q., Evensen, J.F., Berg, K., Western, A. & Rimington, C. (1987) Photosensitizing efficiencies, tumour- and cellular uptake of different photosensitizing drugs relevant for photodynamic therapy of cancer. *Photochem Photobiol* **46**: 713-721
- Moan, J., Berg, K., Kvam, E., Western, A., Malik, Z., Ruck, A. & Schneckenburger, H. (1989) Intracellular localisation of photosensitizers. In: Dougherty, T.J., ed. *Photosensitizing compounds: Their chemistry, biology and clinical use*. John Wiley & Sons, Chichester, pp. 95-111
- Moan, J. (1990) On the diffusion length of singlet oxygen in cells and tissues. *J Photochem Photobiol B: Biol* **6**: 343-344

- Moan, J. & Berg, K. (1992) Photochemotherapy of cancer: experimental research. *Photochem Photobiol* **55** (6): 931-948
- Moan, J. Berg, K., Anholt, H. & Madslie, K. (1994) Sulfonated aluminium phthalocyanines as sensitizers for photochemotherapy. Effects of small light doses on localization, dye fluorescence and photosensitivity in V79 cells. *Int J Cancer* **58**: 865-870
- Modica-Napolitano, J.S., Joyal, J.L., Ara, G., Oseroff, A.R. & Aprille, J.R. (1990) Mitochondrial toxicity of cationic photosensitizers for photochemotherapy. *Cancer Res* **50**: 7876-7881
- Monnier, Ph., Savary, J.F., Wagnieres, G., van den Bergh, H., Mizeret, J & Fontollet, Ch. (1994) Green light irradiation for the prevention of complications in PDT of early squamous cell carcinomas of the oesophagus, in *5th Int Photodynamic Association Biennial Meeting September 21-24, FL. U.S.A. Abstract 27*
- Moor, A.C.E. (2000) Signalling pathways in cell death and survival after photodynamic therapy. *J Photochem Photobiol B: Biol* **57**: 1-13
- Morgan, A.R., Garbo, G.M. Keck, R.W., Eriksen, L.D. & Selman, S.H. (1990a) Metalloporphyrins and light: effect on transplantable rat bladder tumours and murine skin. *Photochem Photobiol* **51**: 589-592
- Morlière, P., Momenteau, M., Candide, C., Simonin, V., Santus, R., Dubertret, L., Goldstein, S. & Hoeppe, G. (1990) Synthesis, cellular uptake of, and cell photosensitization by a porphyrin bearing a quinoline group. *J Photochem Photobiol:B* **5**: 49-67
- Moscow, J.A. & Cowan, K.H. (1988) Multidrug resistance. *J Natl Cancer Inst* **80**: 14-20
- Motsenbocker, M., Masuya, H., Shimazu, H., Miyawaki, T., Ichimori, Y. & Sugawara, T. (1993) Photoactive methylene blue dye derivatives suitable for coupling to protein. *Photochem Photobiol* **58** (5): 648-652
- Murphree, S.A., Tritton, T.L., Smith, P.L. & Sartorelli, A.C. (1981) Adriamycin induced changes in the surface membrane of sarcoma 180 ascites cells. *Biochim Biophys Acta* **649**: 317
- Murrer, L.H.P., Marijnissen, J.P.A., Baas, P., van Zandwijk, N. & Star, W.M. (1997) Applicator for light delivery and *in situ* light dosimetry during endobronchial photodynamic therapy: first clinical measurements. *Lasers Med Sci* **12**: 253-259
- Musser, D.A., Wagner, J.M., Weber, F.J. & Datta-Gupta, N. (1980) The binding of tumour localizing porphyrins to a fibrin matrix and their effects following photoirradiation. *Res Commun Chem Pathol Pharmacol* **28**: 505-525

- Musser, D.A., Wagner, J.M. & Datta-Gupta, N. (1982) The interaction of tumour-localising porphyrins with collagen and elastin. *Res Commun Chem Pathol Pharmacol* **36**: 251-259
- Nadakavukaren, K.K., Nadakavukaren, J.J. & Chen, L.B. (1985) Increased rhodamine 123 uptake by carcinoma cells. *Cancer Res* **45**: 6093-6099
- Nagata, S. (1997) Apoptosis by death factor. *Cell* **88**: 355-365
- Nelson, J.S., Roberts, W.G. & Berns, M.W. (1987) *In vivo* studies on the utilization of mono-L-aspartyl chlorin (Npe₆) for photodynamic therapy. *Cancer Research* **47**: 4681-4685
- Nelson, J.S., -H., Liaw, L, Orenstein, A., Roberts, W.G. & Berns, M.W. (1988) Mechanisms of tumour destruction following photodynamic therapy with haematoporphyrin derivative, chlorin and phthalocyanine. *J Natl Cancer Inst* **80**: 1599-1605
- Neyso, U.O. & Dougherty, T.J. (1986) Photodynamic therapy in the management of resistant bladder cancer. *Lasers Surg Med* **6**: 228 (abstract)
- Nicholson, D.W. (1995) ICE/Ced-3-like proteases as therapeutic targets for the control of inappropriate apoptosis. *Nature Biotech* **14**: 297-301
- Nilsson, R., Merkel, P.B. & Kearns, D.R. (1972) Unambiguous evidence for the participation of singlet oxygen in photodynamic oxidation of amino acids. *Photochem Photobiol* **16**: 117-124
- Noodt, B.B., Rodal, G.H., Wainwright, M., Peng, Q., Horobin, R., Nesland, J.M. & Berg, K. (1998) Apoptosis induction by different pathways with methylene blue derivative and light from mitochondrial sites in V79 cells. *Int J Cancer* **75**: 941-948
- Noodt, B.B., Berg, K., Stokke, T., Peng, Q & Nesland, J.M. (1999) Different apoptotic pathways are induced from various intracellular sites by tetraphenylporphyrins and light. *Br J Cancer* **79**: 72-81
- Oleinick, N.L., Agarwal, M.M.L. & Berger, N.A. (1993) Signal transduction and metabolic changes during tumour cell apoptosis following phthalocyanine sensitized photodynamic therapy. *Proc SPIE Optical methods tumour treatment detection* **1881**: 252-261
- Oleinick, N.L. & Evans, H.H. (1998) The photobiology of photodynamic therapy: cellular targets and mechanisms. *Radiat Res* **150** S146-156
- Orth, K., Rück, A., Stanescu, A. & Beger, H.G. (1995) Intraluminal treatment of inoperable oesophageal tumours by intraluminal photodynamic therapy with methylene blue. *Lancet* **345**: 519-520

- Orth, K., Russ, D., Beck, G., Rück, A. & Beger, H.G. (1998) Photochemotherapy of experimental colonic tumours with intratumorally applied methylene blue. *Langenbecks Archives of Surg* **383** (3-4): 276-281
- Oseroff, A.R.D., Ohuoha, D., Ara, G., McAuliffe, D., Foley, J. & Cincotta, L. (1986) Intramitochondrial dyes allow selective *in vitro* photolysis of carcinoma cells. *Proc Natl Acad Sci USA* **83**: 9729-9733
- Oseroff, A.R. (1993) Photofrin and HpD in the treatment of basal cell carcinoma and Bowen's disease. *Photochem Photobiol* **57**: 108S
- Paquette, B., Ali, H., Langlois, R. & van Lier, J.E. (1988) Biological activities of phthalocyanines-VIII. Cellular distribution in V-79 Chinese hamster cells and phototoxicity of selectively sulphonated aluminium phthalocyanines. *Photochem Photobiol* **47**: 215-220
- Pandey, R.K., Jagerovic, N., Ryan, J.M., Dougherty, T.J. & Smith, K.M. (1993) Efficient syntheses of new classes of regiochemically pure benzoporphyrin derivatives. *Biorg & Med Chem Lett* **3** (12): 2615-2618
- Pangka, V.S., Morgan, A.R. & Dolphin, D. (1986) Diels-Alder reactions of protoporphyrin IX dimethyl ester with electron-deficient alkynes. *J Org Chem* **51**: 1094-1100
- Patterson, M.S., Wilson, B.C. & Wyman, D.G. (1991) The propagation of optical radiation in tissue. 1. Models of transport and their application. *Lasers Med Sci* **6**: 155-168
- Peng, Q., Farrants, G.W., Madslie, K., Bommer, J.C., Moan, J., Danielson, H.E. & Nesland, J.M. (1991) Subcellular localisation, redistribution and photobleaching of sulphonated aluminium phthalocyanine in a human melanoma cell line. *Int J Cancer* **49**: 290-295
- Peng, Q., Moan, J., Farrants, G.W., Danielson, H.E. & Rimington, C. (1991) Localization of potent photosensitizers in human LOX by means of laser scanning microscopy. *Cancer Lett* **58**: 17-27
- Peng, Q., Moan, J. & Nesland, J.M. (1996) Correlation of subcellular and intratumoural photosensitizer localization with ultrastructural features after photodynamic therapy. *Ultrastruct Pathol* **20**: 109-129
- Peng, Q., Warloe, T. & Berg, K. (1997) 5-Aminolaevulinic acid-based photodynamic therapy: clinical research and future challenges. *Cancer* **79**: 2282-2308
- Peng, Q.A., Brown, S.B., Moan, J., Nesland, J.M., Wainwright, M., Griffiths, J., Dixon, B., Cruse Sawyer, J. & Vernon, D. (1993) Biodistribution of a methylene blue derivative in tumours and normal tissues of rats. *J Photochem Photobiol B: Biol* **20**: 63-71

- Penning, L.C., vanSteveninck, J. & Dubbelman, T.M. (1993) HPD-induced changes in intracellular cyclic AMP levels in human bladder transitional carcinoma cells, clone T24. *Biochem Biophys Res Commun* **194**: 1084-1089
- Policard, A. (1924) (cited in Daniell & Hill, 1991) Etude sur les aspects offerts par des tumeurs experimentales examinées à la lumière de Wood. *C R Soc Biol* **91**:1423-1428
- Pooler, J. & Valenzano, D.P. (1979) Physicochemical determinants of the sensitizing effectiveness for photooxidation of nerve membranes by fluorescein derivatives. *Photochem Photobiol* **30**: 491-498
- Potter, W.R., Mang, T.S. & Dougherty, T.J. (1987) The theory of photodynamic dosimetry: consequences of photodestruction of sensitizers. *Photochem Photobiol* **46**: 97-101
- Pottier, R., Chow, Y.F.A., LaPlate, J.P. (1986) Non-invasive technique for obtaining fluorescence excitation and emission spectra *in vivo*. *Photochem Photobiol* **44**: 679-687
- Potts, A.M. (1964) The reaction of uveal pigment *in vitro* with polycyclic compounds. *Invest Ophthalmol* **3**: 405-416
- Prime, J. (1900) (cited in Daniell & Hill, 1991) Les accidentes toxiques par l'eosinate de sodium. Jouve & Boyer, Paris
- Raab, O. (1900) (cited in Daniell & Hill, 1991) Ueber die Wirkung fluorescierenden Stoffe auf Infusorien. *Z Biol* **39**: 524-546)
- Rashid, F. & Horobin, R.W. (1990) Interactions of molecular probes with living cells and tissues. 2. A structure-activity analysis of mitochondrial staining by cationic probes, and a discussion of the synergistic nature of image-based and biochemical approaches. *Histochemistry* **94**: 303-308
- Rasmussen-Taxdal, D.S., Ward, G.E. & Figge, F.M.J. (1955) Fluorescence of human lymphatic and cancer tissues following high doses of intravenous haematoporphyrin. *Cancer* **8**: 78-81
- Razum, N., Snyder, A. & Dorion, D. (1996) SnET2: Clinical update. *Proc SPIE* **2675**: 43-46
- Reed, M.W.R., Miller, F.N., Wieman, T.J., Tseng, M.T. & Pietsch, C.G. (1988) The effect of photodynamic therapy on the microcirculation. *J Surg Res* **45**: 452-459
- Reed, M.W.R., Mullins, A.P., Anderson, G.L., Miller, F.N. & Wieman, T.J. (1989) The effect of photodynamic therapy on tumour oxygenation. *Surgery* **106**: 94-99
- Reers, M., Smiley, S.T., Mottola-Hartshorn, C., Chen, A., Lin, M. & Chen, L.B. (1995) Mitochondrial membrane potential monitored by JC-1 dye. *Methods in Enzymology* **260**: 406-417

- Rennie, J. & Rusting, R. (1996) Making headway against cancer. *Scientific American* **275**: 28-30
- Renschler, M.F., Yuen, A. & Panella, T.J., Wieman, T.J., Julius, C., Panjehpour, M., Taber, S., Fingar, V., Horning, S., Miller, R.A., Lowe, E., Engel, J., Woodburn, K.,
- Ressler, M.M. & Pandey, R.K. (1998) Creating new photosensitizers for cancer therapy. *Chemtech* **28** (3) 39-45
- Reyftman, J.B., Santus, R., Moliere, P. & Kohan, E. (1986) Fluorescent products formed by reaction of amino acids and spermidine with lipid peroxides produced by porphyrin photosensitization in ionic micelles. *Photobiochem Photobiophys* **11**: 197-208
- Richart, R.M. (1963) A clinical staining test for the *in vivo* delineation of dysplasia and carcinoma *in situ*. *Amer J Obstet Gynec* **86**: 703-712
- Richter, A.M., Cerrito-Sola, S., Sternberg, E.D., Dolphin, D. & Levy, J.G. (1990) Biodistribution of tritiated benzoporphyrin derivative (3H-Bpd-MA), a new potent photosensitizer, in normal and tumour-bearing mice. *J Photochem Photobiol, B: Biol* **5**: 231-244
- Richter, C., Schweizer, M., Cossarizza, A. & Franceschi, C. (1996) Control of apoptosis by the cellular ATP level. *FEBS Letters* **378**:107-110
- Rifkin, R., Reed, B. & Hetzel, F. (1997) Photodynamic therapy using SnET2 for basal cell nevus syndrome: a case report. *Clin Ther* **19**(4): 639-641
- Riley, J.F. (1948) Retardation of growth of a transplantable carcinoma in mice fed basic metachromatic dyes. *Cancer Res* **8**: 183-188
- Ris, H.B., Determatt, J.H. & Inderbitzi, R. (1991) Photodynamic therapy with chlorins for diffuse malignant mesothelioma: initial clinical results. *Br J Cancer* **64**: 1116-1120
- Ris, H.B, Altermatt, H.J. & Nachbar, B. (1996) Intraoperative photodynamic therapy with *m*-tetrahydroxyphenylchlorin for chest malignancies. *Lasers Surg Med* **18**: 39-45
- Ritchie, A.C. (1970) The classification, morphology and behaviour of tumours. In *General Pathology* (H. Florey, ed.) 4th ed., Lloyd-Luke, London, pp 668-719
- Rivers, J.K. (1996) Melanoma. *Lancet* **347**: 803-806
- Roberts. W.G. & Berns, M.W. (1989) *In vitro* photosensitization. Cellular uptake and subcellular localization of mono-L-aspartyl chlorin *e*₆, chloro-aluminium sulphonated phthalocyanine and photofrin II. *Lasers Surg Med* **9**: 90-101
- Roberts, W.G., Liaw, L-H. & Berns, M.W. (1989) *In vitro* photosensitization. An electron microscopic study of cellular destruction with mono-L-aspartyl chlorin *e*₆ and photofrin II. *Lasers Surg Med* **9**: 102-108

- Roberts, W.G., Klein, M.K. & Loomis, M. (1991) Photodynamic therapy of spontaneous cancers in felines, canines and snakes with chloro-aluminium sulfonated phthalocyanine. *J Natl Cancer Inst* **83**: 18-23
- Rosenbach, A. & Alster, T. (1996) Cutaneous Laser: A Review. *Ann Plast Surg* **37**: 220-231
- Rosenthal, I. (1991) Phthalocyanines as photodynamic photosensitizers. *Photochem Photobiol* **53**: 859-870
- Rożanowski, M., Ciszewski, J., Korytowski, W. & Sarna, T. (1995) Rose Bengal-photosensitized formation of hydrogen peroxide and hydroxyl radicals. *J Photochem Photobiol B: Biol* **29**: 71-77
- Ruoslahti, E. & Reed, J.C. (1994) Anchorage dependence, integrins and apoptosis. *Cell* **77** (4): 477-478
- Salet, C. & Moreno, G. (1990) New trends in photobiology. Photosensitization of mitochondria. Molecular and cellular aspects. *J Photochem Photobiol B: Biol* **5**: 133-150
- Salet, C., Moreno, G., Ricchelli, F. & Bernardi, P. (1997) Singlet oxygen produced by photodynamic action causes inactivation of the mitochondrial permeability transition pore. *J Biol Chem* **272**: 21938-21943
- Santus, R., Kohen, C., Kohen, E., Reyftmann, J.P. Morliere, P., Dubertret, L. & Tocci, P.M. (1983) Permeation of lysosomal membranes in the course of photosensitization with methylene blue and haematoporphyrin: study by cellular microspectrofluorometry. *Photochem Photobiol* **38** (1): 71-77
- Savary, J.F, Monnier, P., Wagnieres, G., Braichotte, G., Fontolliet, C. & Van den Bergh, H. (1994) Preliminary clinical studies of phototherapy with meso-tetrahydroxyphenyl chlorin (*m*-THPC) as a photosensitizing agent for the treatment of early pharyngeal, oesophageal and bronchial carcinomas. *Proc SPIE*: **2078**: 330-340
- Savary, J.F., Monnier, P., Fontolliet, C., Mizeret, J., Wagnieres, G., Braichotte, D., Van den Bergh, H. (1997) Photodynamic therapy for early squamous cell carcinomas of the oesophagus, bronchi and mouth with tetra(hydroxyphenyl)chlorin. *Arch Otolaryn* **123** (2): 162-168
- Schaap, A.P. (1974) Singlet molecular oxygen and superoxide dismutase. *J Am Chem Soc* **96**: 4025-4026
- Schea, C. R., Chen, N., Wimberly, J. & Hasan, T. (1989) Rhodamine dyes as potential agents for photochemotherapy of cancer in human bladder carcinoma cells. *Cancer Res* **49**: 3961-3965
- Scheibe, G. (1937) *Z Angew Chem* **50**: 212

Schick, E., Ruck, A., Boehnicke, W.H. & Kaufmann, R. (1997) Topical photodynamic therapy using methylene blue and 5-aminolaevulinic acid in psoriasis. *J Dermatol Treatment* **8**: (1): 17-19

Schmidt-Erfurth, U., Miller, J. & Sickenby, M. (1997) Photodynamic therapy for choroidal neovascularisation in a phase II study. Preliminary results of multiple treatments. Abstract. *Assoc Res Vision Ophthalmology* **38**: 74

Schuitmaker, J.J. Baas, P., van Leengoed, H.L.L.M., van der Meulen, F.W., Star, W.M. & van Zandwijk, N. (1996) Photodynamic therapy: a promising new modality for the treatment of cancer. *J Photochem Photobiol B: Biology* **34**: 3-12

Schwartz, S.K., Absolon, K. & Vermund, H. (1955) Some relationships of porphyrins, x-rays and tumours. *Univ Minn Med Bull* **27**: 7-8

Selman, S.H., Kreimer-Birnbaum, M. & Chaudhuri, K. (1986) Photodynamic treatment of transplantable bladder tumours in rodents after pretreatment with chloroaluminium tetrasulphophthalocyanine. *J Urol* **136**: 141-145

Selman, S.H. & Keck, R.W. (1994) The effect of transurethral light on the canine prostate after sensitization with the photosensitizer tin (II) etiopurpurin dichloride: a pilot study. *J Urol* **152**: 2129-2132

Separov, D., He, J. & Oleinick, N.L. (1997) Ceramide generation in response to photodynamic treatment of L5178Y mouse lymphoma cells. *Cancer Res* **57**: 1717-1721

Separov, D., Mann, K.J. & Oleinick, N.L. (1998) Association of ceramide accumulation with photodynamic treatment-induced cell death. *Photochem Photobiol* **68**: 101-109

Separov, D., Pink, J.J., Oleinick, N.A., Kester, M., Boothman, D.A., McLoughlin, M. Pena, L.A. & Haimovitz-Friedman, A. (1999) Niemann-Pick human lymphoblasts are resistant to phthalocyanine 4-photodynamic therapy-induced apoptosis. *Biochem Biophys Res Commun* **258**: 506-512

Sessler, J.L., Murai, T., Lynch, V. & Cyr, M. (1988) An "expanded porphyrin": the synthesis and structure of a new aromatic pentadentate ligand. *J Am Chem Soc* **110**: 5586-5588

Sessler, J.L., Hemmi, G., Mody, T.D., Murai, T., Burrell, A. & Young, S.W. (1994) Texaphyrins: synthesis and applications. *Acc Chem Res* **27**: 43-50

Shea, C.R., Chen, N., Wimberly, J. & Hasan, T. (1989) Rhodamine dyes as potential agents for photochemotherapy of cancer in human bladder carcinoma cells. *Cancer Res* **49**: 3961-3965

Shimizu, S., Eguchi, Y., Kamiike, W., Itoh, H., Hasegawa, J., Yamabe, K., Otsuki, Y., Matsuda, H., & Tsujimoto, Y. (1996) Induction of apoptosis as well as necrosis by hypoxia and predominant prevention of apoptosis by Bcl-2. *Cancer Res* **56** (9): 2161-2166

- Simon, D.I., Woodburn, K.W., Xu, H., Cheong, W.F., Raman, V., Adelman, D., Miller, R.A. & Rogers, C. (1999) Photodynamic therapy with lutetium texaphyrin induces apoptosis of vascular cells. *Circulation* **100** (18SS): 3692
- Singh, A. (1978) Introduction: Interconversion of singlet oxygen and related species. *Photochem Photobiol* **28**: 429-433
- Slominski, A., Paus, R. & Schanderdorf, D. (1993) Melanocytes as sensory and regulatory cells in the epidermis. *J Theor Biol* **164**: 103-120
- Snyder, A.B., Razum, N.J., Trommer, R. & Doiron, D. (1996) Tin ethyl etiopurpurin (SnET2): phase I/II clinical results for the treatment of cutaneous carcinomas, presented at the *Sixth Meeting of the International Photodynamic Association, Melbourne, March 1996*, Abstract
- Soloman, E., Borrow, J. and Goddard, A.D. (1991) Chromosome aberrations and cancer. *Science* **254**: 1153-1160
- Soncin, M., Busetti, A. & Biolo, R. (1998) Photoinactivation of amelanotic and melanotic cells sensitized by axially substituted Si-naphthalocyanines. *J Photochem Photobiol B: Biol* **42**: 202-210
- Specht, K.G. & Rodgers, M.A.J. (1990) Depolarization of mouse myeloma cell membranes during photodynamic action. *Photochem Photobiol* **51**: 319-324
- Spikes, J.D. & Straight, R. (1967) Sensitized photochemical processes in biological systems. *Ann Rev Phys Chem* **18**: 409-436
- Sporn, L.A. & Foster, T. H. (1992) Photofrin and light induces microtubule depolymerisation in cultured human endothelial cells. *Cancer Res* **52**: 3443-3445
- Star, W.M., Marijissen, H.P.A., van der Berg-Blok, A.E., Versteeg, J.A.C., Franken, K.A.P. & Reinhold, H.S. (1986) Destruction of rat mammary tumour and normal tissue microcirculation by haematoporphyrin derivative photoradiation observed *in vivo* sandwich observation chambers. *Cancer Res* **46**: 2532-2540
- Steiner, A., Pehamberger, H. & Wolff, K. (1987) *In vivo* epiluminescence microscopy of pigmented skin lesions. II Diagnosis of small pigmented skin lesions and early detection of malignant melanoma. *J Am Acad Dermatol* **17**: 584-591
- Stockart, J.C., Juarranz, A., Villaneuva, A. & Canete, M. (1996) Photodynamic damage to microtubules induced by thiazine dyes. *Cancer Chemother Pharmacol* **39**: 167-169
- Strekowski, L., Hou, D.F., Wydra, R.L. & Schinazi, R.F. (1993) A synthetic route to 3-(dialkylamino)phenothiazin-5-ium salts and 3,7-disubstituted derivatives containing two different amino groups. *J Heterocyclic Chem* **30**: 1693-1696
- Summerhayes, I.C., Lampidis, T.J. Bernal, S.D., Nadakavukaren, J.J., Nadakavukaren, K.K. Shepherd, E.L. & Chen, L.B. (1982) Unusual retention of rhodamine 123 by mitochondria in muscle and carcinoma cells. *Proc Natl Acad Sci USA* **79**: 5292-5296

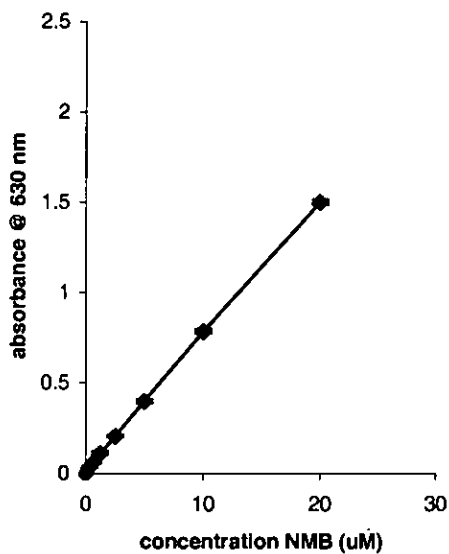
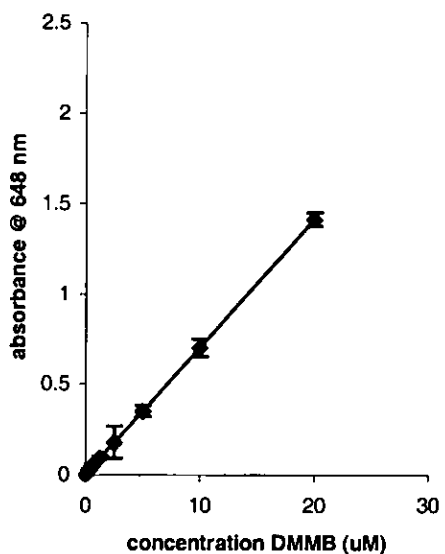
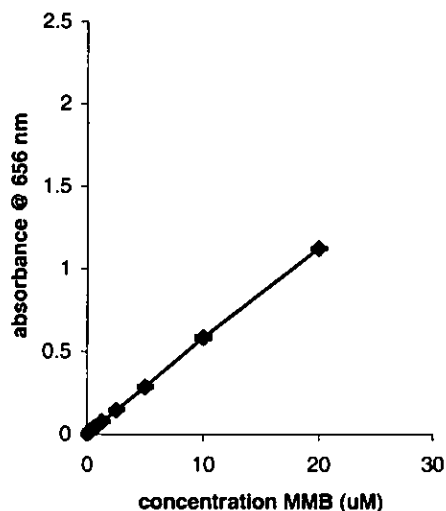
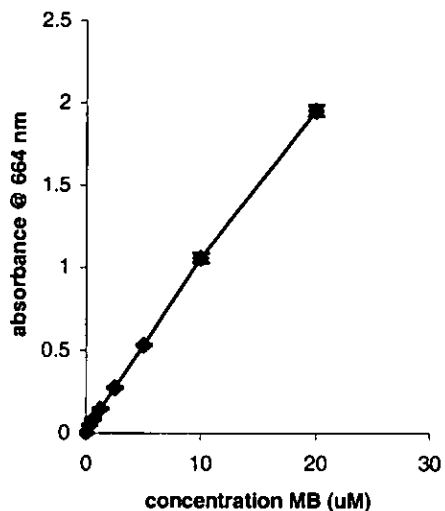
- Svaasand, L.O., Martinelli, E., Gomer, C.J. & Profio, A.E. (1990) Optical characteristics of intraocular tumours in the visible and near-infrared. *Proc SPIE* **1203**: 2-21
- Svetlicec, V., Zutic, V., Clavilier, J. & Chevalet, J. (1987) Organic monolayer formation at a sulphur modified gold electrode. *J Electroanal Chem* **233**: 199-210
- Takemura, T., Ohta, N., Nakajima, S. & Sakata, I. (1989) Critical importance of the triplet lifetime of photosensitizer in photodynamic therapy of tumour. *Photochem Photobiol* **50** (3): 339-344
- Thomas, J.P., Geiger, P.G., Gaffney, D.K. & Girotti, A.W. (1989) Photooxidation of membrane phospholipids and cholesterol in merocyanine 540-sensitized leukaemia cells. *Photochem Photobiol*:**49**: 68-74
- Thomas, J.P. & Girotti, A.W. (1989) Role of lipid peroxidation in haematoporphyrin derivative-sensitized photokilling of tumour cells: protective effects of glutathione peroxidase. *Cancer Res* **49**: 1682-1686
- Thornberry, N.A. & Lazebnik, Y. (1998) Caspases: Enemies within. *Science* **281**: 1312-1316
- Trichopoulos, D., Li, F.P. & Hunter, D.J. (1996) What causes cancer? *Scientific American* **275** (3): 50-57
- Tromberg, B.J., Orenstein, A., Kimel, S., Barker, S.J., Hyatt, J., Nelson, J.S. & Berns, M.W. (1990) *In vivo* tumour oxygen tension measurements for the evaluation of the efficiency of photodynamic therapy. *Photochem Photobiol* **52**: 375-385
- Truscott, T.G., McClean, A.J., Phillips, A.M.R. & Foulds, W.S. (1980) Detection of haematoporphyrin derivative and haematoporphyrin excited states in cell environments. *Canc Lett* **41**: 31-45
- Tuite, E.M. & Kelly, J.M. (1993) Photochemical reactions of methylene blue and analogues with DNA and other biological substrates. *J Photochem Photobiol B: Biol* **21**: 103-124
- Van Hillegersberg, R., Kort, W.J. & Wilson, J.H.P. (1994) Current status of photodynamic therapy in oncology: Review article. *Drugs* **48** (4): 510-527
- Varnes, M.E., Chiu, S.M., Xue, L.Y. & Oleinick, N.L. (1999) Photodynamic therapy-induced apoptosis in lymphoma cells: translocation of cytochrome *c* causes inhibition of respiration as well as caspase activation. *Biochem Biophys Res Commun* **255**: 673-679
- Von Tappeiner, H. (1900) (cited in Daniell & Hill, 1991) Ueber die Wirkung fluoreszierenden Stoffe auf Infusorien nach Versuchen O. Raab. *Munch Med Wochenschr* **47**: 5

- Von Tappeiner, H. & Jesionek, A. (1903) (cited in Daniell & Hill, 1991) Therapeutische Versuche mit fluorescierenden Stoffen. *Munch Med Wochenschr* **47**: 2042-2044
- Von Tappeiner, H. & Jodlbauer, A. (1904) (cited in Daniell & Hill, 1991) Ueber Wirkung der photodynamischen (fluorescierenden) Stoffe auf Protozoan und Enzyme. *Deutsch Arch Klin Med* **80**: 427-487
- Von Tappeiner, H. & Jodlbauer, A. (1907) (cited in Daniell & Hill, 1991) *Die sensibilisierende Wirkung fluorescierender Substanzen. Gasammelte unter Suchungen über die photodynamische Erscheinung*. FCW Vogel, Leipzig
- Wagner, S.J., Skripchenko, A., Robinette, D., Foley, J.W. & Cincotta, L. (1998) Factors affecting virus photoinactivation by a series of phenothiazine dyes. *Photochem Photobiol* **67** (3): 343-349
- Wainwright, M. (1996) Non-porphyrin photosensitizers in biomedicine. *Chem Soc Rev* **25**: 351-359
- Wainwright, M., Phoenix, D.A., Rice, L., Burrow, S.M. & Waring, J.J. (1997) Increased cytotoxicity and phototoxicity in the methylene blue series *via* chromophore methylation. *J Photochem Photobiol B: Biol* **40**: 233-239
- Wainwright, M., Grice, N.J. & Pye, L.E.C. (1999) Phenothiazine Photosensitizers. Part 2. 3,7-Bis(arylamino)phenothiazines. *Dyes Pigments* **42**: 45-51
- Waldow, S.M. & Dougherty, T.J. (1984) Interaction of hyperthermia and photoradiation therapy. *Radiat Res* **97**: 380-385
- Wang, S.Y. & Midden, W.R. (1983) Photodynamic action on nucleic acids and their components. *Stud Biophys* **94**: 7-12
- Wang, K.K. & Densmore, J.C. (1995) A new use for an old drug: methylene blue as a potential photosensitizer for human cholangiocarcinoma. *Hepatology* **14**: 110A
- Weishaupt, K.R., Gomer, C.J. & Dougherty, T.J. (1976) Identification of singlet oxygen as the cytotoxic agent in photoactivation of a murine tumour. *Cancer Res* **36**: 2326-2329
- Wessels, J.M., Seidlitz, H.K., Sroka, R. & Unsoeld, E. (1992) The photodegradation of protoporphyrin in cells: A time-resolved study, in P. Spinelli, M. Dal Fante, R. Marchesini (eds). *Photodynamic therapy and biomedical lasers*. Elsevier Science B.V., pp 684-687
- West, C.M.L., West, D.C., Kumar, S. & Moore, J.V. (1990) A comparison of the sensitivity to photodynamic treatment of endothelial and tumour cells in different proliferative states. *Int J Radiat Biol* **58**: 145-156
- Wieman, T.J., Fingar, V., Taber, S., Panjehpour, M., Julius, C., Panella, T.J., Yuen, A., Horning, S., Woodburn, K., Engel, R., Miller, A., Renschler, M.F. & Young, S.W.

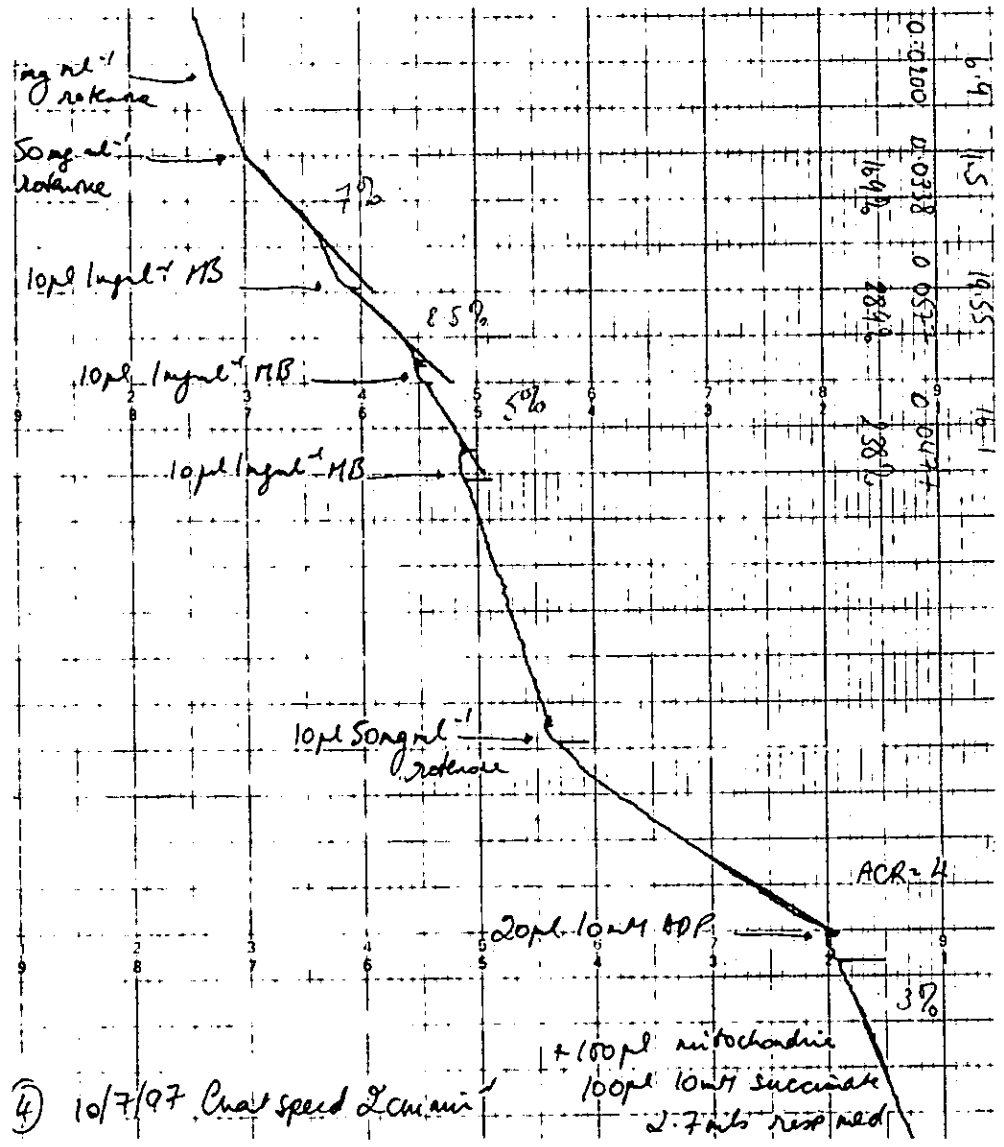
- (1996) Phase I photodynamic trial with lutetium texaphyrin (PCI-0123) in patients with metastatic cancer. *Photochem Photobiol* **80S**
- Wick, M. (1983) The chemotherapy of malignant melanoma. *J Invest Dermatol* **80**: 61S-62S
- Williams, G.T. & Smith, C.A. (1993) Molecular regulation of apoptosis: genetic control of cell death. *Cell* **74**: 777-779
- Williams, J.L., Stamp, J., Devonshire, R. & Fowler, G.J.S. (1989) Methylene blue and the photodynamic therapy of superficial bladder cancer. *J Photochem Photobiol B: Biol* **4**: 229-232
- Wilson, B.C., Jeeves, W.P. & Lowe, D.M. (1985) *In vivo* and post mortem measurements of the attenuation spectra of light in mammalian species. *J Photochem Photobiol B: Biol* **42**: 153-162
- Wilson, B.C. & Patterson, M.S. (1986) The physics of photodynamic therapy. *Phys Med Biol* **31**: 327-360
- Wilson, B.C. (1989) Photodynamic therapy: light delivery and dosage for second-generation photosensitizers. In *Photosensitizing compounds: their chemistry, biology and clinical use*. Ciba Foundation Symposium 146, Wiley, Chichester, pp 60-77
- Wilson, B.D., Mang, T.S., Cooper, M. & Stoll, H. (1989) Use of photodynamic therapy for the treatment of extensive basal cell carcinoma. *Facial Plast Surg* **6**: 185-189
- Wöhrle, D., Hirth, A., Bogdann-Rai, T., Schnurpfeil, G. & Shopova, M. (1998) Photodynamic therapy of cancer: second and third generations of photosensitizers. *Russ Chem Bull* **47** (5) 836-845
- Wolf, P., Rieger, E. & Kerl, H. (1993) Topical photodynamic therapy with endogenous porphyrins after application of 5-aminolaevulinic acid: an alternative treatment modality for solar keratoses, superficial squamous cell carcinomas and basal cell carcinomas? *J Am Acad Dermatol* **28**: 17-21
- Wood, S.R., Holroyd, J.A. & Brown, S.B. (1997) The subcellular localization of Zn(II) phthalocyanines and their redistribution on exposure to light. *Photochem Photobiol* **65**: 397-402
- Woodburn, K.W., Vardaxis, N.J., Hill, J.S., Kaye, A.H. & Phillips, D.R. (1991) Subcellular localization of porphyrins using confocal laser scanning microscopy. *Photochem Photobiol* **54**: 725-732
- Woodburn, K.W., Fan, Q., Miles, D.R., Kessel, D., Luo, Y. & Young, S.W. (1997) localisation and efficacy analysis of the phototherapeutic lutetium texaphyrin (PCI-0123) in the murine EMT6 sarcoma model. *Photochem Photobiol* **65** (3): 410-415
- Wylie, A.H., Kerr, J.F. & Currie, A.R. (1980) Cell death: the significance of apoptosis. *Int Rev Cytol* **68**: 251-306

- Yao, J. & Zhang, G-J. (1996) Loss of lysosomal integrity caused by the decrease of proton translocation in methylene blue-mediated photosensitization. *Biochim Biophys Acta* **1284**: 35-40
- Young, S.W., Woodburn, K.W., Wright, M., Mody, T.D., Fan, Q., Sessler, J.L., Dow, W.C. & Miller, R.A. (1996) Lutetium texaphyrin (PCI-0123): A near infra-red, water-soluble photosensitizer. *Photochem Photobiol* **63**: 892-897
- Yu, D-S., Chang, S-Y. & Ma, C-P. (1990) Photoinactivation of bladder tumour cells by methylene blue: study of a variety of tumour and normal cells. *J Urol* **144**: 164-168
- Yuan, J. & Horvitz, H.R. (1990) The *Caenorhabditis elegans* genes, *ced-3* and *ced-4* act autonomously to cause programmed cell death. *Dev Biol* **138**: 33-41
- Zaidi, S.L., Oleinick, N.L., Zaim, M.T. & Mukhtar, H. (1993) Apoptosis mice: electron microscopic, histopathologic and biochemical evidence. *Ibid.* **58**: 771-776
- Zdolsek, J.M., Olsson, G.M. & Brunk, U.T. (1990) Photooxidative damage to lysosomes of cultured macrophages by acridine orange. *Photochem Photobiol* **51**: 67-76
- Zeiler, T., Riess, H., Wittman, G., Hintz, G., Zimmerman, R., Muller, C., Heuft, H.G. & Huhn, D. (1994) The effect of methylene blue phototreatment on plasma proteins and *in vitro* coagulation capability of single-donor, fresh-frozen plasma. *Transfusion* **34**: 685-689
- Zwang, S., Lynch, M.C. & Kochevar, I.E. (1999) Caspase-8 mediates caspase-3 activation and cytochrome *c* release during singlet oxygen-induced apoptosis of HL-60 cells. *Exp Cell Res* **250**: 203-212
- Zwang, S., Lynch, M.C. & Kochevar, I.E. (1998) Activation of protein kinase C is required for protection of cells against apoptosis induced by singlet oxygen. *FEBS Lett* **437**: 158-162

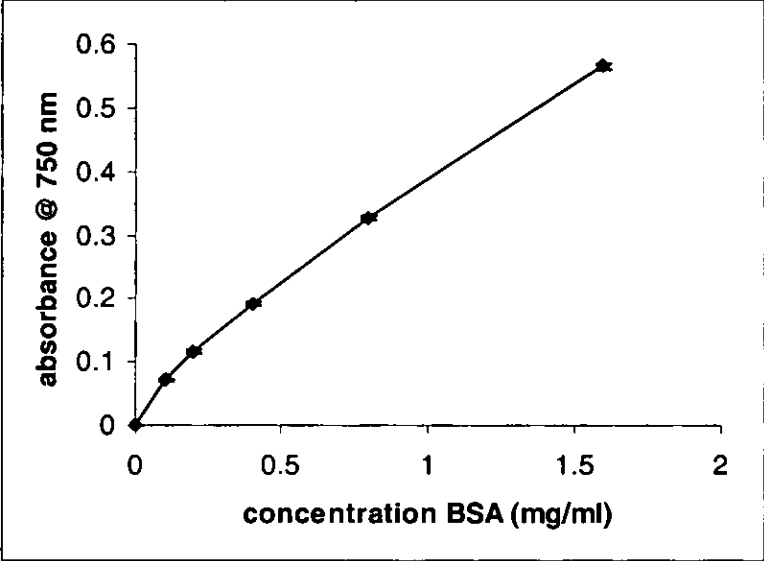
**CHAPTER EIGHT:
APPENDIX**



Appendix 1. Calibration curves for the four photosensitizers, MB, MMB, DMMB and NMB in methanol. Each photosensitizer was read at its maximum absorption value in methanol over a range of concentrations and each point is the mean of 4 experiments \pm SD.



Appendix 2. A typical trace from a chart recorder measuring oxygen utilisation in isolated rat mitochondria that had been incubated with each of the photosensitizers, MB, MMB, DMMB and NMB.



Appendix 3. BSA standard curve.

PRESENTATIONS & PUBLICATIONS

Poster Presentations

1st September 1996- 6th September 1996

"The Effect of Methylation on the Cytotoxicity of Phenothiazinium Dyes"- The 12th Annual Congress on Photobiology, Vienna

31st March 1998- 1st April 1998

"Investigation of methylated Derivatives of Toluidine Blue-O as Photosensitizers for Photodynamic Therapy"- University of Leeds, Colour Science 1998 Exhibition and Conference, Harrogate.

29th July 1998

"Effect of increasing Methylation on the Ability of Methylene Blue to cause diaphorase-catalysed Oxidation of NADH"- Biochemical Society Meeting 666, Sheffield University.

3rd September 1999- 9th September 1999

"Cell Killing by cationic Photosensitizers in the SK-23 and SK-MEL-28 Melanoma Cell Lines"- Biochemical Meeting 670, Cork University, S. Ireland.

Oral Presentations

20th April 1996

"The Effect of Methylation on the Cytotoxicity of Phenothiazinium Dyes"- Lancashire Centre for Medical Studies, Royal Preston Hospital, Preston.

10th February 1999

"Photocytotoxicity of Methylene Blue and its Derivatives in the SK-23 and SK-MEL-28 Melanoma Cell Lines"- Lancashire Centre for Medical Studies, Royal Preston Hospital, Preston.

11th July 2000

"The Effect of Methylation on Methylene Blue Cytotoxicity- (Annual Research Student of the Year Award-Winner), University of Central Lancashire, Preston.

12th October 2000

"The Effect of Methylation on Methylene Blue Cytotoxicity- (Departmental Seminar), University of Central Lancashire, Preston.

Publications

Wainwright, M., Phoenix, D.A., Rice, L., Burrow, S.M. & Waring, J.J. (1997) Increased Cytotoxicity and Phototoxicity in the Methylene Blue Series *via* Chromophore Methylation. *J Photochem Photobiol B*: **40**: 233-239

Rice, L., Wainwright, M., Phoenix, D.A., & Waring, J.J. (1998) Investigation of methylated Derivatives of Toluidine Blue-O as Photosensitizers for Photodynamic Therapy. *Colour Science '98, Proc Ciba Speciality Chemicals Symposium, Volume 1: Dye and Pigment Chemistry*. Pp 327-330

Rice, L., Wainwright, M., Phoenix, D.A., & Waring, J.J. (1998) Effect of increasing Methylation on the ability of Methylene Blue to cause diaphorase-catalysed Oxidation of NADH. *Biochem Soc Transactions* **26**: S319

Rice, L., Wainwright, M., Phoenix, D.A. (1999) Cell Killing by cationic Photosensitizers in the SK-23 and SK-MEL-28 Melanoma Cell Lines. *Biochem Soc Transactions* **28** (1): A30

Rice, L., Wainwright, M., Phoenix, D.A. (2000) Phenothiazine Photosensitizers. III. Activity of Methylene Blue Derivatives against pigmented Melanoma Cell Lines. *J Chemotherapy* **12** (1): 94-104

Increased cytotoxicity and phototoxicity in the methylene blue series via chromophore methylation

Mark Wainwright^{a,*}, David A. Phoenix^b, Lesley Rice^b, Shuna M. Burrow^b, Jack Waring^b

^a Department of Chemistry, University of Central Lancashire, Preston PR1 2HE, UK

^b Department of Applied Biology, University of Central Lancashire, Preston PR1 2HE, UK

Received 21 May 1997; accepted 19 June 1997

Abstract

The cytotoxic and photodynamic activities of the commercially-available biological stains methylene blue (MB), 1,9-dimethyl MB (Taylor's Blue) and a newly synthesised compound, 1-methyl MB, were measured against the murine mammary tumour cell line, EMT-6. Both 1-methyl MB and 1,9-dimethyl MB exhibited increased dark toxicity with concomitant higher phototoxicity compared to MB at a light dose of 7.2 J cm^{-2} . While increasing the light dose as a function of the fluence rate increased the photocytotoxicity of MB, this had little effect on the methylated derivatives. *In vitro* chemical testing proved that successive methylation rendered the phenothiazinium chromophore both more resistant to reduction to its inactive leuco form, and also led to increased levels of singlet-oxygen production, thus providing a possible explanation for the increased toxicities of the methylated derivatives. Comparisons are made with the benzo[*a*]phenothiazinium photosensitizer, EtNBS. © 1997 Elsevier Science S.A.

Keywords: Methylene blue; Phenothiazinium photosensitizers; Phototoxicity; Dark toxicity

1. Introduction

Since the modern development of photodynamic therapy has its foundations in porphyrin-derived drugs, there has been comparatively little interest shown in other compounds such as commercial dyes [1]. Many cationic dyes were tested *in vivo* against animal tumours in the 1940s and exhibited cytotoxic effects [2,3]. Dyes such as methylene blue (MB) have also received widespread use in vital staining [4]. This, coupled with its use as a commercially-available photosensitizer in chemical reactions, led to the testing of MB against various cell lines as a possible candidate for the photodynamic therapy of cancer [5,6]. The photochemistry of the phenothiazinium nucleus has been investigated extensively by several groups, particularly in the area of nucleic acid–MB interactions [7]. On illumination, intercalated MB is known to cause the formation of oxidised guanine residues, notably 8-hydroxyguanosine, via the intermediacy of singlet oxygen.

Abbreviations: MB, methylene blue; LMB, leuco methylene blue; MMB, 1-methyl methylene blue; DMMB, 1,9-dimethyl methylene blue; DPIBF, 1,3-diphenylisobenzofuran; DMSO, dimethyl sulfoxide; EtNBS, 5-ethylamino-9-diethylaminobenzo[*a*]phenothiazinium chloride; MTT, 3-[4,5-dimethylthiazol-2-yl]-2,5-diphenyl-2H-tetrazolium bromide; PBS, phosphate buffered saline

* Corresponding author. E-mail: M.Wainwright@UCLAN.ac.uk

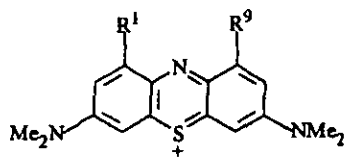
Recent research has also suggested the involvement of MB-induced microtubular photodamage in cell death [8]. In a related area, MB is employed in the eradication of viruses such as HIV from donated blood [9].

In terms of its photodynamic action in clinical malignancy, MB is utilised locally, mainly against accessible tumours such as superficial bladder cancer [10]. Recently, the use of MB has also been reported against inoperable oesophageal tumours [11].

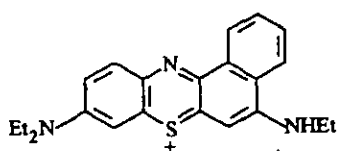
Once in the biological milieu, the metabolism of MB usually occurs via the reduction of the cation to the neutral leucobase (LMB) by standard redox systems [12]. The difference in pK_a of the two forms is sufficient to cause a considerable decrease in DNA binding affinity. Thus MB is cationic at physiological pH, whereas LMB has a pK_a of 5.8, resulting in only 33% protonation. In addition, LMB in either its neutral or its protonated form absorbs only in the ultraviolet region, thus exhibiting negligible photodynamic activity in the therapeutic window (600–900 nm).

Regarding its physicochemical properties, methylene blue is hydrophilic and this determines many aspects of its pharmacology and its intracellular localisation. Because of the presence of dimethylamino groups at positions 3 and 7 (Table 1), MB is normally present as a cation under physiological conditions, unlike other commercially available

Table 1
Physicochemical data for the photosensitizers



	R ¹	R ⁹	λ_{\max} (nm) ^a	Log ϵ_{\max} ^a	Φ_{Δ} ^b	Log <i>P</i> ^c
MB	H	H	656	4.98	0.443	-0.1 ^c
MMB	Me	H	656	4.78	0.491	+0.7
DMMB	Me	Me	650	4.91	0.536	+1.0
EtNBS	-	-	652	4.84	0.025	+2.76



EtNBS

^a Measured in methanol

^b Singlet oxygen quantum yield based on the value for MB given in Ref. [19].

^c Ref. [17] gives Log *P* = 0.

phenothiazinium dyes such as toluidine blue O and new methylene blue N. These dyes contain primary and secondary amino functionality respectively which can lead to the formation of neutral quinoneimines by deprotonation, thus allowing a greater variety of pharmacologically-active species. It is thus unwise to compare these dyes directly, in terms of biological activity, with true derivatives of methylene blue since, because of the presence of the two tertiary amino groups, these are unable to form quinoneimines.

Novel derivatives of methylene blue are scarce, arising mainly from changes in the identity of the amino substituents at positions 3 and 7 of the phenothiazine ring [13–15], although a pentacyclic analogue derived from a substituted tetrahydroquinoline has been prepared and investigated in rats [16]. Commercial MB derivatives are available which have substituents in alternative positions in the ring, e.g. methylene green (4-nitro MB) or Taylor's Blue (1,9-dimethyl MB) which has been used as a metachromatic stain. There is no available literature on the effect of such substitution on the tumour-localising or photosensitizing abilities of the resulting compounds to enable quantitative structure-activity relationships to be derived, although such studies have been carried out on a series of benzo[*a*]phenothiazinium analogues [17].

In the present study, the known biological stains methylene blue and 1,9-dimethyl methylene blue (Taylor's Blue) have been examined, together with a newly-synthesised compound linking these two, 1-methyl methylene blue, in order to investigate the effect on tumour cell toxicity of simple alkylation of the phenothiazinium chromophore. In this way, it was

intended that the weak electron-releasing effect of the methyl group(s) would inhibit the cellular reduction of the chromophore, thus allowing a stronger photosensitizing effect to be exerted.

2. Materials and methods

2.1. Reagents

1,3-Diphenylisobenzofuran (DPIBF), methanol (spectrophotometric grade) and 1-octanol were purchased from Aldrich (Gillingham, UK) and used without further purification. Trypsin, MTT (3-[4,5-dimethylthiazol-2-yl]-2,5-diphenyl-2*H*-tetrazolium bromide) and DMSO (dimethyl sulfoxide) were obtained from Sigma (Poole, UK). All spectrophotometric measurements were carried out on a Hewlett Packard 8452A diode array spectrophotometer. The dyes were found to obey Beer's law in the concentration range 10^{-5} to 10^{-7} M. In addition, the absorption spectra showed no change in the pH range 1–8.

2.2. Photosensitizers

Methylene blue and 1,9-dimethyl methylene blue were purchased from Aldrich and were recrystallised from methanol prior to use. 1-Methyl methylene blue was synthesised from *N,N*-dimethylaniline and 3-(dimethylamino)toluene (both Aldrich) using the oxidative method as described by Fierz-David [18]. The purity of the photosensitizers was ensured by thin layer chromatography (silica gel, eluent methanol/chloroform/acetic acid, 85:10:5). The purity of 1-methyl methylene blue was further examined by high performance liquid chromatography: a 3.3 cm Perkin-Elmer RPC-18 short column was employed with 10% (v/v) methanol/water as the mobile phase. This gave a single peak with the same retention time (0.30 min) when monitored at either 656 nm or 290 nm. Proton magnetic resonance spectroscopy (Bruker WM250) gave the following peaks in D₂O: δ_{H} (ppm) 1.8 (3H, s, CH₃-Ar), 2.7 (12H, s [CH₃]₂N), 6.2–6.9 (5H, m, Ar-H).

2.3. Singlet oxygen production

The three photosensitizers were assayed for efficiency of singlet oxygen production using the decolourisation of 1,3-diphenylisobenzofuran (DPIBF) in methanol. Thus the decrease in absorption at 410 nm was monitored spectrophotometrically with time as in the method of Cincotta et al. [19]. The singlet oxygen yield for MB ($\Phi_{\Delta\text{MB}}$) is given as 0.443 [19]. By assuming that the decrease in absorption of DPIBF at 410 nm is directly proportional to its reaction with singlet oxygen, the time for a 50% decrease in absorption caused by each of the photosensitizers under identical conditions ($t_{1/2\text{MBD}}$) thus gives a measure of its photosensitizing efficiency. Thus, the time for the DPIBF absorption to

decrease by 50% due to MB photosensitization ($t_{1/2MB}$) was taken as 1.0. To calculate the singlet oxygen yield for the methylated methylene blue derivatives ($\Phi_{\Delta MBD}$), the following formula was used:

$$\Phi_{\Delta MBD} = \Phi_{\Delta MB} \cdot \frac{t_{1/2MB}}{t_{1/2MBD}}$$

2.4. Log *P*

The lipophilicities of the photosensitizers were calculated in terms of log *P*, the logarithm of their partition coefficients between phosphate-buffered saline and 1-octanol. The data were calculated using the standard spectrophotometric method [20] based on the relationship:

$$\log P = \log \left\{ \frac{(A - A') \cdot V_w}{A' \cdot V_o} \right\}$$

where *A* and *A'* are the absorption intensities before and after partitioning, respectively, and *V_w* and *V_o* are the respective volumes of the aqueous and 1-octanol phases. Determinations were repeated five times.

2.5. Cell culture

The murine mammary tumour cell line (EMT-6) was originally obtained from Zeneca Pharmaceuticals (Macclesfield, Cheshire). Cultures were routinely maintained at 37°C, 5% CO₂:95% air in RPMI 1640 culture medium (Gibco, Life Technologies, Paisley, UK), supplemented with 10% (v/v) foetal calf serum (M.B. Meldrum Ltd., Bourne End, Bucks, UK), 200 mM glutamine (Sigma) and streptomycin (10 000 μg ml⁻¹)/penicillin (10 000 units ml⁻¹) (Sigma).

2.6. Phototoxicity: dark toxicity experiments

Light from a radial bank of fluorescent tubes (Phillips/Thorn, 8 W), with maximum emission in the 600–700 nm region which provided a fluence rate of 4 mW cm⁻² was used to illuminate the cells which had been exposed to the various photosensitizers. The light dose was measured with a Skye SKP 200 light meter (Skye Instruments Ltd). The temperature of the system was monitored constantly during irradiation but no heating effect was observed.

96 well microtitre plates were seeded with 1000 cells per well (in 200 μl RPMI 1640) and incubated at 37°C, 5% CO₂:95% air for 2 days. Varying concentrations of each dye (0–160 μM) were added and the cells incubated, as previously, for 3 h. The medium containing the drug was then aspirated and the cells rinsed with 200 μl RPMI 1640, before replacing with a further 200 μl RPMI 1640. Each plate was illuminated for 30 min or kept dark. Following this treatment, the cells were grown on again at 37°C, 5% CO₂:95% air for a further 3 days. To evaluate cell viability and thus calculate percentage toxicity, the MTT assay was adapted from Car-

michael et al. [21]. 25 μl MTT (5 mg ml⁻¹) was added to each well and this was incubated at 37°C, 5% CO₂:95% air, for 5 h. The medium and MTT were aspirated, taking care not to disturb the formazan crystals, leaving approximately 30 μl in each well. 200 μl DMSO were then added to each well to solubilise the crystals. The plates were shaken for 10 min and the absorbance read on a plate reader (Anthos HT111, measuring filter, 540 nm; reference filter, 620 nm).

2.7. Light dose study

EMT-6 cells were seeded into 35 mm petri dishes (1000 cells per ml in 2 ml of cell suspension), then grown for two days in RPMI 1640 medium whilst being maintained at 37°C, 5% CO₂:95% air. After two days, the medium was removed and replaced by 2 ml of either 12 μM MB, 2.5 μM MMB or 0.2 μM DMMB in RPMI 1640 (i.e. the doses giving 5% dark toxicity), with each experiment being carried out in triplicate. The cells were incubated in the presence of drug for a further 3 h. The medium and drug were then removed, the cells rinsed with 2 ml of RPMI 1640 and finally 2 ml of medium replaced. The cells were illuminated with a fluence rate of either 9.8 mW cm⁻², 4.7 mW cm⁻², 3.3 mW cm⁻² or 2.0 mW cm⁻² for 30 min (i.e. light dose = 17.6, 8.5, 5.9 or 3.6 J cm⁻² respectively), then grown as above for a further 3 days. The cells in each petri dish were then counted microscopically using the improved Neubauer haemocytometer.

3. Results and discussion

Relevant data concerning the physicochemical properties of MB, MMB and DMMB are given in Table 1. One effect of successive methylation on the methylene blue parent molecule was to increase the lipophilicity. This was expected, since the non-polar character of the methyl group is well established. Indeed Hansch and Leo give a guideline figure for log *P* supplement of +0.65 for the addition of a -CH₂- unit [22]. DMMB exhibited a small hypsochromic shift in long wavelength absorption compared to that of MB and MMB, and both of the methylated derivatives had slightly decreased intensities. However, the three photosensitizers absorb strongly in the 'therapeutic window' for PDT. In addition the methylated derivatives showed increased singlet oxygen yields in the *in vitro* oxidation of DPIBF (Table 2).

Table 2
Relative rates of photosensitized oxidation of DPIBF by MB, MMB and DMMB in methanol at 279 K, measured as the decrease in absorption at 410 nm to half of its original value

	Relative $t_{1/2}$ for A_{410}
MB	1
MMB	0.90
DMMB	0.83

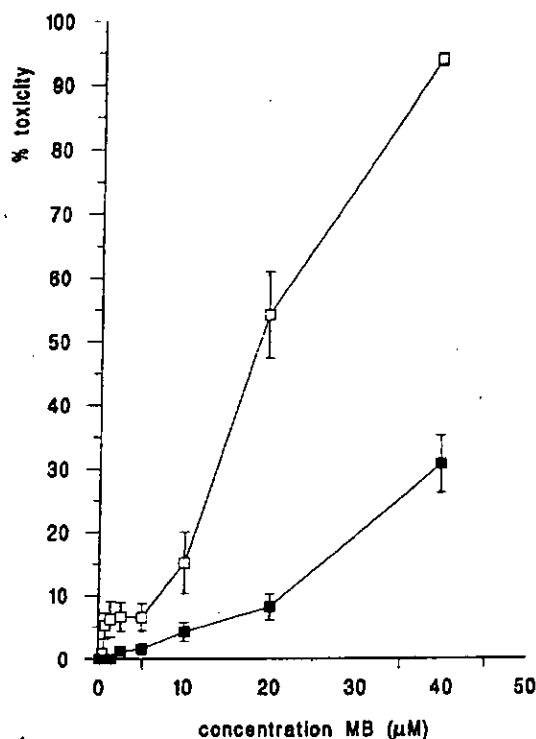


Fig. 1. Photocytotoxicity (□) and dark toxicity (■) of MB against the EMT-6 cell line. Each point is the mean of at least 14 experiments. Error bars represent SEMs.

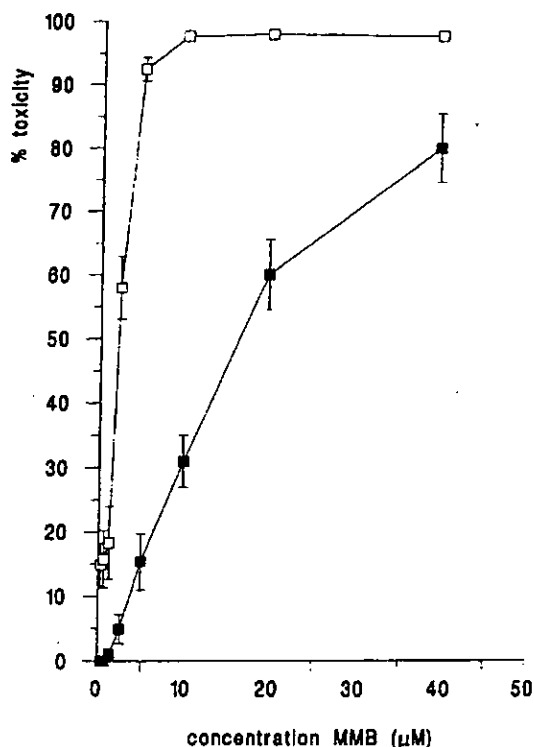


Fig. 2. Photocytotoxicity (□) and dark toxicity (■) of MMB against the EMT-6 cell line. Each point is the mean of at least nine experiments. Error bars represent SEMs.

3.1. Dark toxicity/phototoxicity

The methylated derivatives were more toxic against EMT-6 cells under dark conditions than MB (Figs. 1-3). At 7.2 J cm^{-2} the associated phototoxic effects were also far greater, unsurprisingly in view of the increased Φ_{Δ} values obtained for the methylated derivatives (Table 1). In terms of clinical application, the greater the ratio of light:dark toxicity, the more beneficial the photosensitizer. The IC_{50} for methylene blue at this light dose was $18.7 \mu\text{M}$ (Table 3), with a corresponding dark toxicity of 7.9%. Thus the toxicity ratio (light:dark) here was $50:7.9 = 6.3$. The corresponding values for MMB and DMMB are 11.9 and 17.2 respectively (Table 3). In the authors' opinion, IC_{90} gives a more useful clinical indication. For example, the IC_{90} value for DMMB

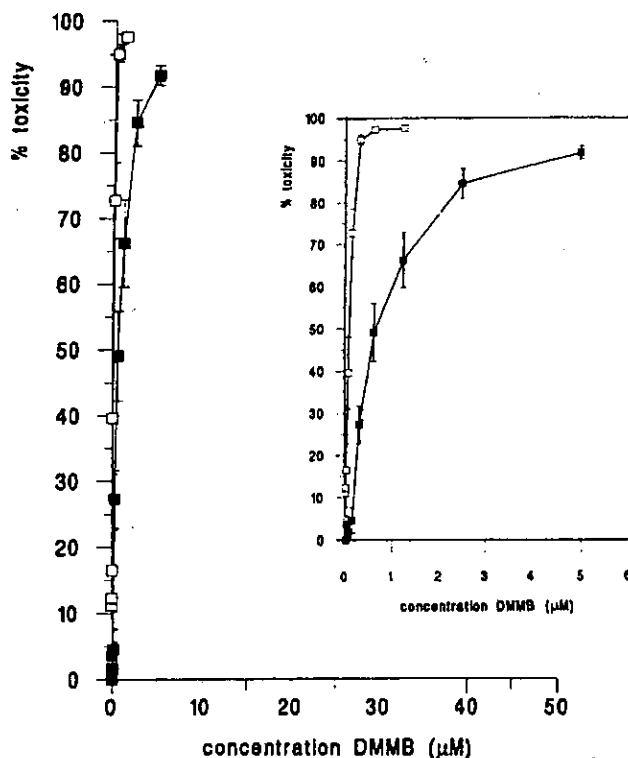


Fig. 3. Photocytotoxicity (□) and dark toxicity (■) of DMMB against the EMT-6 cell line. Each point is the mean of at least eight experiments. Error bars represent SEMs. Insert shows enlargement of responses at low levels.

Table 3

Toxicity data and light:dark ratios for methylene blue and its methylated analogues at a light dose of 7.2 J cm^{-2}

	Dose (μM)	% Light toxicity	% Dark toxicity	Light:dark toxicity
MB	18.7	50	7.9	6.3
MMB	2.20	50	4.2	11.9
DMMB	0.09	50	2.9	17.2
MB	37.7	90	27.9	3.2
MMB	4.80	90	14.2	6.3
DMMB	0.27	90	21.3	4.2

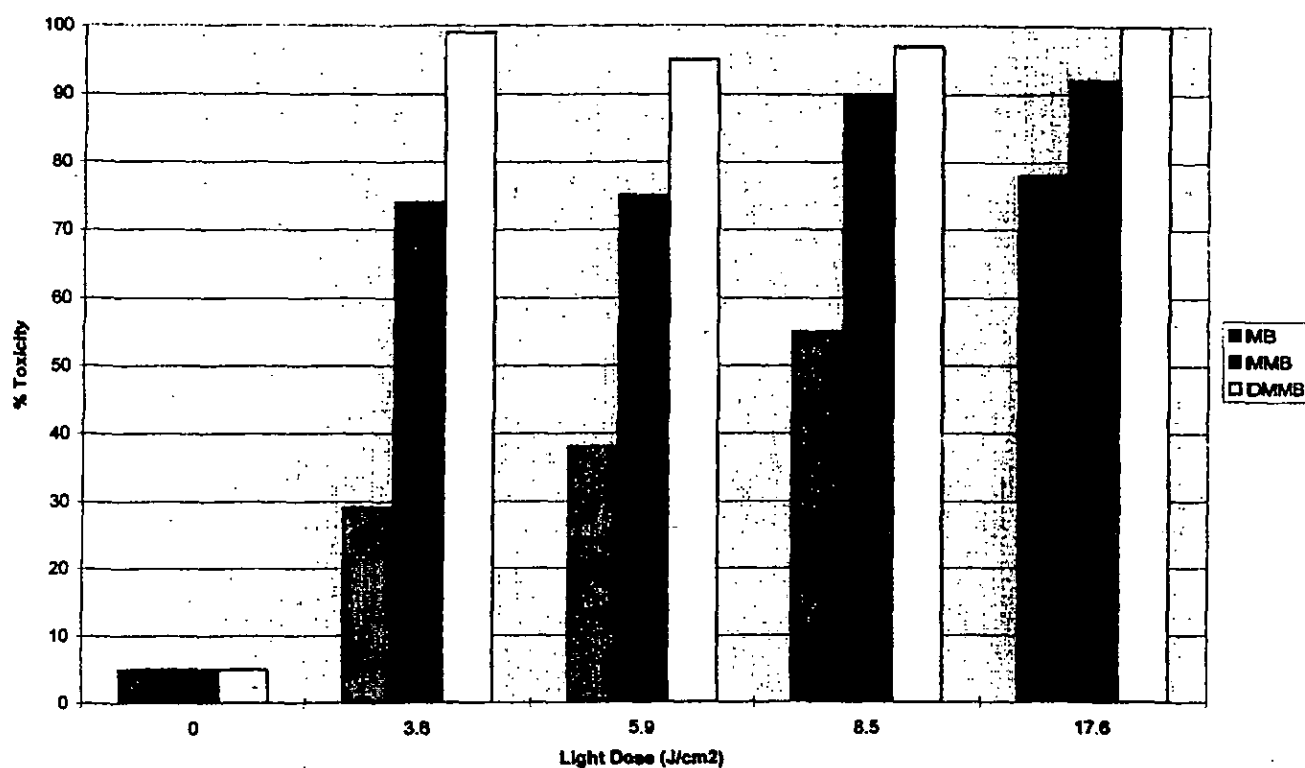


Fig. 4. Photocytotoxicity of the methylene blue derivatives against the EMT-6 cell line as a function of the light dose. Photosensitizer concentration in each case was that giving 5% dark cytotoxicity. Each bar is a mean of ≥ 9 experiments.

on illumination at 7.2 J cm^{-2} is $0.27 \mu\text{M}$, and at this concentration the dark toxicity corresponded to a cell kill of 21.3%, giving a ratio of 4.2. The corresponding ratios for MMB and MB were 6.3 and 3.2 respectively.

The IC_{50} values for the MB derivatives (Table 3) are similar to those exhibited by the benzo[*a*]phenothiazinium compounds investigated by Cincotta et al. [23]. For example, against EMT-6 cells, the promising photosensitizer EtNBS (Table 1) gave an IC_{50} of $0.1 \mu\text{M}$. This is comparable with the value of $0.09 \mu\text{M}$ obtained in the present work for DMMB. Moreover, DMMB gave $>90\%$ photocytotoxicity at a concentration of $0.2 \mu\text{M}$ and a light dose of 3.6 J cm^{-2} (Fig. 4) which is comparable to the 3.3 J cm^{-2} employed with EtNBS. Although the dark toxicity for EtNBS is reportedly much lower for a $0.5 \mu\text{M}$ dose (6% compared to 41% for DMMB), no IC_{90} figure was reported for the phototoxicity [23].

The light dose study alluded to above was carried out at photosensitizer concentrations giving 5% dark toxicity (Fig. 4). At this concentration, MB did not reach 100% phototoxicity even at the highest light dose used (17.6 J cm^{-2}). This was, however, considerably less than that used by Canete et al. who reported $\approx 100\%$ cell death in HeLa cells at 90 J cm^{-2} with $10 \mu\text{M}$ MB [24]. The methylated derivatives were already close to 100% photocytotoxicity at the original light dose used and concentrations giving 5% dark toxicity, so the increased light dose made little improvement on the phototoxicity in these cases. However, it was noticeable that the phototoxicity of 1-methyl methylene blue decreased slightly

at light doses $<7.2 \text{ J cm}^{-2}$ (Fig. 4). In terms of the light:dark toxicity differential, this was greatest (78:5 = 15.6) for MB at the highest light dose used (17.6 J cm^{-2}). The ratio for the monomethylated derivative approached 20 at the maximum light dose, whilst that for DMMB was ≈ 20 across the light dose range. A maximum ratio of 20 (light:dark toxicity) may therefore be possible for MB at further increased light doses.

The higher dark toxicities and phototoxicities of the methylated derivatives may be explained by several factors.

As mentioned earlier, it is apparent from the literature that phenothiazinium photosensitizers and their benzologues are prone to cellular reduction. Indeed this may be advantageous in the clinic as the rate of reduction of EtNBS in mice is reportedly higher in healthy tissue than in tumours, thus increasing the apparent tumour selectivity and decreasing the probability of skin photosensitization [25]. The *in vitro* reduction of MB, MMB and DMMB has been examined in aqueous media using a gold microdisc electrode using the method of Svetlicec et al. [26] (data not shown). The rates of reduction of the three photosensitizers followed the order: MB > MMB > DMMB.

Thus, from a cellular point of view, it can be argued that both MMB and DMMB will be present in their oxidised (cationic) forms for a longer period of time than MB, and therefore that there will be higher concentrations of the photoactive form of the methylated derivatives present. The increased stability to reduction, at least in the *in vitro* electrochemical system used, may be explained by the weak elec-

tron-releasing effect of the methyl groups. This would make the chromophore more electron rich and thus less amenable to reduction. In cell culture this could contribute to the increased levels both of dark toxicity and phototoxicity exhibited by the methylated derivatives.

Methylation of the phenothiazinium chromophore resulted in considerable increases in the lipophilicity of the system. Both MMB and DMMB have positive log *P* values, whereas that for MB is negative. It has been shown previously in fibroblasts that vital stains bearing a unipositive charge and having $0 < \log P < 5$ tend to localise in the mitochondria [27]. Methylene blue is thought to localise mainly in the cell nucleus [7,28–30]. This could indicate that a different cellular localisation pattern for the methylated derivatives is responsible for their greater observed cytotoxicities. Increased levels of photosensitizers in the cell due to lower reduction rates could also explain the higher dark toxicities associated with the methylated derivatives.

The standard DPIBF oxidation test showed that methylation of MB increases the efficiency of singlet oxygen production (Tables 1 and 2). Taken with the increased resistance to reduction and the possibility of more critical intracellular localisation, this may explain the greater phototoxicity of the methylated derivatives against EMT-6 cells relative to that of MB. Additionally, the phototoxicity of MB was increased by increasing the fluence rate of the light source. It is also interesting to note the much greater singlet oxygen efficiencies (approximately 20-fold) of the methylene blue derivatives used in the present study compared to that of the benzo[*a*]phenothiazinium derivative, EtNBS (Table 1).

It is not profitable to include ionisation data for MB and its methylated analogues as each is fully ionised in the pH range 1–8. Such behaviour separates the current range of compounds from other phenothiazinium photosensitizers, such as toluidine blue O, and the benzo[*a*]phenothiaziniums, such as EtNBS (Table 1). Here each structure contains a conjugated primary or secondary amino group, which allows deprotonation to the neutral quinoneimine species. The presence of the neutral species as part of an equilibrium may have important ramifications in terms of *in vitro* uptake and *in vivo* pharmacology. In this respect, the presence of the tertiary dimethylamino groups in positions 3 and 7 of the phenothiazine ring system makes the MB system somewhat simpler.

4. Conclusions

We have shown that, at a light dose of 7.2 J cm^{-2} , the methylation of the established photosensitizer, methylene blue, in position 1 and/or position 9 of the phenothiazinium chromophore leads to increased photocytotoxicity in the murine mammary tumour cell line, EMT-6 compared to that of MB itself. The ratios for light:dark toxicity were also higher at lower light doses for the methylated derivatives and their levels of phototoxicity are comparable to that of the benzo[*a*]phenothiazinium photosensitizer, EtNBS.

Although chromophore methylation gave no change in the degree of ionisation ($\text{p}K_{\text{a}}$) of the system, it did lead to increased lipophilicity, suggesting both potentially different intracellular localisation and different uptakes for the derivatives. Both the resistance to reduction of the chromophores and the singlet oxygen efficiencies were higher in the methylated derivatives. On cellular uptake, the lower reduction rates are expected to give higher viable concentrations of the methylated photosensitizers, and taken with the higher singlet oxygen efficiencies, this provides a feasible explanation for the much improved phototoxicities encountered, relative to methylene blue. The lower reduction rates, together with potential variation in intracellular localisation and uptake may also explain the increased dark toxicities of the methylated derivatives.

References

- [1] M. Wainwright, Non-porphyrin photosensitizers in biomedicine, *Chem. Soc. Rev.*, 25 (1996) 351–359.
- [2] M.R. Lewis, N.A. Sloviter, P.P. Goland, *In vivo* staining and retardation of sarcomata in mice, *Anat. Rec.*, 95 (1946) 89–96.
- [3] J.F. Riley, Retardation of growth of a transplantable carcinoma in mice fed basic metachromatic dyes, *Cancer Res.*, 8 (1948) 183–188.
- [4] T.A. Creagh, M. Gleeson, D. Travis, R. Grainger, T.E.D. M'Dermott, M.R. Butler, Is there a role for *in vivo* methylene blue staining in the prediction of bladder tumour recurrence? *Br. J. Urol.*, 75 (1995) 477–479.
- [5] G.J.S. Fowler, R.C. Rees, R. Devonshire, The photokilling of bladder carcinoma cells *in vitro* by phenothiazine dyes, *Photochem. Photobiol.*, 52 (1990) 489–494.
- [6] K. Koenig, V. Bockhorn, W. Dietel, H. Schubert, Photochemotherapy of animal tumours with the photosensitizer methylene blue using a krypton laser, *J. Cancer Res. Clin. Oncol.*, 113 (1987) 301–303.
- [7] E.M. Tuite, J.M. Kelly, Photochemical reactions of methylene blue and analogues with DNA and other biological substrates *J. Photochem. Photobiol. B*, 21 (1993) 103–124.
- [8] J.C. Stockert, A. Juarranz, A. Villanueva, M. Cañete, Photodynamic damage to HeLa cell microtubules induced by thiazine dyes, *Cancer Chemother. Pharmacol.*, 39 (1996) 167–169.
- [9] T. Zeiler, H. Riess, G. Wittmann, G. Hintz, R. Zimmerman, C. Muller, H.G. Heuft, D. Huhn, The effect of methylene blue phototreatment on plasma proteins and *in vitro* coagulation capability of single-donor fresh-frozen plasma, *Transfusion*, 34 (1994) 685–689.
- [10] J.L. Williams, J. Stamp, R. Devonshire, G.J.S. Fowler, Methylene Blue and the photodynamic therapy of superficial bladder cancer, *J. Photochem. Photobiol. B*, 4 (1989) 229–232.
- [11] K. Orth, A. Ruck, A. Stanescu, H.G. Beger, Intraluminal treatment of inoperable oesophageal tumours by intraluminal photodynamic therapy with Methylene Blue, *Lancet*, 345 (1995) 519–520.
- [12] R.D. Bongard, M.P. Merker, R. Shundo, Y. Okamoto, D.L. Roerig, J.H. Linehan, C.A. Dawson, Reduction of thiazine dyes by bovine arterial endothelial cells in culture, *Am. J. Physiol.*, 269 (1995) L78–L84.
- [13] M. Motsenbocker, H. Masuya, H. Shimazu, T. Miyawaki, Y. Ichimori, T. Sugawara, Photoactive Methylene Blue dye derivatives suitable for coupling to protein, *Photochem. Photobiol.*, 58 (1993) 648–652.
- [14] L. Strekowski, D.F. Hou, R.L. Wydra, R.F. Schinazi, A synthetic route to 3-(dialkylamino)phenothiazin-5-ium salts and 3,7-disubstituted derivatives containing two different amino groups, *J. Heterocyclic Chem.*, 30 (1993) 1693–1696.

- [15] D. Creed, W.C. Burton, N.C. Fawcett, Ground and excited state properties of some new highly water soluble *N*-substituted thiazine dyes for photogalvanic applications, *J. Chem. Soc., Chem. Commun.* (1983) 1521–1523.
- [16] Q.A. Peng, S.B. Brown, J. Moan, J.M. Nesland, M. Wainwright, J. Griffiths, B. Dixon, J. Cruse Sawyer, D. Vernon, Biodistribution of a Methylene Blue derivative in tumors and normal tissues of rats, *J. Photochem. Photobiol. B Biol.*, 20 (1993) 63–71.
- [17] L. Cincotta, J.W. Foley, A.H. Cincotta, Novel phenothiazinium photosensitizers for photodynamic therapy, *SPIE Proc.*, 997 (1988) 145–153.
- [18] H.E. Fierz-David, L. Blangey, *Fundamental Processes in Dye Chemistry*, Interscience, New York, 1949, pp. 311–313.
- [19] L. Cincotta, J.W. Foley, A.H. Cincotta, Novel red absorbing benzo-*[a]*phenoxazinium and benzo-*[a]*phenothiazinium photosensitizers: *in vitro* evaluation, *Photochem. Photobiol.*, 46 (1987) 751–758.
- [20] J. Pooler, D.P. Valenzano, Physicochemical determinants of the sensitizing effectiveness for photooxidation of nerve membranes by fluorescein derivatives, *Photochem. Photobiol.*, 30 (1979) 491–498.
- [21] J. Carmichael, W.G. DeGraff, A.F. Gazdar, J.D. Minna, J.B. Mitchell, Evaluation of a tetrazolium-based semiautomated colourimetric assay: assessment of chemosensitivity testing, *Cancer Res.*, 47 (1987) 936–942.
- [22] C. Hansch, A. Leo, *Substituent Constants for Correlation Analysis in Chemistry and Biology*, Wiley, New York, 1979, pp. 18–43.
- [23] L. Cincotta, J.W. Foley, A.H. Cincotta, Phototoxicity, redox behaviour and pharmacokinetics of benzophenoxazine analogues in EMT-6 murine sarcoma cells, *Cancer Res.*, 53 (1993) 2571–2580.
- [24] M. Cañete, A. Villanueva, A. Juarranz, Uptake and photoeffectiveness of two thiazines in HeLa cells, *Anti-Cancer Drug Design*, 8 (1993) 471–477.
- [25] L. Cincotta, J.W. Foley, T. MacEachern, E. Lampros, A.H. Cincotta, Novel photodynamic effects of a benzophenothiazine on two different murine sarcomas, *Cancer Res.*, 54 (1994) 1249–1258.
- [26] V. Svetlicic, V. Zutic, J. Clavilier, J. Chevalet, Organic monolayer formation at a sulphur modified gold electrode, *J. Electroanal. Chem.*, 233 (1987) 199–210.
- [27] F. Rashid, R.W. Horobin, Interactions of molecular probes with living cells and tissues. 2. A structure–activity analysis of mitochondrial staining by cationic probes, and a discussion of the synergistic nature of image-based and biochemical approaches, *Histochemistry*, 94 (1990) 303–308.
- [28] D.S. Yu, S.Y. Chang, C.P. Ma, Photoinactivation of bladder tumor cells by methylene blue: study of a variety of tumor and normal cells, *J. Urol.* 144 (1990) 164–168.
- [29] D.S. Yu, S.Y. Chang, C.P. Ma, Ultrastructural changes of bladder cancer cells following methylene blue-sensitized photodynamic treatment, *Eur. J. Urol.*, 19 (1991) 322–327.
- [30] D.S. Yu, S.Y. Chang, C.P. Ma, The effect of methylene blue-sensitized photodynamic treatment on bladder cancer cells: a further study on flow cytometric basis, *J. Urol.*, 149 (1993) 1198–1204.

Phenothiazine Photosensitizers. III.¹

Activity of Methylene Blue Derivatives against Pigmented Melanoma Cell Lines

L. RICE - M. WAINWRIGHT* - D.A. PHOENIX

Photochemotherapy Group, Dept of Applied Biology, University of Central Lancashire, Preston PR1 2HE UK

*Author for correspondence: m.wainwright@uclan.ac.uk

Summary

The cytotoxicity and photocytotoxicity of methylene blue and several of its derivatives against two pigmented melanoma cell lines (SK-23 murine melanoma and SK-Mel 28 human melanoma) were investigated in culture. The derivatives were all more effective photosensitizers than methylene blue in both cell lines over a range of light doses (3.6-17.6 J cm⁻²). The increased activity correlated with increased cellular uptake and inherent photosensitizing efficacy. The photosensitizers also showed varying levels of interaction with the biopolymer melanin and although this appeared to affect uptake and activity, there was no direct correlation with toxicity.

Key words: Methylene blue derivatives, photosensitizers, photosensitization, melanin, melanoma.

Abbreviations: MB - methylene blue; LMB - leuco methylene blue; MMB - 1-methyl methylene blue; DMMB - 1,9-dimethyl methylene blue; NMB - new methylene blue; DPIBF - 1,3-diphenylisobenzofuran; DMSO - dimethyl sulfoxide; IC_n - photosensitizer concentration giving n% cell inhibition; MTT - 3-[4,5-dimethylthiazol-2-yl]-2,5-diphenyl-2H-tetrazolium bromide; PBS - phosphate buffered saline.

INTRODUCTION

Among the various types of skin cancer, malignant melanoma poses the greatest risk in terms of mortality. The usual treatment for malignant melanoma is surgical excision but adjuvant chemotherapy may be employed, par-

ticularly dacarbazine (DTIC)² or limb perfusion involving the nitrogen mustards (e.g. melphalan)³. Radiotherapy is also an option. Depending on the progress of the tumour at diagnosis, lymphadenectomy may be indicated although a more conservative approach to dissection may be possible via the use of sentinel

node demarcation⁴. With the traditional therapies there remains the problem of side effects, either due to disfigurement in surgery or to systemic toxicity, immunosuppression etc. after chemotherapy or radiotherapy. Both in terms of morbidity and in patient compliance the minimisation of such side effects is obviously highly desirable. However, even with the increased sophistication of modern cancer treatments, the degree of further improvement of these therapies is limited, mainly due to a fundamental lack of selectivity for tumour tissue. The ongoing search for new drugs and novel therapeutic approaches to cancer treatment which offer greater selectivity thus remains important.

The technique of photodynamic therapy (PDT) is gaining increasing acceptance in cancer treatment, particularly in the area of skin cancer, since here light delivery is not problematic as it might be in the case of internal tumours. The use of either systemic or topical administration of a photosensitizer (or photosensitizer precursor) coupled with superficial light delivery has been shown to be successful in many cases of basal cell and squamous cell carcinoma.⁵ The situation is complicated in the case of metastasising tumours such as malignant melanoma since it may be difficult to trace the secondary foci. Another perceived problem with melanoma is the presence of the pigment melanin in the tumour cells. Melanin is produced in cells which require protection from light (especially ultraviolet) and since melanin absorbs light quite strongly even at long visible wavelengths,⁶ this might decrease the amount of light available to the photosensitizer. In addition, melanin has antioxidant properties⁷ which might interfere with the cell killing processes involving oxygen radicals which are commonly associated with PDT. Such protective effects have been reported against hydrogen peroxide and hydroxyl radicals during Rose Bengal photosensitization (i.e. Type I photosensitization),⁸ whilst the perylenequinone hypericin exhibited significantly higher phototoxicity against amelanotic melanoma cell lines than against a melanin producing melanoma cell line⁹. In order to circumvent any likely effects of melanin, the use of long-wavelength absorbing photosensitizers - i.e. outside the absorption spectrum of melanin - is a logical initial step. Thus benzoporphyrin derivative (BPD-MA) is

reported to be effective *in vivo* against pigmented melanoma in mice, the efficacy being increased by pre-illumination with 1064 nm (near infrared) light in order selectively to break down melanosomes¹⁰. The use of long-wavelength absorbing photosensitizers alone may be insufficient to cause cell death - for example, far-red absorbing (776 nm) silicon naphthalocyanine derivatives were also less effective against melanotic than amelanotic melanoma cell lines¹¹.

The use of methylene blue and its congeners in clinical PDT remains sporadic, mainly because photodynamic therapy has developed from porphyrin-derived drugs¹². Logically, the widespread application of methylene blue and the related phenothiazinium dye toluidine blue O in surgical demarcation - e.g. the tracing of sentinel lymph nodes⁴ in addition to their widespread use in the clinical staining of carcinomata¹³ underlines the low toxicity of the compounds. The efficient photosensitizing behaviour of the phenothiazinium dyes is also well established¹⁴. However, in terms of its use in clinical malignancy, methylene blue is utilised locally, mainly against accessible tumours such as superficial bladder cancer¹⁵ and has been used against inoperable oesophageal tumours¹⁶. Along with many drugs containing fused heteroaromatic chromophores, methylene blue is well known to bind to melanin,^{17,18} and in recent work, Link *et al.* reported the use of radiolabelled methylene blue as a tracer for metastatic melanoma in humans¹⁹.

The authors recently reported the increased efficacy of methylene blue derivatives having increased chromophore methylation²⁰. Thus the two analogues, having methyl groups at positions 1- and/or 9- of the phenothiazinium chromophore, both exhibited increased photosensitizing activities due to increased efficacies of singlet oxygen production, and lower rates of intracellular chromophoric reduction relative to the parent compound. In subsequent work on the photobactericidal activities of phenothiazinium species, the related photosensitizer new methylene blue N (NMB) exhibited similar improvements over the parent compound against methicillin-resistant *Staphylococcus aureus*²¹. NMB also contains a dimethylated phenothiazinium ring system, although the auxochromic amine functionality at positions 3- and 7- is slightly different from that of methyl-

ene blue (Table 1). In each case however, the inclusion of extra methyl groups in the chromophore also led to increased lipophilicity, a property which is often an important factor in drug uptake characteristics.

Studies on the photodynamic action of methylene blue in tumour cells in culture have reported various sites of action for the photosensitizer - for example the formation of oxidised guanine residues, notably 8-hydroxyguanosine, via the intermediacy of singlet oxygen, supports a DNA-based nuclear mechanism^{14, 22-24}. Recent research has also suggested the involvement of MB-induced microtubular photo-damage in cell death²⁵. However it may be that the site of action is variable, depending both on cell type and on the interval between photosensitizer administration and illumination.

Altering the structure of the methylene blue via analogue synthesis should lead to alternative localisation patterns, providing the resulting physicochemical make-up of the analogue is sufficiently different. For example, increased lipophilicity in monocationic dyes has been shown to alter localisation from mainly nuclear to mitochondrial²⁶.

The present study is an investigation into the activity of the phenothiazinium derivatives alluded to above against a murine melanoma cell line (SK-23) and a human melanoma cell line (SK-Mel 28).

MATERIALS AND METHODS

Methylene blue, 1,9-dimethyl methylene blue and new methylene blue were purchased from Aldrich (Gillingham, UK) and recrystallised from methanol before use. 1-Methyl methylene blue was synthesised from *N,N*-dimethyl-*m*-toluidine and *N,N*-dimethylaniline (both Aldrich) as described previously²⁰. 1,3-Diphenylisobenzofuran (DPIBF), methanol (spectrophotometric grade) and 1-octanol were purchased from Aldrich (Gillingham, UK) and used without further purification. Trypsin, MTT (3-[4,5-dimethylthiazol-2-yl]-2,5-diphenyl-2*H*-tetrazolium bromide) and DMSO (dimethyl sulfoxide) were obtained from Sigma (Poole, UK). All spectrophotometric measurements were carried out on a Hewlett Packard 8452A diode array spectrophotometer. The dyes were found to

obey Beer's law in the concentration range 10^{-5} - 10^{-7} M.

The efficiency of production of singlet oxygen of the phenothiaziniums relative to the standard, methylene blue, was measured using the decolourisation of 1,3-diphenylisobenzofuran (DPIBF) in methanol. Details of this procedure are given in the earlier paper²⁰.

The lipophilicities of the photosensitizers were calculated in terms of $\log P$, the logarithm of their partition coefficients between phosphate-buffered saline and 1-octanol. The data were calculated using the standard spectrophotometric method,²⁷ again detailed in the previous work²⁰.

Cell culture

The melanoma cell lines (murine SK-23 and human SK-Mel 28) were originally obtained from the Cancer Research Campaign. Cultures were routinely maintained at 37°C, 5% CO₂ : 95% air in RPMI 1640 culture medium (Gibco, Life Technologies, Paisley, UK), supplemented with 10% (v/v) foetal calf serum (Labtech International, Rigger, East Sussex, UK), 200 mM glutamine (Sigma) and streptomycin (10,000 µg ml⁻¹) / penicillin (10,000 units ml⁻¹) (Sigma).

Phototoxicity: dark toxicity experiments

Light from a radial bank of fluorescent tubes (Phillips/Thorn, 8 W), with maximum emission in the 600-700 nm region which provided a fluence rate of 4.0 mW cm⁻², was used to illuminate the cells which had been exposed to the various photosensitizers. The light dose was measured with a Skye SKP 200 light meter (Skye Instruments Ltd). The temperature of the system was monitored constantly during irradiation but no heating effect was observed.

96-well microtitre plates were seeded with 1000 cells per well (in 200 µl RPMI 1640) and incubated at 37°C, 5% CO₂ : 95% air for 3 days. Varying concentrations of each photosensitizer (0-160 µM) were added and the cells incubated, as previously, for 3 hours. The medium containing the drug was then aspirated and the cells rinsed twice with 200 µl RPMI 1640, before replacing with a further 200 µl RPMI 1640. Each plate was illuminated for 30 minutes or kept dark. Following this treatment,

the cells were grown again at 37°C, 5% CO₂ : 95% air for a further 4 days. To evaluate cell viability and thus calculate percentage toxicity, the MTT assay was adapted from Carmichael *et al*²⁸. 25 µl MTT (5 mg ml⁻¹) were added to each well and this was incubated at 37°C, 5% CO₂ : 95% air, for 5 hours. The medium and MTT were aspirated, taking care not to disturb the formazan crystals, leaving approximately 30 µl in each well. 100 µl DMSO were then added to each well to solubilise the crystals. The plates were shaken for 10 minutes and the absorbance read on a plate reader (Anthos HT111, measuring filter 540 nm; reference filter 620 nm).

Light dose study

SK-23 or SK-Mel 28 cells were incubated in the normal way with the relevant photosensitizer at a dose giving 15% dark toxicity in the initial toxicity test. The cells were illuminated with a fluence rate of either 9.8 mW cm⁻², 4.7 mW cm⁻², 3.3 mW cm⁻² or 2.0 mW cm⁻² for 30 minutes (i.e. light dose = 17.6, 8.5, 5.9 or 3.6 J cm⁻² respectively), then grown on as above for a further 4 days. Toxicity was assayed as above using the MTT assay.

Cellular uptake

Cultures of SK-23 and SKMEL-28 cells in 20 ml RPMI 1640 medium were grown to confluence over 5 days in 75 cm² culture flasks. The medium was then removed and replaced by doubling dilutions of each photosensitizer (0.312 - 5 µM) in 20 ml RPMI 1640 medium or by 20 ml RPMI 1640 medium for the controls. The cultures were then incubated in the presence of the photosensitizers for 3 hours.

Medium and photosensitizers were then discarded and the cell monolayers rinsed twice with PBS. The cells were trypsinised and counted, then the cell suspensions were centrifuged for 10 minutes at 150 g and the supernatants discarded. Each pellet was thus rinsed and resuspended twice in 2 ml PBS. 1 ml methanol was added to each final pellet, mixed and left for 10 minutes before centrifugation at 2000 g for 30 minutes. The absorbances of the photosensitizers in methanol solution were read spectrophotometrically at 664 nm (MB), 650 nm (MMB), 648 nm (DMMB) and 630 nm (NMB).

Melanin binding

The photosensitizers were assayed for melanin binding following the method of Potts¹⁷. Briefly, the light absorption of 5 µM solutions of the photosensitizers in buffer were measured at the relevant λ_{max} value. The solutions were then stirred vigorously with 10 µg of melanin (Sigma, Poole UK) for 15 minutes, centrifuged at 600g and the absorption of the supernatants re-read on the spectrophotometer. The percentage binding to melanin was thus calculated by difference. Measurements were carried out four times.

RESULTS AND DISCUSSION

The photosensitizers used in the present study were selected on evidence obtained in earlier work by the authors^{20,21}. In terms of their physicochemical properties, the methylated derivatives of the lead compound, methylene blue, exhibited increased lipophilicities due to the extra methyl groups (positive Log*P* values, Table 1), although each of the photosensitizers was highly water-soluble. Chromophoric methylation was also found to decrease the reduction potential of the resulting compound²⁰, the reduced (leuco-) form of the phenothiazinium being UV-absorbing only and inactive as a photosensitizer, although reoxidation to the cation is possible. Logically, the longer the time spent in the cellular milieu as a phenothiazinium cation, the greater the potential for photodynamic damage. In addition to the increased lipophilicities encountered, this suggests that the cations might also show a different localisation pattern to that of methylene blue. Chemically, the compounds methylene blue, the 1-methyl and 1,9-dimethyl derivatives are similar in constitution but in new methylene blue the presence of *N*-ethylamino instead of *N,N*-dimethylamino groups at positions 3- and 7-of the phenothiazinium chromophore facilitates deprotonation at the N-H group, leading to a neutral quinoneimine species (Figure 1). This can be shown spectrophotometrically in alcohol, the maximum absorption wavelength (λ_{max}) for the NMB cation being 630 nm at neutral pH, the quinoneimine being formed at higher pH with the λ_{max} shifting to 540 nm. Both cationic and neutral forms exist in equilib-

TABLE 1 - Structures and physicochemical data for the photosensitizers.

	R ¹	R ⁹	λ_{\max} (nm) ^a	Log ϵ_{\max} ^a	Φ_{Δ} ^b	NMB Log P ^c	% Melanin Binding
MB	H	H	664	4.98	1.00	-0.10	82.2 ^c
MMB	Me	H	656	4.78	1.11	+0.7	71.3
DMMB	Me	Me	648	4.91	1.22	+1.0	56.3
NMB	-	-	630	4.95	1.35	+1.2	69.6

^a Measured in methanol; ^b Singlet oxygen yield based on MB = 1.00; ^c Literature ¹⁷ gives 87%.

rium ([cation] \gg [quinoneimine]) at neutral pH, allowing the possibility of differing uptake mechanisms. The importance of such behaviour has been reported previously by Lin *et al.* in their studies on benzo[a]phenothiazinium photosensitizers ²⁹. Such equilibria are not formed by the other photosensitizers in the present study since the dimethylamino group does not allow deprotonation.

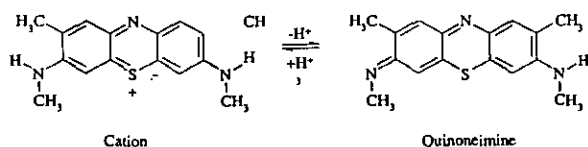


FIGURE 1 - Quinoneimine formation in new methylene blue.

As stated previously, the phenothiazinium dyes are established as efficient photosensitizing compounds. However, this efficiency is affected by the substitution pattern in the periphery of the chromophore. For example, the presence of a fused benzene ring lowers the singlet oxygen efficiency as in the benzo[a]phenothiazinium series alluded to above ²⁹ as does the inclusion of arylamino groups at positions 3- and 7- in place of alkylamino ¹. In the current study the presence of extra methyl groups in the ring-system led to increased singlet oxygen efficiencies in the spectrophotometric assay employed

(Table 1). In terms of inherent ability to photosensitize the production of singlet oxygen, as measured spectrophotometrically, the order was NMB>DMMB>MMB>MB.

At the standard light dose of 7.2 J cm⁻², each of the compounds exhibited higher photosensitizing efficacies in both melanoma cell lines compared to the lead compound, methylene blue (Figures 2 and 3). Using a series of light doses, ranging from 3.6-17.6 J cm⁻², and photosensitizer concentrations giving 15% dark toxicity in the original experiments, methylene blue was clearly the least effective photosensitizer in the human melanoma cell line (SK-Mel 28), and did not in fact achieve a complete cell kill even at the highest light dose (Table 2). As in the previous cell culture study employing the mouse mammary tumour cell line, EMT-6, dimethyl methylene blue was highly phototoxic at very low concentrations (Figures 2c and 3c). The IC₉₀ values for dimethyl methylene blue were 0.1 and 0.4 μ mol for the human and murine melanoma cell lines respectively, which were similar to that for the EMT-6 line in the previous study²⁰ and IC₉₀s were achieved at all light doses (Table 2). New methylene blue also performed well against both melanoma cell lines (SK-Mel 28 IC₉₀ = 0.5 μ mol; SK-23 IC₉₀ = 1.1 μ mol). Methyl methylene blue was less effective in SK-Mel 28 cells than both of the dimethylated photosensitizers, but was still considerably more active than methylene blue (Table 3).

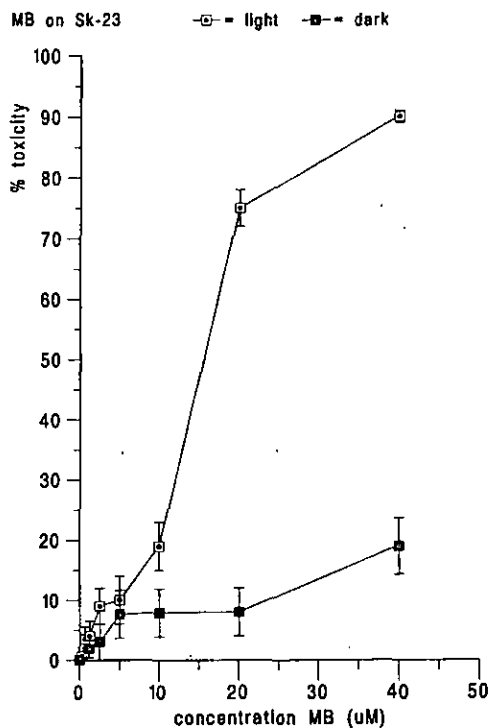


FIGURE 2A - Photocytotoxicity (□) and dark toxicity (■) of MB against the SK-23 cell line. Each point is the mean of at least 14 experiments. Error bars represent SEMs.

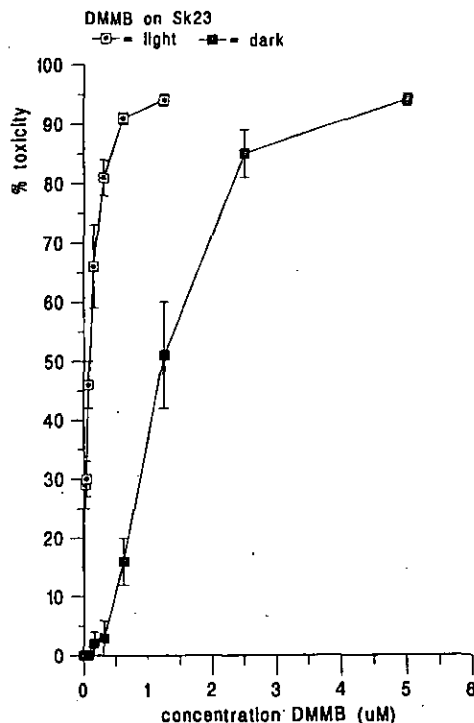


FIGURE 2C - Photocytotoxicity (□) and dark toxicity (■) of DMMB against the SK-23 cell line. Each point is the mean of at least 14 experiments. Error bars represent SEMs.

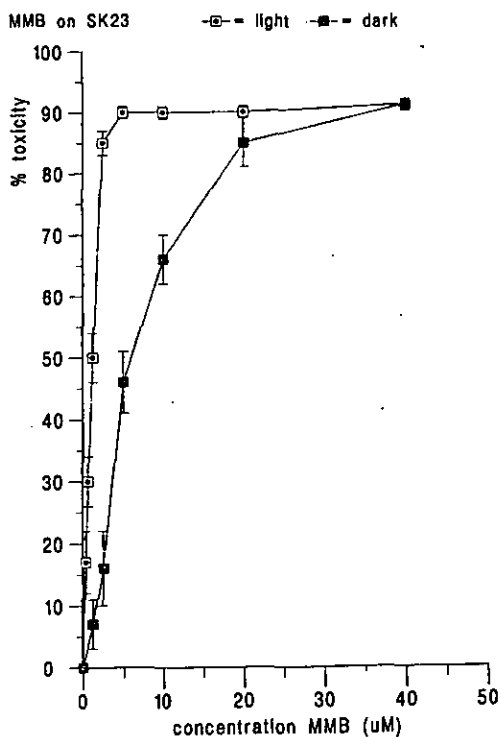


FIGURE 2B - Photocytotoxicity (□) and dark toxicity (■) of MMB against the SK-23 cell line. Each point is the mean of at least 14 experiments. Error bars represent SEMs.

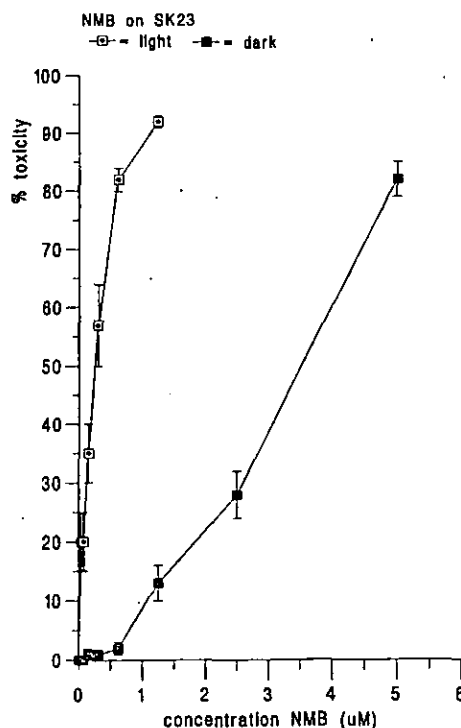


FIGURE 2D - Photocytotoxicity (□) and dark toxicity (■) of NMB against the SK-23 cell line. Each point is the mean of at least 14 experiments. Error bars represent SEMs.

2

Effects of MB on SK-Mel-28 cells in culture, n=at least 16.
 □ - light experiments, ■ - dark experiments.

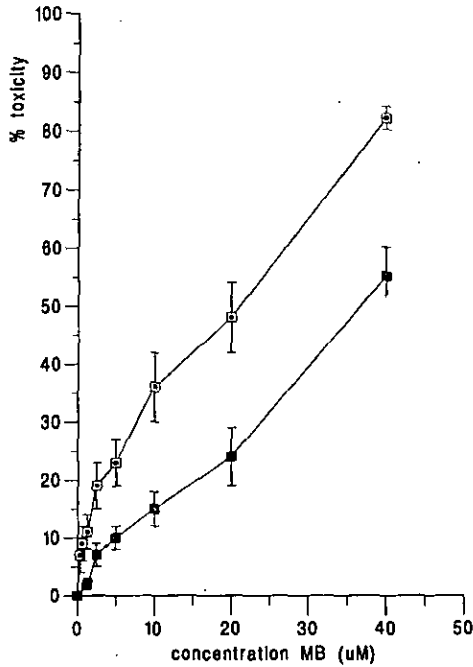


FIGURE 3A - Photocytotoxicity (□) and dark toxicity (■) of MB against the SK-Mel 28 cell line. Each point is the mean of at least 16 experiments. Error bars represent SEMs.

Effect of DMMB on Sk-Mel-28 cells in culture, showing responses at low levels; n= at least 14.
 □ - light experiments, ■ - dark experiments

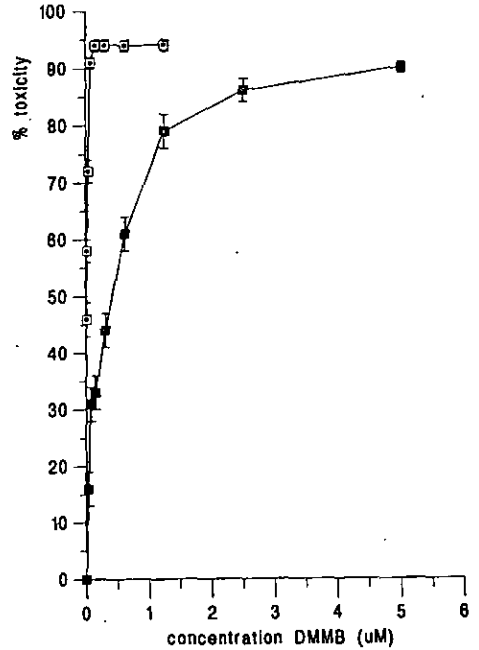


FIGURE 3C - Photocytotoxicity (□) and dark toxicity (■) of DMMB against the SK-Mel 28 cell line. Each point is the mean of at least 14 experiments. Error bars represent SEMs.

Effect of MMB on Sk-mel-28 cells in culture, n=at least 10.
 □ - light experiments, ■ - dark experiments.

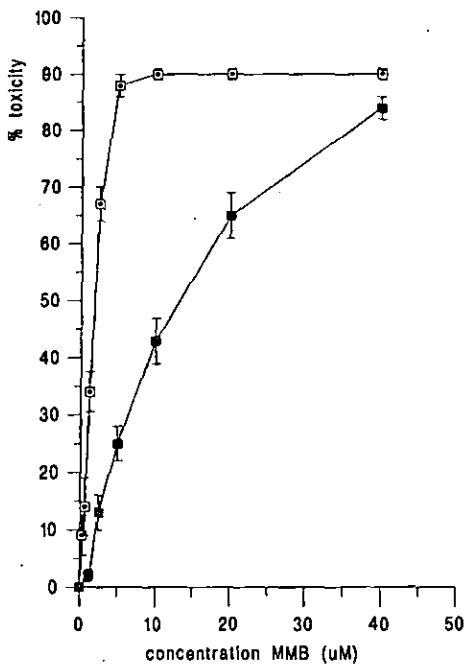


FIGURE 3B - Photocytotoxicity (□) and dark toxicity (■) of MMB against the SK-Mel 28 cell line. Each point is the mean of at least 10 experiments. Error bars represent SEMs.

Effect of NMB on Sk-mel-28 cells showing responses at low levels; n= at least 10.
 □ - light experiments, ■ - dark experiments

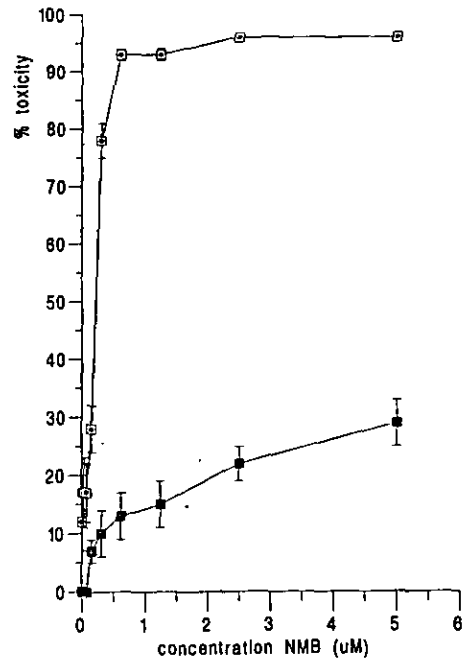


FIGURE 3D - Photocytotoxicity (□) and dark toxicity (■) of NMB against the SK-Mel 28 cell line. Each point is the mean of at least 10 experiments. Error bars represent SEMs.

0

TABLE 2 - Photocytotoxicity of the methylene blue derivatives against the SK-23 and SK-Mel 28 cell lines as a function of the light dose. Photosensitizer concentration in each case was that giving 15% dark cytotoxicity. Each bar is a mean of ≥ 4 experiments.

	% Phototoxicity at light dose				
	0 J cm ⁻²	3.6 J cm ⁻²	5.9 J cm ⁻²	8.5 J cm ⁻²	17.6 J cm ⁻²
vs. SK 23					
MB (32 μ M)	15.0	53.0	62.0	68.0	81.0
MMB (2.5 μ M)	15.0	50.0	53.0	61.0	60.0
DMMB (0.6 μ M)	15.0	91.0	91.0	90.0	97.0
NMB (1.4 μ M)	15.0	42.0	73.0	74.0	95.0
vs. SK Mel 28					
MB (10 μ M)	15.0	13	14	29	57
MMB (3 μ M)	15.0	44	71	86	94
DMMB (0.1 μ M)	15.0	93	95	97	97
NMB (1.25 μ M)	15.0	57	92	97	95

TABLE 3 - Toxicity, phototoxicity and light:dark differential toxicity ratios for the photosensitizers at a light dose of 7.2 J cm⁻².

	SK 23		Light: Dark Toxicity	SK Mel 28	
	IC ₉₀ Light (μ M)	% Dark Toxicity		IC ₉₀ Light (μ M)	% Dark Toxicity
MB	39.6	17.6	5.1	38.8 (80%)	52.6
MMB	5.0	46.0	2.0	9.7	43.2
DMMB	0.4	8.8	10.2	0.1	31.8
NMB	1.1	11.2	8.0	0.5	12.0

	SK 23		SK Mel 28	
	IC ₅₀ Light (μ M)	% Dark Toxicity	IC ₅₀ Light (μ M)	% Dark Toxicity
MB	15.2	7.8	21.0	25.5
MMB	1.6	7.0	2.2	10.1
DMMB	0.05	0	-	-
NMB	0.3	1.0	0.3	9.1

In the SK-23 cell line and with lower light doses methylene blue and its 1-methyl analogue exhibited similar activity (Figures 2a and 2b; Table 2). In addition, when tested against the SK-Mel 28 human melanoma cell line at the standard light dose (7.2 J cm⁻²), it was evident that the dark (inherent) toxicities of methylene blue and 1-methyl methylene blue were appreciable relative to their phototoxicities, even at high phototoxicity values. Thus 38.8 μ M methylene blue caused 80% phototoxicity and

52.6% dark toxicity, while methyl methylene blue at 9.7 μ M gave 90% photo- and 43.2% dark toxicity (Figures 3a and 3b). The corresponding light:dark toxicity ratios were 1.5 and 2.1. These values were increased at higher light doses, moreso for methyl methylene blue than for methylene blue, underlining the greater inherent photosensitizing efficacy of the methylated derivatives (Tables 1 and 2). Methylene blue also exhibited the lowest uptake in this cell line (Figure 4a).

Uptake of MB and its derivatives into SK-23 cells. N=4.

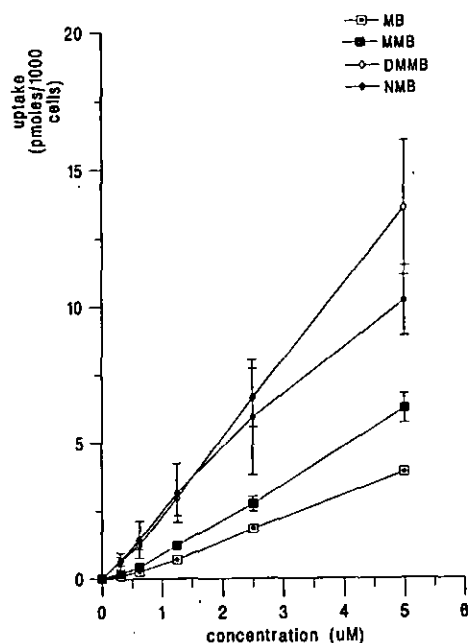


FIGURE 4A - Uptake of the photosensitizers into the SK-23 melanoma cell line as a function of photosensitizer concentration. \square - MB; \blacksquare - MMB; \diamond - DMMB; \blacklozenge - NMB.

Uptake of MB and its derivatives into SK-MEL-28 cells. N=6.

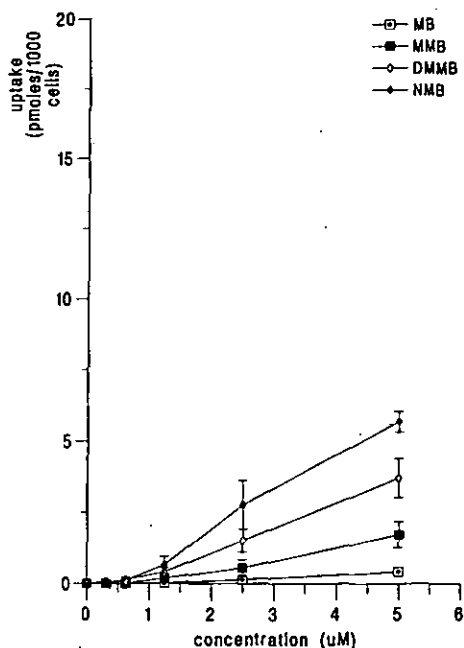


FIGURE 4B - Uptake of the photosensitizers into the SK-Mel 28 melanoma cell line as a function of photosensitizer concentration. \square - MB; \blacksquare - MMB; \diamond - DMMB; \blacklozenge - NMB.

In the SK-Mel 28 cell line, dimethyl methylene blue and new methylene blue both exhibited high levels of phototoxicity at relatively low corresponding dark toxicities, thus having higher light:dark toxicity ratios than the lead compound, methylene blue. New methylene blue was particularly interesting in this respect, having by far the highest ratio at 7.5 (Table 3). The low dark toxicity of new methylene blue is underlined by the greater uptake of this photosensitizer compared to the more dark toxic dimethyl methylene blue in the human melanoma cell line (Figure 4b).

The behaviour of the photosensitizers against the SK-23 murine melanoma cell line was broadly similar to that in the human melanoma cell line. At the standard light dose methyl methylene blue exhibited higher dark toxicity than methylene blue which had a much improved light:dark toxicity ratio (5.1, Table 3). In this cell line the activity of dimethyl methylene blue was higher than that of new methylene blue, although both showed improved light:dark toxicities (10.2 and 8.0 respectively, Table 3). The relative uptakes of the two photosensitizers in this cell line were similar at the IC_{90} s (Figure 4a).

The sites of action of the phenothiazinium photosensitizers in melanoma cells are, as yet, unknown. As suggested earlier, they may be various and time-dependent, although Link *et al.* found a fourfold increase in the uptake of radiolabelled methylene blue in melanotic B16 melanoma cells compared to an amelanotic sub-line and also reported that radiolabelled methylene blue is localised in melanosomes³⁰. Using the method of Potts¹⁷ the melanin affinities of the phenothiazinium photosensitizers employed in the current study were found to follow the order: MB>MMB>NMB>DMMB which, taken with the photocytotoxicity data, suggests that melanin may have had an inhibitory effect on their photodynamic action. This is in agreement with comparative studies utilising other types of photosensitizer, e.g. naphthalocyanines,¹¹ in melanotic and amelanotic strains. However, uptake in the murine melanoma cell line (SK-23) was considerably higher for each of the photosensitizers than in the human melanoma cells which contained visibly lower levels of melanin (Figures 4a and 4b). This suggests that melanin is important in cellular uptake, but that intracellular redistribu-

tion is probable for the methylene blue derivatives²⁶. Since cellular uptake data suggest that NMB and DMMB exhibit greater uptake in both cell lines than do MB or MMB (Figures 4a and 4b) it is suggested that different sites of action exist for the photosensitizers. Thus, for example, dimethyl methylene blue, which showed the least affinity for melanin, might be expected to show cellular localisation other than in the melanosomes - e.g. mitochondria as suggested in the previous work²⁰. This, coupled with a high photosensitizing efficacy would explain the high levels of photocytotoxicity encountered, even at low light doses. NMB showed similar melanin binding to MMB (Table 1) but exhibited higher uptake than the monomethylated derivative in both cell lines and gave the highest yield of singlet oxygen. It was thus more photocytotoxic than MMB. The variation in dark toxicities encountered in both cell lines for the different photosensitizers also indicates localisation at sites other than melanosomes, which are not vital to cell viability.

In order to investigate this, the cellular localisation of each of the photosensitizers was examined in both cell lines using fluorescence microscopy. However, only new methylene blue exhibited any detectable fluorescence, showing a diffuse pattern throughout the cytoplasm in both cell lines (data not shown). It is suggested that the cation-quinoneimine character of NMB (Figure 1) could facilitate intracellular distribution, as has been reported for the related benzo[a]phenothiazinium photosensitizers²⁹.

The toxicity levels and ratios encountered in the SK-23 and SK-Mel 28 melanoma cell lines were expected to differ from those in the earlier study on a murine mammary carcinoma line (EMT-6) due to the presence of the photoprotective and antioxidant melanin. That the toxicity trends were similar indicates that - with phenothiazinium photosensitizers at least - the protective effect of melanin against photodynamic action in cell culture is limited. In addition, cellular uptake of the phenothiaziniums by the melanin-expressing cells exhibited a gross correlation with melanin content, indicating that the biopolymer may be important in the uptake mechanism. This has been demonstrated previously in studies on melanotic and amelanotic sublines.

In terms of the possible clinical application of the current work, PDT employing pheno-

thiazinium photosensitizers is not suggested procedurally for the removal of primary melanoma, since this is routinely performed by excision. However, due to the demonstrated efficacy of methylene blue in tracing microsatelites and its use in sentinel lymph node tracing, it may be of use in the photodynamic treatment of local metastatic lymph infiltration immediately post-surgery i.e. as an alternative to lymphadenectomy. At present, methylene blue is used routinely in various tracing or demarcative procedures, either visible or scintillographic, without reported toxicity. The derivatives used in the present *in vitro* study were all more effective in terms of the photodynamic effect and it is thus suggested that future clinical developments in this direction may be feasible.

ACKNOWLEDGEMENTS: The authors wish to acknowledge the studentship bursary (L.R.) provided by the University of Central Lancashire, and the financial assistance provided by the Preston and Chorley Acute NHS Hospitals Trust:

REFERENCES

- 1 Wainwright M, Grice NJ, Pye LEC. Phenothiazine Photosensitizers. Part 2. 3,7-Bis(arylamino)phenothiazines. *Dyes Pigments* 1999; 42: 45-51.
- 2 Ho RCS. Medical management of stage IV malignant melanoma. *Cancer* 1995; 75: 735-741.
- 3 Kremenz ET, Carter RD, Sutherland CM, Muchmore JH, Ryan RF, Creech O. Regional chemotherapy for melanoma: a 35-year experience. *Ann Surg* 1994; 220: 520-535.
- 4 Rivers JK. Melanoma. *Lancet* 1996; 347: 803-806.
- 5 Roberts DJH, Cairnduff F. Photodynamic therapy of primary skin cancer: a review. *Br J Plastic Surg* 1995; 48: 360-370.
- 6 Herd RM, Dover JS, Arndt KA. Basic laser principles. *Dermatol Clin* 1997; 15: 355-374.
- 7 Corsaro C, Scalia M, Blanco AR, Aiello I, Sichel G. Melanins in physiological conditions protect against lipoperoxidation. A study on albino and pigmented *Xenopus*. *Pigment Cell Res* 1995; 8: 279-282.
- 8 Rozanowska M, Ciszewska J, Korytowski W, Sarna T. Rose Bengal-photosensitized formation of hydrogen peroxide and hydroxyl radicals. *J Photochem Photobiol B Biol* 1995; 29: 71-77.
- 9 Hadjur C, Richard MJ, Parat MO, Jardon P, Favier A. Photodynamic effects of hypericin on lipid peroxidation and antioxidant status in melanoma cells. *Photochem Photobiol* 1996; 64: 375-381.
- 10 Busetti A, Soncin M, Jori G, Rodgers MAJ. High efficiency of benzoporphyrin derivative in the photodynamic therapy of pigmented malignant melanoma. *Br J Cancer* 1999; 79: 821-824.
- 11 Soncin M, Busetti A, Biolo R, et al. Photoinactivation of amelanotic and melanotic cells sensitized by axially substituted Si-naphthalocyanines. *J Photochem Photobiol B Biol* 1998; 42: 202-210.
- 12 Wainwright M. Non-porphyrin photosensitizers in biomedicine. *Chem Soc Rev* 25 (1996) 351-359.

- ¹³ Creagh TA, Gleeson M, Travis D, Grainger R, McDermott TED, Butler MR. Is there a role for *in vivo* methylene blue staining in the prediction of bladder tumour recurrence? *Br J Urol* 1995; 75: 477-479.
- ¹⁴ Tuite EM, Kelly JM. Photochemical reactions of methylene blue and analogues with DNA and other biological substrates. *J Photochem Photobiol B Biol* 1993; 21: 103-124.
- ¹⁵ Williams JL, Stamp J, Devonshire R, Fowler GJS. Methylene Blue and the photodynamic therapy of superficial bladder cancer. *J Photochem Photobiol B Biol* 1989; 4: 229-232.
- ¹⁶ Orth K, Ruck A, Stanescu A, Beger HG. Intraluminal treatment of inoperable oesophageal tumours by intraluminal photodynamic therapy with Methylene Blue. *Lancet* 1995; 345: 519-520.
- ¹⁷ Potts AM. Further studies concerning the accumulation of polycyclic compounds on uveal melanin. *Invest Ophthalmol* 1964; 3: 399-405.
- ¹⁸ Knorle R, Schnitz E, Feuerstein TJ. Drug accumulation in melanin: an affinity chromatographic study. *J Chromatog B* 1998; 714: 171-179.
- ¹⁹ Link EM, Blower PJ, Costa DC et al. Early detection of melanoma metastases with radiiodinated methylene blue. *Eur J Nucl Med* 1998; 25: 1322-1329.
- ²⁰ Wainwright M, Phoenix DA, Rice L, Burrow SM, Waring J. Increased cytotoxicity and phototoxicity in the methylene blue series via chromophore methylation. *J Photochem Photobiol B Biol* 1997; 40: 233-239.
- ²¹ Wainwright M, Phoenix DA, Laycock SL, Wareing DRA, Wright PA. Photobactericidal activity of phenothiazinium dyes against methicillin-resistant strains of *Staphylococcus aureus*. *FEMS Microbiol Lett* 1998; 160: 177-81.
- ²² Yu DS, Chang SY, Ma CP. Photoinactivation of bladder tumor cells by methylene blue: study of a variety of tumor and normal cells. *J Urol* 1990; 144: 164-168.
- ²³ Yu DS, Chang SY, Ma CP. Ultrastructural changes of bladder cancer cells following methylene blue-sensitized photodynamic treatment. *Eur J Urol* 1991; 19: 322-327.
- ²⁴ Yu DS, Chang SY, Ma CP. The effect of methylene blue-sensitized photodynamic treatment on bladder cancer cells: a further study on flow cytometric basis. *J Urol* 1993; 149: 1198-1204.
- ²⁵ Stockert JC, Juarranz A, Villanueva A, Cañete M. Photodynamic damage to HeLa cell microtubules induced by thiazine dyes. *Cancer Chemother Pharmacol* 1996; 39: 167-169.
- ²⁶ Rashid F, Horobin RW. Interactions of molecular probes with living cells and tissues. 2. A structure-activity analysis of mitochondrial staining by cationic probes, and a discussion of the synergistic nature of image-based and biochemical approaches. *Histochemistry* 1990; 94: 303-308.
- ²⁷ Pooler J, Valzeno DP. Physicochemical determinants of the sensitizing effectiveness for photooxidation of nerve membranes by fluorescein derivatives. *Photochem Photobiol* 1979; 30: 491-498.
- ²⁸ Carmichael J, DeGraff WG, Gazdar AF, Minna JD, Mitchell JB. Evaluation of a tetrazolium-based semiautomated colourimetric assay: assessment of chemosensitivity testing. *Cancer Res* 1987; 47: 936-942.
- ²⁹ Lin CW, Shulok JR, Kirley SD, Cincotta L, Foley JW. Lysosomal localization and mechanism of uptake of Nile blue photosensitizers in tumor cells. *Cancer Res* 1991; 51: 2710-2719.
- ³⁰ Link EM, Brown I, Carpenter RN, Mitchell JS. Uptake and therapeutic effectiveness of ¹²⁵I- and ²¹¹At-methylene blue for pigmented melanoma in an animal model system. *Cancer Res* 1989; 49: 4332-4337.